



Università degli Studi della Basilicata

International PhD programme

“APPLIED BIOLOGY AND ENVIRONMENTAL SAFEGUARD”

DISSERTATION TITLE

“Advanced Oxidation Processes (AOPs): solutions for the degradation of emerging contaminants in liquid phases”

Settore Scientifico-Disciplinare

“ AGR/13 – Chimica Agraria ”

PhD Coordinator

Prof. Patrizia Falabella

PhD Student

Dr. Foti Luca

Supervisor

Prof. Laura Scrano

Cycle: XXXIV

A. Y. 2020-2021

Index

Chapter 1

Literature review	1
1.1 Water pollution and Legislative Decree 152/06	1
1.2 Wastewater: origin, classification, and characteristics	3
1.2.1 <i>Definition of wastewater</i>	3
1.2.2 <i>Wastewater composition: physical, chemical, and biological characteristics</i>	4
1.2.2.1 <i>Physical parameters</i>	5
1.2.2.2 <i>Chemical parameters</i>	6
1.2.2.3 <i>Biological parameters</i>	10
1.3 Wastewater treatment plants (WWTPs)	10
1.3.1 <i>Preliminary treatment</i>	12
1.3.2 <i>Primary treatment</i>	13
1.3.3 <i>Secondary treatment</i>	14
1.3.4 <i>Tertiary treatment</i>	16
1.4 Emerging contaminants (ECs)	18
1.5 Occurrence of pharmaceuticals in wastewater	20
1.6 Occurrence of antibacterial compounds in the environment and antibacterial resistance	23
1.6.1 <i>Quinolones: discovery, mechanism of action and global consumption</i>	25
1.6.1.1 <i>Quinolones in the soil environment</i>	28
1.6.1.2 <i>Quinolones in wastewater and surface water</i>	30
1.7 Advanced Oxidation Processes (AOPs)	35
1.7.1 <i>Photolysis</i>	37
1.7.2 <i>UV/H₂O₂ processes</i>	38
1.7.3 <i>Ozonation</i>	39
1.7.4 <i>O₃/UV process</i>	40
1.7.5 <i>O₃/UV/H₂O₂ process</i>	41
1.7.6 <i>Process involving iron catalysts: Fenton process (H₂O₂/Fe²⁺)</i>	41
1.7.7 <i>Photo-Fenton process (UV/H₂O₂/Fe²⁺)</i>	42

1.7.8	<i>Heterogeneous catalysis/photocatalysis</i>	43
1.7.9	<i>Sulphate radicals</i>	45
1.8	Toxicity bioassays: methods to evaluate the dangerousness of organic wastewater contaminants	46
1.8.1	<i>Bacterial bioassay (Vibrio fischeri, Escherichia coli, Micrococcus flavus)</i>	48
1.8.2	<i>Phytotoxicity bioassays (Lepidium sativum and Solanum lycopersicum)</i>	50
1.8.3	<i>3-(4,5-dimethylthiazol-2-yl)-2,5-diphenyltetrazolium bromide (MTT) bioassay</i>	52
1.9	Aim of thesis	53

Chapter 2

	Case study #1: photolysis and heterogeneous photocatalysis with suspended TiO₂ for the degradation of levofloxacin in ultrapure water	55
2.1	Introduction	55
2.2	Experimental section	56
2.2.1	<i>Chemicals</i>	56
2.2.2	<i>Experimental device for photodegradation process (in batch)</i>	56
2.2.3	<i>Photolysis and heterogeneous photocatalysis with suspended TiO₂</i>	57
2.2.4	<i>HPLC-UV condition</i>	57
2.3	Results and discussion	58
2.4	Conclusions	62

Chapter 3

	Case study #2: heterogeneous photocatalysis with supported TiO₂ on borosilicate tube for the degradation of levofloxacin in ultrapure water	63
3.1	Introduction	63
3.2	Experimental section	64

3.2.1	<i>Chemicals</i>	64
3.2.2	<i>Experimental devices for photocatalysis in continuous</i>	65
3.2.3	<i>Photolysis and heterogeneous photocatalysis with supported TiO₂</i>	66
3.2.4	<i>HPLC-UV conditions</i>	66
3.2.5	<i>MicroTox[®] bioluminescence assay on Vibrio fischeri</i>	66
3.2.6	<i>Phytotoxicity assays on Lepidium sativum and Solanum lycopersicum</i>	68
3.3	Results and discussion	69
3.3.1	<i>Kinetic study</i>	69
3.3.2	<i>Vibrio fischeri toxicity evaluation</i>	72
3.3.3	<i>Phytotoxicity evaluation</i>	75
3.4	Conclusions	79
3.5	Supplementary material	79

Chapter 4

Case study #3: homogeneous photocatalysis with hydrogen peroxide (H₂O₂), peroxymonosulphate (PMS, HSO₅⁻) and peroxydisulphate (PS, S₂O₈²⁻) for the degradation of levofloxacin	89
--	-----------

4.1	Introduction	89
4.2	Material and methods	91
4.2.1	<i>Reagents, catalyst and wastewater</i>	91
4.2.2	<i>AOPs and experimental conditions</i>	92
4.2.3	<i>Analytical methods</i>	93
4.2.3.1	<i>HPLC-UV and MS method</i>	93
4.2.3.2	<i>Spectrophotometric method for PDS quantification</i>	93
4.2.4	<i>Antibacterial activity assessment (E. coli and M. flavus)</i>	93
4.3	Results and discussion	94
4.3.1	<i>Degradation efficiency of levofloxacin by simulated irradiation-drive processes</i>	94

4.3.2	<i>Kinetic study of simulated irradiation/PDS system in simulated wastewater (SWW), and optimisation of the process</i>	98
4.3.3	<i>Antibacterial activity evaluation</i>	101
4.3.4	<i>Elucidation on degradation pathways of levofloxacin</i>	102
4.4	Conclusions	104

Chapter 5

Scientific activity in University of Ioannina (Department of Chemistry)	106
--	------------

5.1	MTT assay for the toxicity evaluation of photocatalytic treatment of levofloxacin with PDS	106
5.2	Chemicals	106
5.3	Experimental section	106
5.4	Results and discussion	109
5.5	Conclusions	109

Chapter 6

Training period at Hydros S.r.l.	110
General conclusions and perspectives	112
References	114

LIST OF FIGURES

Figure 1.1	Characteristics of wastewater.	4
Figure 1.2	Typical composition of a wastewater treatment plant (WWTP).	11
Figure 1.3	Categories of emerging contaminants listed in the NORMAN substance database.	19
Figure 1.4	Main categories of human pharmaceuticals detected in the environment (Nikolaou et al., 2007).	23
Figure 1.5	Chemical structure of the main quinolones.	26
Figure 1.6	Classification of advanced oxidation processes (Mokhbi et al, 2019)	36
Figure 1.7	Representative scheme of TiO ₂ -semiconductor photocatalysis process (Ibhadon and Fitzpatrick, 2013).	44
Figure 1.8	<i>Vibrio fischeri</i> bacterium (www.deviantart.com).	48
Figure 1.9	A simplified schematic of the molecular basis of bioluminescence in <i>Vibrio fischeri</i> (Williams et al., 2019).	49
Figure 1.10	(A) <i>Lepidium sativum</i> and (B) <i>Solanum lycopersicum</i> .	51
Figure 1.11	Conversion reaction of MTT to formazan by mitochondrial reductase.	52
Figure 2.1	(A) Photochemical reactor used for direct photolysis and heterogeneous photocatalysis with suspended TiO ₂ , and (B) solar simulator device.	57
Figure 2.2	HPLC-UV separation of photo-degraded solution using direct photolysis and heterogeneous photocatalysis with TiO ₂ powder. (A) Initial solution 10 mg·L ⁻¹ in ultrapure water before irradiation, (B) photocatalysis after 10 min, (C) photocatalysis after 60 min, (D) photocatalysis after 120 min, (E) photolysis after 120 min, (F) photolysis after 420 min. In all chromatograms the last peak on the right is LFX.	59

Figure 2.3	Evaluation of LFX degradation measured as $C/C_0\%$ versus irradiation time.	60
Figure 2.4	(A) Photodegradation of levofloxacin catalysed by TiO_2 powder; Ct_{calc} , values calculated using Equation 2.1 ; Ct_{exp} , experimental values. (B) The trend of the second-order linearized equation used to estimate kinetic parameters reported in Table 2.1 .	61
Figure 3.1	(A) Photochemical reactor used for direct heterogeneous photocatalysis with immobilised TiO_2 , and (B) schematic diagram of the photodegradation system.	65
Figure 3.2	MicroTox system used for bioluminescence assay on <i>Vibrio fischeri</i> . Water Research Institute (IRSA-CNR), Taranto (Italy).	67
Figure 3.3	Evaluation of LFX degradation measured as $C/C_0\%$ versus irradiation time.	70
Figure 3.4	(A) Photodegradation of levofloxacin catalysed by TiO_2 -coated tube; Ct_{calc} , values calculated using Equation 3.1 ; Ct_{exp} , experimental values. (B) The trend of the first-order linearized equation used to estimate kinetic parameters reported in Table 3.1 .	71
Figure 3.5	Percentage of toxic effect after 30 minutes of exposure to the samples obtained from (A) photolysis and (B) TiO_2 -coated tube photocatalysis experiments.	74
Figure 3.6	Effect of the tested samples on (A) seed germination, (B) radical elongation, (C) growth index of <i>Lepidium sativum</i> .	77
Figure 3.7	Effect of the tested samples on (A) seed germination, (B) radical elongation, (C) growth index of <i>Solanum lycopersicum</i> .	78
Figure 3.8	Toxicity results of the T0 sample ($C_{LFX} = 20.56 \text{ mg}\cdot\text{L}^{-1}$).	80
Figure 3.9	Toxicity results of the sample obtained after 150 minutes of irradiation in the photolysis experiment (T150 ; $C_{LFX} = 13.18 \text{ mg}\cdot\text{L}^{-1}$).	80

- Figure 3.10** Toxicity results of the sample obtained after 300 minutes of irradiation in the photolysis experiment (**T300**; $C_{LFX} = 9.012 \text{ mg}\cdot\text{L}^{-1}$). **81**
- Figure 3.11** Toxicity results of the sample obtained after 600 minutes of irradiation in the photolysis experiment (**T600**; $C_{LFX} = 5.36 \text{ mg}\cdot\text{L}^{-1}$). **81**
- Figure 3.12** Toxicity results of the sample obtained after 1140 minutes of irradiation in the photolysis experiment (**T1140**; $C_{LFX} = 0.81 \text{ mg}\cdot\text{L}^{-1}$). **82**
- Figure 3.13** Toxicity results of the sample obtained after 1560 minutes of irradiation in the photolysis experiment (**T1560**; $C_{LFX} = 0 \text{ mg}\cdot\text{L}^{-1}$). **82**
- Figure 3.14** Toxicity results of the **T0** sample ($C_{LFX} = 22.08 \text{ mg}\cdot\text{L}^{-1}$). **83**
- Figure 3.15** Toxicity results of the sample obtained after 120 minutes of irradiation in the TiO_2 -coated tube photocatalysis experiment (**T120**; $C_{LFX} = 13.71 \text{ mg}\cdot\text{L}^{-1}$). **83**
- Figure 3.16** Toxicity results of the sample obtained after 420 minutes of irradiation in the TiO_2 -coated tube photocatalysis experiment (**T420**; $C_{LFX} = 7.45 \text{ mg}\cdot\text{L}^{-1}$). **84**
- Figure 3.17** Toxicity results of the sample obtained after 840 minutes of irradiation in the TiO_2 -coated tube photocatalysis experiment (**T840**; $C_{LFX} = 3.09 \text{ mg}\cdot\text{L}^{-1}$). **84**
- Figure 3.18** Toxicity results of the sample obtained after 1320 minutes of irradiation in the TiO_2 -coated tube photocatalysis experiment (**T1320**; $C_{LFX} = 0.76 \text{ mg}\cdot\text{L}^{-1}$). **85**
- Figure 3.19** Toxicity results of the sample obtained after 1980 minutes of irradiation in the TiO_2 -coated tube photocatalysis experiment (**T1980**; $C_{LFX} = 0 \text{ mg}\cdot\text{L}^{-1}$). **85**
- Figure 3.20** Toxicity results of the sample obtained after 2340 minutes of irradiation in the TiO_2 -coated tube photocatalysis experiment (**T2340**; $C_{LFX} = 0 \text{ mg}\cdot\text{L}^{-1}$). **85**

Figure 3.21	Chromatograms of tested samples obtained from photolysis experiment.	86
Figure 3.22	Chromatograms of tested samples obtained from TiO ₂ -coated tube photocatalysis experiment.	87
Figure 4.1	Chromatograms of LFX 10 mg·L ⁻¹ in distilled water and after adding PMS [400 μM] in distilled water, acetate buffer solution pH = 5 and phosphate buffer solution pH = 7.	95
Figure 4.2	Photodegradation curve of LFX in A) distilled water, B) acetate buffer solution and C) phosphate buffer solution, by different simulated irradiation/oxidant system (t = 10 min; C ₀ = 10 mg·L ⁻¹).	97
Figure 4.3	Kinetics degradation by simulated irradiation/PDS system at different PDS concentrations [400 μM; 200 μM; 100 μM] in simulated wastewater (pH=7.8; t = 10 min; C ₀ = 10 mg·L ⁻¹).	99
Figure 4.4	Trends of the first-order linearised equation used to calculate kinetic parameters reported in Table 4.2 .	100
Figure 4.5	Possible degradation pathway of LFX in SWW by simulated irradiation/PDS system, after 5 minutes of irradiation.	102
Figure 5.1	Elisa's plate positions used for MTT assay of tested samples.	108
Figure 5.2	Schematic procedure of MTT assay.	108
Figure 6.1	Process flow diagram of Giugliano-Naple's wastewater treatment plant.	111

LIST OF TABLES

Table 2.1	Kinetic parameters of LFX degradation under photolysis and photocatalysis experiments.	60
Table 3.1	Kinetic parameters of LFX degradation under photolysis and supported-TiO ₂ photocatalysis experiments.	70
Table 3.2	Percentage (%) of toxic effect after 30 minutes of exposure to the samples obtained from photolysis and TiO ₂ -coated tube photocatalysis experiments and toxicity classification.	73
Table 3.3	Results of phytotoxicity assays against <i>Lepidium sativum</i> and <i>Solanum lycopersicum</i> .	76
Table 3.4	List of transformation products obtained from photolysis and TiO ₂ -coated tube photocatalysis, based on retention time observed by HPLC-UV analyses.	88
Table 4.1	Percentage (%) of LFX degraded in acetate buffer solution, distilled water and phosphate buffer solution by different simulated irradiation/oxidant systems (t = 10 min).	96
Table 4.2	Kinetic parameters of LFX degradation in synthetic wastewater with three different concentrations of PDS.	100
Table 5.1	Results of MTT assay on A549 cells.	109

LIST OF ABBREVIATIONS

ACN: acetonitrile

AIFA: Agenzia Italiana del Farmaco

AOPs: Advanced Oxidation Processes

ATC: Anatomical Therapeutic and Chemical classification

AWaRe: Access, Watch, Reserve

BOD: Biochemical Oxygen Demand

CB: conduction band

CHMP: Committee for medicinal products for human use

CIP: ciprofloxacin

COD: Chemical Oxygen Demand

DAD: Diode Array Detector

DDD: Defined Daily Dose

DKA: β -diketone antibiotics

DMSO: dimethylsulfoxide

EC10: 10% of effect concentration

EC20: 20% of effect concentration

EC50: half maximal effective concentration

ECs: Emerging Contaminants

EDCs: endocrine-disrupting compounds

EEA: European Economic Area

EFSA: European Food Safety Authority

EMA: European Medicine Agency

ENR: enrofloxacin

ESPR: Environmental Science and Pollution Research

FMN: flavine mononucleotide

FQs: fluoroquinolones

GC-MS: Gas Chromatography - Mass Spectrometry

GI: growth index

HPLC-UV: High-Performance Liquid Chromatography - Ultraviolet

HR-AOPs: hydroxyl radicals based advanced oxidation processes

HRS: hospital raw sewage

IC20: 20% of inhibitory concentration

LB: Lysogeny Broth

LC-MS: Liquid Chromatography - Mass Spectrometry

LFX: levofloxacin

MedFil: media filtration

MemFil: membrane filtration

MTT: [3-(4,5-dimethylthiazol-2-yl)-2,5-diphenyltetrazolium bromide]

NADPH: reduced nicotinamide adenine dinucleotide phosphate

NSAID: non-steroidal anti-inflammatory drugs

PAOs: polyphosphate accumulating organisms

PBS: phosphate-buffered solution

PDS: peroxydisulphate

PMS: peroxymonosulphate

PRAC: Pharmacovigilance Risk Assessment Committee

PTFE: polytetrafluoroethylene

QSAR: Quantitative Structure-Activity Relationship

RE: roots elongation

RGI: relative growth index

SG: seed germination

SR-AOPs: sulphate radicals based advanced oxidation processes

STP: sewage treatment plant

SurFil: surface filtration

TDS: total dissolved solids

TKN: total Kjeldahl nitrogen

TOC: total organic carbon

TPs: transformation products

TS: total solids

TSB: Tryptic Soy Broth

TSS: total suspended solids

TW: treated wastewater

US: ultrasound

USEPA: United States Environmental Protection Agency

UV: ultraviolet

VB: valence band

VFBI: *Vibrio fischeri* bioluminescence inhibition assay

WHO: World Health Organization

WRRF: water resource recovery facility

WWTP: wastewater treatment plant

ABSTRACT

Wastewater is the main source of micropollutants and although treated in urban wastewater treatment plants (WWTPs), it can continue to contain recalcitrant substances, potentially dangerous for the health of living organisms and for the environment. It is therefore necessary to implement appropriate actions to limit its diffusion. Advanced oxidation processes (AOPs), which use hydroxyl radicals for the remediation of organic contaminants in wastewater, are highly effective innovative methods to accelerate the remediation process. AOPs can amplify their action if combined with ozone (O₃) and if subjected to mono and polychromatic irradiation. The main objective of the PhD thesis was precisely to apply heterogeneous and homogeneous photolysis and photocatalysis systems in the liquid phase, for the removal of levofloxacin (LFX), a widely used antibiotic belonging to the quinolone family. Comparison of degradation kinetics, chromatographic detection of degradation products and evaluation of toxicity were some of the steps of the work. In detail, this thesis consists of **six chapters**.

Chapter 1 provides an accurate bibliographic analysis, with the aim of giving an overview of the numerous fields of investigation connected with the topic of this thesis: a description of wastewater characteristics and of the Italian legislative decree 152/06 which regulates discharges into the environment, the organization of wastewater treatment plants, the problem of emerging contaminants, including antibiotics and in particular the class of fluoroquinolones, taken into consideration as case study of this thesis, the advanced oxidation processes (AOPs), and, finally, a brief review on the toxicity tests used in this work.

Chapter 2 contains the first experiment of this thesis, which consists in the degradation of levofloxacin in distilled water, through the processes of photolysis and heterogeneous photocatalysis with titanium dioxide (TiO₂). The first purpose of this chapter was to evaluate the efficiency of heterogeneous photocatalysis with TiO₂, a process that in the literature is taken as a "reference" model, a very effective technique. Experimental results obtained demonstrate that this process is effective to remove levofloxacin and its by-products in almost 4 hours, and seems to follow a second-order kinetic. However, this process cannot be applied on a large scale due to the high costs of treatment for the recovery and separation of the photocatalyst from the solution.

Chapter 3 provides an evaluation of the efficiency of TiO₂ as photocatalyst immobilized on the surface of a borosilicate tube for the degradation of levofloxacin through a "continuous" irradiation system, different from the "static" system used in chapter 2. In particular, not only a kinetic study was carried out, but also some toxicity tests, including the *Vibrio fischeri*

bioluminescence inhibition test and the phytotoxicity tests on *Lepidium sativum* and *Solanum lycopersicum*, in order to better understand the potential applicability of this system. More specifically, in the case of phytotoxicity tests, the last sample of each photodegradation test carried out with the "continuous" system (with and without the TiO₂-coated tube) was tested; in the case of the *Vibrio fischeri* assays, the most representative samples were tested, i.e. those that seemed to present the greatest number of transformation products, on the basis of the chromatograms obtained by liquid chromatography analysis. From experimental results, both photolysis and photocatalysis follow a very similar trend and degradations seem to be modelled with a first-order kinetic. The toxicity tests on *Vibrio fischeri* showed a low toxicity of the starting solution containing only levofloxacin. All the solutions subjected to photolysis were found to be toxic, while the solutions subjected to photocatalysis highly toxic. This unexpected result has been attributed to the probable detachment of titanium dioxide nanoparticles from the surface of the tube, whose toxicity is also being confirmed by the European Food Safety Authority (EFSA). Phytotoxicity tests confirmed these results showing an inhibition of seed germination, root elongation and growth index in both the plants tested.

Chapter 4 is reported in this thesis as an under review article submitted to "*Environmental Science and Pollution Research (ESPR)*". In this scientific work, levofloxacin solution was treated using hydrogen peroxide (H₂O₂), peroxymonosulfate (PMS) and peroxodisulfate (PDS), as oxidizing agents, which respectively provide only OH[•] radicals, both OH[•]/SO₄^{•-} radical, and SO₄^{•-} radicals. The efficiency of the three oxidizing agents was tested in different pH conditions, and the most efficient treatment (simulated radiation/PDS) was applied (and optimized) to remove levofloxacin from a simulated wastewater (SWW). In this case the main transformation products (TPs) were identified by liquid chromatography coupled with mass spectrometry, the degradation pathway was suggested and toxicity tests on *Escherichia coli* (LMG2092), a Gram-negative bacterium, and *Micrococcus flavus* (DSM1790), a Gram-positive bacterium, were performed. Experimental results demonstrated that simulated irradiation/H₂O₂ treatment showed less impact on LFX reduction than the combined AOPs of simulated irradiation/PMS and simulated irradiation/PDS. In contrast, PMS and PDS were able to degrade levofloxacin completely. In particular, the PMS resulted the best in phosphate buffer because it has been able to completely transform LFX into LFX N-oxide in 30 seconds, through a non-radicals mechanism. However, except for phosphate buffer, simulated irradiation/PDS system showed the best performance achieving a complete degradation of LFX after 10 minutes of irradiation in all mediums investigated. This system was successfully applied in simulated wastewater (SWW) by using three different concentrations of PDS to optimize the process, and in all cases the

degradation followed a first-order kinetic. Selected samples obtained from the photocatalytic treatment of LFX in SWW with the highest concentration tested of PDS were tested on *Escherichia coli* and *Micrococcus flavus*. Both the cultures of Gram-positive and Gram-negative bacteria were not affected after the effective degradation of levofloxacin by the sulphate radical based AOP.

Chapter 5 provides a further insight into the potential eco-friendliness of sulphate radicals treatment for the degradation of levofloxacin. In particular, some of the samples obtained from the treatment of levofloxacin with peroxodisulfate in distilled water were subjected to the MTT (3-(4,5-dimethylthiazol-2-yl)-2,5-diphenyltetrazolium) bioassay on human epithelial-like lung cancer cell line A549. These experimental tests were carried out in Greece, at the University of Ioannina. Experimental results demonstrated that there was no toxicity effect on the cells viability.

Finally, **chapter 6** provides a brief description of the internship period carried out at Hydros S.r.l. (Tito, Potenza). During this experience, I participated in the design of fumes and wastewater treatment systems, and in the optimization of the parameters of the biological process of nitrification/denitrification/oxidation present within a real wastewater treatment plant.

In conclusion, I can say that this PhD thesis demonstrates that AOPs may be an alternative eco-friendly treatment for the removal of contaminants from wastewater effluents. The experimental results tends to demonstrate that solar advanced oxidation processes has the potential to open new feasible remediation strategies for WWTPs effluent tertiary treatment before wastewater reuse in irrigation for instance. However, most investigations are done at lab-scale. For a practical view and commercial uses, much more work is necessary to switch from batch work to a large scale to find out the efficiency and ecotoxicity of the processes.

RIASSUNTO

Le acque reflue sono la principale fonte di microinquinanti e, sebbene siano trattate negli impianti di trattamento delle acque reflue (WWTP), esse possono continuare a contenere sostanze recalcitranti, potenzialmente pericolose per la salute degli organismi viventi e per l'ambiente. Pertanto è necessario mettere in atto opportune azioni per limitarne la diffusione. I processi di ossidazione avanzata (AOPs), che utilizzano i radicali idrossilici per la distruzione dei contaminanti organici nelle acque reflue, sono metodi innovativi altamente efficaci per accelerare il processo di rimozione. Questi processi possono amplificare la loro azione se vengono combinati con l'ozono (O₃) o se vengono sottoposti ad irraggiamento per mezzo di una radiazione mono- e poli- cromatica. L'obiettivo principale di questa tesi di dottorato è stato proprio quello di applicare sistemi di fotolisi e fotocatalisi eterogenei ed omogenei in fase liquida, per la rimozione del levofloxacin (LFX), un antibiotico ampiamente utilizzato appartenente alla famiglia dei chinoloni. Nella diverse fasi del lavoro sono state confrontate le cinetiche di degradazione, la separazione cromatografica dei prodotti di degradazione e la valutazione della tossicità. In dettaglio, questa tesi consiste di **6 capitoli**.

Il **capitolo 1** fornisce un'attenta analisi bibliografica, con l'intento di dare un quadro generale dei numerosi campi di indagine connessi con l'argomento di questa tesi: una descrizione delle caratteristiche delle acque reflue e del decreto legislativo italiano 152/06 che ne regola gli scarichi nell'ambiente, l'organizzazione degli impianti di trattamento delle acque reflue, il problema dei contaminanti emergenti, tra cui gli antibiotici ed in particolar modo la classe dei fluorochinoloni, presi in considerazione come caso di studio di questa tesi, i processi di ossidazione avanzata (AOPs), ed infine una breve rassegna sui test di tossicità utilizzati in questo lavoro.

Il **capitolo 2** contiene il primo esperimento di questa tesi, che consiste nella degradazione del levofloxacin in acqua ultrapura, tramite i processi di fotolisi e fotocatalisi eterogenea con biossido di titanio (TiO₂) in polvere. Il primo scopo di questo capitolo è stato quello di valutare l'efficienza della fotocatalisi eterogenea con TiO₂, un processo che in letteratura viene preso come modello di "riferimento", quindi una tecnica molto efficace che però non può essere applicata su larga scala a causa degli alti costi del trattamento dovuti alla necessità di recupero e separazione del fotocatalizzatore dalla soluzione.

Il **capitolo 3** fornisce una valutazione sull'efficienza del TiO₂ come fotocatalizzatore immobilizzato sulla superficie di un tubo di borosilicato per la degradazione del levofloxacin attraverso un sistema di irraggiamento "in continuo", diverso dal sistema "statico" utilizzato nel

capitolo 2. In particolare, non è stato effettuato solo uno studio cinetico, ma anche alcuni test di tossicità, tra cui il test di inibizione della bioluminescenza di *Vibrio fischeri* ed il test di fitotossicità su *Lepidium sativum* e *Solanum lycopersicum*, al fine di comprendere meglio la potenziale applicabilità di questo sistema. Più specificamente, nel caso dei saggi di fitotossicità, è stato testato l'ultimo campione di ciascuna prova di fotodegradazione effettuata con il sistema "in continuo" (con e senza il tubo rivestito di TiO₂); nel caso dei saggi su *Vibrio fischeri*, invece, sono stati testati i campioni più rappresentativi, ossia quelli che sembravano presentare il maggior numero di prodotti di trasformazione, sulla base dei cromatogrammi ottenuti tramite analisi di cromatografia liquida. Dai risultati sperimentali è emerso che sia la fotolisi sia la fotocatalisi seguono un andamento molto simile e le degradazioni sembrano seguire una cinetica del primo ordine. I test di tossicità su *Vibrio fischeri* hanno mostrato una bassa tossicità della soluzione di partenza contenente solo levofloxacin. Tuttavia, tutte i campioni ottenuti dal processo di fotolisi sono risultati tossici, mentre quelli ottenuti dal processo di fotocatalisi con TiO₂ immobilizzato sono risultati altamente tossici. Questo risultato inaspettato è stato attribuito al probabile distacco dalla superficie del tubo di nanoparticelle di biossido di titanio, la cui tossicità è stata confermata anche dall'Autorità Europea per la Sicurezza Alimentare (EFSA). I test di fitotossicità hanno confermato questi risultati mostrando un'inibizione della germinazione dei semi, dell'allungamento delle radici e dell'indice di crescita in entrambe le piante testate.

Il **capitolo 4** è riportato in questa tesi sotto forma di articolo ancora in fase di revisione, sottomesso alla rivista "*Environmental Science and Pollution Research (ESPR)*". In questo lavoro, una soluzione di levofloxacin è stata trattata con agenti ossidanti quali il perossido di idrogeno (H₂O₂), il perossimonosolfato (PMS) ed il perossidisolfato (PDS), i quali forniscono rispettivamente solo radicali OH[•], un radicale OH[•] ed un radicale SO₄^{•-}, e radicali SO₄^{•-}. L'efficienza dei tre agenti ossidanti è stata testata in diverse condizioni di pH, ed il trattamento risultato più efficiente (radiazione simulata/PDS) è stato successivamente applicato (e ottimizzato) per rimuovere il levofloxacin da un'acqua di scarico simulata. In questo caso sono stati identificati i principali prodotti di trasformazione (TPs) mediante cromatografia liquida accoppiata a spettrometria di massa, è stato suggerito il pathway di degradazione e sono stati effettuati test di tossicità su *Escherichia coli* (LMG2092), un batterio Gram-negativo, e *Micrococcus flavus* (DSM1790), un batterio Gram-positivo. I risultati sperimentali hanno dimostrato che il trattamento radiazione/H₂O₂ aveva un impatto minore sulla degradazione del levofloxacin, rispetto ai trattamenti radiazione/PMS e radiazione/PDS. Invece, PMS e PDS sono stati in grado di rimuovere completamente il levofloxacin. In particolare, il PMS è risultato essere il migliore in tampone fosfato perché, attraverso un meccanismo di tipo non radicalico, ha

portato alla completa trasformazione del LFX nel rispettivo LFX N-ossido in 30 secondi. Comunque, fatta eccezione per il tampone fosfato, il sistema che ha mostrato la miglior performance portando alla completa degradazione del LFX dopo 10 minuti in tutte le matrici investigate è stato il sistema radiazione/PDS. Questo sistema è stato applicato con successo in acqua reflua simulata (SWW) utilizzando tre diverse concentrazioni di PDS per ottimizzare il processo, ed in tutti i casi la degradazione ha seguito una cinetica del primo ordine. Alcuni campioni ottenuti durante il trattamento fotocatalitico in SWW con la concentrazione più alta di PDS sono stati selezionati per essere testati su *Escherichia coli* e *Micrococcus flavus*. Nessuno dei campioni testati ha mostrato effetto tossico nei confronti delle due colture batteriche.

Il **capitolo 5** fornisce un ulteriore approfondimento riguardo la potenziale eco-compatibilità del trattamento con radicali solfato per la degradazione del levofloxacin. In particolare, alcuni dei campioni ottenuti dal trattamento del levofloxacin con perossidissolfato in acqua distillata sono stati sottoposti al saggio biologico MTT (3-(4,5-dimetiltiazol-2-il)-2,5-difeniltetrazolio) sulla linea cellulare di carcinoma polmonare simil-epiteliale A549. Tali prove sperimentali sono state effettuate in Grecia, presso l'Università di Ioannina. Dai risultati sperimentali non si è osservato alcun effetto negativo sulla vitalità cellulare.

Infine, il **capitolo 6** prevede una breve descrizione del periodo di tirocinio svolto presso l'azienda Hydros S.r.l. (Tito, Potenza). Durante queste esperienze ho partecipato alla progettazione di impianti per il trattamento di fumi e di acque reflue, ed all'ottimizzazione dei parametri del processo biologico di nitrificazione/denitrificazione/ossidazione presenti all'interno di un reale impianto di depurazione.

In conclusione, questa tesi di dottorato dimostra che i processi di ossidazione avanzata possono essere un trattamento ecologico alternativo per la rimozione dei contaminanti dagli effluenti delle acque reflue. I risultati sperimentali tendono a dimostrare che tali processi hanno il potenziale per aprire nuove strategie di bonifica per il trattamento terziario degli effluenti degli impianti di depurazione, prima del riutilizzo delle acque, per esempio, nell'irrigazione. Tuttavia la maggior parte delle indagini viene eseguita in ambito di laboratorio. Per una visione più pratica e per usi commerciali, è necessario molto più lavoro per passare all'applicazione di tali processi su larga scala, in modo da capirne l'efficienza e l'ecocompatibilità.

CHAPTER 1

Literature review

1.1 Water pollution and Legislative Decree 152/06

Many of humanity's major problems are water quantity and water quality issues in the twenty-first century. These problems will be more aggravated in the future by climate change, resulting in higher water temperatures, melting of glaciers, and an intensification of the water cycle, with potentially more floods and droughts. Concerning human health, the most direct and most severe impact is the lack of improved sanitation and related to it is the scarcity of safe drinking water, which currently affects more than a third of the people in the world. Additional threats include, for example, exposure to pathogens or chemical toxicants via the food chain (e.g., the result of irrigating plants with contaminated water and of bioaccumulation of toxic chemicals by aquatic organisms, including seafood and fish) or during recreation (e.g., swimming in polluted surface water) (Schwarzenbach et al., 2010).

Indeed, global industrialisation has led to an uncontrolled increase in water pollution due to the continuous spillage of harmful substances into water bodies. **Water pollution** is defined as “*any direct or indirect alteration of the physical, thermal, chemical, biological, radioactive properties of any part of the environment by, discharge, emission or deposit of wastes to affect any beneficial use adversely or to cause a condition, which is hazardous to public health, safety or welfare of animals, birds, wildlife, aquatic life or to plants of every description*” (Balasuriya, 2018). There are various causes of water pollution:

1. **Industrial waste**: industries and industrial sites worldwide significantly contribute to water pollution. Many industrial sites produce waste in the form of toxic chemicals and pollutants, and though regulated, some still do not have proper waste management systems.
2. **Marine dumping**: is exactly what it sounds like, dumping garbage into the waters of the ocean. It might seem crazy, but household garbage is still collected and dumped into oceans by many countries worldwide.
3. **Sewage and wastewater**: harmful chemicals, bacteria and pathogens can be found in sewage and wastewater even when it's been treated. Each household's sewage and wastewater are released into the sea with fresh water. The pathogens and bacteria found in

that wastewater breed disease, and therefore are a cause of health-related issues in humans and animals alike.

4. ***Oil leaks and spills***: large oil spills and oil leaks, are a significant cause of water pollution while often accidental. Leaks and spills are usually caused by oil drilling operations in the ocean or ships transporting oil.
5. ***Agriculture***: to protect their crops from bacteria and insects, farmers often use chemicals and pesticides. When these substances seep into the groundwater, they can harm animals, plants and humans. Additionally, when it rains, the chemicals mix with rainwater, which then flows into rivers and streams that filter into the ocean, causing further water pollution.
6. ***Global warming***: rising temperatures due to global warming are a significant concern for water pollution. Global warming causes water temperatures to increase, which can kill water-dwelling animals. When large die-offs occur, it further pollutes the water supply, exacerbating the issue.
7. ***Radioactive waste***: radioactive waste from facilities that create nuclear energy can be highly hazardous to the environment and must be disposed of properly. This is because uranium, the element used to develop atomic energy, is highly toxic.

All our social and productive activities lead to the production of discharges that must necessarily be subjected to purification to be returned to the environment. The number of pollutants is greater than the self-purifying capacity of the land, seas, lakes and rivers. Several programs are planned to mitigate this issue and to protect the good status of water bodies.

In Italy, water protection and regulation of environmental discharges are currently included in Part III of **Legislative Decree 152/2006**, “*Testo Unico ambientale*”. This decree defines “**discharge**” as “*any introduction of wastewater carried out exclusively through a stable collection system that connects the wastewater production cycle with the receiving body (surface water, soil, subsoil and sewage system), regardless of their nature pollutant, also subjected to preventive purification treatment*” (**Repubblica Italiana, 2006**).

The regulation of discharges is contained in Art. 101, in which it is reported that all discharges are governed according to compliance with the quality objectives of the receiving water bodies and must in any case comply with the limit values set out in Annex 5 of Part III of Decree 152/2006. These acceptability limit values are indicated in a series of different tables, according to the type of discharge and the receptor waterbody:

- **Table 1**: emission limits for urban wastewater treatment plants;

- **Table 2:** emission limits for urban wastewater treatment plants in sensitive areas;
- **Table 3:** emission limits in surface water and sewer;
- **Table 3/A:** emission limits per unit of a product referred to specific production cycles;
- **Table 4:** emission limits for urban and industrial wastewater discharging on the ground;
- **Table 5:** substances for which less restrictive limits than those indicated in table 3 cannot be adopted, for discharge into surface water and for release into the sewer system, or in table 4 for release to the ground.

1.2 Wastewater: origin, classification, and characteristics

1.2.1 Definition of wastewater

The wastewater is defined as “*all those waters whose quality has been compromised by human action after their use in domestic, agricultural and industrial activities, thus becoming unsuitable for their direct use as they are contaminated by different types of dangerous organic and inorganic substances for public health and the natural environment*”. According to Legislative Decree 152/06 (Art. 74), wastewater is divided into four classes depending on its source of origin:

- **Domestic wastewater:** wastewater from residential settlements and services and deriving mainly from human metabolism and domestic activities;
- **Industrial wastewater:** any wastewater discharged from buildings or plants in which commercial or production activities take place, other than domestic wastewater and run-off rainwater;
- **Urban wastewater:** domestic wastewater or the mixture of domestic and industrial wastewater or run-off rainwater conveyed into sewer networks and coming from agglomerations;
- **Industrial wastewater similar to domestic:** wastewater from commercial or production installations which, by law or due to particular qualitative and quantitative requirements, can be considered domestic wastewater (Art. 101).

1.2.2 Wastewater composition: physical, chemical, and biological characteristics

Domestic sewage contains approximately 99.9% water. The remaining part includes organic and inorganic, suspended and dissolved solids, together with microorganisms. Because of this 0.1%, water pollution occurs and wastewater needs to be treated. The composition of wastewater is a function of the uses to which the water was submitted. These uses, and the form with which they were exercised, vary with climate, social and economic situation and population habits.

In designing a wastewater treatment plant (WWTP), there is usually no interest in determining various compounds that make up wastewater. This is due to the difficulty in undertaking the laboratory tests. The results themselves cannot be directly used as elements in design and operation (we will discuss later the organisation of a typical WWTP). Therefore, it is often preferable to utilise indirect parameters representing the character or the polluting potential of the wastewater in question. These parameters define the quality of the sewage and can be divided into three categories: *physical*, *chemical* and *biological* parameters (Von Sperling, 2007) (Fig. 1.1).

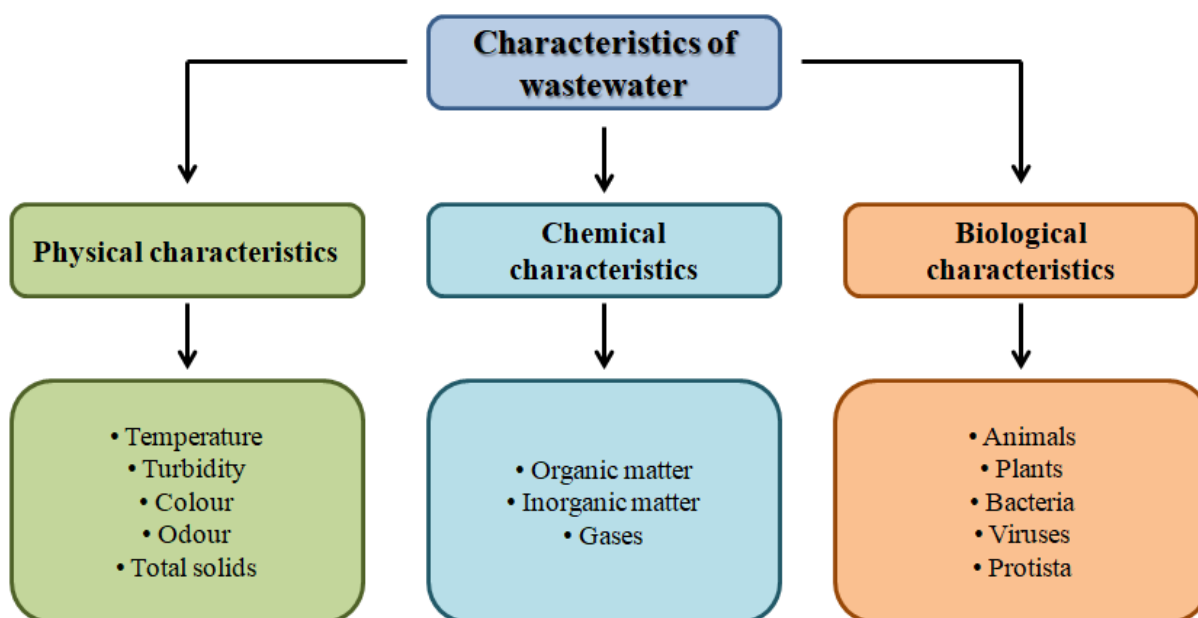


Fig. 1.1: Characteristics of wastewater.

1.2.2.1 *Physical parameters*

The physical characteristics identify the basic properties of wastewater and represent the first approach to characterisation. Some of these measurements must be performed *in situ* because transporting the sample to the laboratory can alter its values. The main physical characteristics are:

- **Temperature:** depends on the water temperature delivered to the sewer before entering the treatment plant. Civil and industrial uses may require hot water, subsequently conveyed to the sewer, with temperatures above environmental temperature. The temperature of wastewater influences microbial activity, the solubility of gases and viscosity of the liquid;
- **Colour:** an abnormal colour of wastewater indicates industrial discharges, and, in some cases, it can also persist after the purification treatment. The introduction of coloured water into the environment can alter the transparency of the water and the photosynthesis reactions. Thus the legislation provides that, when discharged, the wastewater must not be coloured. Colour is a parameter of particular interest because its immediate and straight forward detectability allows getting information on the nature of the phenomena in progress. Usually, a slight grey colouration indicates fresh sewage, while a dark grey or black colouration indicates septic sewage;
- **Odour:** common odours lingering in and around treatment plants smell like rotten eggs, ammonia, or garlic, among other things. Sometimes the scent is described as earthy or organic. Generally, foul odours at treatment plants originate from the anaerobic decomposition of organic compounds. A natural by-product of anaerobic digestion is hydrogen sulphide (H_2S), which gives off a strong, disgusting smell. Due to its low solubility in wastewater, is released into the atmosphere, producing an offensive odour. Amines and mercaptans are two other odour-causing offenders at treatment plants. These organic compounds contain sulphur or nitrogen, making odours that are detectable by the human nose at deficient concentrations;
- **Turbidity:** is an optical property that broadly describes the clarity or cloudiness of water. It is related to colour, but has more to do with the loss of transparency due to suspended particles and colloidal material. Suspended particles also contribute to the adhesion of many heavy metals and other toxic compounds. Turbidity is considered a measure of water quality: the more turbid the water, the lower quality.

- **Total solids (TS):** the term "total solids" refers to matter suspended or dissolved in water or wastewater and is related to both specific conductance and turbidity. Higher solids decrease the passage of light through water, thereby slowing photosynthesis by aquatic plants. Water will heat up more rapidly and hold more heat; this, in turn, might adversely affect aquatic life that has adapted to a lower temperature regime. Total solids are used for material left in a container after evaporation and drying of a water sample. Total Solids includes both **total suspended solids (TSS)**, the portion of total solids retained by a filter and **total dissolved solids (TDS)**, the amount that passes through a filter.

1.2.2.2 Chemical parameters

The chemical characteristics can be divided into organic matter, inorganic matter and gases.

- **Organic matter:** represent a heterogeneous mixture of various organic compounds; the main components are proteins, carbohydrates and lipids. Along with the proteins, carbohydrates, fats and oils, wastewater contains small quantities of many different synthetic organic molecules such as pharmaceutical, agricultural pesticides, hormones, and other organic pollutants. The most frequent parameters used to measure amounts of organic matter in wastewater are Biochemical Oxygen Demand (BOD), Chemical Oxygen Demand (COD), Total Organic Carbon (TOC).

✓ **Biochemical Oxygen Demand (BOD):** represents the quantity of oxygen per unit of volume (and, therefore, the concentration) required by aerobic microorganisms to assimilate and degrade the biodegradable organic matter present in the sewage. In this sense, BOD provides an indirect measure of the biodegradable organic matter present within the sewage and is typically expressed in mg/L of O₂. In general, biodegradation is the set of biochemical transformations of organic molecules mediated by aerobic microorganisms that need to take in free oxygen from the environment to explain their metabolic reactions. The greater the biodegradable organic substance, the greater the oxygen required by the aerobic microorganisms to assimilate and degrade it. The analysis of the BOD depends on three fundamental factors: time, temperature and light radiation. The quantity of oxygen that the microorganisms use to assimilate and degrade the biodegradable organic matter varies according to the time allowed for the biodegradation process. The longer the time, the greater the quantity of organic matter assimilated and degraded and,

therefore, the greater the amount of oxygen consumed by the microorganisms themselves. A characteristic value of the biochemical oxygen demand is BOD_5 , i.e. the oxygen consumption after five days (biochemical oxygen demand at five days);

- ✓ **Chemical Oxygen Demand (COD)**: represents the quantity of oxygen necessary to chemically oxidise the organic and inorganic substances (biodegradable and non-biodegradable) present in the sewage and is expressed in mg/L of O_2 . The chemical oxygen demand is a critical index proportional to the polluting content present in the wastewater. In practice, wastewater treatment plants are often sized based on COD, although the literature parameter used for these purposes is commonly BOD_5 . The measurement of COD is essential in industrial wastewater where BOD_5 is not easily determined or is significantly influenced by the contaminants present. However, for urban and domestic sewage, BOD_5 is commonly preferred;
- ✓ **Total Organic Carbon (TOC)**: is a test that allows measuring the organic carbon directly, and not indirectly, by determining the oxygen consumed, like the two tests above. This method measures the organic carbon existing in the wastewater by injecting a sample in the particular device in which the carbon is oxidised to carbon dioxide. Then carbon dioxide is measured and used to quantify the amount of organic matter. To guarantee that the carbon being measured is only the organic carbon, the inorganic forms like CO_2 and HCO_3^- already present in the sample must be removed before the analysis or be corrected when calculated.
- **Inorganic matter**: inorganic load in water results from discharges of treated and untreated wastewater, various geologic formations, and inorganic substances left in the water after evaporation. Many inorganic constituents found in natural waters are also found in sewage, and most of these constituents are added via human use. These inorganic constituents include nitrogen, phosphorus, sulphur, chlorides, pH, alkalinity, toxic inorganic compounds, and heavy metals.
 - ✓ **Nitrogen**: is present in wastewater in various forms, is an essential nutrient for microorganisms growth in biological wastewater treatment, and its determination is necessary for the sizing of the biological treatment phases needed for its removal (nitrification and denitrification), as well as the equipment that must provide the required oxygen for the treatment. Total nitrogen includes organic nitrogen ($N-N_{org}$), ammonia ($N-N_{amm}$), nitrites (NO_2^-) and nitrates (NO_3^-). Organic nitrogen and

ammonia together are called *Total Kjeldahl Nitrogen (TKN)*. **Organic nitrogen** is bound to proteins and other organic nitrogen compounds, and it is converted into ammonia nitrogen as a result of purification treatments. **Ammonia nitrogen** is the main form of nitrogen found in untreated wastewater. It must be nitrified and possibly denitrified in wastewater treatment plants to avoid negative impacts on aquatic environments. **Nitrous nitrogen ($N-NO_2^-$)** is the partially oxidised form of nitrogen before converting into **nitric nitrogen ($N-NO_3^-$)**, a more stable form of nitrogen. We will discuss more in detail nitrification/denitrification processes in chapter 6.

- ✓ **Phosphorus**: is an essential nutrient in biological wastewater treatment and exists in inorganic and organic forms. Phosphorus reduction is often needed to prevent eutrophication before discharging effluent into lakes, reservoirs, and estuaries. Phosphorus can be removed biologically in a process called enhanced biological phosphorus removal. In this process, specific bacteria, called **polyphosphate accumulating organisms (PAOs)**, are selectively enriched and get large quantities of phosphorus within their cells (up to 20% of their mass). When the biomass enriched in these bacteria is separated from the treated water, these biosolids have a high fertiliser value. Phosphorus removal can also be achieved by chemical precipitation by adding aluminium sulphate, ferric chloride or lime. This may lead to excessive sludge production as hydroxides precipitate, and the added chemicals are expensive.
- ✓ **Sulphur**: is perhaps the least understood element and one of the most critical factors of sewage disposal problems. It is generally the chief odour source, either in the sewerage system or the treatment plant. Sulphur in sewage as inorganic sulphate or combined in organic matter may be perfectly inodorous, but some time later, during treatment or flow through sewers, decomposition may set in and give rise to the odours of hydrogen sulphide. Not only are offensive odours given off, but the hydrogen sulphide in time attacks the sewers and maintenance holes above the waterline, thus causing severe damage to the collection system (**Mahlie, 1934**).
- ✓ **Chlorides**: are necessary for water habitats to thrive, yet high chloride levels adversely affect an ecosystem. Chloride may impact freshwater organisms and plants by altering reproduction rates, increasing species mortality, and changing the characteristics of the entire local ecosystem. In addition, as chloride filters down to the water table, it can stress plant respiration and change the quality of our drinking water (**University of Minnesota, 2013**);

- ✓ **pH**: strong acids and bases can alter the pH of a generic solvent. This, of course, also applies to the final receiver of a water discharge (watercourse, lake, sewage, etc.). This form of pollution requires careful monitoring, as the alterations that it produces can block the purification processes, cause corrosion and promote the toxicity of other contaminants. The pH of the environment has a profound effect on the rate of microbial growth involved in biological treatments because it affects the function of metabolic enzymes. Acidic conditions (low pH) or primary conditions (high pH) alter the enzyme's structure and stop growth. Most microorganisms do well within a pH range of 6.5 to 8.5. However, some enzyme systems can tolerate extreme pHs and thrive in acidic or basic environments. However, most bacteria and protozoa grow best in neutral (pH 7) environments. Abnormal or irregular pH in biological treatment processes can result in a significant decrease in the rate of removal of organic compounds from the environment, which will affect the biochemical oxygen demand (BOD) measurements.
- ✓ **Alkalinity**: is defined as the ability of water to neutralise acid to absorb hydrogen ions. It is the sum of all acid-neutralising bases in the water. In municipal and industrial wastewater, many factors contribute to alkalinity. Factors that contribute to alkalinity include the type of dissolved inorganic and organic compounds present in the water, the amount of suspended organic matter in the water, whether the water is strongly or weakly buffered, the presence or absence of free hydroxyl alkalinity, the amount of bicarbonate in the water, the bicarbonate to dissolved CO₂ ratio and is indirectly correlated to the number of dissolved solids in the water. One of the most common alkalis used to provide alkalinity in wastewater treatment is caustic soda. However, magnesium hydroxide has properties that make it a superior product in providing alkalinity to wastewater treatment systems (**Martin Marietta Magnesia Specialities, 2015**);
- ✓ **Toxic inorganic compounds**: copper, lead, silver, arsenic, boron, and chromium are classified as priority pollutants and are harmful to microorganisms. Thus, they must be considered in the design and operation of a biological treatment process. When introduced into a treatment process, these contaminants can kill off the microorganisms needed for treatment and thus stop the treatment process;
- ✓ **Heavy metals**: are significant toxicants found in industrial wastewater and may adversely affect the biological treatment of sewage. Heavy metals of chromium (Cr), iron (Fe), selenium (Se), vanadium (V), copper (Cu), cobalt (Co), nickel (Ni),

cadmium (Cd), mercury (Hg), arsenic (As), lead (Pb), and zinc (Zn) represent the primary toxic, hazardous materials to humans and other forms of life. Any of these metals in excessive quantities will interfere with beneficial water uses because of their toxicity. The uptake of heavy metals from wastewater is essential to eliminate their toxic impact and recover precious materials. Conventional methods for removing these pollutants from wastewater include chemical precipitation, ion exchangers, chemical oxidation/reduction, reverse osmosis, electrodialysis, and ultra-filtration (Alalwan et al., 2020).

- **Gases:** the most common gases found in untreated wastewater include nitrogen (N₂), oxygen (O₂), carbon dioxide (CO₂), hydrogen sulphide (H₂S), ammonia (NH₃) and methane (CH₄). The first three are gases of the atmosphere found in all waters exposed to air. The latter three are derived from the decomposition of the organic matter present in wastewater. Gases like chlorine (Cl₂) and ozone (O₃) (disinfection and odour control) and the oxides of sulphur and nitrogen (combustion processes) can be present in treated wastewater.

1.2.2.3 *Biological parameters*

The presence or absence of specific biological organisms - pathogens - is of primary importance to the water/wastewater quality. Pathogens are organisms capable of infecting or transmitting diseases in humans and animals. It should be pointed out that these organisms are not native to aquatic systems and usually require an animal host for growth and reproduction. They can, however, be transported by natural water systems. These waterborne pathogens include bacteria, viruses, protozoa, and parasitic worms (helminths).

1.3 **Wastewater treatment plants (WWTPs)**

Given the dangerousness of wastewater, they cannot be discharged as such into the environment but must necessarily undergo a series of treatments aimed at their purification and clarification. **Wastewater treatment** is defined as “*a process used to remove contaminants from wastewater and convert it into an effluent that can be returned to the water cycle. Once returned to the water cycle, the effluent creates an acceptable impact on the environment or is reused for various purposes (called water reclamation)*” (Ambulkar and Nathanson, 2021). The treatment process takes place in a **wastewater treatment plant (WWTP)**, often referred to as a Water Resource

Recovery Facility (WRRF) or a Sewage Treatment Plant (STP) and defined as “a facility in which a combination of various processes (e.g., physical, chemical and biological) are used to treat wastewater and remove pollutants” (Hreiz et al., 2015). Most traditional WWTPs are designed to control various substances, such as particulates, carbonaceous substances, nutrients and pathogens. While these substances can be efficiently and consistently eliminated, removing micropollutants is often insufficient. Evaluating the fate and removal of micropollutants during wastewater treatment is imperative optimisation of treatment to prevent the release of these potentially harmful micropollutants. Although there are different wastewater treatment plants, most will have the following steps: *preliminary* (physical and mechanical), *primary* (physicochemical and chemical), *secondary* (chemical and biological), rarely, *tertiary* (physical and chemical) treatments (Fig. 1.2). Preliminary and primary treatments aim to eliminate above all suspended substances and is carried out by mechanical means (screening, homogenisation, primary sedimentation, etc.); for the industrial waste, it may also be necessary to use chemical-physical systems such as chemical coagulation followed by sedimentation. Secondary treatment is typically based on biological processes in which microorganisms degrade the organic and nitrogenous substances present in the wastewater. The tertiary treatment is generally based on sand filtration, activated carbon filtration, and disinfection techniques. Especially in the primary and secondary treatments, considerable quantities of sludge are formed, which must be eliminated without danger of further pollution; therefore, this sludge is subjected to other treatments such as thickening and drying.

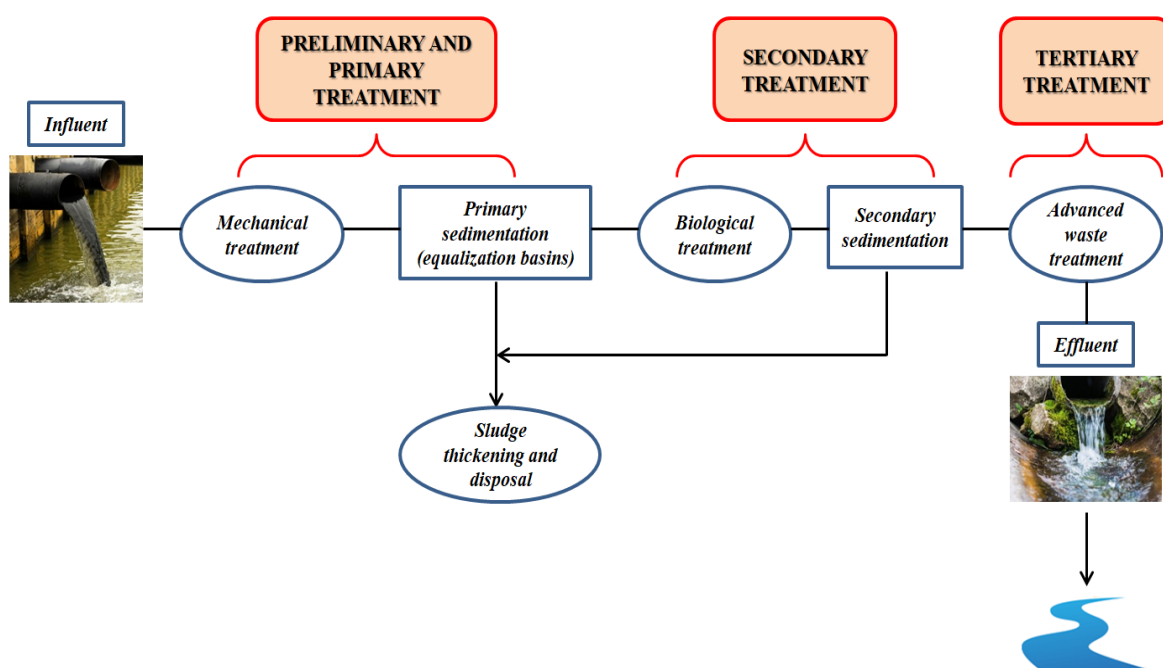


Fig. 1.2: Typical composition of a wastewater treatment plant (WWTP).

1.3.1 Preliminary treatment

The purpose of *preliminary treatment* is to protect plant equipment (e.g. pumps and valves) by removing untreatable solids that first enter a wastewater treatment plant from the sewer. Initial treatment may include many different processes; each is designed to remove a specific material that poses a potential problem for the treatment process. Methods include *screening*, *shredding*, *grit removal*, *chemical addition* and *flow equalisation*.

- **Screening**: removing floatable or suspended coarse solids in raw wastewater, including rags, paper, plastic, rubber, and vegetable matter. *Bar screens* are the most commonly used screening devices, which trap debris as wastewater influent passes through. Typically, a bar screen consists of parallel, evenly spaced (spacing between 15 to 25 mm) bars or a perforated screen placed in a channel. The waste stream passes through the screen, and large solids (screenings) are trapped on the bars for removal;
- **Shredding**: usually is used as an alternative to screening to reduce solids to a size that can enter the plant without causing mechanical problems or clogging. Shredding processes include comminution and barminution devices. The *comminutor* is the most common shredding device used in wastewater treatment. All of the wastewater flow passes through the grinder assembly in this device. The grinder consists of a screen or slotted basket, a rotating or oscillating cutter, and a stationary cutter. Solids pass through the screen and are chopped or shredded between the two sedges. The *barminutor* uses a bar screen to collect solids, which are then sliced and passed through the bar screen for removal at a later process. The cutter alignment and sharpness of each device are critical factors in practical operation. Solids that are not shredded must be removed daily, stored in closed containers, and disposed of by burial or incineration;
- **Grit removal**: is used to remove the heavy inorganic solids that could cause excessive mechanical wear. Grit is heavier than inorganic solids and includes sand, gravel, clay, eggshells, coffee grounds, metal filings, seeds, and similar materials. Several processes or devices are used for grit removal. The functions are based on the fact that grit is heavier than the organic solids that should be kept in suspension for treatment in the following procedures. Grit removal may be accomplished in grit chambers or by the centrifugal separation of sludge. Methods use gravity/velocity, aeration, or centrifugal force to separate the solids from the wastewater. Gravity/velocity-controlled grit removal is usually

accomplished in a channel or tank where the speed or velocity of the wastewater is controlled, so the grit will settle while the organic matter remains suspended;

- **Chemical addition:** is made to the waste stream to improve settling, reduce odours, neutralise acids or bases, reduce corrosion, reduce BOD₅, improve solids and grease removal, reduce loading on the plant, add or remove nutrients, add organisms, or aid subsequent downstream processes. The particular chemical and amount used to depend on the desired result. Chemicals must be added at a point where sufficient mixing will occur to obtain maximum benefit. Chemicals typically used in wastewater treatment include chlorine, peroxide, acids and bases, mineral salts (e.g., ferric chloride, alum), and bio-additives and enzymes;
- **Flow equalisation:** is used to reduce or remove the wide swings in flow rates usually associated with wastewater treatment plant loading; it minimises the impact of storm flows. Usually, the *equalisation basins* are designed to prevent discharges above the maximum plant design hydraulic capacity, reduce the magnitude of diurnal flow variations, and eliminate flow variations. Flow equalisation is accomplished using mixing or aeration equipment, pumps, and flow measurement. Equalised flows allow the plant to perform at optimum levels by providing stable hydraulic and organic loading.

1.3.2 Primary treatment

The purpose of **primary treatment** (primary sedimentation or primary clarification) is to remove settleable organic and floatable solids that pass through screens and grit chambers from the sewage in specific tanks called *sedimentation tanks*. These tanks are large basins where primary settling is achieved under relatively quiescent conditions. Within these basins, mechanical scrapers collect the primarily settled solids into a hopper, from which they are pumped to a sludge processing area. In contrast, suspended solids like oil, grease, and other floating materials (scum) are skimmed from the surface. Solids heavier than water settle to the bottom, while solids lighter than water float to the top. Settled solids are removed as sludge, and floating solids are removed as scum. Wastewater leaves the sedimentation tank over an effluent weir and moves on to the next step of the treatment. Factors affecting primary clarifier performance include flow rate through the clarifier and wastewater characteristics (strength, temperature, amount and type of industrial waste, and the density, size, and shapes of particles). The main features of primary treatment are listed below:

- Reduction of the organic loading on downstream treatment processes by removing a large amount of settleable, suspended, and floatable materials;
- Reduction of the velocity of the wastewater through a clarifier, so settling and flotation can take place. Slowing the flow enhances the removal of suspended solids in wastewater;
- Elimination of floated grease and scum, as well as the settled sludge solids, and collecting them for pumped transfer to disposal or further treatment;
- Clarifiers may be rectangular or circular. In *rectangular clarifiers*, wastewater flows from one end to the other. The settled sludge is moved to a hopper at the one end, either by flights set on parallel chains or by a single bottom scraper set on a travelling bridge. A surface skimmer collects floating material (mostly grease and oil). In *circular clarifiers*, the wastewater usually enters the middle and flows outward. Settled sludge is pushed to a hopper in the middle of the tank bottom, and a surface skimmer removes floating material.

Upon completion of screening, de-gritting, and settling in sedimentation basins, large debris, grit, and many settleable materials have been removed from the waste stream. What is left is referred to as *primary effluent*. Usually grey, primary effluent still contains large amounts of dissolved food and other chemicals (nutrients) treated in the secondary treatment. Two of the essential nutrients left to remove are phosphorus and ammonia. Excessive removal of these compounds from the waste stream is unnecessary because microorganisms in secondary treatment (biological treatment) require phosphorus and ammonia to explain their activities.

1.3.3 *Secondary treatment*

Secondary treatment is designed to substantially degrade the sewage's biological content derived from human waste, food waste, soaps and detergent. These processes use microorganisms to remove contaminants from wastewater biologically and can be aerobic or anaerobic (each utilises a different bacterial community). However, coupled anaerobic-aerobic processes may also be employed under certain circumstances. Most municipal WWTPs use aerobic biological processes as a secondary treatment step. To be effective, the biota requires both oxygen and nutrients to live. The bacteria and protozoa consume biodegradable soluble organic contaminants (e.g. sugars, fats, organic short-chain carbon molecules) and bind much of the less soluble fractions into floc. Due to the production of suspended solid material, all biological processes must include a step to remove them (e.g., settling tank, filter). Secondary treatment processes can be separated into two large categories: *fixed-film systems* and *suspended-*

growth systems. Fixed-film systems are processes that use a biological growth (biomass or slime) attached to some form of media (for example, stone, redwood, synthetic materials, any other durable substance). Wastewater passes over or around the media and the dirt. When the wastewater and dirt are in contact, the organisms remove and oxidise the organic solids. The media provides a large area for slime growth that can be an open space for ventilation and is not toxic to the organisms in the biomass. Fixed-film devices include trickling filters and rotating biological contactors. *Suspended-growth systems* are processes based on biological growth mixed with wastewater. Typical suspended-growth systems consist of various modifications of the activated sludge process. The **activated sludge** process is most commonly used for secondary wastewater treatment. As a suspended-growth biological treatment process, activated sludge utilises a dense microbial culture in suspension to biodegrade organic material under aerobic conditions and form a biological floc for solid separation in the settling units. Diffused or mechanical aeration maintains the aerobic environment in the reactor (Stott, 2003). The activated sludge process follows primary settling. The essential components of an activated sludge sewage treatment system include an *aeration tank* and a *secondary basin, settling basin, or clarifier*. Primary effluent is mixed with settled solids recycled from the secondary clarifier and introduced into the aeration tank. Compressed air is injected continuously into the mixture through porous diffusers located at the bottom of the tank, usually along one side. Wastewater is constantly fed into an aerated tank, where the microorganisms metabolise and biologically flocculate the organics. Microorganisms (activated sludge) are settled from the aerated mixed liquor under quiescent conditions in the final clarifier and are returned to the aeration tank. Left uncontrolled, the number of organisms would eventually become too great; therefore, some must periodically be removed (wasted). A portion of the concentrated solids from the bottom of the settling tank must be removed from the process. The clear supernatant from the final settling tank is the *plant effluent* (Spellman, 2013). Several factors affect the performance of an activated sludge system. These include *temperature, amount of oxygen available, amount of organic matter available, pH* (ideal in the range 6.0 - 8.0), *aeration time* and *wastewater toxicity*. To obtain the desired level of performance in an activated sludge system, a proper balance must be maintained among the amounts of food (organic matter), organisms (activated sludge), and oxygen (dissolved oxygen).

1.3.4 Tertiary treatment

Tertiary treatment is the final cleaning process that improves wastewater quality before it is reused, recycled or discharged to the environment. Tertiary treatment of effluent involves additional steps after secondary treatment to further reduce organics, turbidity, nitrogen, phosphorus, metals, and pathogens. Most processes involve physicochemical treatment such as coagulation, filtration, activated carbon adsorption of organics, reverse osmosis, and additional disinfection. Tertiary wastewater treatment is practised for additional wildlife protection after discharge into rivers or lakes. It may take several different treatments depending on the quality of the final effluent required. Even more commonly, it is performed when the wastewater is to be reused for irrigation (e.g., food crops, golf courses), for recreational purposes (e.g., lakes, estuaries), or drinking water (Gerba and Pepper, 2019). Following processes have been studied (Van der Graaf et al., 2005):

- **Media filtration (MedFil)**: is the process used for removal of particles by filtration through media consisting of sand or anthracite;
- **Surface filtration (SurFil)**: is mainly concerned with retaining particles on the surface. The particles had to form a layer of material, commonly called the “cake layer”, to increase filtration efficiency. If the rate of filtration initially is around 50-60%, then after the layer of cake is formed, it grows to 100%;
- **Membrane filtration (MemFil)**: is applied to remove particles and other components bypassing the liquid through a membrane; pore sizes of the membrane can differ widely, giving various results (microfiltration, ultrafiltration, nanofiltration, reverse osmosis);
- **Adsorption**: is a surface phenomenon with the standard mechanism for organic and inorganic pollutants removal. When a solution containing absorbable solute comes into contact with a solid with a highly porous surface structure, liquid-solid intermolecular forces of attraction cause some solute molecules from the solution to be concentrated or deposited at the solid surface. The solute retained (on the solid surface) in adsorption processes is called *adsorbate*, whereas the solid on which it is contained is called an *adsorbent*. This surface accumulation of adsorbate on adsorbent is called *adsorption*. This creation of an adsorbed phase having a composition different from that of the bulk fluid phase forms the basis of separation by adsorption technology (Rashed, 2013);
- **Air stripping**: is a process by which wastewater is brought into intimate contact with a gas, usually air, so that some undesirable volatile substances present in the liquid phase can be

released and carried away by the gas. Processes such as mechanical surface aeration, diffused aeration, spray fountains, spray or tray towers, and the term *air stripping* encompasses countercurrent packed towers. These procedures produce a condition in which a large surface area of the water to be treated is exposed to air, promoting the contaminant's transfer from the liquid phase to the gaseous phase. This process is mainly applied for the removal of ammonia (**Srinivasan et al., 2009**);

- ***Ion exchange***: is a process in which ions replace ions of a particular species in solution with a similar charge but of different species attached to an insoluble resin. In essence, ion exchange is a sorption process and can also be considered a reversible chemical reaction. The typical ion exchange applications are *water softening* (removing "hardness" ions such as Ca^{2+} and Mg^{2+}) and nitrate removal in advanced wastewater treatment operations. These ion exchange resins naturally occur inorganic zeolites or synthetically produced organic resins. Synthetic organic resins are the predominant type used today because their characteristics can be tailored to specific applications. An organic ion exchange resin consists of an organic or inorganic network structure with attached functional groups that exchange their mobile ions for ions of similar charge from the surrounding medium. Each resin has many mobile ion sites that set the maximum quantity of exchanges per resin unit. Ion exchange resins are called cationic if they exchange positive ions and anionic if they exchange negative ions (**Climate Policy Watcher, 2021**);
- ***Disinfection***: is the primary process used to remove bacteria and viruses by chemical oxidation (chloride, ozone), UV or membrane filtration. Undisinfected wastewater effluents represent a potentially important source of pathogenic microorganisms in the environment and a possible vector for disease transmission among human populations. Although bacterial pathogens are present in wastewater effluents, it is generally believed that enteric viruses represent the most significant risk to human health of all waterborne pathogens. Most wastewater disinfection operations have used chlorine as the disinfectant. Chlorine is known to be effective for the inactivation of common bacterial indicator organisms; however, several essential drawbacks to chlorine-based disinfection have been identified, including its relative ineffectiveness against some microbial pathogens and repair or regrowth of pathogens post-disinfection. UV irradiation, a broad-spectrum antimicrobial agent, is widely recognised as an alternative to chlorination/dechlorination for disinfection of municipal wastewater (**Blatchley et al., 2007**);
- ***Advanced oxidation processes (AOPs)***: are the technologies that generally use the hydroxyl radicals, the ultimate oxidant for the remediation of organic contaminants in

wastewater. These are highly effective novel methods speeding up the oxidation process. AOP can combine with ozone (O₃), catalyst, or ultraviolet (UV) or solar irradiation to offer a powerful treatment of wastewater (**Ghime and Ghosh, 2020**).

As said above, most of the traditional WWTPs are designed to control a wide range of substances, such as particulates, carbonaceous substances, nutrients and pathogens. While these substances can be efficiently and consistently eliminated, removing micropollutants is often insufficient. Wastewater effluents are the primary source of micropollutants in the environment. These recalcitrant compounds escaping from wastewater treatment plants (WWTPs) are called *emerging contaminants (ECs)*.

1.4 Emerging contaminants (ECs)

Industries, agriculture, and the general population use water daily and release many compounds in wastewaters. Indeed, agriculture practices, industrial discharges and human beings play an essential role in the issue of pollutants in wastewater. These practices have generated various pollutants and altered the water cycle causing a global concern linked to their eventual impact on wildlife and human health (**Deblonde et al., 2011**). For more than 20 years, many articles have reported the presence of new compounds, called “*emerging contaminants*”, in wastewater and aquatic environments (**Rosal et al., 2010; Vogelsang et al., 2006**). Emerging contaminants (ECs) are defined as *synthetic or naturally occurring chemicals that are not commonly monitored in the environment but have the potential to enter the environment and cause known or suspected adverse ecological and (or) human health effects*. Nowadays, more than 700 emerging contaminants, their metabolites and transformation products are listed as present in the European aquatic environment (www.norman-network.net). ECs are currently not included in (inter)national routine monitoring programmes, and their fate, behaviour and ecotoxicological effects are often not well understood. They can be released from point pollution sources, e.g. wastewater treatment plants from urban or industrial areas, diffuse sources through atmospheric deposition, or crop and animal production. ECs are categorised into more than 20 classes related to their origin (<http://www.norman-network.net>). The prominent classes are surfactants, antibiotics and other pharmaceuticals, steroid hormones and endocrine-disrupting compounds (EDCs), fire retardants, sunscreens, disinfection byproducts, new pesticides and pesticide metabolites (**Fig. 1.3**). In light of the potential impact of these substances on aquatic life and human health, the lack of knowledge regarding their behaviour in the environment and the

deficiency in analytical and sampling techniques, action is urgently required at multiple levels (Geissen et al., 2015).

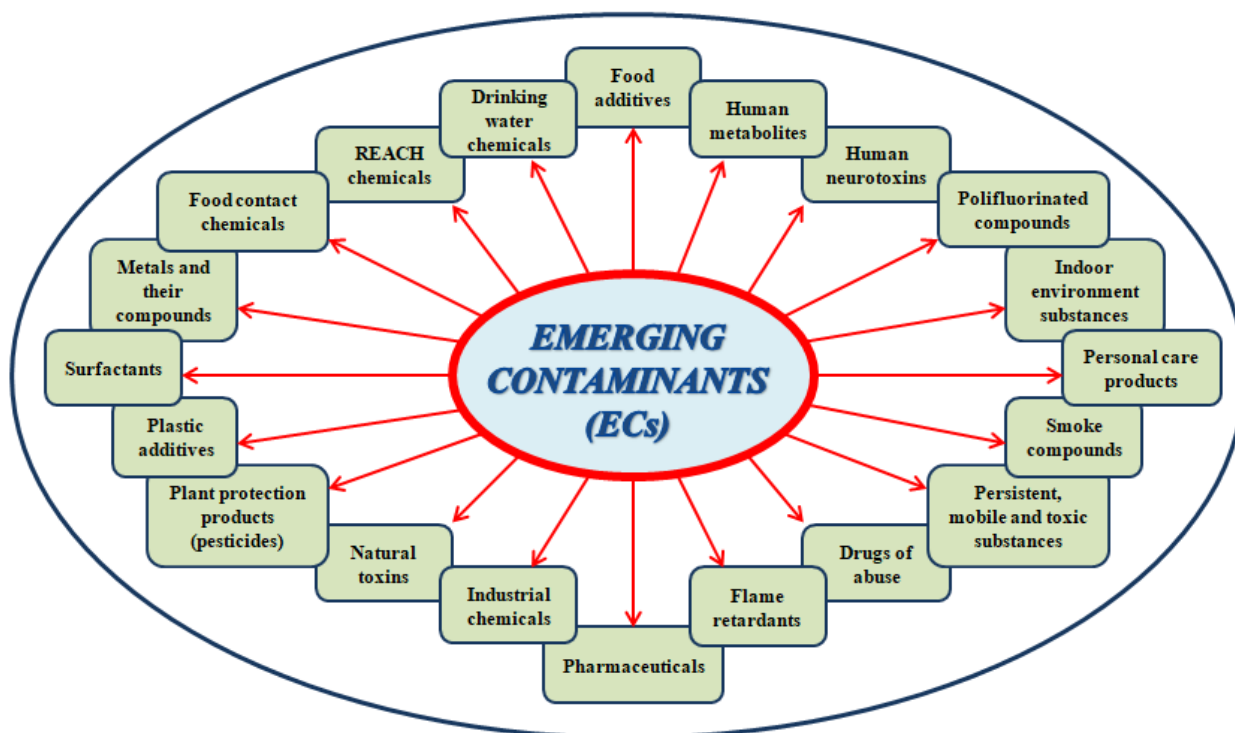


Fig. 1.3: Categories of emerging contaminants listed in the NORMAN substance database.

Current demographic trends, the rise of chronic diseases, the accessibility of inexpensive generic treatments, and the emergence of “lifestyle” drugs have been the key to increased pharmaceutical medicine use worldwide. These *pharmaceuticals* are now the group of emerging contaminants with rising concern in the scientific world due to their presence in surface water, such as lake and river, groundwater, soil, and even drinking water and their associated impact on invertebrates, vertebrates, and ecosystem structure and function. The two main routes of their spread in the environment are (1) when taken drugs are excreted in faeces and urine and (2) when unused drugs are thrown down. Research undertaken has found that 60–80% of these pharmaceutical medicines are flushed down the toilet or dumped as regular household waste that ends up in sewage treatment plants, which are generally not designed to remove such pollutants from wastewater (Chhaya et al., 2020).

1.5 Occurrence of pharmaceuticals in wastewater

In the last decade, traces of pharmaceuticals, typically at range levels of nanograms to micrograms per litre have been reported in the water bodies, including surface waters, wastewater, groundwater and, to a lesser extent, drinking water.

Advances in analytical technology have been a key factor driving their increased detection. Even at these very low concentrations, scarce water has raised concerns among stakeholders, such as drinking water regulators, governments, water suppliers, and the public, regarding the potential risks to human health from exposure to traces of pharmaceuticals via drinking-water (**World Health Organization, 2012**). Pharmaceuticals and their metabolites can reach water bodies through sewage systems, industrial discharges, effluents from sewage treatment facilities, aquaculture and livestock farming (**Bottoni and Fidente, 2005**).

Pharmaceuticals include many very different substances regarding their chemical and physical properties and environmental behaviour, although they may have potent biochemical activity. Nevertheless, their presence in the aquatic environment and their impact on aquatic biota and human health have not been adequately studied. There is some experimental evidence that pharmaceuticals may cause harmful effects such as morphological and metabolic alterations on aquatic species and induction of antibiotic resistance in aquatic pathogenic bacteria (**Bottoni et al., 2010**).

Pharmaceutical compounds are designed to have a specific mode of action, and many are persistent in the body. However, many pharmaceuticals transform in the human body, resulting in the release of their metabolites into the aquatic environment. They have been detected in low concentrations in many countries in many environmental samples, for example, sewage-treatment-plant effluents, surface water, seawater, and groundwater (**Nikolaou et al., 2007**). Prolonged exposure over time of these substances, at low concentrations, can cause:

- Allergies;
- Development of antibiotic resistance (antibiotics);
- Effects of the endocrine system (hormone-acting drugs);
- Cytolytic or cytostatic effects (antitumoral drugs).

The main categories of human pharmaceuticals and the most commonly used products include *non-steroidal anti-inflammatory drugs (NSAID)*, *beta-blockers*, *lipid regulators*, *steroids and related hormones*, *antibiotics*, as shown in **Fig. 1.4**.

- **Non-steroidal anti-inflammatory drugs (NSAID):** are the most frequently and ubiquitously environmentally detected drugs of various chemical structures with anti-inflammatory, antipyretic and analgesic effects. Pharmaceuticals from the NSAID group are of a diverse and complex chemical nature. They include derivatives of indoleacetic (indomethacin, sulindac, etodolac), phenylacetic (diclofenac), propionic (ibuprofen, naproxen, flurbiprofen, ketoprofen) acids, salicylates (acetylsalicylic acid), pyrazolidines (metamizole), oxicams (meloxicam), alkanones (nabumetone), and sulfonamide derivatives (nimesulide). NSAID molecules have high reactivity and stability with the reactive groups (particularly hydroxyl amide). This determines their resistance to biodegradation, ecotoxicity, persistence and therefore threat to the environment (**Tyumina et al., 2020**);
- **Beta-blockers:** are a class of medications that are predominantly used to manage abnormal heart rhythms and protect the heart from a second heart attack (myocardial infarction) after a first heart attack (secondary prevention). They are also widely used to treat high blood pressure (hypertension), although they are no longer the first choice for the initial treatment of most patients. The most frequently identified in wastewater are atenolol, metoprolol, propranolol, sotalol. These compounds were also found in surface waters in $\text{ng}\cdot\text{L}^{-1}$ to low $\mu\text{g}\cdot\text{L}^{-1}$ due to the incomplete removal during wastewater treatment (**Gros et al., 2010**); the ecotoxicity of some beta-blockers have been analysed with various phytoplankton, zooplankton and fish species. The results obtained indicate the detection of acute toxicity towards phytoplankton and zooplankton species (*Synechococcus leopolensis* and *Daphnia magna*), in particular, due to the activity of propranolol (**Huggett et al., 2001; Stanley et al., 2006**). Sub-chronic effects of propranolol and metoprolol have also been documented in the growth, reproduction and physiology of *D. magna*, showing a higher toxic action in the case of propranolol (**Hernando et al., 2007**);
- **Lipid regulators:** are used to treat dyslipidemias, cardiovascular problems, osteoporosis and post-menopause complications. This is why these lipid regulators come under the class of most prescribed medications. Clofibric acid, due to its environmental persistence and refractory, is one of the most widely and routinely reported drug metabolites found in open waters (**Salgado et al., 2012**). Other lipid regulators commonly prescribed and found in wastewater are gemfibrozil, bezafibrate and fenofibrate. **Rosal et al. (2009)** reported the ecotoxicity of all lipid regulators on *Vibrio fischeri*, *Daphnia magna*, and *Anabaena CPB4337* as a novel and more sensitive bioassay. The results obtained showed that the toxicity of fenofibric acid was exceptionally high for *V.fischeri* and reclassification of

bezafibrate and clofibric acid from “non-toxic” to “harmful to aquatic organisms”, thanks to the greater sensitivity of the novel *Anabena* bioassay;

- ***Steroids and related hormones***: are a group of hormones derived from cholesterol that act as chemical messengers in the body and regulate many physiologic processes, including the development and function of the reproductive system (**Whirledge and Cidlowski, 2019**). Steroid hormones are ubiquitous in aquatic environments at trace concentrations ranging from a few $\text{ng}\cdot\text{L}^{-1}$ to $\mu\text{g}\cdot\text{L}^{-1}$ (**Fent, 2015**). Several studies have confirmed the adverse effects of steroid hormones on aquatic organisms, such as sexual disorders, feminisation, masculinisation and infertility (**Yarahmadi et al., 2018**). 17β -Estradiol and 17α -Ethinylestradiol are the steroids most frequently identified in the environment due to their vast consumption (**Vallejo-Rodríguez et al., 2017**);
- ***Antibiotics***: are a type of antimicrobial substance active against bacteria. They are the most important antibacterial agents for fighting bacterial infections, and antibiotic medications are widely used to treat and prevent such diseases. We will discuss more in detail about antibiotics in the next section.

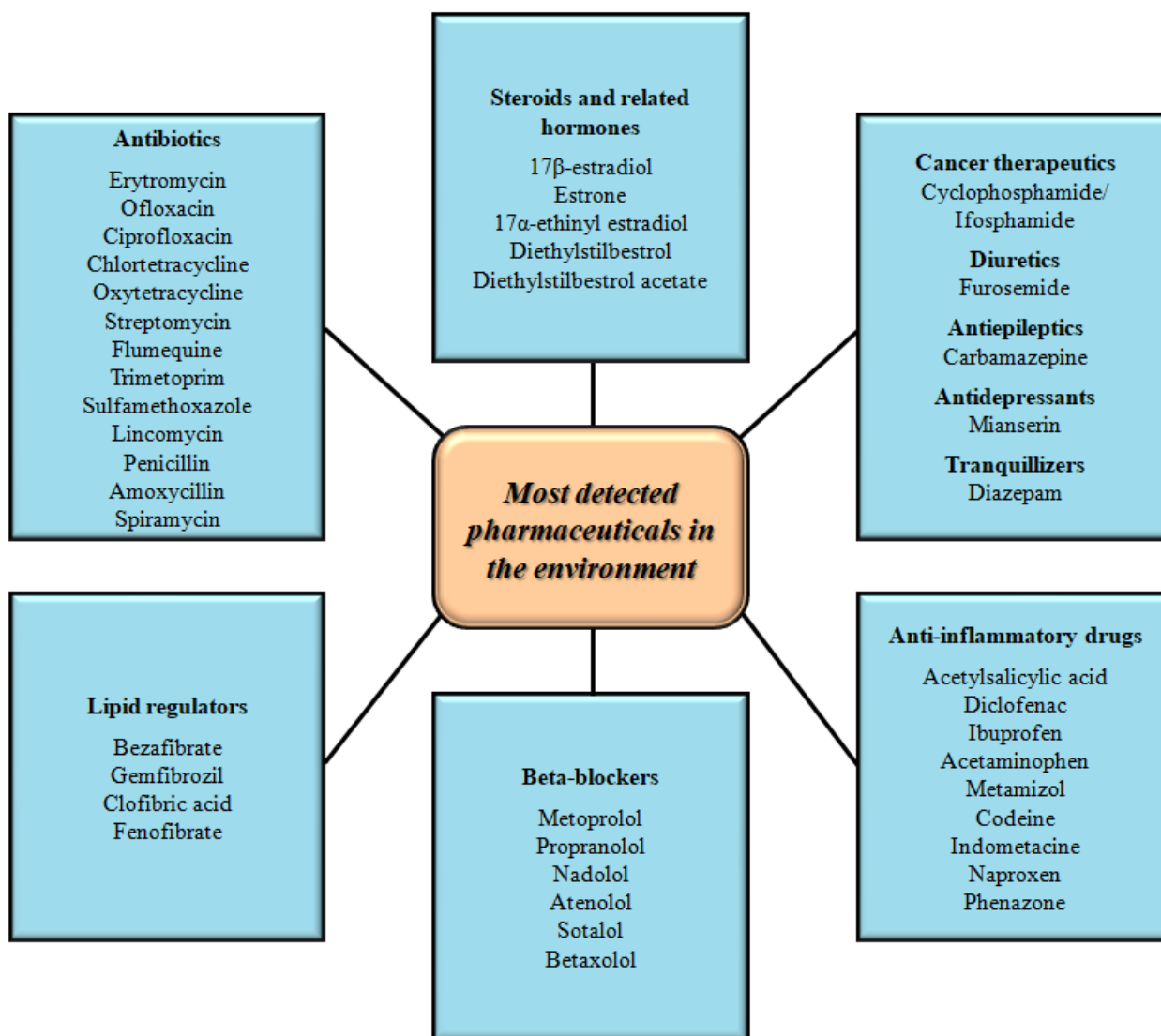


Fig. 1.4: Main categories of human pharmaceuticals detected in the environment (Nikolaou et al., 2007).

1.6 Occurrence of antibacterial compounds in the environment and antibacterial resistance

The category of drugs on which the scientific community's attention is most focused is that of antibiotics present in the aquatic environment and foods, about the possibility of inducing the formation of antibiotic-resistant bacteria and the health risks that may arise. In addition, many drugs can exert their inhibitory effect against degrading microorganisms present in water purification plants (activated sludge), thus compromising the quality of the water product that comes out (Nzila et al., 2016).

In fact, among the most prescribed pharmaceuticals, there are general antimicrobials for systemic use (classified according to the anatomical therapeutic and chemical classification system with the ATC code J01) which include different classes of compounds: J01A tetracyclines; J01B

amphenicols; J01C beta-lactam antibacterials and penicillins; J01D other beta-lactam antibacterials; J01E sulfonamides and trimethoprim; J01F macrolides, lincosamides and streptogramins; J01G aminoglycoside antibacterials; J01M quinolone antibacterials.

The generic term “*antibiotic*” denotes any class of organic molecule that inhibits or kills microbes by specific interactions with bacterial targets, without considering the source of the particular compound or class (**Davies and Davies, 2010**). Because of the intensive use of antibiotics for human (domestic and hospital use), veterinary and agricultural purposes, these compounds are continuously released into the environment from anthropogenic sources, such as urban wastewater treatment plants, which are considered as one of the leading “hotspots” of potential evolution and spreading of antibiotic resistance into the environment. The presence of antibiotics in environmentally relevant concentration levels has been associated with chronic toxicity and the prevalence of resistance to antibiotics in bacterial species (**Michael et al., 2013**). Worldwide, antimicrobial resistance is increasing at an alarming rate: in 2019, WHO listed antimicrobial resistance as one of the top ten threats to global health (**Scheres and Kuszewski, 2019**). A primary driver of antimicrobial resistance is antibiotic overuse and misuse. For example, in 2000-2015, global antibiotic use in humans increased by 65% from 21.1 billion defined daily doses (DDD) in 2000 to 34.8 billion DDDs in 2015 (**Klein et al., 2018**). The rate of antibiotic consumption also increased during this period, from 11.3 DDDs per 1000 inhabitants per day to 15.7 DDDs per 1000 inhabitants per day (an increase of 39%). The researchers estimated that if all countries continue to increase their antibiotic consumption rates at their compounded annual growth rates and do so with no policy changes, the total consumption will increase by 202% to 128 billion DDDs by 2030, and the antibiotic consumption rate will increase by 161% to 41.1 DDDs per 1000 inhabitants per day. Therefore, reducing global consumption and increasing global surveillance is critical to reducing the threat of antibiotic resistance (**The Pharmaceutical Journal, 2018**).

Moreover, in 2020/2021, the world was faced with a pandemic linked to the spread of the SARS-COV-2 virus, responsible for the disease that we all know as COVID-19, and in this period, a lot of antibiotics have been prescribed. During the first wave, it was observed that most patients admitted with COVID-19 had been prescribed antibiotics, including broad-spectrum antibiotics in a percentage of cases. The first meta-analyses conducted in China in 2020 (**Langford et al., 2020**) showed that despite the prevalence of bacterial co-infections being less than 4%, the prescription of antibiotics exceeded 70%, mainly with broad-spectrum molecules, and in particular, fluoroquinolones and third-generation cephalosporins. In Europe, the drug prescription rises to 78% and focuses on 3rd generation cephalosporins, macrolides and

penicillins (Moretto et al., 2021). A meta-analysis from 2021 (Langford et al., 2021), in addition to confirming the use of antibiotics in 78% of cases (with a prevalence of co-infection at 9%) on a sample of over 30000 patients, highlighted a considerable heterogeneity in antibiotic prescribing, with lower values at European level than in the Asian and American continent and a different distribution among the countries of the various classes of antibiotics: in Europe, the use of macrolides and beta-lactams (in particular of the cephalosporin subclass) prevails, while in China the most used class was that of fluoroquinolones; the United States, on the other hand, has a more varied distribution of all types of drugs. The increase in the use of these molecules was also highlighted by AIFA in the report released in July 2020, where azithromycin showed a rise of almost 200% from the pre-COVID period with considerable variability between regions (D'Arienzo and Carmignani, 2021). As said above, one of the most feared secondary effects of inappropriate antibiotic use is increased microbial resistance. It is well known that the spread of multidrug-resistant bacteria is closely related to antibiotic exposure. Therefore, several groups have sounded the alarm and requested the intervention of antibiotic stewardship programs in these patients (Calderón-Parra et al., 2021).

Although the ideal antibiotic is toxic to bacteria without affecting humans/animals, the reality is more complicated, and directly toxic side effects are common for several classes of antibiotics at doses used for therapy (Larsson, 2014). A few relatively persistent antibiotics have been found in drinking water at very low $\text{ng}\cdot\text{L}^{-1}$ levels (Ye et al., 2007). Near manufacturing discharges, ground-water contamination has led to levels up to low $\mu\text{g}\cdot\text{L}^{-1}$ in drinking-water wells (Fick et al., 2009). The antibiotics most commonly found in the waters belong to tetracyclines, sulphonamides, macrolides, lincosamides and quinolones.

1.6.1 *Quinolones: discovery, mechanism of action and global consumption*

A quinolone antibiotic is a member of a large group of broad-spectrum bacteriocidal that share a bicyclic core structure related to the substance *4-quinolone*. The first quinolone, *nalidixic acid*, was discovered in 1962 as an impurity in the chemical manufacture of a batch of the antimalarial agent *chloroquine*. It demonstrated anti-Gram-negative antibacterial activity, with minor anti-Gram-positive activity but its potency and antimicrobial spectrum were not significant enough to be helpful in therapy. However, building on this lead, subsequently, nalidixic acid was commercialised (Mitscher, 2005). Since then, structural modifications have resulted in second-, third-, and fourth-generation quinolones, which have improved coverage of Gram-positive organisms. Quinolones rapidly inhibit DNA synthesis by promoting cleavage of bacterial DNA in the DNA-enzyme complexes of DNA gyrase and type IV topoisomerase, resulting in rapid

bacterial death. As a general rule, Gram-negative antibacterial activity correlates with inhibition of DNA gyrase, and Gram-positive antibacterial activity corresponds with inhibition of DNA type IV topoisomerase (**Oliphant and Green, 2002**).

The basic quinolone structure (**Fig. 1.5**) consists of a bicyclic aromatic core displaying the R1-substituted nitrogen at the 1 position, the ketone group at the C4 position, and a carboxylic group at the C3 position. The atom attached at the 8 position can be carbon, in the case of true quinolones, or nitrogen, in which case the structure formed is a naphthyridone. However, both structures are considered quinolone agents. The analogues have different substituents at the C2, C6, C7, or C8 positions. These structural differences modify their antibacterial activity, half-life, and toxicity (**Doña et al., 2018**).

Quinolones can be classified into four generations based on antimicrobial activity. First-generation agents used less often today include nalidixic acid and cinoxacin which have moderate gram-negative activity and minimal systemic distribution. Second-generation quinolones have expanded gram-negative activity and atypical pathogen coverage but limited gram-positive activity. These agents are most active against aerobic gram-negative bacilli. Ciprofloxacin remains the quinolone most active against *Pseudomonas aeruginosa*. Third-generation quinolones retain expanded gram-negative and atypical intracellular activity but have improved gram-positive coverage. Finally, fourth-generation agents improve gram-positive coverage, maintain gram-negative coverage, and gain anaerobic coverage (**Oliphant and Green, 2002**). The most popular quinolones are *fluoroquinolones (FQs)* (with a fluorine atom on C6) which include ciprofloxacin, lomefloxacin, norfloxacin, ofloxacin, moxifloxacin and levofloxacin (**Fig. 1.5**).

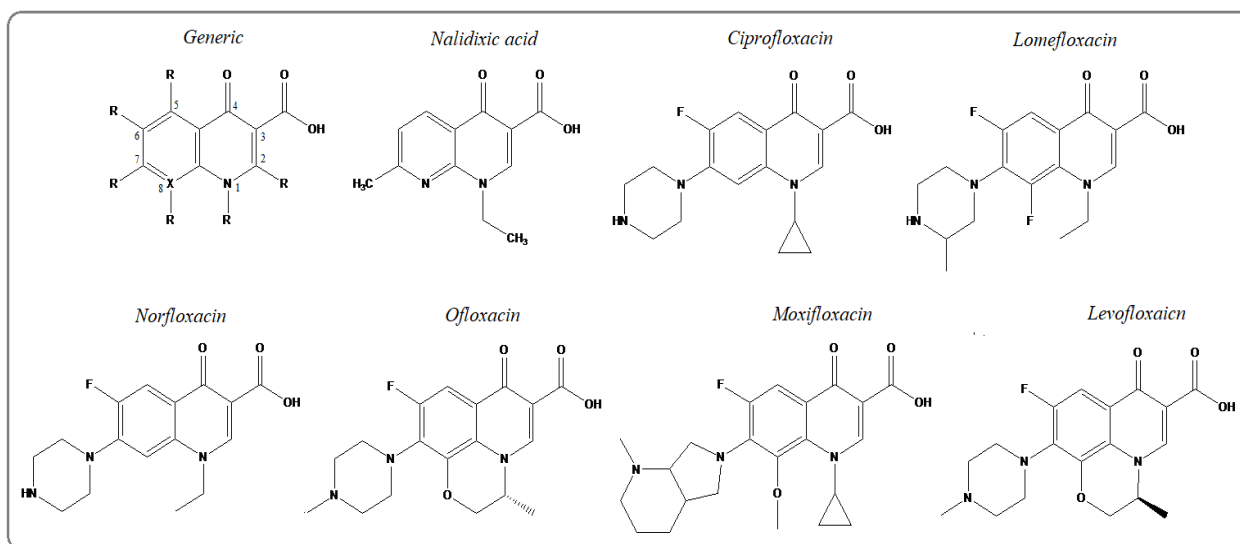


Fig. 1.5: Chemical structure of the main quinolones.

In 2017, in 28 EU/EEA countries, four substances accounted for 90% of quinolone consumption in the community expressed in DDD per 1000 inhabitants per day: ciprofloxacin (48.6% in 2017 compared with 50.8% in 2009), levofloxacin (28.8% in 2017 compared with 11.8% in 2009), norfloxacin (10.4% in 2017 compared with 18.2% in 2009) and moxifloxacin (7.2% in 2017 compared with 7.4% in 2009). First-generation quinolones (mostly norfloxacin) represented the most consumed quinolone subgroup in Croatia and represented >20% of quinolone consumption in the community in Estonia, Lithuania, Poland and Romania. Pipemidic acid was used in five countries. Among the other first-generation quinolones, nalidixic acid was only reported in Romania and flumequine was only used in France. Second-generation quinolones were the most widely consumed quinolones in EU/EEA countries. Their consumption exceeded 50% (median 85%) of quinolone consumption in the community in all countries except Croatia. Ciprofloxacin was the most consumed second-generation quinolone in 24 countries; levofloxacin was the most consumed in Bulgaria, Cyprus, Hungary and Italy; and ofloxacin was the most consumed in France (**Adriaenssens et al., 2021**). However, ciprofloxacin remained the most consumed quinolone in most countries. Yet, an emerging trend to consume more levofloxacin and moxifloxacin, mainly in countries with a high quinolone consumption, should be noted.

Quinolones have attracted particular attention cause of the recent toxicity episodes found in some treated patients. Indeed, fluoroquinolone medicines (which contain ciprofloxacin, levofloxacin, lomefloxacin, moxifloxacin, norfloxacin, ofloxacin, pefloxacin, prulifloxacin and rufloxacin) can cause long-lasting, disabling, and potentially permanent side effects involving tendons, muscles, joints and the nervous system. These severe side effects include inflamed or torn tendons, muscle pain or weakness, joint pain or swelling, walking difficulty, feeling pins and needles, burning pain, tiredness, depression, problems with memory, sleeping, vision and hearing, and altered taste and smell. For these reasons, in April 2019, the EMA's Committee for medicinal products for human use (CHMP) endorsed the recommendations of EMA's safety committee (PRAC). It concluded that the marketing authorisation of medicines containing cinoxacin, flumequine, nalidixic acid, and pipemidic acid should be suspended. The CHMP confirmed that the use of the remaining fluoroquinolone antibiotics should be restricted. In addition, the prescribing information for healthcare professionals and information for patients will describe the disabling and potentially permanent side effects and advise patients to stop treatment with a fluoroquinolone antibiotic at the first sign of a side effect involving muscles, tendons or joints and the nervous system (**European Medicines Agency, 2018**).

As quinolone consumption should be restricted and mainly reserved for well-defined indications, the high consumption and seasonal variation of quinolones in the community observed in some

countries probably indicate non-adherence to prescribing guidelines. From a public health perspective, this is an important consideration, as excessive and inappropriate use of quinolones is associated with the development of quinolone resistance, requires more resources and exposes patients to the additional risk of side effects. All quinolones are listed as Watch group antibiotics in the 2019 WHO Access, Watch or Reserve (AWaRe) classification list (**World Health Organization, 2019**). The continuous monitoring of quinolone consumption in the community can help assess the impact of future interventions promoting better use of these antibiotics.

Administered fluoroquinolones are primarily excreted as unchanged compounds in urine and consequently discharged into hospital or municipal sewage (**Fink et al., 2012; Pena et al., 2007**). These fluoroquinolones are not entirely removed at WWTPs, and consequently, their continuous introduction into the environment makes fluoroquinolones ‘pseudo-persistent’ compounds (**Frade et al., 2014**). The excellent chemical stability of the heterocyclic ring makes these drugs highly persistent (to thermal decomposition, hydrolysis and biodegradation) widespread in the environment, with possible insertion into the food chain through plants. Biosolids, animal manure, antibiotic manufacturing, and WWTP effluents contaminated with fluoroquinolones all constitute potential reservoirs of active fluoroquinolone compounds either as residues in the parent form or as metabolites. The flow of fluoroquinolone compounds from these sources into surrounding watersheds contributes to increased concentrations present in tested water and a negative impact on water quality (**Janecko et al., 2016**).

Initially present in water bodies, the fluoroquinolones rapidly transfer into the soil and sediments due to strong adsorption on minerals and organic matter (**Sturini et al., 2012**). Besides their potential to promote antibiotic resistance, fluoroquinolones also have an unfavourable ecotoxicity profile (**Golet et al., 2002a**). They may contribute to a significant portion of the measured bacterial genotoxicity in hospital effluents (**Zhang and Huang, 2005**).

1.6.1.1 Quinolones in the soil environment

Fluoroquinolones have become one of the major contaminants in wastewater bodies, which are not even wholly removed during treatment. Furthermore, their abundance in agricultural resources, such as irrigation water, bio-solids and livestock manure, can also affect the soil micro-environment. These antibiotics in soil tend to interact in several different ways to affect soil flora and fauna (**Riaz et al., 2018**).

Although the antibiotics have been detected in soil in relatively low concentrations compared to other pollutants, they might have long-lasting effects on plants, animals and humans. A few studies have reported the sorption and degradation mechanism of quinolone antibiotics in soil

using high concentrations (up to $\text{mg}\cdot\text{kg}^{-1}$ levels) to gain insight into their behaviour, including persistence and mobility in the soil. The presence of fluoroquinolone residues in the food chain, even at low concentrations, is a potential risk factor for consumers. Fluoroquinolone antibiotics have been reported in concentrations as high as $\text{mg}\cdot\text{kg}^{-1}$ in soil (Golet et al., 2002b; Prat et al., 2006; Uslu et al., 2008). They were initially present in wastewater and transported to the soil compartment due to irrigation or sorption on minerals and organic matter. Furthermore, the manure produced from animal husbandry and biosolids in the wastewater treatment plants serves as a source of fertiliser for agricultural soil in many regions which further enhances the concentration of these antibiotics in that compartment (Turiel et al., 2007).

The FQs result in high sorption in the soil micro-environment since a smaller portion undergoes transformation through biodegradation. When they enter the soil environment through irrigation of wastewater or biosolids and manure, they can cause toxicity to soil flora and fauna. For example, veterinary antibiotics such as enrofloxacin (ENR) pose threats to soil fauna, i.e. earthworms, usually used as bio-indicators of chemical contamination in soils. A past study showed that the earthworms undergo oxidative stress, reduced burrowing activity and CO_2 production when exposed to ENR concentrations at $10 \text{ mg}\cdot\text{kg}^{-1}$ soil (Li et al., 2016). For what concern the effects on the flora, the toxicity of FQs to plants varies from species to species and greatly depends on the sorption of these compounds in soil (Kumar et al., 2012). For example, the research evaluated the toxicity of levofloxacin towards seedlings of yellow lupin (*L. luteus* L. cv. Dukat) by considering the length of roots and shoots, seedling fresh and dry weight as morphological parameters, the activity of enzymes (catalase and peroxidase), protein profile and location of free radicals as physiological and biochemical parameters. The results showed a wide range of changes in protein synthesis in lupin roots. In contrast, on a morphological level, the levofloxacin soil contamination resulted in over 50% inhibition of root and shoot growth and a similar reduction in seedling fresh mass (Orzol and Piotrowicz-Cieślak, 2017). Another study evaluated the effects of three FQ antibiotics (ofloxacin, ciprofloxacin and levofloxacin) in the presence of three organic amendments (rice husk, farmyard manure and poultry litter) with rice (*Oryza sativa* L.) as a model plant. Organic amendments were mixed with soil ($5 \text{ g}\cdot\text{kg}^{-1}$), and after three weeks, antibiotics were applied ($10 \text{ mg}\cdot\text{kg}^{-1}$), and plants were allowed to grow for four months. After which plants were harvested, physical growth parameters (root/shoot length, biomass) and nutritional composition (grain protein content, carbohydrates, phosphorous and iron) were monitored. It was observed that germination rate, seedling root/shoot length, seedling biomass and vigour index were negatively impacted. Among all antibiotics, the most damaging was ofloxacin at the germination stage followed by ciprofloxacin and levofloxacin. Similarly, at

the maturity stage, the most harmful drug was ofloxacin then levofloxacin and ciprofloxacin (Mukhtar et al., 2020b).

1.6.1.2 Quinolones in wastewater and surface water

Until recently, pharmaceutical compounds in the environment have drawn very little attention. Although their presence in the effluents of WWTPs had been reported, it was believed these compounds were readily biodegradable in the background as most could be metabolised and transformed to some extent in humans. However, many recent studies have demonstrated the persistence of these pharmaceuticals in the aquatic environment (Frade et al., 2014). Because of their extensive usage, the presence and accumulation of fluoroquinolone antibacterial agents in aquatic environments have been widely reported. In fact, due to their strong sorption properties and a degree of resistance to microbial degradation, fluoroquinolones can persist in environmental waters (Ramos Payán et al., 2011; Robinson et al., 2005). Rivers become contaminated with fluoroquinolones through the domestic, urban, hospital, and industrial wastewaters (Adachi et al., 2013; Van Doorslaer et al., 2014). In addition, the rainfall-runoff from agricultural fields fertilised with contaminated manure or sludge can contribute to the dispersion of fluoroquinolones into soil and water bodies. Fluoroquinolone residues can negatively affect aquatic and terrestrial organisms, such as altering microbial activity and community composition in groundwater and causing antibiotic resistance (Ory et al., 2016). These chemicals in the environment are alarming because they can appear individually and as a complex mixture, leading to unwanted synergistic effects (Liu et al., 2018; Petrie et al., 2015). Moreover, contamination of water bodies can result in their bioaccumulation in aquatic ecosystems (Zhang et al., 2019; Zhao et al., 2018).

Researchers have focused on antibiotics with high persistence or high concentrations in aquatic environments (Bendz et al., 2005). Contamination with fluoroquinolones has been widely reported worldwide in different aquatic matrices at variable concentrations, including surface water, groundwater, sewage or sediment samples (Janecko et al., 2016). For example, 249-405 ng·L⁻¹ of ciprofloxacin and 45-120 ng·L⁻¹ of norfloxacin were detected in domestic sewage in Switzerland (Golet et al., 2002a). Higher concentrations of some fluoroquinolones (0.6-2 µg·L⁻¹) were also detected in wastewaters in the United States. Median concentrations of 0.02 µg·L⁻¹ and 0.12 µg·L⁻¹ were reported for ciprofloxacin and norfloxacin, respectively, for samples from 139 surface streams across the United States. Additionally, ciprofloxacin in the range 0.7-124.5 µg·L⁻¹ was found in wastewater of a Swiss hospital (Fink et al., 2012). Ciprofloxacin and norfloxacin were also detected in sewage and at WWTPs in Switzerland in the

range 45-568 ng·L⁻¹ and 36-367 ng·L⁻¹, respectively. The removal efficiency of these drugs in WWTPs was 79-87% (**Kümmerer et al., 2000**). In samples obtained from wastewater treatment plants in Portugal, ciprofloxacin was measured at 856 ng·L⁻¹ in the influent (**Maia et al., 2020**).

Jia et al. (2012) developed a method for analysing nineteen quinolone and fluoroquinolone antibiotics in sludge samples. They investigated the occurrence and fate of the FQs in a municipal sewage treatment plant (STP) with anaerobic, anoxic, and aerobic treatment processes. Ten compounds of the 19 target antibiotics, including pipemidic acid, fleroxacin, ofloxacin, norfloxacin, ciprofloxacin, enrofloxacin, lomefloxacin, sparfloxacin, gatifloxacin, and moxifloxacin, were detected in wastewater samples from Qinghe STP (Beijing, China). Ofloxacin (128 ± 97 ng·L⁻¹) and norfloxacin (775 ± 87 ng·L⁻¹) were the dominant FQs in the raw sewage, accounting for $50 \pm 1\%$ and $30 \pm 0.6\%$ of total concentrations, respectively. Relatively low concentrations were detected in the raw sewage for lomefloxacin (162 ± 4 ng·L⁻¹), ciprofloxacin (99 ± 21 ng·L⁻¹), pipemidic acid (86 ± 17 ng·L⁻¹), moxifloxacin (72 ± 34 ng·L⁻¹), gatifloxacin (66 ± 7 ng·L⁻¹), fleroxacin (14 ± 1 ng·L⁻¹), enrofloxacin (8.3 ± 3.2 ng·L⁻¹), and sparfloxacin (4.4 ± 0.3 ng·L⁻¹).

Fluoroquinolones were also detected in hospital wastewaters. However, reports focusing on their traces in these waters are scarce. Worldwide, some authors (**Gros et al., 2013; Lima Gomes et al., 2015; Watkinson et al., 2009**) reported that the predominant fluoroquinolones present in hospital raw wastewater effluents were ciprofloxacin (0.85-101 ng·mL⁻¹), ofloxacin (25-35 ng·mL⁻¹) and norfloxacin (0.2-17 ng·mL⁻¹). Unexpectedly, enrofloxacin, a veterinary drug, was also identified in hospital wastewater (0.1 ng·mL⁻¹) (**Watkinson et al., 2009**). Norfloxacin is observed in tap water and effluents from the wastewater treatment plant and surface water (**Watkinson et al., 2007; Yiruhan et al., 2010**). In another study, it was reported that the ciprofloxacin concentration in hospital wastewater (8.3-13.8 ng·mL⁻¹) was approximately ten times higher than in the effluents of a wastewater treatment plant (0.6-1.3 ng·mL⁻¹) (**Rodriguez-Mozaz et al., 2015**). **Rodrigues-Silva et al. (2019)** investigated the occurrence of fluoroquinolones in hospital raw sewage (HRS). They treated wastewater (TW) using a solid online phase extraction-ultra high-performance liquid chromatography-tandem mass spectrometry method (SPE-UHPLC-MS/MS). All HRS samples contained ciprofloxacin (1-34 ng·mL⁻¹) and ofloxacin (0.9-27 ng·mL⁻¹), while norfloxacin was detected in 17% of the samples (0.8-4.4 ng·mL⁻¹). Only ciprofloxacin (0.5-5.6 ng·mL⁻¹) was detected in TW samples.

Levofloxacin and Ciprofloxacin were also detected in raw and finished drinking water from Al-Rasheed and Al-Wihda plants in Baghdad (Iraq). The results showed that all target analytes were detected in the drinking water treatments. Ciprofloxacin was detected in 11 out of 36 water

samples, with a maximum concentration of $1.270 \mu\text{g}\cdot\text{L}^{-1}$; nine species confirmed the presence of levofloxacin, with a maximum concentration of $0.177 \mu\text{g}\cdot\text{L}^{-1}$ (**Mahmood et al., 2019**).

Ciprofloxacin and enrofloxacin were also detected in actual water river samples by **Alcaraz et al. (2016)**, and their concentrations were found to be 0.4 and $3.6 \mu\text{g}\cdot\text{L}^{-1}$, respectively. Currently, the presence of $0.97 \mu\text{g}\cdot\text{L}^{-1}$ of enrofloxacin shows the continuous existence of fluoroquinolones in this water source. Many studies have noted the ubiquity of enrofloxacin worldwide. Concerning the presence of this fluoroquinolone in river waters, the highest reported concentration (due to vast discharges of domestic and industrial wastewaters [$123 \mu\text{g}\cdot\text{L}^{-1}$]) was found in the Musi River in India (**Gothwal and Thatikonda, 2017**). Ciprofloxacin was also found in marine environments and freshwaters (**He et al., 2012; Hughes et al., 2013**).

Next to surface water, groundwater is threatened by FQs pollution due to (i) percolation from sludge or manure fertilised acres into the deeper soil layers, (ii) landfill leachate if there are no collection barriers, and (iii) via FQs polluted surface waters. Extreme ciprofloxacin (CIP) groundwater pollution ($0.7\text{--}14 \mu\text{g}\cdot\text{L}^{-1}$) is observed in the Pantacheru region in India, where also high CIP surface water concentrations are detected (**Fick et al., 2009**). Densely populated areas are also vulnerable to FQs groundwater pollution, as is observed by **López-Serna et al. (2013)**, where FQ concentrations up to $0.5 \mu\text{g}\cdot\text{L}^{-1}$ are reported in the region of the metropolis of Barcelona.

As said above, fluoroquinolones in the environment can pose a severe threat to the ecosystem and human health due to their high consumption globally. In 1998, around 120 tons were produced. The consequences of fluoroquinolones in the environment are not fully understood but are toxic to plants and aquatic organisms.

In mammals, norfloxacin causes neurotoxicity, embryotoxicity and genotoxicity (**Yang et al., 2020**). Ciprofloxacin affects the metabolism of the bacteria's carbon source in marine environments (**Johansson et al., 2014**). In addition, ciprofloxacin is toxic to other aquatic organisms, such as green algae and cyanobacteria. Moreover, ciprofloxacin ($10 \mu\text{g}\cdot\text{L}^{-1}$), combined with other pharmaceuticals such as ibuprofen ($6 \mu\text{g}\cdot\text{L}^{-1}$) and fluoxetine ($10 \mu\text{g}\cdot\text{L}^{-1}$), causes death in fish (**Richards et al., 2009**).

Although most fluoroquinolones have been observed at concentrations below $1 \text{mg}\cdot\text{L}^{-1}$ in aquatic environments, the studies of toxic mechanisms at higher concentrations may enable the establishment of clear regulatory rules for the use of fluoroquinolone antibiotics. The combined exposure of β -diketone antibiotics (DKA), including ciprofloxacin, ofloxacin, norfloxacin, and enrofloxacin, significantly reduced the normal formation of zebrafish larvae and hatching rate compared to the control at concentrations higher than $37.5 \text{mg}\cdot\text{L}^{-1}$ (**Wang et al., 2014**).

Yamashita et al. (2006) evaluated the toxic effects of the antibacterial agent levofloxacin, widely used in Japan, on aquatic organisms. In particular, ecotoxicity tests were carried out on a marine fluorescent bacterium (*Vibrio fischeri*), an alga and marine crustacean (*Daphnia magna*). Microtox[®] bioluminescence test on *Vibrio fischeri* and *Daphnia magna* immobilisation test showed no acute toxicity of levofloxacin. Meanwhile, an algal growth inhibition test revealed that levofloxacin has high microalgae toxicity. However, from the *Daphnia* reproduction test, levofloxacin showed chronic toxicity to the crustacean.

One year before, **Robinson et al. (2005)** performed some toxicity tests of seven fluoroquinolone antibiotics (ciprofloxacin, lomefloxacin, ofloxacin, levofloxacin, clinafloxacin, enrofloxacin and flumequine) on five aquatic organisms. The cyanobacterium *Microcystis aeruginosa* was the most sensitive organism (5-day growth and reproduction, effective concentrations [EC50s] ranging from 7.9 to 1.960 $\mu\text{g}\cdot\text{L}^{-1}$ and a median of 49 $\mu\text{g}\cdot\text{L}^{-1}$), followed by duckweed (*Lemna minor*, 7-day reproduction, EC50 values ranged from 53 to 2.470 $\mu\text{g}\cdot\text{L}^{-1}$ with a median of 106 $\mu\text{g}\cdot\text{L}^{-1}$) and the green alga *Pseudokirchneriella subcapitata* (3-day growth and reproduction, EC50 values ranged from 1.100 to 22.700 $\mu\text{g}\cdot\text{L}^{-1}$ with a median 7.400 $\mu\text{g}\cdot\text{L}^{-1}$). Tests with the crustacean *Daphnia magna* (48h survival) and fathead minnow (*Pimephales promelas*, 7-day early life stage survival and growth) showed limited toxicity with no-observed effect concentrations at or near 10 $\text{mg}\cdot\text{L}^{-1}$. Fish dry weights obtained in the ciprofloxacin, levofloxacin, and ofloxacin treatments (10 $\text{mg}\cdot\text{L}^{-1}$) were significantly higher than in control fish. The hazard of adverse effects occurring to the tested organisms in the environment was quantified using hazard quotients. An estimated environmental concentration of 1 $\mu\text{g}\cdot\text{L}^{-1}$ was chosen based on measured ecological concentrations previously reported in surface water; at this level, only *M. aeruginosa* resulted in being at risk in surface water. However, the selective toxicity of these compounds may have implications for aquatic community structure, especially if they are present in combination in the water environment by acting with a synergistic effect.

The individual and combined toxicities of levofloxacin and norfloxacin have been examined by **González-Pleiter et al. (2013)** in two organisms representative of the aquatic environment, the cyanobacterium *Anabaena* CPB4337 as a target organism and the green alga *Pseudokirchneriella subcapitata* as a non-target organism, and results were obtained after 72h of exposure. The antibiotic concentrations tested ranged from 0.01-200 $\text{mg}\cdot\text{L}^{-1}$ for levofloxacin and 0.01-100 $\text{mg}\cdot\text{L}^{-1}$ for norfloxacin. Levofloxacin and norfloxacin were more toxic to the cyanobacterium, most probably due to its higher sensitivity thanks to its prokaryotic nature than to the green alga. However, based on EC10 and EC20 values, levofloxacin was more toxic than

norfloxacin to the green alga. The two antibiotics were also tested in combination, and the results showed that they could be dangerous due to the synergistic interaction found at low-level effects. In another study (Ebert et al., 2011), the growth inhibition effect of the fluoroquinolone antibiotics enrofloxacin and ciprofloxacin was investigated on four photoautotrophic aquatic species: the freshwater microalga *Desmodesmus suspiciosus*, the cyanobacterium *Anabaena flos-aquae*, the monocotyledonous macrophyte *Lemna minor*, and the dicotyledonous macrophyte *Myriophyllum spicatum*. Both antibiotics demonstrated high toxicity to *A. flos-aquae* and *L. minor* and moderate to slight toxicity to *D. suspiciosus* and *M. spicatum*. Also, in this study, the cyanobacterium was the most sensitive species with median effective concentration (EC50) values of 173 and 10.2 $\mu\text{g}\cdot\text{L}^{-1}$ for enrofloxacin and ciprofloxacin, respectively. *Lemna minor* proved to be similarly sensitive, with EC50 values of 107 and 62.5 $\mu\text{g}\cdot\text{L}^{-1}$ for enrofloxacin and ciprofloxacin, respectively. While enrofloxacin was more toxic to green algae, ciprofloxacin was more harmful to cyanobacterium. Calculated EC50s for *D. suspiciosus* were 5.568 $\mu\text{g}\cdot\text{L}^{-1}$ and $>8.042 \mu\text{g}\cdot\text{L}^{-1}$ for enrofloxacin and ciprofloxacin, respectively.

Acute toxicity of 21 quinolone antibiotics (cinoxacin, ciprofloxacin, danofloxacin, difloxacin hydrochloride, enoxacin, enrofloxacin, fleroxacin, levofloxacin, lomefloxacin hydrochloride, moxifloxacin hydrochloride, norfloxacin, ofloxacin, pazufloxacin, pipemidic acid, sarafloxacin hydrochloride, sparfloxacin, balofloxacin, gatifloxacin, nadifloxacin, pefloxacin, rufloaxcin hydrochloride) was also assessed from Li et al., (2014) using photobacterium *Vibrio fischeri* assay. The results suggested that difloxacin, moxifloxacin and cinoxacin showed relatively high acute toxicity among all tested compounds, with IC20 values of 18.86, 22.85 and 35.02 $\mu\text{mol}\cdot\text{L}^{-1}$, respectively. Additionally, the action mode of quinolones to *V. fischeri* was investigated with the established QSAR (Quantitative Structure-Activity Relationship) model. The electronegative atoms in quinolone molecules, such as F, N, and O atoms, donated electrons to photobacterium and thus inhibited the luminance emission. Although the quinolones showed limited acute toxicity, the coexistence of multiple quinolones in environmental matrices may lead to severe overall toxicity.

High fluoroquinolone compound concentrations were present in urban centres where conventional WWTPs processed wastewater influent. The removal fraction accumulated higher concentrations of fluoroquinolones in the treated byproduct sludge (biosolids portion) (Janecko et al., 2016). As said above, a small % of the fluoroquinolones present in influents can be removed by conventional wastewater treatment plants (approximately 85%). Still, the extracted fraction is frequently accumulated in the sludge, sometimes used as fertiliser, representing an additional input route into the environment. In contrast, the remaining % is founded into

WWTPs effluents and surface water. The removal of fluoroquinolones by biological treatment is ineffective, and it is believed that only advanced oxidation technologies can destroy these emerging contaminants (Frade et al., 2014).

1.7 Advanced Oxidation Processes (AOPs)

In the last decades, industrial processes have generated many molecules that polluted air and waters due to negative impacts for ecosystems and humans (toxicity, carcinogenic and mutagenic properties) (Busca et al., 2008). Organic substances are refracted to biological degradation processes, but chemical technologies can remove them in many cases. Different chemical oxidation processes can be used. For high concentrations of organic substances, i.e., COD major than 20 g/mL, incineration or wet air oxidation processes are the most convenient, even if high pressure and high temperature have to be settled. *Advanced oxidation processes* (AOPs) are recommended for low concentrations of organics. These processes can be broadly defined as aqueous phase oxidation methods based on the intermediacy of highly reactive species such as hydroxyl radicals (HO^\bullet) or sulphate radicals ($\text{SO}_4^{\bullet-}$) in the mechanisms leading to the destruction of the target pollutant (Comninellis et al., 2008). A chemical wastewater treatment using AOPs completely mineralises pollutants to CO_2 , water, and inorganic compounds, or their transformation into more innocuous products (Poyatos et al., 2009). In particular, the decomposition of non-biodegradable organic pollutants can lead to biodegradable intermediates. Thus it can be recommended in some cases to set AOPs as pre-treatments, followed by biological processes.

The basic principle of advanced oxidation processes entails the generation of hydroxyl free radical (HO^\bullet), a non-selective chemical oxidant, as a strong oxidant for destroying organic compounds that conventional oxidants cannot oxidise as ozone, oxygen and chlorine (Munter, 2001). Hydroxyl radicals effectively destroy organic chemicals because they are reactive electrophiles that react rapidly and non-selectively with almost all organic compounds that are electron-rich (Glaze et al., 1987). Their oxidation potential is quantified as 2.80V, which makes them exhibit faster rates of oxidation reactions than conventional oxidations. Once the hydroxyl radicals are generated, they can attack organic chemicals through electron transfer, hydrogen abstraction and radical combination (Al Mayyahi and Ali Abed Al-Asadi, 2018).

Key AOPs include photocatalysis based on near-ultraviolet (UV) or solar visible irradiation, electrochemical processes, ultrasound (US), and chemical oxidation using oxidants, especially ozone and Fenton's reagent. These methods produce HO^\bullet radicals. These radicals are very

reactive, attack most organic molecules and are not highly selective (Skoumal et al., 2006). Furthermore, less conventional but evolving processes exist, including ionising radiation, microwaves, pulsed plasma, and ferrate reagent utilisation. Moreover, it has been shown that coupled AOPs can lead to higher removal efficiencies. Thus, more AOPs are often used simultaneously as UV/O₃, UV/H₂O₂, photo-Fenton, O₃/H₂O₂ and others. Some researchers have classified AOPs, both singles and combined, differentiating them as homogeneous or heterogeneous. Homogeneous processes have been further subdivided into methods that use energy and techniques that don't use energy, as shown in Fig. 1.6 (Poyatos et al., 2009).

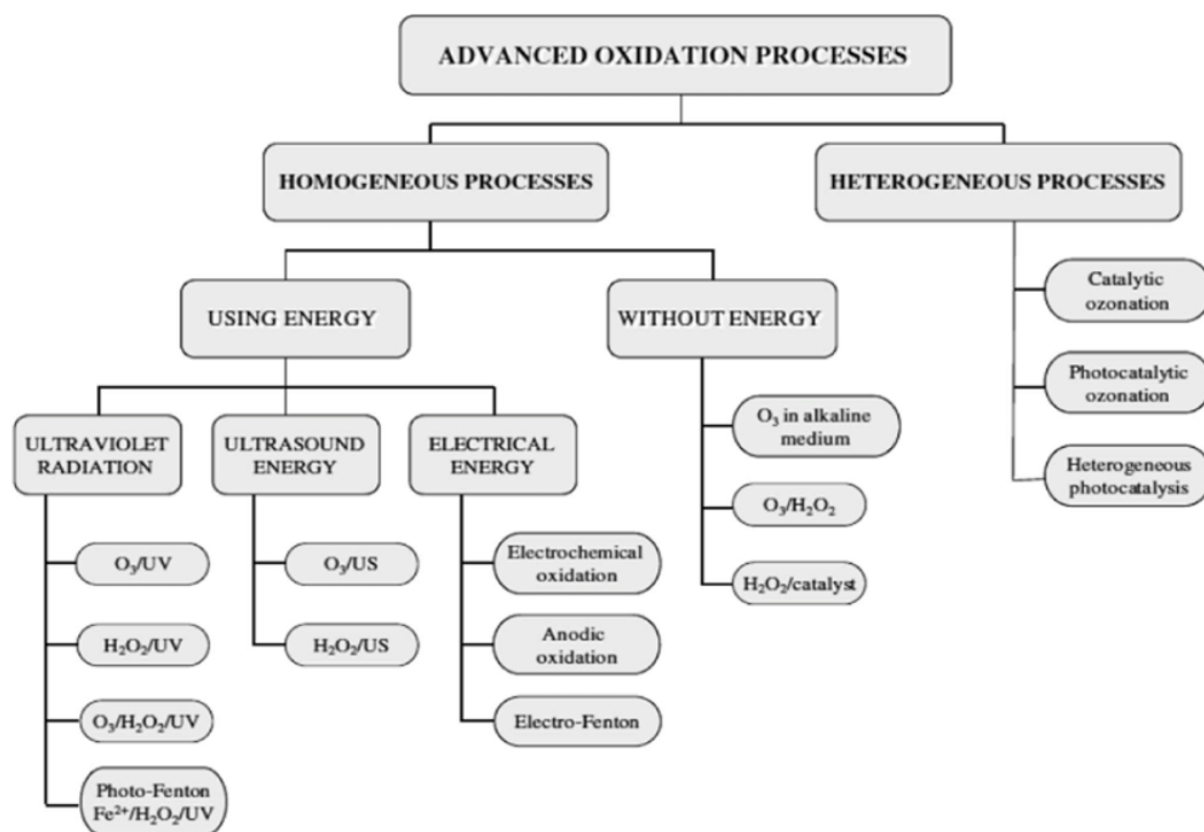


Fig. 1.6: Classification of advanced oxidation processes (Mokhbi et al., 2019).

Homogeneous AOPs using energy in the form of ultraviolet (UV) radiation, ultrasonic (US) energy or electrical energy have been applied to remove several pollutants from wastewater. Especially homogeneous treatments employing *UV light* have generally been used to degrade compounds that absorb within the corresponding range of the spectrum. UV radiation has been more often applied in the presence of other oxidants such as UV/O₃, UV/H₂O₂, UV/O₃/H₂O₂, UV/Fe²⁺/H₂O₂ (photo-Fenton) etc. (Babuponnusami and Muthukumar, 2014). **Ultrasounds (US)** constitute a particular type of AOPs in which the formation of reactive radicals (HO[•], HO₂[•], O[•]) can proceed either through a primary physical (direct) mechanism, where sonolysis of water

molecules takes place or through the chemical (indirect) mechanism, where homolytic fragmentation of water and dioxygen molecules occur (**Ghatak, 2014; Oturan and Aaron, 2014**). However, ultrasound in AOPs is not very energy efficient because 50% of the input energy is lost in thermal dissipation (**Zouaghi et al., 2011**). For this reason, various combinations of ultrasounds with other oxidants, such as H_2O_2 and O_3 , as well as with UV irradiation and with various AOPs, including the Fenton's reagent (with different forms of iron: Fe^0 , Fe^{2+} and Fe^{3+}) and Fenton-type reactions (called sono-Fenton AOPs) have been developed. **Electrochemical AOPs** are a form of degradation treatment based on electrical energy to break up organic pollutants contained in wastewater effluents. This group of homogeneous AOPs is subdivided into electrochemical oxidation, anodic oxidation and electro-Fenton, which are all techniques based on the transfer of electrons.

Homogeneous AOPs without energy include ozonation in alkaline medium and ozonation with hydrogen peroxide. O_3 , especially in $\text{pH} > 7$, is unstable and undergo spontaneous degradation to generate hydroxyl radicals, which attack the molecules of organic contaminant. In the presence of H_2O_2 , ozonation proceeds through a different set of reactions in which H_2O_2 is partially dissociated to hydroperoxide anion that reacts with the ozone to produce more radicals.

Heterogeneous AOPs require the addition of catalysts (metal oxides of Ti, Al, Zn, V, Cr, Mn, etc., or organometal catalysts) for the degradation reactions. Compared with the homogeneous AOPs, the heterogeneous AOPs have the advantage of easier separation from the product (meaning the treated effluents). Catalytic ozonation ($\text{Fe}^{2+}/\text{O}_3$, TiO_2/O_3), photocatalytic ozonation (UV/ TiO_2/O_3), and heterogeneous photocatalysis (UV/ TiO_2) are the most commonly used applications (**Vagi and Petsas, 2017**).

The AOP variety comes from the fact that there are many ways to hydroxyl radical production; this allows to meet the needs of any treatment. The hydroxyl radicals can be generated by different oxidation processes, such as ultraviolet (UV) (**Mansilla et al., 1997**), hydrogen peroxide combined with ultraviolet radiation ($\text{H}_2\text{O}_2/\text{UV}$), Fenton process ($\text{Fe(II)}/\text{H}_2\text{O}_2$) (**Walling, 1975**), photo-Fenton process (**Pignatello, 1992**), ozone (O_3), O_3/UV (**Baxendale and Wilson, 1957**) and heterogeneous photocatalysis using semiconductors such as titanium dioxide (TiO_2)-UV/ TiO_2 process.

1.7.1 *Photolysis*

Photolysis (also called *photochemical reaction* or *photodissociation*) is a chemical process by which chemical bonds are broken as the result of the transfer of light energy (direct photolysis) or radiant energy (indirect photolysis) to these bonds. The photolysis rate depends upon

numerous chemical and environmental factors, including the light adsorption properties and reactivity of the chemical and the intensity of solar radiation. In the process, the photochemical mechanism of photolysis is divided into three stages: (I) the adsorption of light, which excites electrons in the molecule, (II) the primary photochemical processes which transform or de-excite the excited molecule, and (III) the secondary (“dark”) thermal reactions which transform the intermediates produced in the previous step (Speight, 2017). Solar energy can be used as the source of such radiation energy to degrade some compounds. Still, the photons’ energy level that composes the solar spectrum is insufficient in many cases. Hence, ordinarily, ultraviolet light radiation and, more specifically, UVC correspond to radiation at a very low wavelength. The direct photolysis happens thanks to the direct interaction of a photon cross-reactive with a target molecule leading to the "photodissociation" or "photodecomposition" of the chemical. Different investigations indicate that several organic contaminants can be decomposed partial or totally into other substances less toxic and more biodegradable by oxidation based on UV light (Mokrini et al., 1997).

In photochemical reactions, one other possible way to generate the hydroxyl radical is the photolysis of the water according to **equation 1.1**.



If this reaction could be considered an essential source of radicals, it would happen at a very low rate. To increase the production rate of oxidative species, some additives are added, like adding oxidant H_2O_2 and O_3 , adding a catalyst (Photo-Fenton) or photocatalysis (TiO_2).

1.7.2 *UV/H₂O₂ processes*

The *ultraviolet/H₂O₂* (UV/H₂O₂) process involves the photolysis of hydrogen peroxide. The most accepted mechanism for this H_2O_2 photolysis is the cleavage of the O-O bond by the action of ultraviolet light forming two hydroxyls radical. This process is effected by irradiating the pollutant solution containing H_2O_2 with UV light having wavelengths smaller than 280 nm. This causes the homolytic cleavage of H_2O_2 (Eq. 1.2) (Beltrán et al., 1997).



Since H_2O_2 itself is attacked by OH radicals:



When these reactions occur in solutions containing organic contaminants, the reaction begins forming different radicals that degrade these contaminants. The hydroxyl radical generated in the presence of an organic substrate can react in three different ways:

1. With hydrogen abstraction: $HO^{\bullet} + RH \rightarrow R^{\bullet} + H_2O$
2. With electrophilic addition: $HO^{\bullet} + PhX \rightarrow HOPhX^{\bullet}$
3. With electron transfer: $HO^{\bullet} + RX \rightarrow RX^{\bullet+} + HO^{-}$

The major drawback of this process is due to the small molar extinction coefficient of H_2O_2 , which is only $18.6 \text{ M}^{-1} \cdot \text{cm}^{-1}$ at 254 nm; only a relatively small fraction of incident light is therefore exploited, particularly in the cases where organic substrates will act as inner filters. The photolysis rate of aqueous H_2O_2 is pH-dependent and increases when more alkaline conditions are used (**Legrini et al., 1993**). This may be primarily due to the higher molar absorption coefficient of the peroxide anion HO_2^{-} which at 254 nm is $240 \text{ M}^{-1} \cdot \text{cm}^{-1}$.

1.7.3 Ozonation

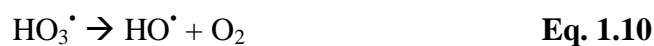
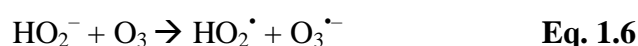
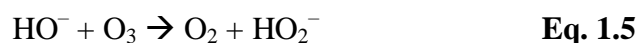
Ozonation is usually adopted for water disinfection, but it also has a high pretreatment method potential. As the most potent oxidising reagent, ozone can degrade several phenolic compounds effectively, with the advantage that oxidised products are usually less toxic than the parental compounds. In oxidation systems, by using ozone, it is possible:

- to convert inorganic components into higher oxidation stages;
- to cleave hardly biodegradable organic compounds;
- to kill bacteria;
- to destroy especially odorous, taste-causing and colouring substances.

The ozonation process involves compressing air from the atmosphere and feeding this air through valves into a chamber containing pellets. The valves switch back and forth to vary the pressure in the room from alternating vacuum and pressure cycles. The air breaks down to separate nitrogen and oxygen, with nitrogen merging with the pellets, leaving free O_2 that goes to an oxygen tank and is stored there until needed. The free O_2 progresses to an ozone generator, where the electric current is used to charge the O_2 to reform as O_3 charged molecules with electricity. The O_3 is then applied to the wastewater, where it violently disinfects the water and dissipates in it. The wastewater is further subjected to traditional water treatment, such as

filtration and chlorination, with any excess ozone recycled to the inlet water where it joins the water system (Arvanitoyannis and Kassaveti, 2008).

The ozonation of dissolved compounds in water can constitute an AOP by itself, as hydroxyl radicals are generated from the decomposition of ozone, which is catalysed by the hydroxyl ion or initiated by traces of other substances, like transition metal cations (Hoigné et al., 1985). As the pH increases, so does the ozone decomposition rate in water. Ozone decomposition in aqueous solution develops through the formation of OH radicals, and HO⁻ ion has the role of initiator in the reaction mechanism:



In an ozonation process, two possible pathways have to be considered: the direct pathway through the reactions with molecular ozone and the radical pathway through the reactions of hydroxyl radicals generated in the ozone decomposition and the dissolved compounds. The molecular ozone reactions commonly occur through ozonolysis of a double bond or attack of nucleophilic centres, where aldehydes, ketones or carboxylic acids are obtained from double bonds; amides from nitriles; amine oxides from amines, etc. The radical mechanism predominates in less reactive molecules, such as aliphatic hydrocarbons, carboxylic acids, benzenes or chlorobenzenes (Hoigne and Bader, 1979). An essential factor for this process is the pH; usually, the direct pathway dominates under acidic conditions (pH<4); above pH 10, it changes to the radical.

1.7.4 O₃/UV process

O₃/UV process is an advanced water treatment method for the effective oxidation and destruction of toxic and refractory organics in water. Ozone readily absorbs ultraviolet radiation at 254 nm wavelength (the extinction coefficient is 3600 M⁻¹·cm⁻¹), producing H₂O₂ as an intermediate that decomposes to HO[•] (Peyton and Glaze, 1988).

This system contains three components to produce HO[•] radicals and oxidises the pollutant for subsequent reactions: UV radiation, ozone and hydrogen peroxide. Therefore, the reaction mechanism of O₃/H₂O₂ and the combination UV/H₂O₂ is of great importance.

However, suppose water solutions contain organic compounds strongly absorbing UV light. In that case, UV radiation usually does not give any additional effect to ozone because of the screening of ozone from the UV by optically active compounds (**Munter, 2001**).

1.7.5 O₃/UV/H₂O₂ process

When hydrogen peroxide is used in an O₃/UV process, it accelerates the decomposition of ozone and increases the generation of OH radicals. This process is the result of the combination of two binary systems, O₃/UV and O₃/H₂O₂, in such a way that the resulting action is the following:



O₃/H₂O₂/UV processes are the most expensive because of the use of two types of reagents compared to methods that use only one. In processes involving pollutants that are weak absorbers of UV radiation, it is more cost-effective to add hydrogen peroxide externally at a reduced UV flux. If direct photolysis of contaminants is not a significant factor, O₃/H₂O₂ should be considered an alternative to photooxidation processes. The capital and operating costs for the UV/O₃ and H₂O₂ systems vary widely depending on the wastewater flow rate, types and concentrations of contaminants present, and the degree of removal required (**Munter, 2001**).

1.7.6 Process involving iron catalysts: Fenton process (H₂O₂/Fe²⁺)

The Fenton reagent is a homogeneous catalytic oxidation process that combines an oxidising agent (hydrogen peroxide) and a catalyst (an oxide or metal salt, usually iron) to produce hydroxyl radicals. Fenton H. J. H. Discovered the Fenton reaction in 1894 when intended to oxidise polycarboxylic acids (malic acid and tartaric acid) with H₂O₂ and noted a strong promotion in the presence of ferrous ions (Fe²⁺). Forty years later, the **Haber-Weiss (1934)** mechanism was postulated, revealing that the effective oxidative agent in the Fenton reaction was the hydroxyl radical (HO[•]). The use of Fenton's reagent is one of the most effective ways for HO[•] radical generation. In addition, due to the simplicity of equipment and mild operation conditions (atmospheric pressure and room temperature), this method has been postulated as the most economical oxidation alternative.

The mechanism of HO[•] generation is quite complex. Briefly, H₂O₂ decomposes catalytically by means of Fe²⁺ at acid pH giving rise to hydroxyl radicals (**Eq. 1.13**):



The rate constant for the reaction of a ferrous ion with hydrogen peroxide is high, and Fe(II) oxidises to Fe(III) in a few seconds to minutes in the presence of excess amounts of hydrogen peroxide. Furthermore, Fe³⁺ can react, at acid pH, with H₂O₂ regenerating the catalyst and producing the HO₂[•] radical, thus sustaining the process (**Eq. 1.14**). The technique becomes operative if the contaminated solution is at the optimum pH of 2.8-3.0, where it can be propagated by the catalytic behaviour of the Fe³⁺/Fe²⁺ couple. Interestingly, only a tiny catalytic amount of Fe²⁺ is required, whereas this ion is regenerated (see **Eq. 1.14**) (**Brillas et al., 2009**).

This process can lead to the complete mineralisation of the organics and is considered an attractive oxidative system for wastewater treatment because iron is a very abundant and non-toxic element even if usually significant quantities of ferric salts need to be disposed of.

The Fenton reagent has been successfully used in the degradation of several compounds such as chlorophenols (**Kwon et al., 1999**), surfactants (**Lin et al., 1999**), the oxidation of the leaching of landfill waste (**Kang and Hwang, 2000**) and the degradation of dyes (**Szpyrkowicz et al., 2001**).

However, technical requirements for optimising or monitoring the Fenton's reaction efficiency are complex and costly (i.e., GC-MS), limiting its common usage. Moreover, it is necessary to control pH carefully to prevent iron hydroxide precipitation, which occurs at basic pH. Even with optimisation of the reaction efficiency, this treatment technique implies high operative costs, significantly limiting treatment choice.

1.7.7 *Photo-Fenton process (UV/H₂O₂/Fe²⁺)*

A combination of hydrogen peroxide and UV radiation with Fe²⁺ or Fe³⁺ ions (photo-Fenton process) produces more HO[•] compared to the conventional Fenton method. Fenton reaction rates are enormously increased by irradiation with UV/visible light (**Ruppert et al., 1993; Sun and Pignatello, 1993**). Fe³⁺ ions are accumulated in the system during the reaction, and after Fe²⁺ ions are consumed, the reaction practically stops. Photochemical regeneration of ferrous ions (Fe²⁺) by photoreduction of ferric ions (Fe³⁺) is the proposed mechanism (**Eq. 1.15**) (**Faust and Hoigné, 1990**). The new generated ferrous ions react with H₂O₂ generating a second HO[•] radical

and ferric ion, and the cycle continues. In these conditions, iron can be considered a natural catalyst.



Furthermore, direct photolysis of H_2O_2 produces HO^{\bullet} , which can be used to degrade organic compounds, increasing the rate of degradation of organic pollutants. However, photo-Fenton gives a better degradation of low concentration organic pollutants. Because the high concentration of organic pollutants could reduce the absorb radiation of iron complex, which needs a longer radiation time and more H_2O_2 dosage. Compared with the classic Fenton, photo-Fenton has many advantages. A photo-induced $\text{Fe}^{3+}/\text{Fe}^{2+}$ redox cycle could decrease the catalyst dosage in Fenton, which effectively reduces iron sludge formation. Meanwhile, solar or UV light can increase the utilisation of H_2O_2 and possess photolysis on several small molecule organics. However, photo-Fenton has many disadvantages, such as low utilisation of visible light, the required UV energy for a long time, high energy consumption, and cost (**Bustillo-Lecompte, 2020**).

1.7.8 *Heterogeneous catalysis/photocatalysis*

Many catalytic processes in which the catalyst and the reactants are not present in the same phase are *heterogeneous catalytic reactions*. They include responses of gases (or liquids) at the surface of a solid catalyst. The cover is where reactions occur, so the catalysts are generally prepared to provide large surface areas per unit. Metals, metals coated onto supporting materials, metalloids, metallic films, and doped metals have been used as heterogeneous catalysts. With solid catalysts, at least two of the reactants are chemisorbed by the catalyst, and they will react at the surface of the catalyst, with which the products are formed as readily as possible. Then, the products are released from the catalyst surface. Heterogeneous catalysts can be divided into *unsupported catalysts* (bulk catalysts) and *supported catalysts*. Unsupported catalysts include metal oxide catalysts, such as TiO_2 , Al_2O_3 , SiO_2 , and B_2O_3 . Supported catalysts often employ porous materials as supporters, and active components, metals or metal oxides, for example, are coated on the surface of the supporters to form the catalysts.

As an efficient green method coping with organic wastewater, the heterogeneous catalytic process has attracted considerable attention in the last two decades. The highly reactive and non-selective hydroxyl radicals can oxidise and mineralise most organic compounds at near diffusion-limited rates, mainly unsaturated organic compounds (**Bustillo-Lecompte, 2020**).

Heterogeneous photocatalysis is the process of light-induced redox reactions upon the surrounding molecules to produce radical species for the subsequent utilisation in various pollutant degradations. Photocatalysis has many advantages: low reaction temperature, high oxidizability, complete purification, and solar energy sources. Furthermore, the careful selection of materials and structures of photocatalysts for photocatalysis is essential to perform photocatalytic reactions efficiently. An ideal photocatalyst is bound to possess good performances such as narrow bandgap energy, suitable band edge potential, reduced recombination, enhanced charge separation, and improved charge transportations (**Reddy et al., 2019**).

The principle of photocatalysis is based on the theory of a solid energy band. When the energy of light irradiation absorbed by the semiconductor catalyst is larger than the photon band gap width, the electron-hole pairs are generated due to the transition of electrons. The light irradiation on the semiconductor causes the excitation of electrons from the valence band (VB) to the conduction band (CB) and the creation of holes in the valence band (VB) (**Ibhadon and Fitzpatrick, 2013**). Electrons and holes stimulated by light radiation will migrate to the surface of semiconductor particles after various interactions and react with water or organics adsorbed on the surface of semiconductor catalyst particles to produce a photocatalytic effect, as shown in **Fig. 1.7** for the specific case of TiO_2 catalyst.

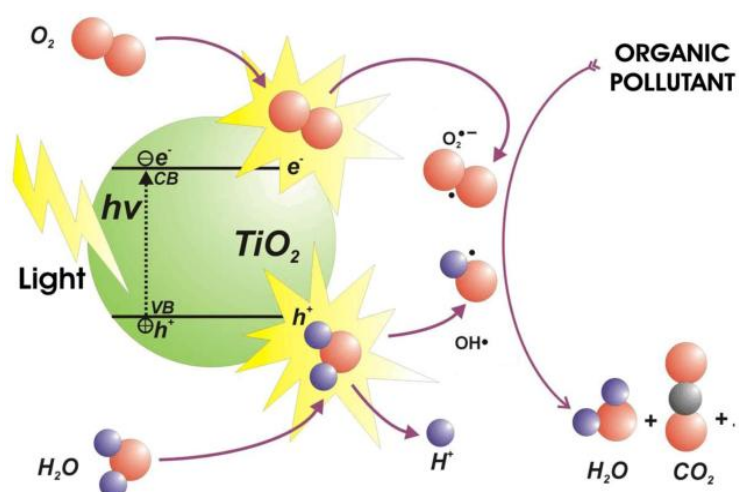


Fig. 1.7: Representative scheme of TiO_2 -semiconductor photocatalysis process (**Ibhadon and Fitzpatrick, 2013**).

Various materials are candidates to act as photocatalysts such as, for example, TiO_2 , ZnO , CdS , iron oxides, WO_3 , ZnS , etc. These materials are economically available, and many of them participate in chemical processes in nature. Besides, most of these materials can be excited with light of a wavelength in the range of the solar spectrum ($\lambda > 310 \text{ nm}$), therefore increasing the interest in the possible use of sunlight. So far, the most investigated photocatalysts are metallic

oxides, particularly TiO₂ in the anatase form seems to possess the most exciting features, such as high stability, it can be used in a wide pH range, being able to produce electronic transitions by light absorption in the near-ultraviolet range (UV-A) (**Fig. 1.7**). So, it can have good performance and low cost (**Andreozzi et al., 1999**). Still, the disadvantage of the catalyst available in nanoparticles is its recovery and separation from solution and the fouling of the catalyst by organic matter.

1.7.9 Sulphate radicals

Recently, sulphate radicals (SO₄^{•-}) based AOPs have been introduced to degrade organic pollutants. The most common initiators of sulphate radicals are peroxydisulphate (PDS, S₂O₈²⁻) and peroxymonosulfate (PMS, HSO₅⁻), which are two solid oxidising oxidants with a half-life span of 3–4 × 10⁻⁵ s. Instantaneously once activated, they can engender the extremely reactive SO₄^{•-}. Compared with HO[•], SO₄^{•-} has a more significant oxidation potential of 2.5-3.1 V and is wide-ranging operative at pH range. SO₄^{•-} expresses a superior standard reduction potential than HO[•] at neutral pH and under acidic conditions. Additional SO₄^{•-} has a half-life span of 30-40 μs, which is comparatively higher than HO[•] radical with a half-life span of 1 μs, that can oxidise micro-pollutants ranging 106-109 M·s⁻¹ (**Ushani et al., 2020**).

For the past few decades, SO₄^{•-} has been widely used to degrade a wide variety of organic materials in wastewater (**Anipsitakis and Dionysiou, 2003; Rastogi et al., 2009**). According to the United States Environmental Protection Agency (USEPA), SO₄^{•-} is virtually inert and regarded as non-pollutant. Taking taste and odour as a keen factor in secondary drinking water standards, such radical has been listed underneath the standards with a maximum concentration of 250 mg·L⁻¹. Thus, instantaneous oxidations of SO₄^{•-} occur in the aqueous phase that has been utilised in wastewater treatment.

Through their activation, sulphate radicals can be produced to remove many organic contaminants, including pharmaceuticals and pesticides (**Kan et al., 2021**). The activation of PMS and PS can be achieved mainly by acidic conditions (**House, 1962**), thermal (**Liang and Bruell, 2008**), photolytic, sonolytic (**Wei et al., 2017**), and the reactions of the oxidants with iron oxide magnetic composites, including in situ formed iron hydroxides and quinines (**Waclawek et al., 2017**).

Under the acid condition, the breakdown of peroxydisulphate into sulphate free radical (**House, 1962**) can be further acid-catalyzed through **Eqs. 1.16** and **1.17**:





Raising temperature is one approach to increasing the decomposition of peroxydisulphate into reactive $\text{SO}_4^{\bullet-}$ (Johnson et al., 2008). At ambient temperatures, sulfate radical's kinetics become slow while reacting with many organics (Saïen et al., 2011). $\text{S}_2\text{O}_8^{2-}$ decomposition rate increases with the temperature and concentration of organic compounds due to the occurrence of radical chain reactions that enhance $\text{S}_2\text{O}_8^{2-}$ decomposition (Liang and Su, 2009). In heterogeneous catalytic reactions, $\text{SO}_4^{\bullet-}$ reacts freely with the organic pollutants due to its long life span ($t_{1/2} = 30\text{--}40 \mu\text{s}$) when compared with OH^\bullet ($t_{1/2} = < 1 \mu\text{s}$). At constant temperature, numerous features affect the production of $\text{SO}_4^{\bullet-}$ such as pH, catalyst load and dosage of PS oxidant.

The peroxydisulphates oxidation process can be activated through the homolysis of peroxide bond, which can be performed in several ways, such as thermolysis and photolysis. When UV light is radiated on the single mole of peroxydisulphate, it generates double moles of $\text{SO}_4^{\bullet-}$; in the case of peroxymonosulfate, it generates one mole of $\text{SO}_4^{\bullet-}$ and one mole of HO^\bullet , as reported in the Eqs. 1.18 and 1.19:



Overall, the UV-activated peroxydisulphate oxidation process has better degradation efficiency for an organic pollutant, but the enhancement effect in sludge conditioning and anaerobic digestion is minimal. In addition, the generation of UV irradiation is usually expensive, thus restricting the actual application of UV techniques.

The peroxydisulphate oxidation process has been successfully activated by numerous transition metals such as Cu^{2+} , Mn^{2+} , Ce^{3+} , Ni^{2+} , V^{3+} , Ru^{3+} and Co^{2+} since these species can act as electron donors peroxydisulphate for $\text{SO}_4^{\bullet-}$ formation (Yin et al., 2018). Grounded on the reduction mechanism, the activation of PS and PMS shows a significant relationship with the redox potential of metal. Depending upon the present form, i.e. transition metal or metal oxide, they are categorised into homogeneous and heterogeneous activators.

1.8 Toxicity bioassays and their importance: some methods to evaluate the dangerousness of organic wastewater contaminants

Besides controlling the removal efficiency of essential substances, it is crucial to evaluate advanced treatments with appropriate toxicity tests to evaluate wastewater effluents globally. The *ecotoxicological test* is a biological experiment designed to verify if a potentially toxic

compound, or an environmental sample, causes a relevant biological response in the organisms used for the test. Usually, organisms are exposed to different concentrations or doses of a test substance or sample (wastewater, sewage sludge, soil, river or marine sediment) diluted in a suitable medium. Typically, at least one group of organisms (control group) is not subjected to the test substance or sample but is treated similarly to the exposed organisms. The observed and measured parameter (endpoint) in the different groups of organisms can be mobility, survival, size or growth, or any biochemical or physiological variable that can be quantified. Observations can be made after one or more predetermined exposure periods. The aim is to establish the relationship between the endpoint and the concentration of the test substance or sample.

Ecotoxicological tests are generally applied on the following matrices:

- *Surface water;*
- *Groundwater;*
- *Civil discharges;*
- *Industrial waste;*
- *Soils of contaminated sites;*
- *River sediments.*

In many countries, ecotoxicity tests are already used in wastewater management. This kind of test presents a definitive advantage in the impact assessment of complex wastewaters, for which a detailed and accurate pollution composition is almost complex. Such tests are helpful, for example, to protect biological treatment plants from toxic influents (**Hongxia et al., 2004**); to monitor the effectiveness of wastewater treatment plants (**Emmanuel et al., 2005**). Consequently, a range of acute and chronic toxicity bioassays have been developed to establish the toxicity levels of compounds for aquatic organisms. These tests are based on the use of micro-organisms (bacteria, algae, protozoa), plants (germinal test, radical elongation), invertebrates (shellfish, rotifers) and vertebrates (fish and small mammals). The biological response induced in different living organisms challenged by a chemical substance is diverse and depends on their sensitivity to toxicants. So, a series of methodologies may be applied to evaluate and monitor water quality with an ample variety of bioindicators. Toxicity bioassays can be classified according to the test species involved.

1.8.1 Bacterial bioassay (*Vibrio fischeri*, *Escherichia coli*, *Micrococcus flavus*)

A range of bacterial methods has been developed for toxicity screening. Studies of the effects of microbial metabolic activity on function constitute a direct, rapid, sensitive and cost-effective approach to assessing chemical stress. Several bioassays have been described, and different methods using microorganisms have been standardised and classified according to the parameter measured. The most common toxicity test is based on inhibiting the bioluminescence of luminescent bacteria *Vibrio fischeri* (**Fig. 1.8**).

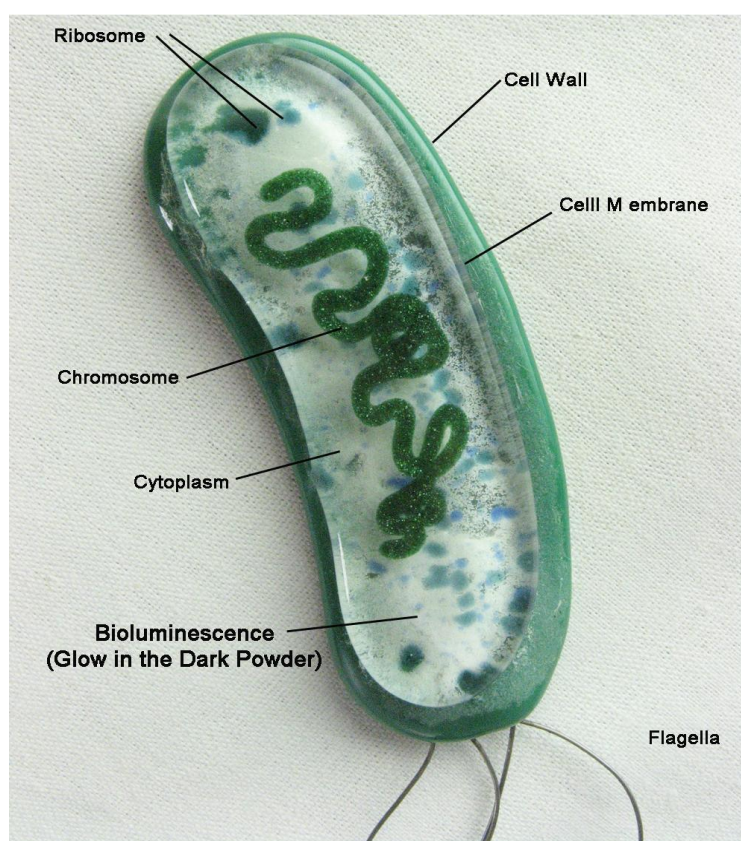


Fig. 1.8: *Vibrio fischeri* bacterium (www.deviantart.com).

Bioluminescence is a type of chemiluminescence reaction triggered by enzyme catalysis. Luminous bacteria are omnipresent and primarily inhabit the marine ecosystem as free-living or parasitic organisms (**Kaeding et al., 2007**). The underlying principle of the bioluminescent assay is the correlation of changes in kinetic attributes of bioluminescent reaction with the toxicity of test substance (**Dunn et al., 2015**). *Vibrio fischeri* is a Gram-negative, rod-shaped, flagellated, non-pathogenic bacterium ubiquitously distributed in subtropical and temperate marine environments. The biochemical and genetic basis of bacterial bioluminescence and its regulatory mechanism has been fully elucidated (**Meighen, 1993**). *Vibrio fischeri* possesses two substrates,

including a reduced flavin mononucleotide (FMNH₂) called luciferin and a long-chain fatty aldehyde. Exogenous reducing agents induce the reduction of flavin mononucleotide (FMN) to form FMNH₂ via the enzymatic action of luciferase (flavin mono-oxygenase oxidoreductase). The resultant FMNH₂ reacts with O₂ to yield an intermediate substance called 4a-peroxy-flavin, which oxidises the fatty aldehyde to its corresponding acid and a luciferase-hydroxyflavin complex. This stable intermediate slowly decomposes while emitting a blue-green light with its highest intensity at 490 nm (Meighen, 1991) (Fig. 1.9).

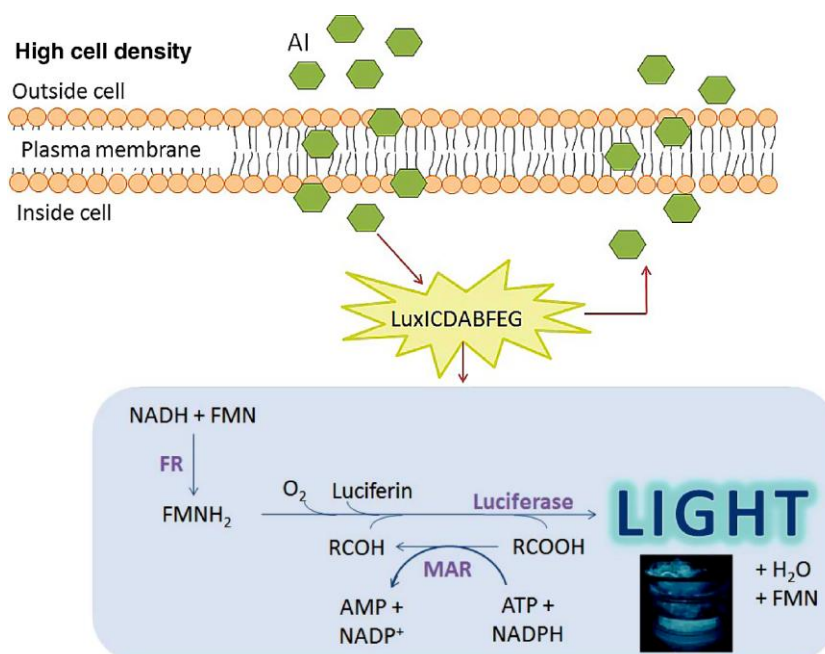


Fig. 1.9: A simplified schematic of the molecular basis of bioluminescence in *Vibrio fischeri* (Williams et al., 2019).

Bioluminescence is directly linked to respiration through the electron transport chain and thereby reflects the cellular metabolic status as a determinant of xenobiotic-mediated toxicity. The presence of toxic substances diminishes the resultant luminescence. The inhibition of bacterial metabolism is manifested by attenuation of light emittance, which corresponds to the toxicity level of the tested substance. As said above, the light emission is directly proportional to the metabolic status of the cell, so any inhibition of this activity is reflected in a decrease in bioluminescence expressed in percentage (I%). Toxicity is defined as EC50, the effective concentration of a toxic substance causing light to be reduced by 50%. This test has the advantage of being rapid, sensitive and reproducible. However, it presents also some disadvantages. *Vibrio fischeri* is a marine bacterium, so this test works only in saline solution, and filtration is required before every test. Because of the salinity, some organic substances' solubility is enhanced, thus producing turbid solutions (Abbas et al., 2018).

Vibrio fischeri bioluminescence inhibition assay (VFBIA) is extensively used to assess wastewater toxicity and provides a convenient, rapid, and cost-effective approach to monitor the remediation process. The assay has been applied for the toxicity evaluation of effluents derived from different sources such as forest products (Svenson et al., 1996), textile (Wang et al., 2002), paper (Rigol et al., 2004) and pharmaceutical (Maselli et al., 2015) industries.

Often, other bacterial species (such as *Escherichia coli* or *Micrococcus flavus*) can also be used as indicators for toxicity tests. In these cases, some plates of the corresponding bacteria species are prepared, and the test compound is pipetted in specific places of the plate: if the microorganism is susceptible to the action of the compound, an inhibition halo forms around it. Then, the toxicity results are expressed by measuring the inhibition halo diameter.

Monitoring the microbiological quality of water relies largely on examination of indicator bacteria. *Escherichia coli* is a member of the faecal coliform group and is a more specific indicator of faecal pollution than other faecal coliforms. Two key factors have led to the trend toward the use of *E. coli* as the preferred indicator for the detection of faecal contamination, not only in drinking water, but also in other matrices as well: first, the finding that some faecal coliforms were non faecal in origin, and second, the development of improved testing methods for *E. coli*. At present, *E. coli* appears to provide the best bacterial indication of faecal contamination in drinking water. This is based on the prevalence of thermotolerant (faecal) coliforms in temperate environments as compared to the rare incidence of *E. coli*, the prevalence of *E. coli* in human and animal faeces as compared to other thermotolerant coliforms, and the availability of affordable, fast, sensitive, specific and easier to perform detection methods for *E. coli* (Odonkor and Ampofo, 2013). In this thesis we also used *Micrococcus flavus* as water quality bioindicator, a Gram-positive cocci isolated from activated sludge of a wastewater-treatment bioreactor (Liu et al., 2007).

1.8.2 Phytotoxicity bioassays (*Lepidium sativum* and *Solanum lycopersicum*)

Plants interact directly with the terrestrial and atmospheric environment, are highly sensitive to various contaminants and possess cellular responses similar of animal organisms. Still, from an ethical point of view, their use in experimentation is more acceptable and more easily achievable (Blinova, 2004). Therefore, the use of plants for toxicity tests has acquired considerable importance in recent decades. The seed germination process represents the most critical event in forming the future plant (Dash and Panda, 2001).

Phytotoxicity is defined as a delay of seed germination, inhibition of plant growth or any adverse effect on plants caused by specific substances or growing conditions (Blok et al., 2019). Different toxicity bioassays based on plants have been developed. Plant biomarkers offer general advantages, such as an extensive array of assessment endpoints (germination rate, biomass weight, enzyme activity, etc.), low maintenance cost and rapid test activation. The phytotoxicity test represents the most direct experimental approach to evaluate the effect of a potential contaminant on seed germination and sprout growth (acute effect) and, in longer times, at the level of the plant life cycle (chronic effect). The commonly used plant model species are *Lepidium sativum* L. (Fig. 1.10A), *Cucumis sativus* L., *Lactuca sativa* L., and *Solanum lycopersicum* (Fig. 1.10B).



Fig. 1.10: (A) *Lepidium sativum* and (B) *Solanum lycopersicum*.

There are several standard phytotoxicity criteria, such as the frequency (number of plants at some stage or which have a visual symptom) or criteria based on measurements (height, length, diameter, weight of plants or organs from a sample). Further criteria for the appraisal of phytotoxicity refer to visual estimates such as changes of colour, plant deformation etc. In this case, the effect is often marked by a standard. Among the most commonly used criteria to evaluate phytotoxicity symptoms, the following are mainly applied: changes in root weight, root length, root system development; alterations of germination rate, stem length; colour changes; plant necrosis, deformation of organs (stem, leaf) (Pavel et al., 2013).

Phytotoxicity tests present several advantages: (I) these tests are simple, quick and reliable; (II) they are inexpensive and do not require significant equipment; (III) plants can be more sensitive to environmental stress over other organisms (Valerio et al., 2007).

Thanks to the importance of plants in ecotoxicology studies, phytotoxicity and genotoxicity tests provide immediate and essential information for evaluating the effects of environmental contaminants. The multidisciplinary approach makes it possible to assess many biological and

ecological parameters, favouring a greater understanding of the cellular mechanisms involved in the plant's response to different substances and contaminant-matrix-plant interactions.

1.8.3 3-(4,5-dimethylthiazol-2-yl)-2,5-diphenyltetrazolium bromide (MTT) bioassay

The MTT assay is a colorimetric assay for assessing cell metabolic activity. NAD(P)H-dependent cellular oxidoreductase enzymes may reflect, under defined conditions, the number of viable cells present. These enzymes are capable of reducing the tetrazolium dye MTT [3-(4,5-dimethylthiazol-2-yl)-2,5-diphenyltetrazolium bromide] to its insoluble *formazan*, which has a purple colour, and this reaction occurs only in living cells (**Fig. 1.11**).

Then, a solubilisation solution (usually dimethyl sulfoxide) is added to dissolve the insoluble purple formazan product into a coloured solution. The absorbance of this coloured solution can be quantified by measuring at a specific wavelength (usually between 500 and 600 nm) by a spectrophotometer. The degree of light absorption is dependent on the degree of formazan concentration accumulated inside the cell and on the cell surface. The greater the formazan concentration, the deeper the purple colour and thus the higher the absorbance.

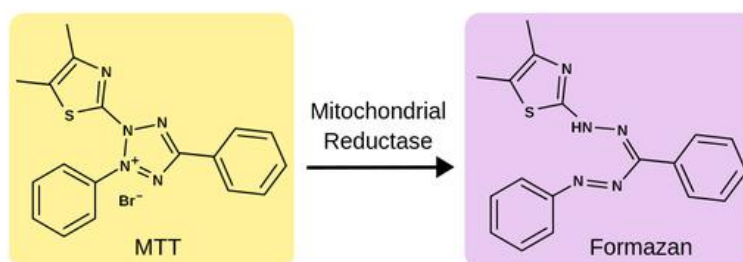


Fig. 1.11: Conversion reaction of MTT to formazan by mitochondrial reductase.

Tetrazolium dye reduction is generally assumed to depend on NAD(P)H-dependent oxidoreductase enzymes, mainly in the cytosolic compartment of the cell. Therefore, the reduction of MTT and other tetrazolium dyes depends on the cellular metabolic activity due to NAD(P)H flux (**Berridge et al., 2005; Berridge and Tan, 1993**). Cells with a low metabolism reduce very little MTT. In contrast, rapidly dividing cells exhibit high rates of MTT reduction: for this reason, this test is usually carried out on cancer cells. It is essential to remember that assay conditions can alter metabolic activity and thus reduce tetrazolium dye without affecting cell viability (**Ghasemi et al., 2021**).

MTT assays are usually done in the dark since the MTT reagent is sensitive to light. Tetrazolium dye assays can be used to measure cytotoxicity (loss of viable cells) or cytostatic activity (shift

from proliferation to quiescence) of potential medicinal agents and toxic materials. A treated cell population with tested compounds can show a reduction of absorbance if these molecules have cytotoxic or cytostatic activity on living cells concerning an untreated cell population.

1.9 Aim of thesis

From the bibliographic part dedicated to the most commonly tested AOPs for removing specific compounds and the organic wastewater contamination, representative AOPs have been selected to remove levofloxacin (LFX), one of the most used antibiotics, as the main aim of this thesis. Considering the different conclusions described and directly coming from state of the art, the objectives of the experimental works carried out in this dissertation and presented in the form of cases of studies and papers published, accepted and under review are:

- 1. Photolysis and heterogeneous photocatalysis with TiO₂:** the simplest and most basic case to evaluate the treatment and compare these two AOPs. This experiment was necessary to compare these two processes because it is well known the efficiency of TiO₂ as a heterogeneous photocatalyst in increasing the removal rate of organic compounds, but the high costs of the treatment due to the necessity of recovery and separation from solution is the main applicative limitation. However, it was not surprising to observe that heterogeneous photocatalysis using TiO₂ can give satisfactory results in this field;
- 2. Heterogeneous photocatalysis with supported TiO₂ on borosilicate tube:** supported catalysts often employ porous materials as supporters, and active components, metals or metal oxides, for example, are coated on the surface of the supporters to form the catalysts. Titanium dioxide has been already tested as immobilised on borosilicate glass plates for the degradation of fenamiphos (an insecticide) in water (El Yadini et al., 2014) and glass spheres for the photocatalytic degradation of methylene blue (Cunha et al., 2018). In our case study, the efficiency of TiO₂ as a supported catalyst on the surface of a borosilicate tube was assessed. Finally, the last sample of each photodegradation test (with and without TiO₂-coated tube) was used for phytotoxicity assays on *Lepidium sativum* and *Solanum lycopersicum*, while selected samples obtained during the entire process were successively used for acute ecotoxicology assay with MicroTox[®] system on *Vibrio fischeri*, at Water Research Institute (IRSA-CNR) in Taranto (Italy);
- 3. Homogeneous photocatalysis with hydrogen peroxide (H₂O₂), peroxymonosulphate (PMS, HSO₅⁻) and peroxydisulphate (PDS, S₂O₈²⁻):** for this case of study, the aim was to give a comprehensive view of the different aspects linked to the degradation of

levofloxacin with sulphate radicals based AOPs (SR-AOPs) and hydroxyl radicals based AOPs (HR-AOPs). In the first step, the performance of different AOPs was investigated in different pH conditions according to essential kinetic criteria, mainly the comparison between apparent first-order kinetic rate constants obtained by different SR-AOPs and HR-AOPs. Then, in a second step, the more efficient treatment was performed in a complex matrix such as simulated wastewater to assess the potential application of SR-AOPs at a larger scale, considering the eco-friendly proprieties based on antibacterial activity against *Escherichia coli* and *Micrococcus flavus*. All these results are reported in this dissertation as an under review paper;

- 4. Scientific activity in University of Ioannina (Department of Chemistry):** the aim was to obtain another critical feedback about the potential eco-compatibility of sulphate radicals treatment for levofloxacin removal. The toxicity of selected samples obtained during the photocatalytic process was assessed by MTT assays, carried out at the University of Ioannina (Greece). In particular, we tested the toxicity of the samples obtained from levofloxacin treatment with peroxydisulphate in pure water, through MTT bioassay, on human epithelial-like lung carcinoma cell line A549.
- 5. Training period at Hydros S.r.l.:** the aim of this experience was to participate in designing of fumes and wastewater treatment systems, and in the optimization of the parameters of the biological process of nitrification/denitrification/oxidation present within a real wastewater treatment plant.

CHAPTER 2

Case study #1: photolysis and heterogeneous photocatalysis with suspended TiO₂ for the degradation of levofloxacin in ultrapure water

2.1 Introduction

With the development of human society and rampant industrial growth, the consumption of fossil fuels is rapidly increasing. As a result, environmental pollution (such as the release of toxic agents and industrial waste) and the shortage of resources for renewable energy are two major problems that the world is facing. Thus, developing environmentally friendly, clean, safe, and sustainable energy technologies is one of the most urgent challenges faced by researchers today (Schneider et al., 2014). Solar energy is one of the most importantly clean and renewable energy sources on Earth that can be easily converted into electricity and chemical energy. Thus, environmentally friendly energy technologies using solar energy should be primarily developed and harnessed to solve the world's environmental and energy problems. Among the various technologies, photocatalysis, in which solar energy is used to drive chemical and energy processes, is one of the significant advances in this direction. Photocatalysis has been widely applied in various areas, such as solar cells, water splitting and pollutant degradation. Therefore, the photochemical mechanisms and basic principles of photocatalysis, especially TiO₂ photocatalysis, have been extensively investigated by various surface science methods in the last decade, aiming to provide vital information for TiO₂ photocatalysis under natural environmental conditions (Guo et al., 2019). In addition to TiO₂, various new semiconductor materials, such as SrTiO₃, BiVO₄, Ag₃PO₄, TaON, CdS, MoS₂, and their nanoparticles, have been applied to exploit solar energy for various photocatalytic reactions directly. Among the various photocatalysts, TiO₂, the most widely employed “golden” photocatalyst, has mainly been used in heterogeneous photocatalysis, due to its chemical stability and low cost (Chen et al., 2011; Nakata and Fujishima, 2012; Schneider et al., 2014). In the last two decades, TiO₂ heterogeneous photocatalysis has expanded very quickly. There are enormous fields where the photocatalytic activity of TiO₂ nanoparticles have been explored, e.g. in photocatalytic water splitting for hydrogen production (Ni et al., 2007), photocatalytic self-cleaning (Hashimoto et al., 2005), purification of wastewater (Liu et al., 2006; Pekakis et al., 2006), photovoltaics

(Umadevi et al., 2013) and antibacterial/antimicrobial activity (Yu et al., 2011). The most promising area of TiO₂ photocatalysis is the photodegradation of a large variety of environmental contaminations such as complex organic compounds and inorganic material turn into CO₂ and harmless inorganic anions respectively. TiO₂, as a photocatalyst, has shown an excellent potential for detoxification or remediation of wastewater (Jain and Vaya, 2017).

We used Aeroxide-TiO₂ P25 as a heterogeneous photocatalyst to degrade levofloxacin (LFX) in this case study. For the photocatalytic experiment, we used a TiO₂ concentration of 200 mg·L⁻¹, according to Khalaf et al., 2017, and an initial LFX concentration of 10 mg·L⁻¹.

2.2 Experimental section

2.2.1 Chemicals

For chemical analysis, acetonitrile (ACN) and formic acid were LC-MS grade from Honeywell (Wabash, Indiana, US), and water was ultrapure Milli-Q grade (18.2 MΩ cm⁻¹ resistivity at 25°C, VWR European). Analytical standard of levofloxacin (LFX) (purity 99.4%) was purchased from Lab Instruments S.r.l. (Castellana Grotte, Puglia, Italy), Aeroxide-TiO₂ P25 from Degussa AG (Frankfurt, Germany). Chemicals were used as received without further purification.

2.2.2 Experimental device for photodegradation process (in batch)

Photodegradation experiments (photolysis and heterogeneous photocatalysis with suspended TiO₂) were carried out in batch using a cylindrical reactor covered with a quartz cap (Fig. 2.1A). All reactions were performed by placing the photochemical reactor in a solar simulator device (Heraeus-Atlas Suntest CPS+, Chicago, USA) (Fig. 2.1B). This device is equipped with a Xenon Arc lamp (1.8 KW), the irradiation source having a light power of 400 W/m², with a spectral wavelength range 290 - 800 nm. The temperature was kept constant (30 ± 0.1°C) using an air conditioning system, and the solutions were maintained under continuous stirring, ensuring an optimum mixing flow.

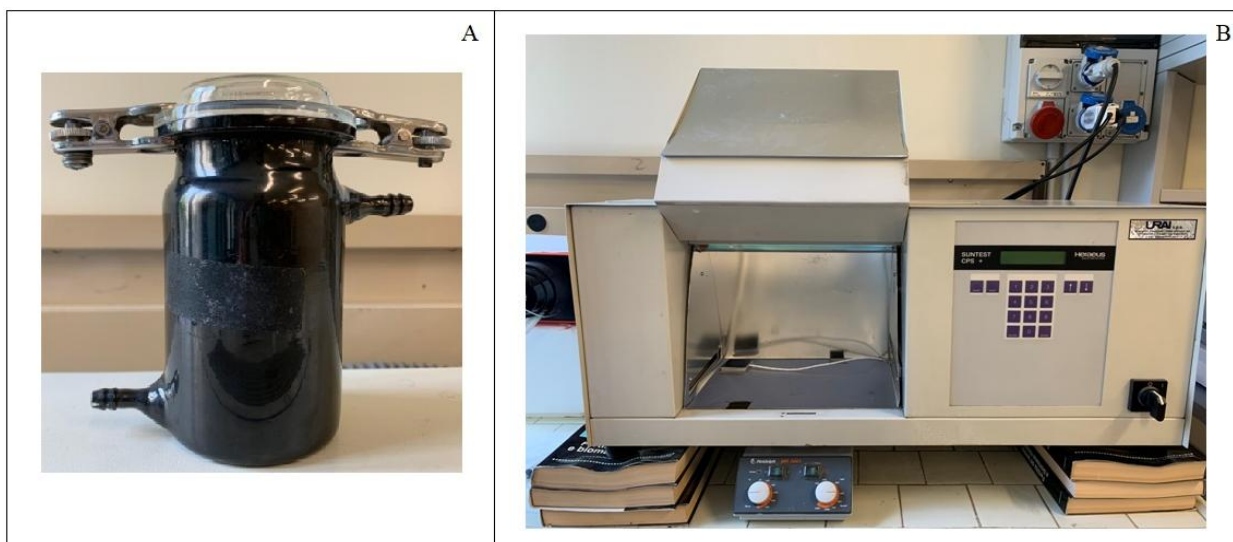


Fig. 2.1: (A) Photochemical reactor used for direct photolysis and heterogeneous photocatalysis with suspended TiO_2 , and (B) solar simulator device.

2.2.3 *Photolysis and heterogeneous photocatalysis with suspended TiO_2*

For photolysis and heterogeneous photocatalysis experiments, a $2000 \text{ mg}\cdot\text{L}^{-1}$ stock solution of levofloxacin in methanol was used to prepare 500 mL of a solution with an initial concentration of $10 \text{ mg}\cdot\text{L}^{-1}$ in ultrapure water. From this solution, 250 mL were used for photolysis experiments, and the other 250 mL were used for heterogeneous photocatalysis experiments after adding 50 mg of TiO_2 powder ($C_{\text{TiO}_2} = 200 \text{ mg}\cdot\text{L}^{-1}$); both solutions were stirred throughout the experiment. All the analysed samples were taken (1 mL for each sample) at prefixed time intervals; moreover, those from the heterogeneous photocatalysis were filtered using PTFE (polytetrafluoroethylene) filters $0.2 \mu\text{m}$ pore size, to remove the suspended catalyst before the HPLC-UV analysis.

2.2.4 *HPLC-UV conditions*

LFX concentration was monitored using a high-performance liquid chromatography (HPLC) system (Agilent Technologies 1200 series, USA) equipped with a Kinetex C18 100\AA column ($250 \times 4.6 \text{ mm}$ i.d., $5 \mu\text{m}$ particle size) and a diode array detector (DAD), set at $\lambda = 295 \text{ nm}$. The mobile phase consists of a bifasic gradient, ultrapure water with 0.1% formic acid (solvent A) and acetonitrile (solvent B), structured as follows: 0 - 3 min, 0% B; 3 - 5 min, 15% B; 5 - 16 min, 15% B; 16 - 18 min, 100% B; 18 - 22 min, 100% B; 22 - 23 min, 0% B; 23 - 25 min, 0% B. The flow rate is $1.0 \text{ mL}\cdot\text{min}^{-1}$, and the injection volume was $20 \mu\text{L}$.

2.3 Results and discussion

The concentration of levofloxacin during photolysis and heterogeneous photocatalysis reactions was monitored using High-Performance Liquid Chromatography - Ultra Violet (HPLC-UV). The standard solution used showed a peak of levofloxacin at a 12.7 min retention time (**Fig. 2.2A**). Before the photodegradation, the pharmaceutical adsorption on the catalyst surface in TiO₂ powder suspension was assessed. After adding the TiO₂ powder, the levofloxacin solution was left under stirring in dark conditions for 30 minutes to determine the percentage of TiO₂ particles' adsorption, and a slight decrease (7.1%) of free LFX concentration in 200 mg·L⁻¹ TiO₂ suspension was achieved. Then the solution was placed into the solar simulator and irradiated by the Xenon Arc lamp. After 10 minutes of sample irradiation, a marked decrease in the LFX concentration was observed (54.7% of the initial concentration) along with the appearance of new photoproducts. After 60 min of irradiation, an approximately 87% reduction in LFX initial concentration was obtained, while the complete disappearance of LFX and their photoproducts was achieved after 240 min. Instead, as for photolysis, after 240 minutes of sample irradiation, just a 59% reduction in LFX initial concentration was observed. The degradation test was stopped after 420 minutes of irradiation when the LFX concentration was still present at 1.6 mg·L⁻¹. In **Fig. 2.2**, some chromatograms for photolysis and heterogeneous photocatalysis are reported.

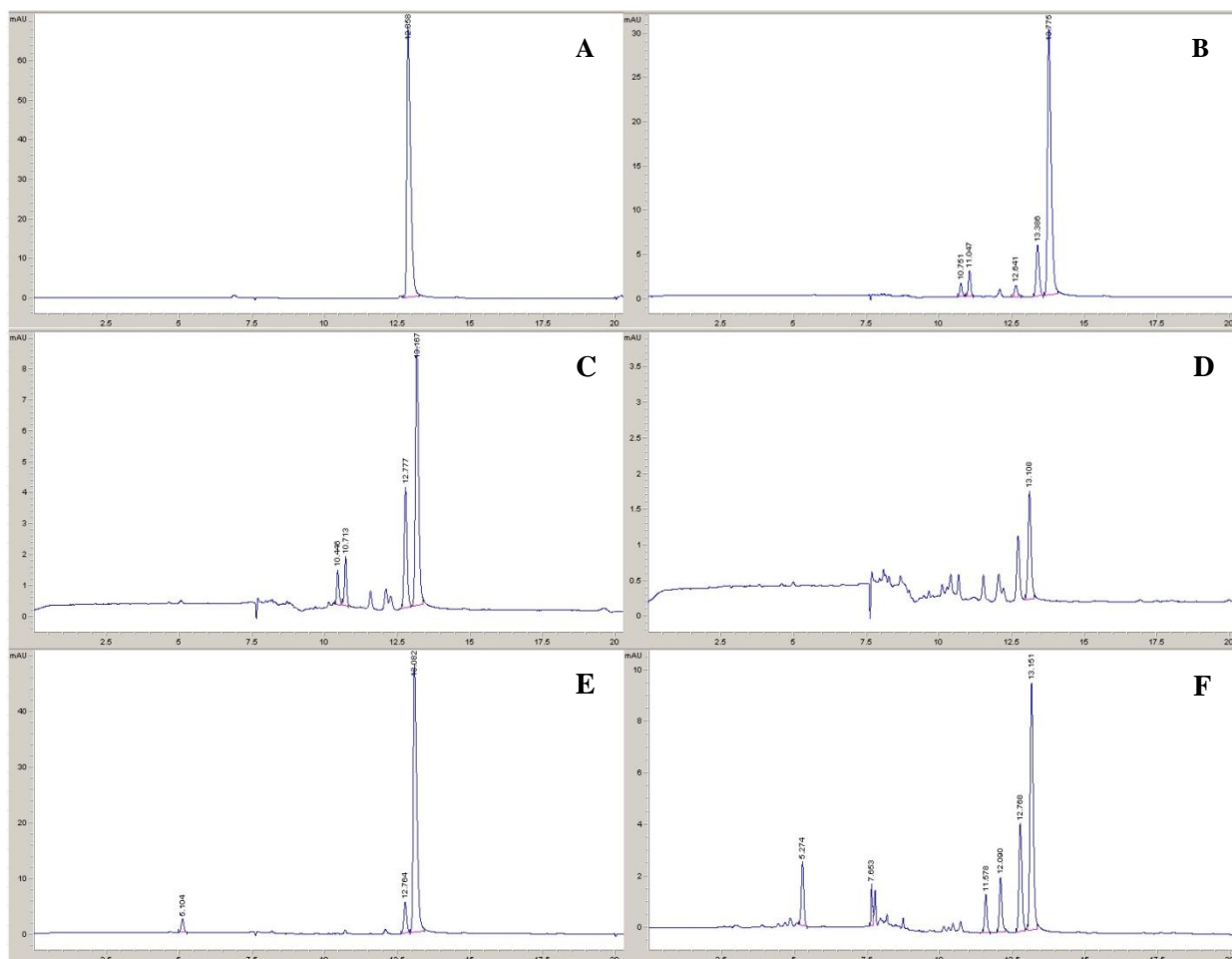


Fig. 2.2: HPLC-UV separation of photo-degraded solution using direct photolysis and heterogeneous photocatalysis with TiO_2 powder. (A) Initial solution $10 \text{ mg}\cdot\text{L}^{-1}$ in ultrapure water before irradiation, (B) photocatalysis after 10 min, (C) photocatalysis after 60 min, (D) photocatalysis after 120 min, (E) photolysis after 120 min, (F) photolysis after 420 min. In all chromatograms the last peak on the right is LFX.

No degradation of LFX was observed in the dark conditions. Direct photolysis under simulated sunlight didn't achieve the desired goal. Accordingly, we can conclude that the direct interaction of LFX with sunlight (both via thermal hydrolytic reactions and photolysis) cannot lead to LFX's quick degradation. However, in the presence of TiO_2 , complete removal of this antibiotic was obtained, although a xenon lamp with low UV energy was used for irradiation aiming at the simulation of sunlight effect. **Fig. 2.3** illustrates the depletion trend of LFX measured as $C/C_0\%$ (where C is the compound concentration at time t , C_0 is the initial compound concentration) versus irradiation time using the two different photodegradation methods.

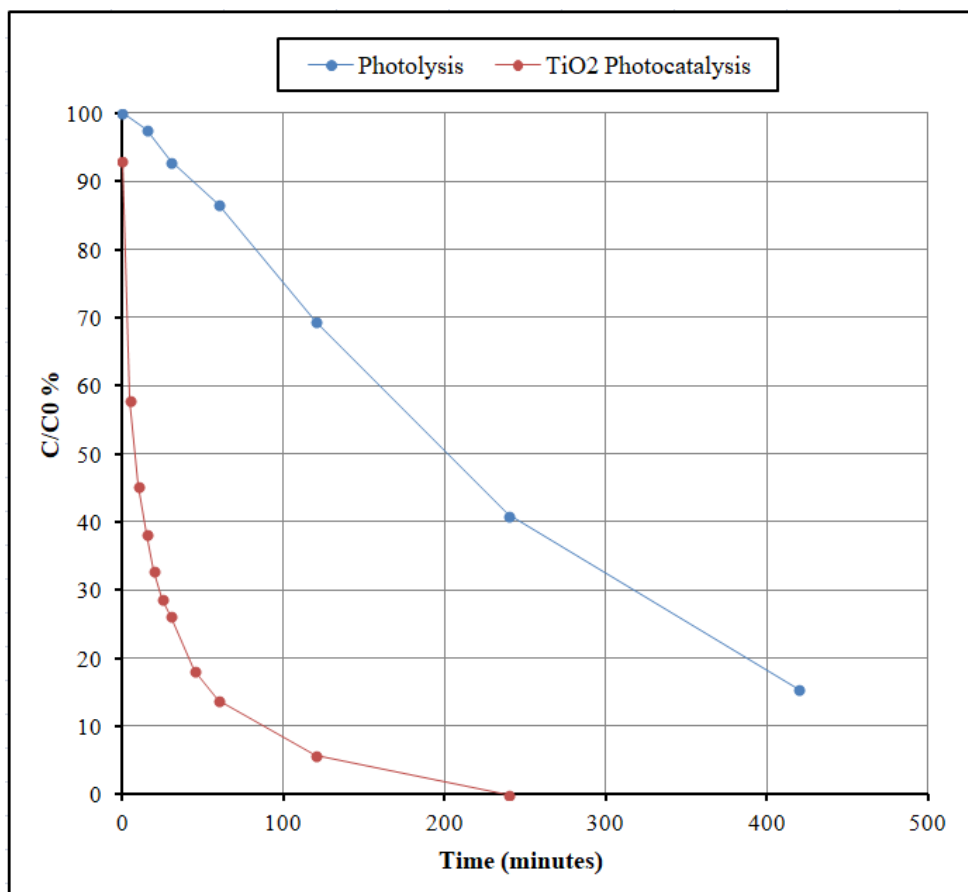


Fig.2.3: Evaluation of LFX degradation measured as $C/C_0\%$ versus irradiation time.

To find the kinetics model, kinetics parameters were calculated using integrated equations describing zero-, first-, and second-order (Langmuir-Hinshelwood) equations (Scrano et al., 1999). According to Snedecor & Cochran, 1989, the least square method should be utilised to find the best fit. Table 2.1 summarises the kinetic parameters of LFX degradation under photolysis and TiO₂ heterogeneous photocatalysis experiments.

Table 2.1: Kinetic parameters of LFX degradation under photolysis and photocatalysis experiments.

System	Reaction Order	Linearised Rate Equation	$(C_{\text{exp}}-C_{\text{calc}})^2$	R^2	$t_{1/2}$ (min)	k
Photolysis	Zero-order	$C_t = C_0 - kt$	1.0706	0.9843	235.30	$0.0218 \text{ mg}\cdot\text{L}^{-1}\cdot\text{min}^{-1}$
	First-order	$\text{Ln } C_t = \text{Ln } C_0 - kt$	3.3859	0.9879	155.75	0.0045 min^{-1}
	Second-order	$C_0/C_t = 1 + (1/t_{1/2})t$	27.8388	0.8632	80.61	$0.0012 \text{ L}\cdot\text{mg}^{-1}\cdot\text{min}^{-1}$
TiO ₂ powder	Zero-order	$C_t = C_0 - kt$	28.1803	0.5649	50.37	$0.0566 \text{ mg}\cdot\text{L}^{-1}\cdot\text{min}^{-1}$
	First-order	$\text{Ln } C_t = \text{Ln } C_0 - kt$	56.0970	0.9182	32.97	0.0210 min^{-1}
	Second-order	$C_0/C_t = 1 + (1/t_{1/2})t$	1.9206	0.9696	8.19	$0.0123 \text{ L}\cdot\text{mg}^{-1}\cdot\text{min}^{-1}$

C_{exp} , experimental concentrations; C_{calc} , the value of concentrations calculated from rate equations; k, kinetic constant; $t_{1/2}$, half-life.

The measured reaction rate of LFX under irradiation conditions using TiO_2 powder as a catalyst was best the fit by a Langmuir-Hinshelwood-type equation:

$$C_t = C_0 t_{1/2}/(t + t_{1/2}) \quad \text{Eq. 2.1}$$

Where C_0 is the initial amount (mg) of LFX per litre of solution, C_t is the remaining concentration at time t , and $t_{1/2}$ is the half-life of the reactant. **Equation 2.1** describes a second-order reaction governed by the kinetic law:

$$v = -dC_t/dt = kC_t^2 \quad \text{Eq. 2.2}$$

where v is the reaction rate, and k is the rate (or kinetic) constant, which in our case can be calculated as:

$$k = 1/(C_0 t_{1/2}) \quad \text{Eq. 2.3}$$

The half-life value for a second-order reaction, calculated using the linearized form of **Equation 2.1** (**Table 2.1**), was just 8.19 minutes. The second-order kinetics shown in **Fig. 2.4A** was confirmed by the linear behaviour of (C_0/C_t) as a function of irradiation time (**Fig. 2.4B**).

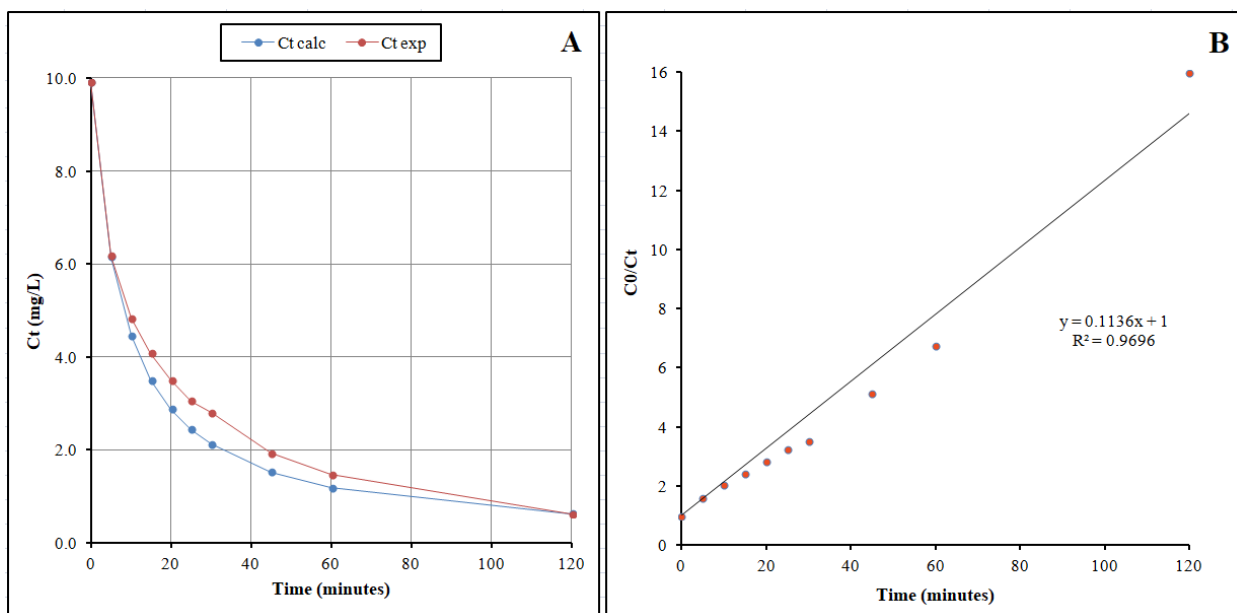


Fig. 2.4: (A) Photodegradation of levofloxacin catalysed by TiO_2 powder; C_t calc, values calculated using **Equation 2.1**; C_t exp, experimental values. (B) The trend of the second-order linearized equation used to estimate kinetic parameters reported in **Table 2.1**.

The results show that the initial degradation rate was high; however, it decreased rapidly as the reaction proceeded. The degradation was fast during the first 30 minutes, and then it gradually decreased; this trend is typical of second-order reactions. Several observations can be related to

such behaviour: (1) the high concentration of LFX at the beginning of the reaction facilitates the practical attack by the hydroxyl radicals, resulting in a high degradation rate; however, when LFX concentration gradually decreases, the degradation rate subsequently decelerates due to the dilution effect that reduces the possibility of valuable collisions with the hydroxyl radicals; (2) the competitive reactions of the hydroxyl radicals with LFX degradation products that are produced during the reaction; (3) the recombination reactions of radical–radical.

2.4 Conclusions

From the results obtained, we can conclude that photocatalysis by using TiO_2 powder removes LFX and its by-products in four hours and seems to follow a second-order kinetic. Still, the photocatalysis with TiO_2 immobilised system could be promising for use in the wastewater treatment field since it is totally clean and does not require an additional post-treatment stage to recover TiO_2 , the main disadvantage of heterogeneous photocatalysis process.

CHAPTER 3

Case study #2: heterogeneous photocatalysis with supported TiO₂ on borosilicate tube for the degradation of levofloxacin in ultrapure water

3.1 Introduction

Since the past decades, immobilisation of titanium dioxide (TiO₂) on different substrates has been drawing a lot of attention because it eliminates the need for expensive post-treatment separation processes. Considering the various substrates that have been tried for supporting TiO₂ photocatalysts, polymer substrate seems to be very promising due to its several advantages such as flexible nature, low-cost, chemical resistance, mechanical stability, low density, high durability and ease of availability. Titanium dioxide is conventionally available in the form of powder. It can be applied to wastewater either as suspended powder or supported over a suitable substrate (**Han and Bai, 2009**). Although in powder form it shows the greater surface area and efficiency, it suffers from the following drawbacks:

- Low light utilisation efficiency of the suspended photocatalyst. This is attributed to the attenuation loss suffered by light rays. It has been reported that less than 1% of UV light or about 20% of visible light penetrates at a depth of 0.5m under the water surface (**Han and Bai, 2010**);
- Post-treatment recovery is both time and money consuming. This is because the catalyst requires a long settling time and efficient solid-liquid (phase) separation techniques (**Byrne et al., 1998; Krýsa et al., 2006**). It also leads to loss of catalyst;
- Unfavourable human health problems are also associated with the mobility of the powder form (**Sriwong et al., 2008**).

To overcome the drawbacks mentioned above, continuous efforts are being made to coat TiO₂ on various substrates. Immobilisation of TiO₂ has the following advantages:

- Easy of post-treatment recovery that would reduce the operational cost when used for large scale practical applications;
- Minimizing catalyst loss;

- Availability of longer contact time of the photocatalyst with pollutants to be degraded.

However, also the immobilisation has a series of drawbacks, such as the reduction in the surface area available for reaction and the need of various suitable techniques involving well-defined procedures and equipment unlike powder form of TiO₂, which is available in “ready to be used form” (Singh et al., 2013).

As said above, to date, most investigations and applications on heterogeneous photocatalysis (TiO₂) have employed the suspension form of semiconducting particles, and the performances of such systems were well documented. Fixation or immobilisation of catalyst over a stationary substrate would circumvent the need for post-treatment stages to recover the catalyst from the reaction mixture. Several research groups have supported TiO₂ on glass beads or glass surfaces in the past years. Both systems exhibited efficacious and stable catalysts for photodegradation of the organic compounds tested (Matthews, 1987; Serpone et al., 1986). In another study, the photocatalytic oxidation of an anionic monoazo dye of acid class was performed over an anatase-TiO₂ catalytic bed in a continuous flow photoreactor system (Behnajady et al., 2007). Some examples of TiO₂ immobilised include immobilisation on alumina, polyvinylidene difluoride, cellulose fibres and glass through various immobilisation techniques, such as sol-gel techniques, chemical vapour deposition, electrospinning and film casting (Bedford et al., 2012; Liu et al., 2012; Romanos et al., 2012). Immobilisation of TiO₂ on rigid substrates is mainly done on the glass due to the system’s transparency obtained after the immobilisation. This can facilitate light penetration, resulting in improved photocatalysis (Chen et al., 2008; Khalaf et al., 2019; Lelario et al., 2016).

In this case study, the immobilisation of TiO₂ over a borosilicate tube has been investigated to assess its potential to remove levofloxacin in the water system. In particular, for photocatalytic experiments we used a TiO₂-coated borosilicate tube, contained into a photochemical reactor, to degrade an initial levofloxacin concentration of 20 mg·L⁻¹, using a continuous flow photoreactor system.

3.2 Experimental section

3.2.1 Chemicals

For chemical analysis, acetonitrile (ACN) and formic acid were LC-MS grade from Honeywell (Wabash, Indiana, US), and water was ultrapure Milli-Q grade (18.2 MΩ cm⁻¹ resistivity at 25°C, VWR European). Analytical standard of levofloxacin (LFX) (purity 99.4%) was

purchased from Lab Instruments S.r.l. (Castellana Grotte, Puglia, Italy). Chemicals were used as received without further purification.

3.2.2 *Experimental devices for photocatalysis in continuous*

Heterogeneous photocatalysis with immobilised TiO_2 on the surface of a borosilicate tube was carried out by using the photochemical reactor shown in **Fig. 3.1A**. The diameter and length of the photochemical reactor are 5 and 19 cm, respectively. The diameter and size of the borosilicate tube inside the photochemical reactor are 3.3 and 14.9 cm, respectively, and the thickness is 3 mm. The photochemical reactor can load up to 420 ml of the treating water. The reacting fluid flows continuously into the photochemical reactor, assembled such as the active coated borosilicate tube that can be fixed inside it. The flow of liquid through the reactor provides both a continuous fresh feed and complete immersion of the TiO_2 -coated tube inside the reactor, and thus, the solution is in contact with both the internal and external surfaces of the tube. A peristaltic pump (Autoclude model V, Velp Scientifica Usmate, Milano, Italy) recirculates the reactant solution from a storage tank to the photochemical reactor placed in the chamber of the solar simulator device (Heraeus-Atlas Suntest CPS+, Chicago, USA) (**Fig. 3.1B**). This device is equipped with a Xenon Arc lamp (1.8 KW), the irradiation source having a light power of 400 W/m^2 , with a spectral wavelength range of 290 - 800 nm. All experiments were done on solutions of levofloxacin with an initial concentration of $20 \text{ mg}\cdot\text{L}^{-1}$ in pure water. The temperature was kept constant ($30.0 \pm 0.1^\circ\text{C}$) using an air conditioning system, and the solutions were maintained under continuous flow, thanks to the peristaltic pump.

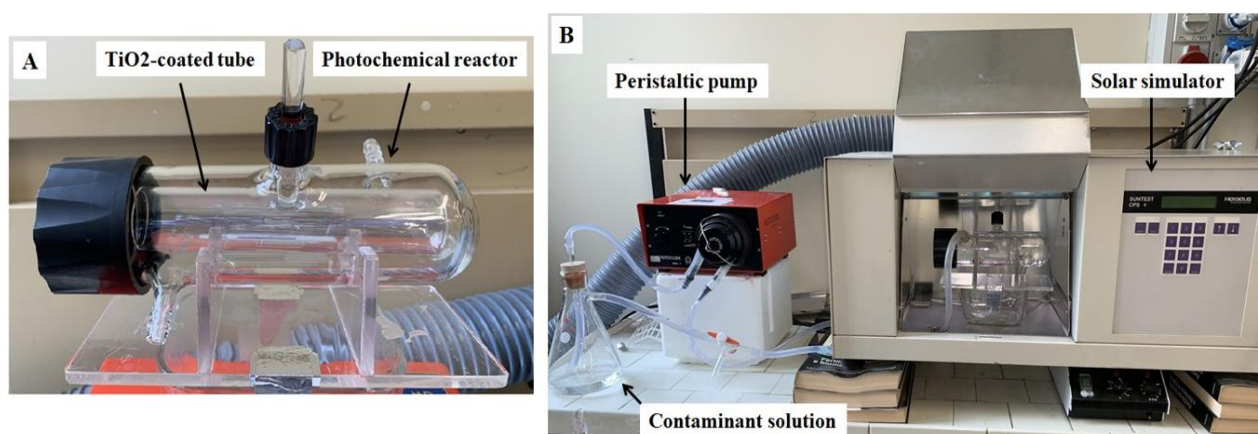


Fig. 3.1: (A) Photochemical reactor used for direct heterogeneous photocatalysis with immobilised TiO_2 , and (B) schematic diagram of the photodegradation system.

3.2.3 *Photolysis and heterogeneous photocatalysis with supported TiO₂*

For photolysis and heterogeneous photocatalysis experiments, a 2000 mg·L⁻¹ stock solution of levofloxacin in methanol was used to prepare 2000 mL of a solution with an initial 20 mg·L⁻¹ concentration in ultrapure water. From this solution, 900 mL were used for photolysis experiments, and the other 900 mL were used for heterogeneous photocatalysis experiments. Both the experiments were carried out using the photochemical reactor shown in **Fig. 3.1A**. Still, in the first case (photolysis), we removed the TiO₂-tube from the reactor and used the same continuous system described previously. All the samples were taken (1 mL for each sample) at determined intervals time and injected into the HPLC-UV system. Finally, selected samples obtained during the entire process were used for acute ecotoxicology assay with MicroTox[®] system on *Vibrio fischeri*, at Water Research Institute (IRSA-CNR) in Taranto (Italy). In contrast, the last sample of each photodegradation test (with and without TiO₂-coated tube) was used for phytotoxicity assays on *Lepidium sativum* and *Solanum lycopersicum*.

3.2.4 *HPLC-UV conditions*

LFX concentration was monitored using a high-performance liquid chromatography (HPLC) system (Agilent Technologies 1200 series, USA) equipped with a Kinetex C18 100Å column (250 x 4.6 mm i.d., 5 µm particle size) and a diode array detector (DAD), set at $\lambda = 295$ nm. The mobile phase consists of a bifasic gradient, ultrapure water with 0.1% formic acid (solvent A) and acetonitrile (solvent B), structured as follows: 0 - 3 min, 0% B; 3 - 5 min, 15% B; 5 - 16 min, 15% B; 16 - 18 min, 100% B; 18 - 22 min, 100% B; 22 - 23 min, 0% B; 23 - 25 min, 0% B. The flow rate is 1.0 mL·min⁻¹, and the injection volume was 20 µL.

3.2.5 *MicroTox[®] bioluminescence assay on Vibrio fischeri*

Selected samples obtained during photolysis and photocatalysis with TiO₂-coated tube were used for acute ecotoxicology assay with MicroTox[®] system (**Fig. 3.2**) on *Vibrio fischeri*. In the case of the photolysis experiment, we selected the samples obtained after 0, 150, 300, 600, 1140 and 1560 minutes of irradiation; in the case of the photocatalysis experiment, we set the samples obtained after 0, 120, 420, 840, 1320, 1980 and 2340 minutes of irradiation. All the samples taken were chosen based on the number of transformation products obtained after the correspondent time of irradiation.

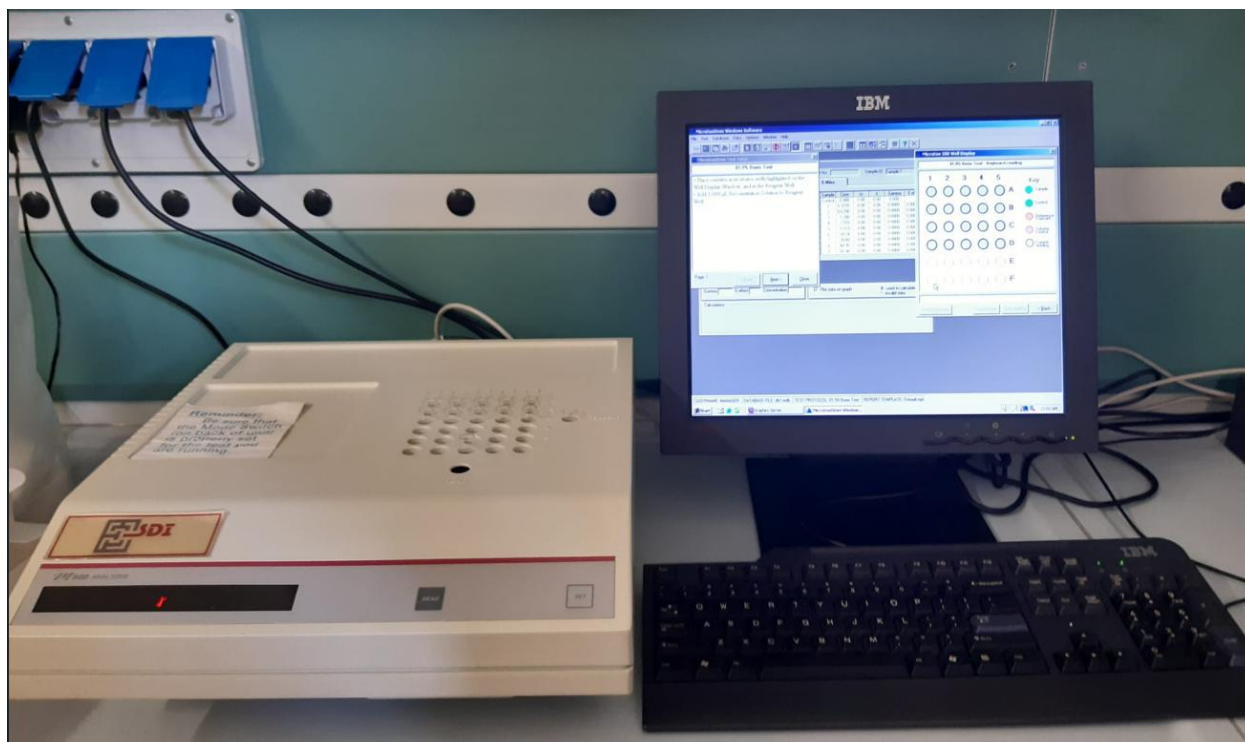


Fig. 3.2: MicroTox system used for bioluminescence assay on *Vibrio fischeri*. Water Research Institute (IRSA-CNR), Taranto (Italy).

The protocol used for bioluminescent assay includes a series of steps:

1. Place cuvettes in incubator wells: A1 through A5, B1 through B5, C1 through C5, D1 through D5, F3 and reagent well;
2. Add 1000 μL reconstitution solution to reagent well;
3. Add 1500 μL diluent to F3;
4. Add 1000 μL diluent to A1 through A5, and C1 through C4 (no diluent in C5);
5. Add 2500 μL investigated sample and 250 μL osmotic adjustment solution (OAS) to C5, and mix; then discard 750 μL to C5 (total volume in C5 = 2000 μL);
6. Make 1:2 serial dilutions by transferring 1000 μL , mixing after each transfer: C5 to C4, C4 to C3, C3 to C2, C2 to C1, C1 to A5, A5 to A4, A4 to A3, A3 to A2 (no sample in A1); then discard 1000 μL to A2 and wait 5 minutes (total volume in all wells = 1000 μL);
7. Reconstitute a vial of MicroTox[®] Acute Toxicity Reagent in the following way:
 - Remove a single vial of reagent from the freezer and open it with the minimum of handling, thereby reducing warming of the vial;
 - Shake and tap the vial gently to ensure the pellet of bacteria is seated on the bottom of the vial;

- Take the precooled cuvette of reconstitution solution from the Reagent well, then quickly pour the solution into the opened vial;
 - Swirl the vial 3 or 4 times, then quickly pour the mixture back into the cuvette and return it to the Reagent well;
 - Mix the bacteria thoroughly using the pipettor by aspirating and dispensing 0.5 mL of solution at least ten times.
8. Transfer 150 μL reagent (reconstituted bacteria) to F3 and mix;
 9. Add 100 μL diluted reagent (reconstituted bacteria) to B1 through B5 and D1 through D5; then wait 15 minutes;
 10. Place B1 cuvette in READ well, then press the SET button;
 11. READ zero time I_0 light levels as prompted by the computer monitor: B1, B2, B3, B4, B5, D1, D2, D3, D4, D5;
 12. Immediately add 900 μL of diluted samples from lanes A to B and from C to D: A1 to B1, A2 to B2, A3 to B3, A4 to B4, A5 to B5, C1 to D1, C2 to D2, C3 to D3, C4 to D4 and C5 to D5;
 13. Read the light levels of all samples after 5, 15 and 30 minutes of exposure to diluted samples.

3.2.6 *Phytotoxicity assays on *Lepidium sativum* and *Solanum lycopersicum**

A standard solution of levofloxacin at concentration $20 \text{ mg}\cdot\text{L}^{-1}$ and the last sample of each photodegradation experiments (with and without TiO_2 -coated tube) were used for phytotoxicity assays on *Lepidium sativum* and *Solanum lycopersicum*: the sample obtained after 1560 minutes of irradiation in the case of photolysis and the sample obtained after 2340 minutes of irradiation in the case of photocatalysis with supported TiO_2 . The samples were tested as they are and after a 1:2 dilution.

The bioassay was based on seed germination (SG) and roots elongation (RE). It was carried out to evaluate the possible phytotoxic effect of levofloxacin and its transformation products on *Solanum lycopersicum* L. (tomatoes) and *Lepidium sativum* L. (garden cress) seeds (Ceglie et al., 2011; Elshafie et al., 2019). Seeds were sterilised in 3% H_2O_2 solution for 1 min and then were rinsed twice with deionised sterile water (dH_2O). Seeds were put either in dH_2O (control), or the solutions collected during the degradation treatments and were shaken gently for 2 hours. All seeds were subsequently transferred into 15 mm \times 100 mm Petri dishes containing one piece of filter paper (\O 90 mm, Whatman No.1). Ten seeds of each species were evenly spaced on top

of the filter paper in each Petri dish, filled with 2 mL of dH₂O or treatment solutions, and sealed with parafilm. All Petri dishes were incubated in a growth chamber at 24 ± 2°C with 60% relative humidity in dark conditions for four days. The number of germinated seeds was counted, and length of the roots was measured in cm. The experiment was conducted in triplicate, and the germination index (GI) was calculated using the formula:

$$\text{G.I. \%} = [(SG_t \times RE_t) / (SG_c \times RE_c)] \times 100$$

where: GI: germination index; SG_t: average number of germinated treated seeds; RE_t: average root elongation for treated seeds; SG_c: average number of germinated seeds for dH₂O control; RE_c: average radical elongation for dH₂O control. Data are expressed as the mean ± SDs for the number of germinated seeds, radicle elongation and germination index. Data were analysed using SPSS statistical program with Tukey test at $P < 0.05$.

3.3 Results and discussion

3.3.1 Kinetic study

Photolysis (without TiO₂-coated tube) and heterogeneous photocatalysis (with TiO₂-coated tube) of a levofloxacin solution with an initial concentration of 20 mg·L⁻¹ was carried out under artificial irradiation simulating solar light. Before undertaking the LFX photodegradation studies, a control experiment was carried out under dark conditions. No degradation was observed. The degradation profile of levofloxacin during photolysis and heterogeneous photocatalysis reactions was monitored using High-Performance Liquid Chromatography - Ultra Violet (HPLC-UV). **Fig. 3.3** illustrates the degradation behaviour during the experiments.

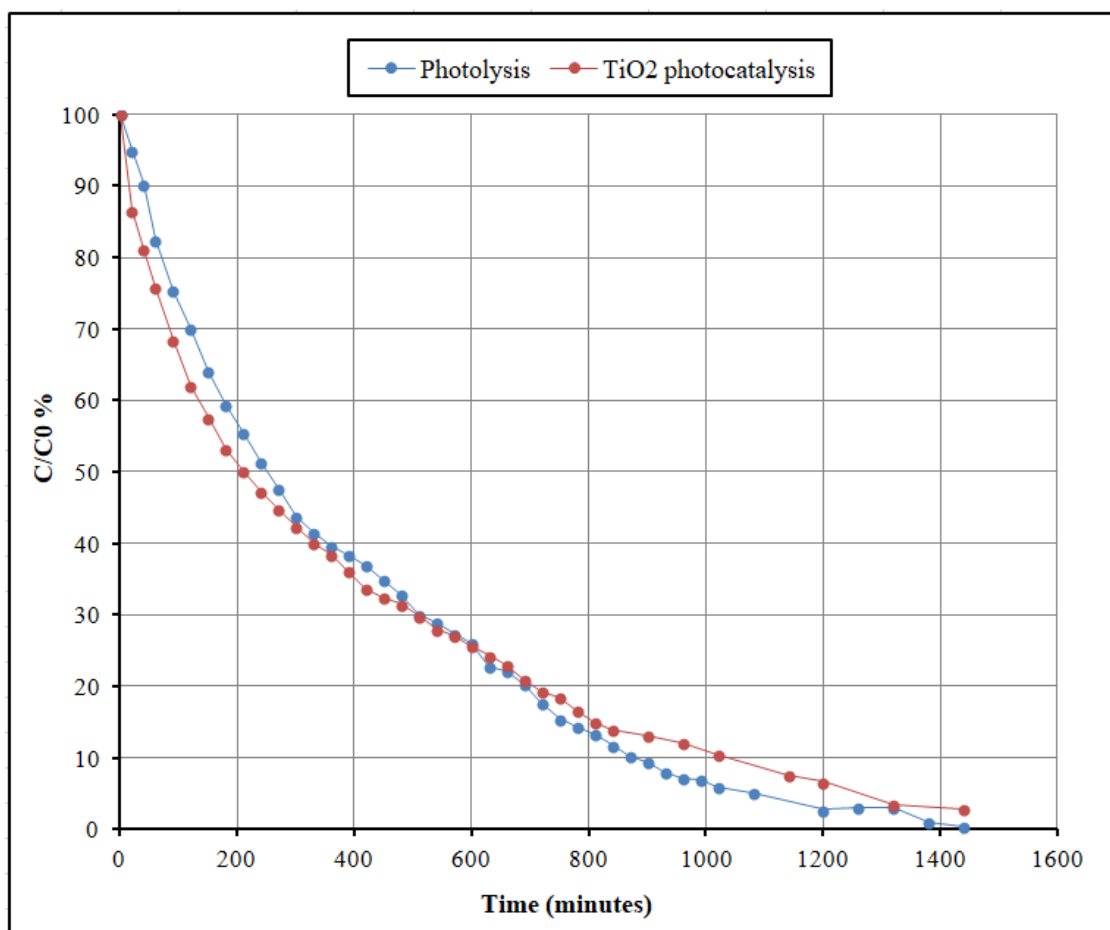


Fig. 3.3: Evaluation of LFX degradation measured as $C/C_0\%$ versus irradiation time.

The direct irradiation of the levofloxacin solution was conducted for almost 40 h with regular sampling at determined intervals time. HPLC-UV analysis show a gradual degradation for levofloxacin and a steady decrease in the concentrations versus the time of irradiation. Kinetic parameters are summarised in **Table 3.1**.

Table 3.1: Kinetic parameters of LFX degradation under photolysis and supported-TiO₂ photocatalysis experiments.

System	Reaction Order	Linearised Rate Equation	$(C_{\text{exp}} - C_{\text{calc}})^2$	R^2	$t_{1/2}$ (min)	k
Photolysis	Zero-order	$C_t = C_0 - kt$	202.10	0.8499	785.40	$0.0131 \text{ mg}\cdot\text{L}^{-1}\cdot\text{min}^{-1}$
	First-order	$\ln C_t = \ln C_0 - kt$	50.01	0.9417	227.78	0.0030 min^{-1}
	Second-order	$C_0/C_t = 1 + (1/t_{1/2})t$	1750.88	0.2359	16.55	$0.00294 \text{ L}\cdot\text{mg}^{-1}\cdot\text{min}^{-1}$
TiO ₂ -coated tube	Zero-order	$C_t = C_0 - kt$	179.56	0.8096	574.02	$0.0129 \text{ mg}\cdot\text{L}^{-1}\cdot\text{min}^{-1}$
	First-order	$\ln C_t = \ln C_0 - kt$	90.824	0.9856	314.06	0.0022 min^{-1}
	Second-order	$C_0/C_t = 1 + (1/t_{1/2})t$	573.327	0.5898	64.33	$0.0007 \text{ L}\cdot\text{mg}^{-1}\cdot\text{min}^{-1}$

C_{exp} , experimental concentrations; C_{calc} , the value of concentrations calculated from rate equations; k , kinetic constant; $t_{1/2}$, half-life.

Due to their similar degradation trend, both photolysis and photocatalysis degradations seem to be modelled with a first-order kinetic as in **Eq. 3.1**.

$$\ln(C_t) = \ln(C_0) - k \cdot t \quad \text{Eq. 3.1}$$

The plot of $\ln(C_t)$ versus irradiation time (where C is the concentration of the compound at time t , C_0 is its initial concentration) provides an almost straight line (**Fig. 3.4B**), which suggests the first-order kinetics of the photocatalysis reaction (**Fig. 3.4A**). The reaction rate constant (k) was determined from the slope of the straight line and the reaction half time ($t_{1/2}$) as in **Eq. 3.2**.

$$t_{1/2} = (\ln 2) / k \quad \text{Eq. 3.2}$$

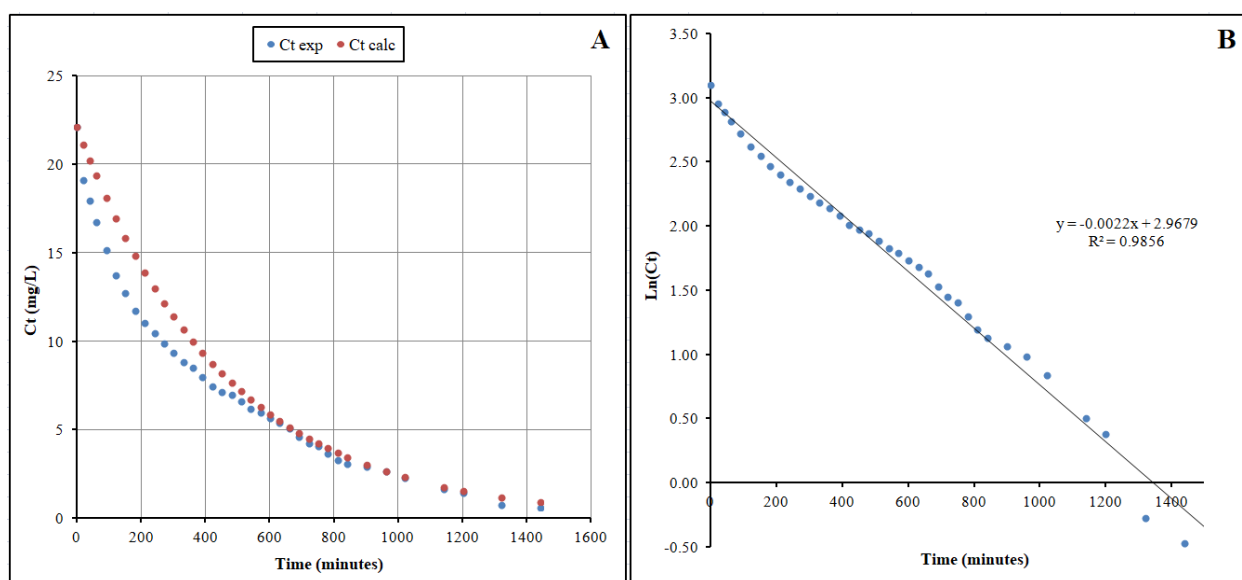


Fig. 3.4: (A) Photodegradation of levofloxacin catalysed by TiO_2 -coated tube; C_t calc, values calculated using **Equation 3.1**; C_t exp, experimental values. (B) The trend of the first-order linearized equation used to estimate kinetic parameters reported in **Table 3.1**.

In photocatalysis processes, the amount of the catalyst is an essential factor. Kinetic results demonstrated that the amount of coated TiO_2 was not sufficient to improve the levofloxacin degradation in this case. The only action of the solar irradiation gives the half time of 223 minutes; it means that 50% of the target compound was degraded at this time. Instead, with the presence of titanium dioxide, the degradation is slower and the half-life is reached after more than 300 minutes of irradiation. Coated catalyst technology is applied to avoid after treatment a filtration step and to be able to reuse the catalyst that will reduce the cost of using technologies. Several scientific works reported the efficiency of TiO_2 , coated on ceramic plates by sol-gel method for the photocatalytic degradation of atenolol, chlorpromazine and metronidazole (**Khataee et al., 2013**), or on spinning disk reactors for the removal of antipyrine (**Expósito et**

al., 2017). However, sometimes happens that the quantity of catalyst is not sufficient to improve the processes. This can be explained by the fact that when catalysts are coated on materials, they cannot adequately absorb visible radiation. In addition, this is a fundamental limitation for this process because the choice of titanium dioxide is given precisely by its ability to absorb solar radiation and make this technology low cost. Moreover, another negative consequence of the slow kinetics of degradation is the persistence and co-presence of many degradation products that may be more toxic than the parent compound. It was necessary to go deeper on this aspect, and phytotoxicity on *Lepidium sativum* and *Solanum lycopersicum* and toxicity evaluation on *Vibrio fischeri* were investigated.

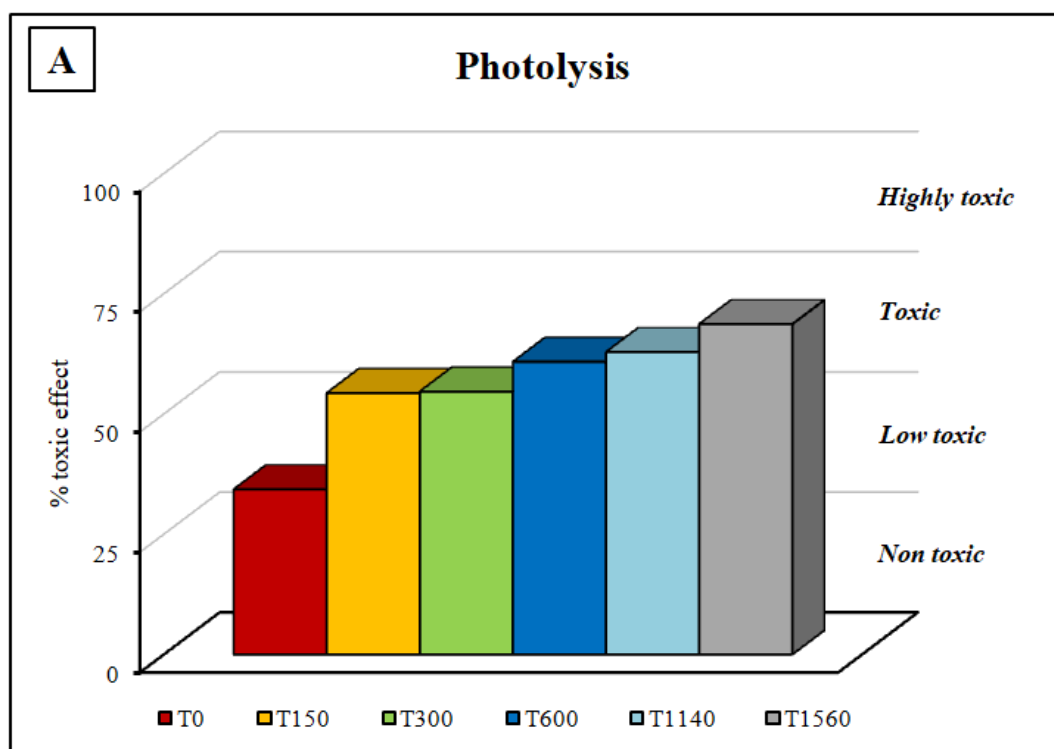
3.3.2 *Vibrio fischeri* toxicity evaluation

Toxicological analysis of water solutions is a method of assessing the biological effect of the tested samples and leads to an indirect assessment of the formation of oxidation by-products of the tested parent compound. Toxicity evaluation about the applied treatment was obtained using the MicroTox[®] acute toxicity test developed by IRSA-CNR (Taranto), based on the inhibition of the bioluminescence of the Gram- *Vibrio fischeri* bacterium. The method involves using a bacterial suspension obtained by dispersing a vial of freeze-dried bacteria in 1 mL of an isotonic reconstitution solution. Then, 150 μL of reconstituted bacteria were mixed with a diluent solution, and, finally, an aliquot (100 μL) was placed in selected MicroTox[®] wells. Simultaneously, serial 1:2 dilutions of each sample tested were prepared to observe a concentration-dependent response (these data are available as *supplementary material* at the end of this chapter). Then 900 μL of each dilution were added to the bacteria to test their toxicity after 5, 15 and 30 minutes of exposure. Firstly, the influence of the tested antibiotic water solutions, before its treatment in selected oxidation processes, on the indicator organisms was tested. In the case of the photolysis experiment, the samples tested were obtained after 0, 150, 300, 600, 1140 and 1560 minutes of irradiation; in the case of the TiO₂-coated tube photocatalysis experiment, the samples tested were obtained after 0, 120, 420, 840, 1320, 1980 and 2340 minutes of irradiation. **Table 3.2** and **Fig. 3.5** present the obtained results of the toxicological assessment and the classification of water samples to toxicological classes. **Santana et al. (2009)** proposed four classes of solution toxicity. Water solutions, which incurs an inhibition of bacterial bioluminescence of over 75% are classified as highly toxic. The levofloxacin water solution was characterised by low toxicity (35%).

Table 3.2: Percentage (%) of toxic effect after 30 minutes of exposure to the samples obtained from photolysis and TiO₂-coated tube photocatalysis experiments and toxicity classification.

Photolysis	% Effect (after 30 minutes of exposure)	Toxicity classification
T0 ($C_{LFX} = 20.56 \text{ mg}\cdot\text{L}^{-1}$)	34.30 %	<i>Low toxic</i>
T150 ($C_{LFX} = 13.18 \text{ mg}\cdot\text{L}^{-1}$)	54.34 %	<i>Toxic</i>
T300 ($C_{LFX} = 9.012 \text{ mg}\cdot\text{L}^{-1}$)	54.64 %	<i>Toxic</i>
T600 ($C_{LFX} = 5.36 \text{ mg}\cdot\text{L}^{-1}$)	60.83 %	<i>Toxic</i>
T1140 ($C_{LFX} = 0.81 \text{ mg}\cdot\text{L}^{-1}$)	62.85 %	<i>Toxic</i>
T1560 ($C_{LFX} = 0 \text{ mg}\cdot\text{L}^{-1}$)	68.66 %	<i>Toxic</i>
Photocatalysis with TiO₂-coated tube		
T0 ($C_{LFX} = 22.08 \text{ mg}\cdot\text{L}^{-1}$)	35.95 %	<i>Low toxic</i>
T120 ($C_{LFX} = 13.71 \text{ mg}\cdot\text{L}^{-1}$)	41.38 %	<i>Low toxic</i>
T420 ($C_{LFX} = 7.45 \text{ mg}\cdot\text{L}^{-1}$)	52.70 %	<i>Toxic</i>
T840 ($C_{LFX} = 3.09 \text{ mg}\cdot\text{L}^{-1}$)	75.84 %	<i>Highly toxic</i>
T1320 ($C_{LFX} = 0.76 \text{ mg}\cdot\text{L}^{-1}$)	86.47 %	<i>Highly toxic</i>
T1980 ($C_{LFX} = 0 \text{ mg}\cdot\text{L}^{-1}$)	97.15 %	<i>Highly toxic</i>
T2340 ($C_{LFX} = 0 \text{ mg}\cdot\text{L}^{-1}$)	98.72 %	<i>Highly toxic</i>

The results reported in **Table 3.2.** are graphically represented in **Fig. 3.5A** and **Fig. 3.5B.**



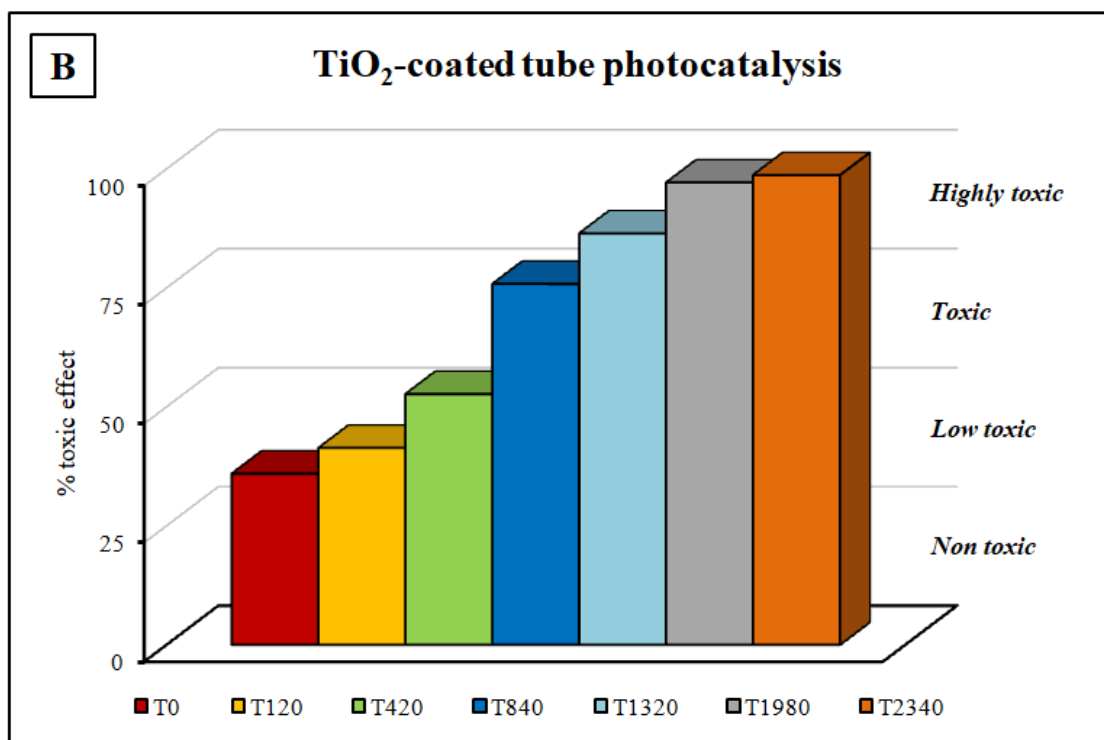


Fig. 3.5: Percentage of toxic effect after 30 minutes of exposure to the samples obtained from (A) photolysis and (B) TiO₂-coated tube photocatalysis experiments.

The treatment of levofloxacin water solutions in chosen oxidation processes resulted in an increase in their toxicity. **Figure 3.5** summarises the toxic effect of the treated water solution during photolysis and photocatalysis using coated TiO₂. The highest toxicity increase was observed for the LFX after the TiO₂ process, which incurred an inhibition of bacterial bioluminescence of over 99%.

The significant increase in the toxicity of the levofloxacin solution after the proposed treatments may result from the formation of several by-products. A similar trend was observed by (**El Najjar et al., 2013**): although quinolones exhibited limited acute toxicity to *V. fischeri*, an acute toxicity elevation was observed after chlorination treatment on levofloxacin, which was attributed to the formation of toxic transformation products. Furthermore, **Yamashita et al. (2006)** already reported in their study that light emission released from luminescent bacterium was not reduced, which meant that levofloxacin had a little toxic effect at the highest concentration tested (8.2 mg/L), thus confirming that the high increase in the toxicity observed from our results may be attributed to the presence toxic by-products. In addition, the slow kinetics degradation observed under TiO₂-coated tube photocatalytic processes allows the coexistence of many of them, increasing the toxicity.

Calza et al. (2008) and **Juretic et al. (2013)** reported that dihydroxy-derivatives of some organic compounds with their corresponding quinone structure are more toxic than their monohydroxy-

precursors. Moreover, open ring by-products are generally less toxic than aromatic compounds (Milovac et al., 2014). Another possible cause of the increase in toxicity, may be the detachment of titanium dioxide nanoparticles from the surface of the TiO₂-coated tube. The toxicity of TiO₂ on living organisms and in aquatic environment was confirmed from Hou et al., 2019 and Sharma, 2009.

In general, the oxidation of micropollutants does not lead to complete mineralisation and the formed products are still biologically active compounds; for this reason, the toxicity information has to be complete also with a phytotoxicity test.

3.3.3 Phytotoxicity evaluation

In order to compare the phytotoxicity between untreated and post-treatment, toxicity endpoint and global phytotoxicity were determined on *Lepidium sativum* and *Solanum lycopersicum*. Data of germinated seeds and root elongation for each concentration of untreated (LFX 20 mg·L⁻¹) and post-treated (after 1560 minutes of treatment for photolysis and 2340 minutes for TiO₂-coated tube photocatalysis) were used to determine three phytotoxicity indexes: seed germination (SG), root elongation (RE) and relative growth index (RGI). SG and RE were calculated using equations Eq. 3.3 and Eq. 3.4 respectively, according to Bagur-González et al. (2011). Values of these indexes were used to classify each concentration as causing low, moderate, high or very high toxicity. Currently, there is no unified approach regarding the use of these indexes, as different authors select which to use according to the specific aim of each evaluation.

$$SG = \frac{(GS-GC)}{GC} \quad \text{Eq. 3.3}$$

$$RE = \frac{(RS-RC)}{RC} \quad \text{Eq. 3.4}$$

The control complied with the established criteria for quality controls, hence the toxicity test was deemed valid. In fact, the coefficient of variation of root elongation was 1.0 ± 0.0 cm and the percentage of germinated seeds was 100 ± 0.0% using both plants.

The untreated solution containing 20 mg·L⁻¹ of levofloxacin inhibited seed germination at 60 ± 0.0% and 10 ± 0.0% in *L. sativum* and *S. Lycopersicum*, respectively shown in Table 3.3 and Fig. 3.6 and Fig. 3.7. The inhibition of seed germination is related to the stress caused by pollutants present in a water solution that penetrate the seed and affect its metabolism (Aguar et al., 2016). In addition, the increased seed germination percentage after two proposed treatments, indicated that both AOPs could remove or mitigate the number of pollutants harmful to germination, especially for *S. Lycopersicum*.

Table 3.3: Results of phytotoxicity assays against *Lepidium sativum* and *Solanum lycopersicum*.

		The concentration of the sample ($\text{mg}\cdot\text{L}^{-1}$)	Seed germination (%)	Radical elongation (cm)	Growth index (%)
<i>L. sativum</i>	LFX t_0 min	20	$60.0 \pm 7.5c$	$9.7 \pm 4.1bc$	$0.19 \pm 0.05c$
	LFX t_{1560} min (photolysis)	Taken as it is	$80.0 \pm 5.4b$	$10.4 \pm 1.4bc$	$0.26 \pm 0.07c$
	LFX t_{2340} min (TiO_2 -coated photocatalysis)	Taken as it is	$100.0 \pm 0.0a$	$5.1 \pm 0.8b$	$0.22 \pm 0.03b$
	CONTROL	H_2O	$100.0 \pm 0.0a$	$25.1 \pm 1.7a$	$1.0 \pm 0.0a$
<i>S. lycopersicum</i>	LFX t_0 min	20	$10.0 \pm 2.4c$	$0.42 \pm 0.80d$	$0.0 \pm 0.0d$
	LFX t_{1560} min (photolysis)	Taken as it is	$50.0 \pm 3.1b$	$0.74 \pm 0.70d$	$0.03 \pm 0.00d$
	LFX t_{2340} min (TiO_2 -coated photocatalysis)	Taken as it is	$50.0 \pm 4.2ab$	$2.0 \pm 1.9b$	$0.09 \pm 0.02c$
	CONTROL	H_2O	$100.0 \pm 0.0a$	$15.11 \pm 1.80a$	$1.0 \pm 0.0a$

All values are recorded as the average values of three replicates.

Values followed by the different letters in each vertical column for each tested plant are significantly different according to the Tukey B test at $P < 0.05$.

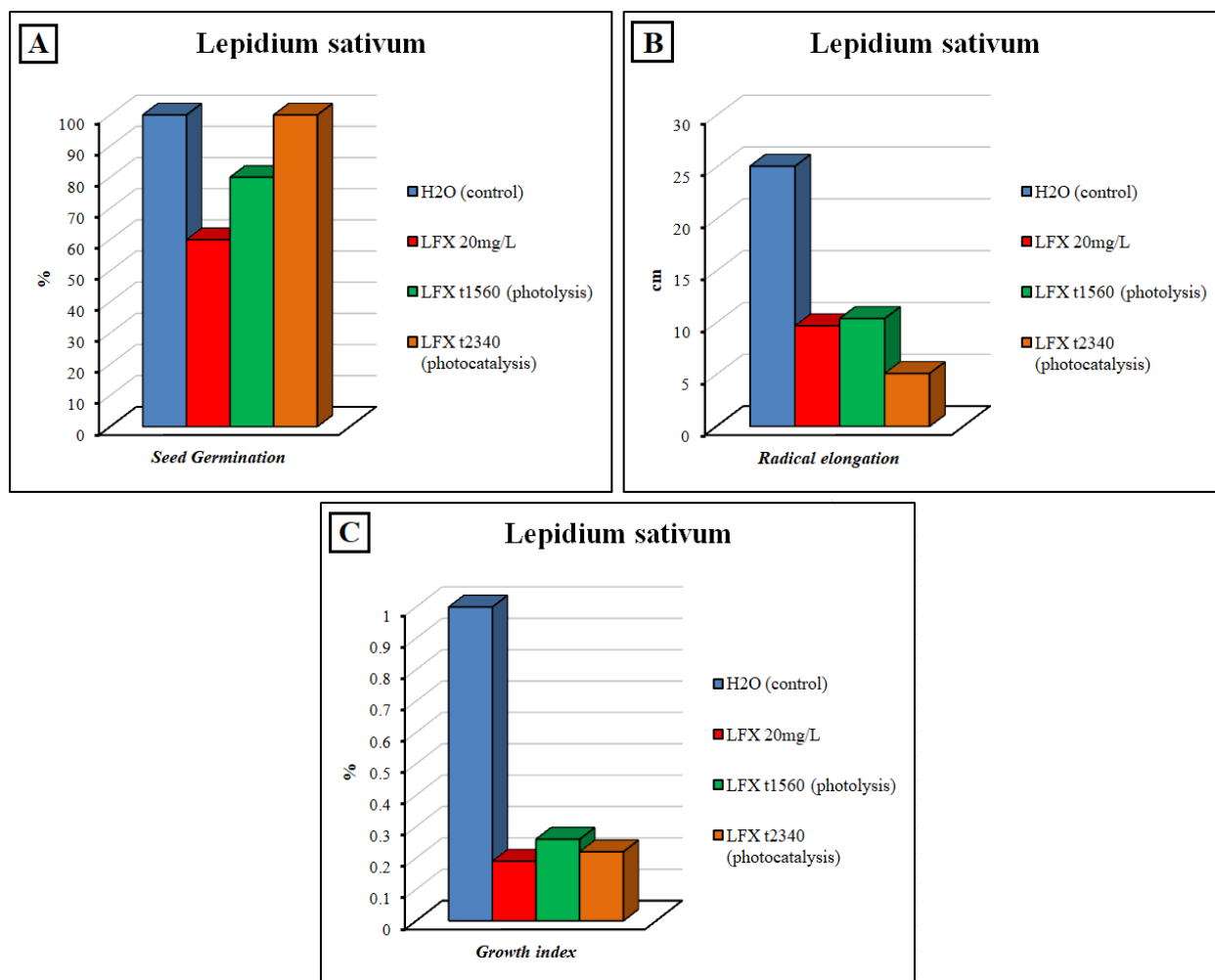


Fig. 3.6: Effect of the tested samples on **A)** seed germination, **B)** radical elongation, **C)** growth index of *Lepidium sativum*.

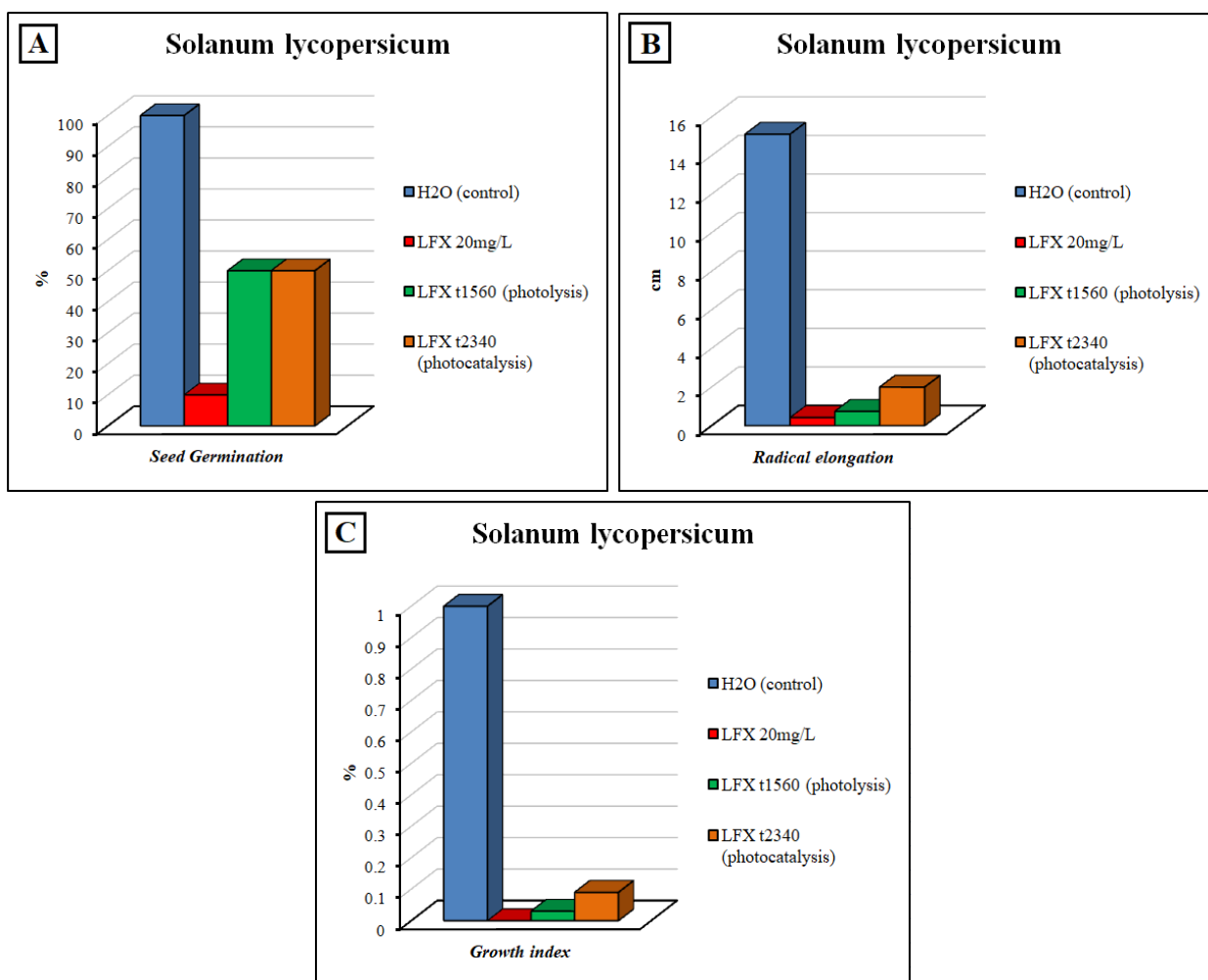


Fig. 3.7: Effect of the tested samples on **A)** seed germination, **B)** radical elongation, **C)** growth index of *Solanum lycopersicum*.

An increase in the inhibition of root elongation by using coated-TiO₂ on *L. sativum* was observed in the present study. This effect is represented by not only RE but also GI phytotoxicity indexes. Due to the low inhibition on seed germination (20% under photolysis and 0% using coated TiO₂), growth index (GI) show inhibition at the same concentrations for both AOP applied. Root elongation inhibition turned out to be a more sensitive biological response than seed germination inhibition. These results coincide with those reported by **Pan & Chu (2016)**. Seedling growth may be affected by reduced adsorption of the compounds necessary for development, caused by inhibition of cell division in the root (**Pan & Chu, 2016**).

A different response was observed using *S. Lycopersicum*. The sensitivity of this species is more sensitive, but in general, the behaviour is similar, but it is not highly sensitive on root elongation.

3.4 Conclusions

The present study demonstrates that the degradation of levofloxacin using coated TiO₂ on the surface of a borosilicate tube was not an efficient treatment, as we initially supposed. The kinetic results showed that the applied treatment was slower than the natural photolysis under simulated solar radiation, giving an half time of 300 minutes and 223 minutes, respectively. Moreover, due to their similar degradation trend, both photolysis and photocatalysis degradations seem to be modelled with a first-order kinetic. Using a simple tool like the toxicity test using *Vibrio fischeri* and test seed inhibition of germination and root elongation allowed assessing the quality and effectiveness of the effluent treatment systems. The results obtained from the ecotoxicity tests on *Vibrio fischeri* demonstrated that the treatment of levofloxacin water solutions in chosen oxidation processes resulted in an increase in their toxicity. The highest toxicity increase was observed after the treatment with the TiO₂-coated tube. In particular, the last two samples obtained from photocatalysis experiment after 1980 and 2340 minutes of irradiation showed 97.15% and 98.72% of bioluminescence inhibition, respectively. This unexpected result has been attributed to the probable detachment of titanium dioxide nanoparticles from the surface of the tube, whose toxicity is also being confirmed by the European Food Safety Authority (EFSA). An increase in the toxicity was also observed with phytotoxicity tests, because the final sample obtained from photolysis and TiO₂-coated tube photocatalysis treatments showed an inhibition in seed germination, roots elongation and growth index in both the plants tested. This suggests that effluent toxicity from these processes must be reduced using another potential treatment that could also accelerate the kinetic degradation of the process.

3.5 Supplementary material

This section reports all concentration-dependent toxicity plots (from **Fig. 3.8** to **Fig. 3.20**) for each sample tested, obtained by MicroTox analysis, some chromatograms obtained from HPLC-UV analysis (**Fig 3.21** and **Fig 3.22**), for photolysis and TiO₂-coated tube photocatalysis experiments, and the list of transformation products obtained from these two processes, based on retention time observed by HPLC-UV analyses (**Table 3.4**). For the *Vibrio fischeri* toxicity assessment through the MicroTox system, each sample was diluted by 1:2 serial dilutions for the analyses. The LFX concentration in the actual sample obtained from photolysis and TiO₂-coated tube photocatalysis experiments is indicated in all tables as 81.90, followed by all 1:2 dilutions.

Photolysis: t0			
Concentration	% effect (5 min)	% effect (15 min)	% effect (30 min)
0.3199	-0.9219	0.1845	-0.3423
0.6398	1.757	1.744	1.734
1.28	-0.0288	0.1845	-1.034
2.559	3.043	2.378	-0.8442
5.119	-0.223	-3.35	-6.443
10.24	2.17	-3.723	3.893
20.48	4.79	0.0902	21.49
40.95	7.722	2.676	28.50
81.9	14.33	5.92	34.30

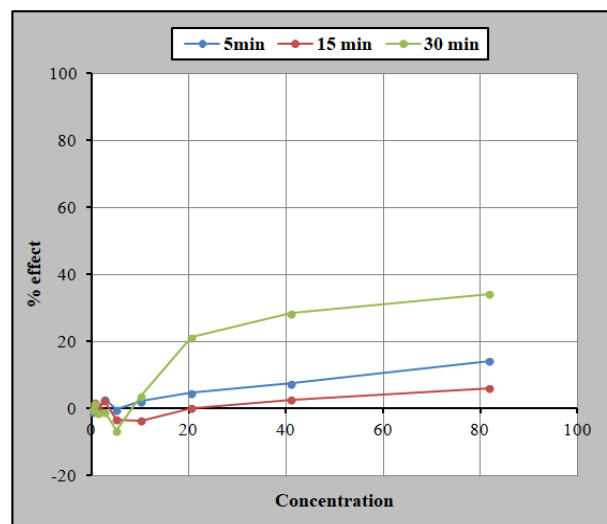


Fig. 3.8: Toxicity results of the T0 sample ($C_{LFX} = 20.56 \text{ mg}\cdot\text{L}^{-1}$).

Photolysis: t150			
Concentration	% effect (5 min)	% effect (15 min)	% effect (30 min)
0.3199	7.634	6.569	6.849
0.6398	13.85	10.76	10.54
1.28	8.984	6.008	6.085
2.559	12.95	7.065	6.727
5.119	15.45	10.76	8.388
10.24	17.47	11.75	15.6
20.48	24.4	18.01	24.72
40.95	30.46	23.8	37.6
81.9	48.12	40.82	54.34

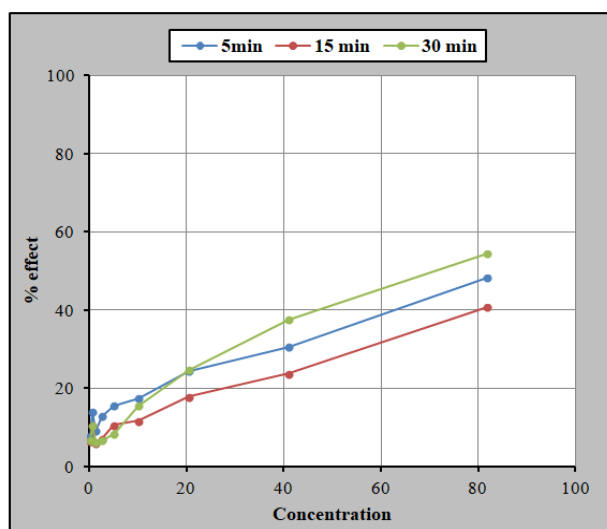


Fig. 3.9: Toxicity results of the sample obtained after 150 minutes of irradiation in the photolysis experiment (T150; $C_{LFX} = 13.18 \text{ mg}\cdot\text{L}^{-1}$).

Photolysis: t300			
Concentration	% effect (5 min)	% effect (15 min)	% effect (30 min)
0.3199	-3.548	-3.079	-0.2165
0.6398	0.5132	2.544	6.636
1.28	-0.0578	-0.1389	4.023
2.559	0.8087	-0.4219	2.809
5.119	4.798	2.02	7.67
10.24	9.97	6.24	7.481
20.48	21.01	19.31	26.24
40.95	32.37	27.34	41.07
81.9	48.97	40.85	54.645

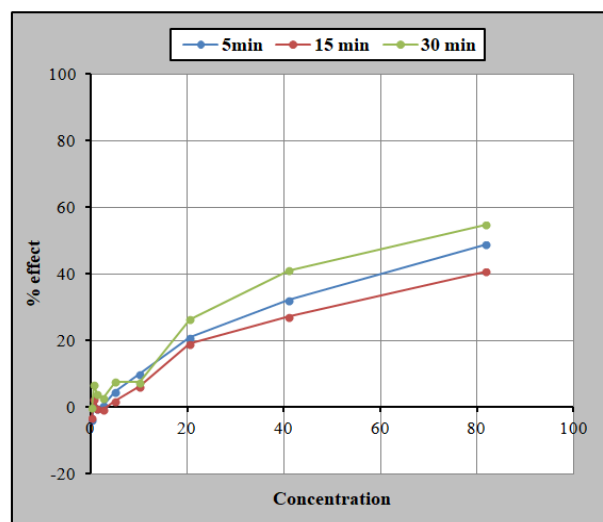


Fig. 3.10: Toxicity results of the sample obtained after 300 minutes of irradiation in the photolysis experiment (**T300**; $C_{LFX} = 9.012 \text{ mg}\cdot\text{L}^{-1}$).

Photolysis: t600			
Concentration	% effect (5 min)	% effect (15 min)	% effect (30 min)
0.3199	4.095	6.469	2.502
0.6398	4.616	6.862	2.748
1.28	7.003	7.612	5.943
2.559	12.87	13.76	10.57
5.119	11.09	11.86	8.475
10.24	22.69	23.61	18.31
20.48	37.18	33.6	30.17
40.95	49.2	44.12	47.02
81.9	69.54	64.88	60.835

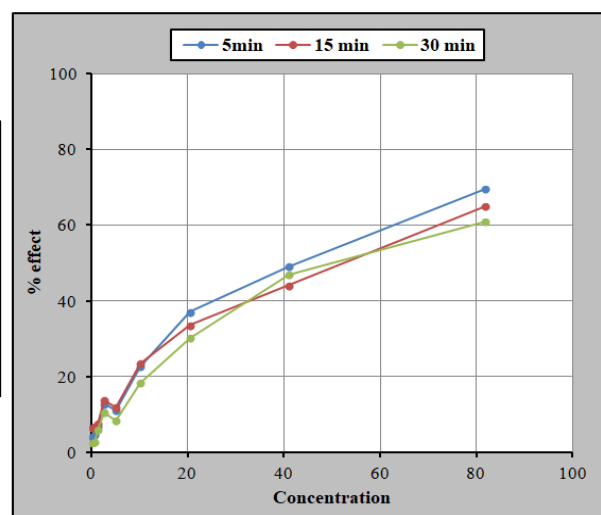


Fig. 3.11: Toxicity results of the sample obtained after 600 minutes of irradiation in the photolysis experiment (**T600**; $C_{LFX} = 5.36 \text{ mg}\cdot\text{L}^{-1}$).

Photolysis: t1140			
Concentration	% effect (5 min)	% effect (15 min)	% effect (30 min)
0.3199	9.784	5.499	5.976
0.6398	0.1181	-2.807	-4.965
1.28	1.214	-0.01	0.1436
2.559	2.893	-0.0774	-0.6275
5.119	13.79	7.733	9.359
10.24	19.51	15.29	13.96
20.48	38.04	31.77	28.87
40.95	55.22	46.05	42.56
81.9	65.82	64.34	62.85

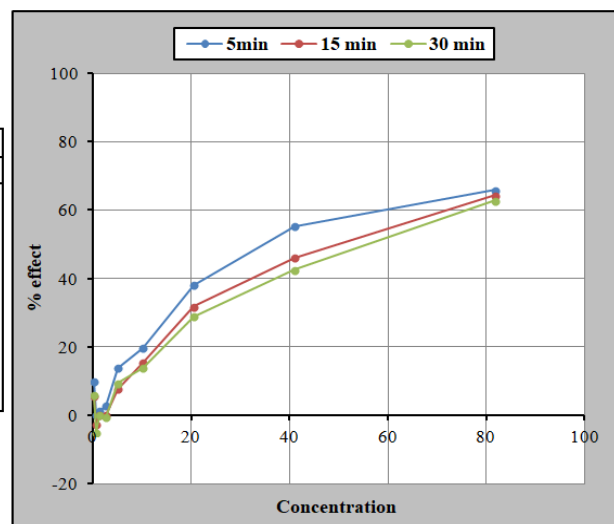


Fig. 3.12: Toxicity results of the sample obtained after 1140 minutes of irradiation in the photolysis experiment (T1140; $C_{LFX} = 0.81 \text{ mg}\cdot\text{L}^{-1}$).

Photolysis: t1560			
Concentration	% effect (5 min)	% effect (15 min)	% effect (30 min)
0.3199	8.148	8.392	12.58
0.6398	6.603	4.869	9.215
1.28	15.12	12.99	15.7
2.559	22.05	19.72	18.01
5.119	24.77	23.63	23.8
10.24	37.92	33.78	34.14
20.48	51.35	45.17	44.53
40.95	65.7	58.43	56.76
81.9	75.58	68.07	68.66

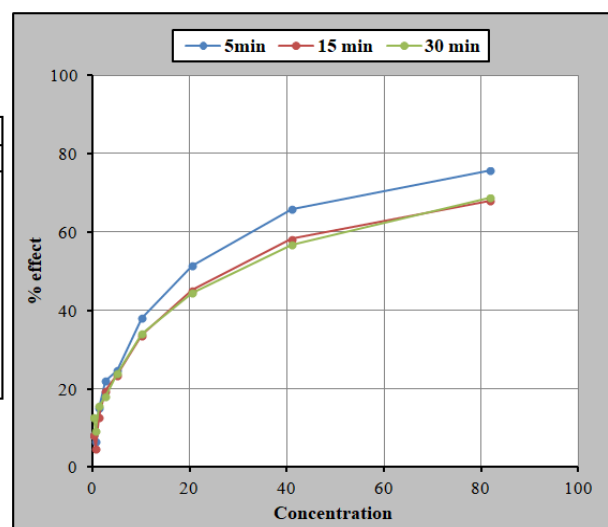


Fig. 3.13: Toxicity results of the sample obtained after 1560 minutes of irradiation in the photolysis experiment (T1560; $C_{LFX} = 0 \text{ mg}\cdot\text{L}^{-1}$).

TiO ₂ -coated tube: t0			
Concentration	% effect (5 min)	% effect (15 min)	% effect (30 min)
0.3199	10.53	10.18	9.508
0.6398	13.64	11.89	9.56
1.28	14.38	9.447	11.27
2.559	14.89	11.76	12.07
5.119	16.44	13.03	16.29
10.24	14.26	8.533	18.99
20.48	15.31	8.116	26.35
40.95	10.65	5.54	27.25
81.9	15.43	10.77	35.95

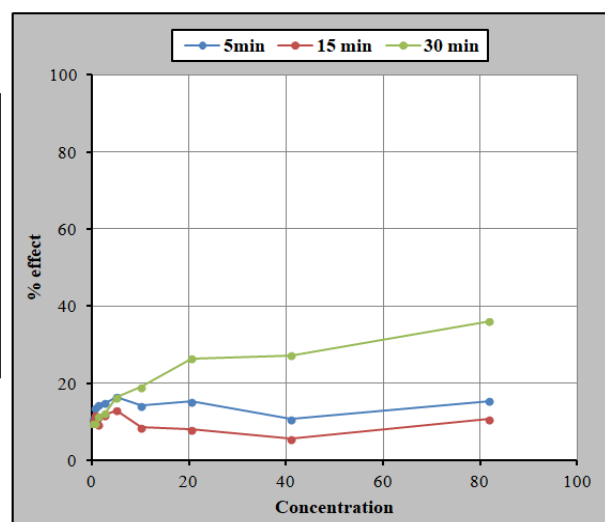


Fig. 3.14: Toxicity results of the T0 sample ($C_{LFX} = 22.08 \text{ mg}\cdot\text{L}^{-1}$).

TiO ₂ -coated tube: t120			
Concentration	% effect (5 min)	% effect (15 min)	% effect (30 min)
0.3199	-3.012	-1.786	-6.456
0.6398	-2.305	-3.012	-6.877
1.28	-6.202	-7.53	-9.462
2.559	0.3236	0.2907	-1.485
5.119	0.5397	-2.586	-6.074
10.24	9.135	6.461	5.955
20.48	15.32	8.235	20.05
40.95	16.06	9.81	25.74
81.9	36.46	28.57	41.38

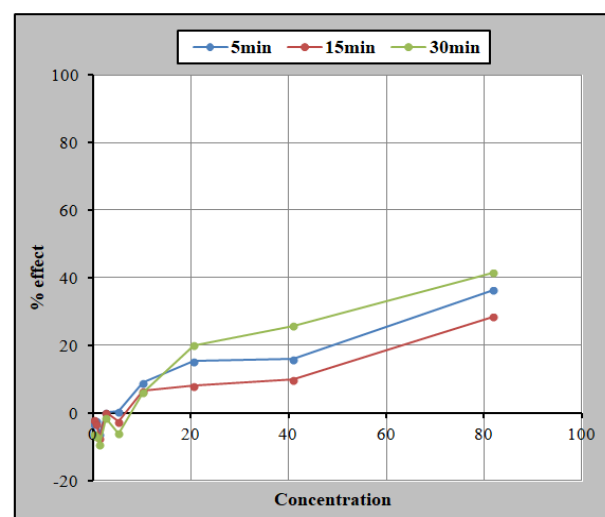


Fig. 3.15: Toxicity results of the sample obtained after 120 minutes of irradiation in the TiO₂-coated tube photocatalysis experiment (T120; $C_{LFX} = 13.71 \text{ mg}\cdot\text{L}^{-1}$).

TiO ₂ -coated tube: t420			
Concentration	% effect (5 min)	% effect (15 min)	% effect (30 min)
0.3199	0.0961	0.7256	2.006
0.6398	2.367	2.145	2.637
1.28	1.755	1.591	2.942
2.559	-5.496	-5.8	-3.588
5.119	7.916	5.956	7.142
10.24	8.053	5.86	8.539
20.48	20.59	16.59	19.63
40.95	31.92	28.11	37.12
81.9	54.91	50.36	52.7

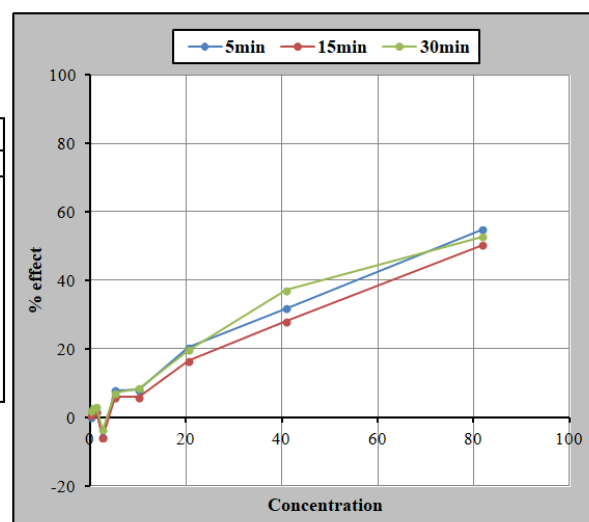


Fig. 3.16: Toxicity results of the sample obtained after 420 minutes of irradiation in the TiO₂-coated tube photocatalysis experiment (T420; C_{LFX} = 7.45 mg·L⁻¹).

TiO ₂ -coated tube: t840			
Concentration	% effect (5 min)	% effect (15 min)	% effect (30 min)
0.3199	4.386	5.882	4.098
0.6398	9.919	8.773	7.008
1.28	2.642	4.093	2.16
2.559	10.65	10.25	8.406
5.119	10.13	8.687	5.842
10.24	20.05	18.9	16.5
20.48	36.63	34.01	32.2
40.95	58.24	56.52	57.79
81.9	78.07	78.15	75.84

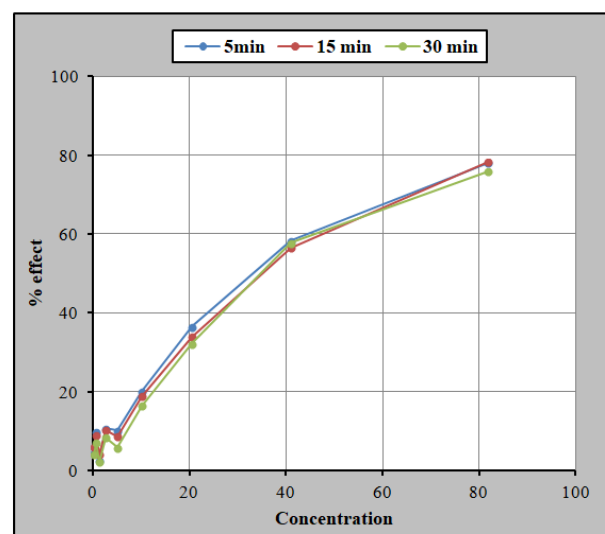


Fig. 3.17: Toxicity results of the sample obtained after 840 minutes of irradiation in the TiO₂-coated tube photocatalysis experiment (T840; C_{LFX} = 3.09 mg·L⁻¹).

TiO ₂ -coated tube: t1320			
Concentration	% effect (5 min)	% effect (15 min)	% effect (30 min)
0.3199	6.47	5.80	4.86
0.6398	6.67	5.93	6.00
1.28	6.97	5.43	5.57
2.559	12.32	12.89	11.00
5.119	18.96	17.69	14.91
10.24	28.05	26.23	25.49
20.48	45.21	41.97	41.39
40.95	71.75	69.65	69.34
81.9	84.04	86.52	86.47

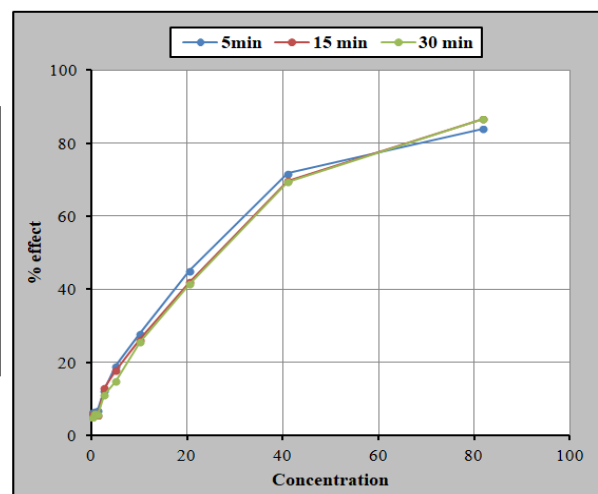


Fig. 3.18: Toxicity results of the sample obtained after 1320 minutes of irradiation in the TiO₂-coated tube photocatalysis experiment (T1320; C_{LFX} = 0.76 mg·L⁻¹).

TiO ₂ -coated tube: t1980			
Concentration	% effect (5 min)	% effect (15 min)	% effect (30 min)
0.3199	4.63	3.67	4.464
0.6398	1.107	0.07738	-1.97
1.28	6.103	3.128	2.922
2.559	7.881	5.782	7.35
5.119	20.49	16.53	18.77
10.24	40.87	37.44	40.08
20.48	64.34	60.74	61.79
40.95	80.19	82.33	84.72
81.9	93.99	96.03	97.15

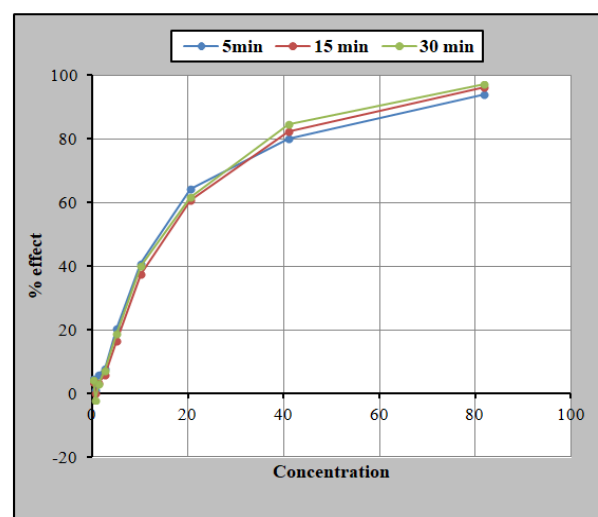


Fig. 3.19: Toxicity results of the sample obtained after 1980 minutes of irradiation in the TiO₂-coated tube photocatalysis experiment (T1980; C_{LFX} = 0 mg·L⁻¹).

TiO ₂ -coated tube: t2340			
Concentration	% effect (5 min)	% effect (15 min)	% effect (30 min)
0.3199	3.729	2.848	4.861
0.6398	4.379	4.145	7.368
1.28	9.244	8.594	12.06
2.559	15.19	14.19	17.19
5.119	25.89	26.56	29.21
10.24	45.69	44.92	50.00
20.48	69.09	66.47	69.57
40.95	83.37	84.54	87.37
81.9	96.64	97.66	98.72

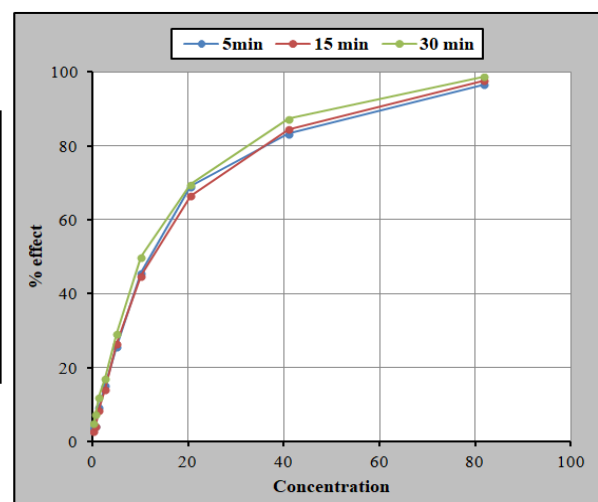


Fig. 3.20: Toxicity results of the sample obtained after 2340 minutes of irradiation in the TiO₂-coated tube photocatalysis experiment (T2340; C_{LFX} = 0 mg·L⁻¹).

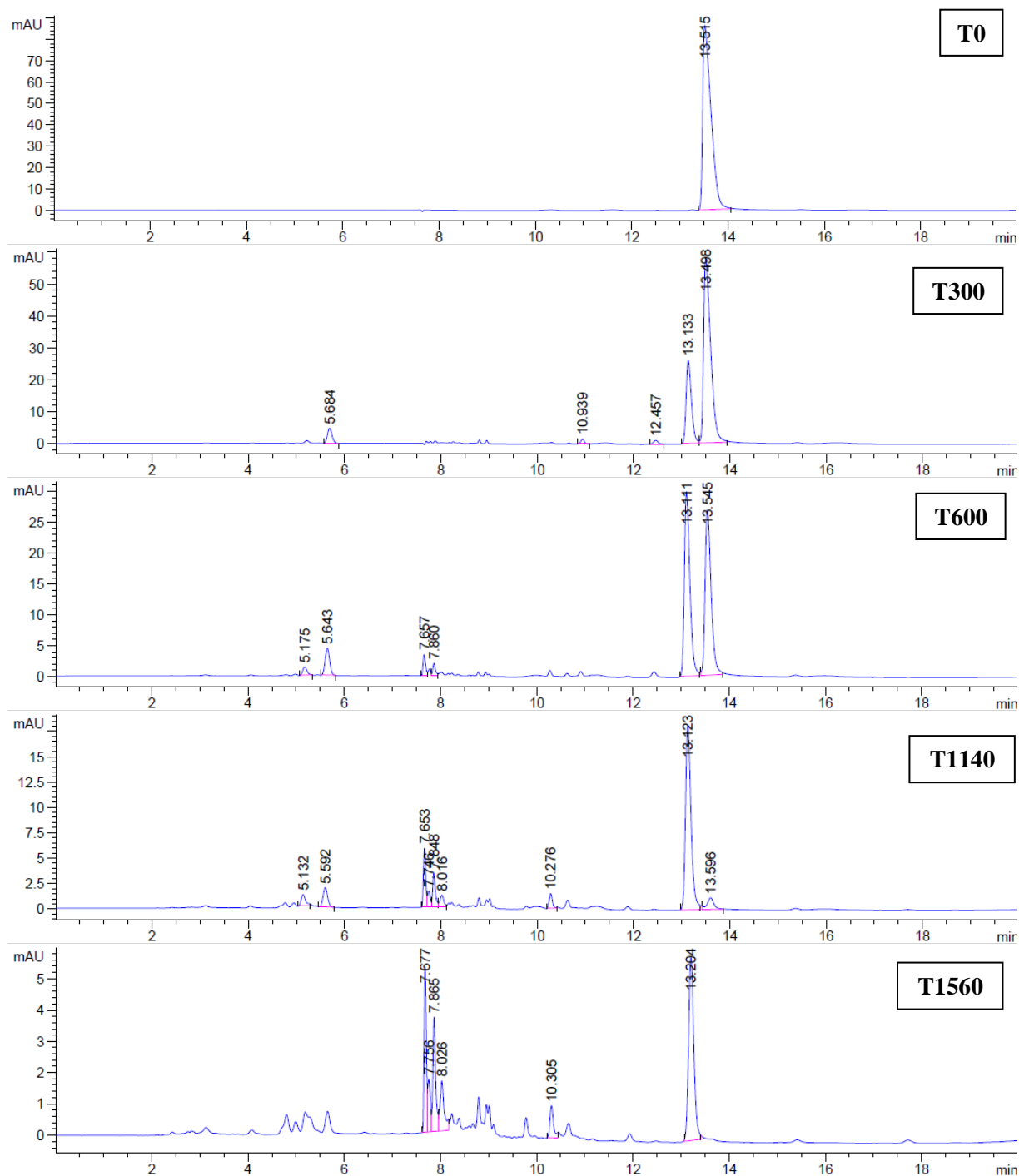


Fig. 3.21: Chromatograms of tested samples obtained from photolysis experiment.

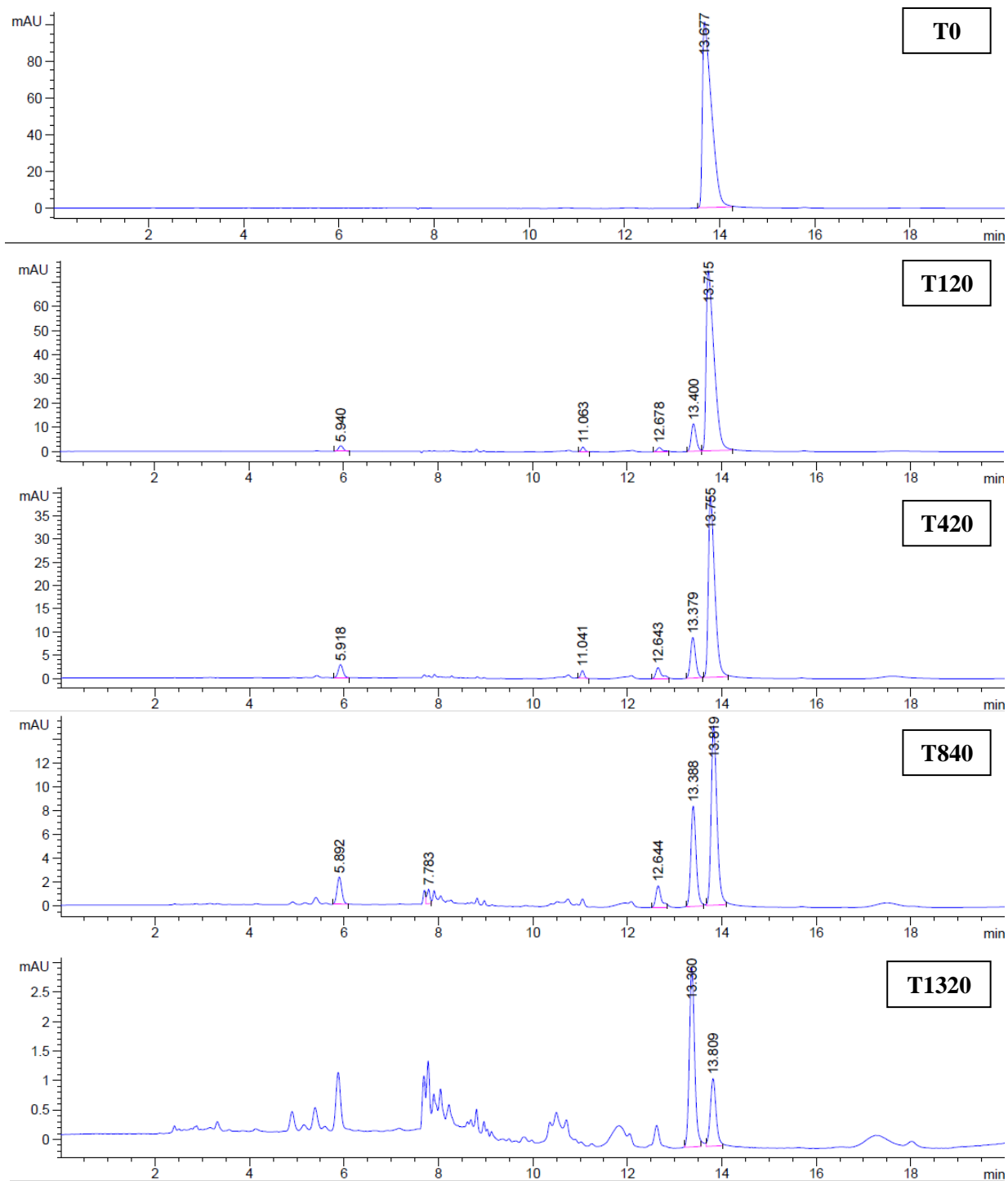


Fig. 3.22: Chromatograms of tested samples obtained from TiO₂-coated tube photocatalysis experiment.

Table 3.4: List of transformation products obtained from photolysis and TiO₂-coated tube photocatalysis, based on retention time observed by HPLC-UV analyses.

	Time (min)	TPs 1 (T _R = 5.1)	TPs 2 (T _R = 5.7)	TPs 3 (T _R = 7.6)	TPs 4 (T _R = 7.7)	TPs 5 (T _R = 7.8)	TPs 6 (T _R = 8.0)	TPs 7 (T _R = 10.3)	TPs 8 (T _R = 10.9)	TPs 9 (T _R = 12.4)	TPs 10 (T _R = 13.1)	
Photolysis	0	/	/	/	/	/	/	/	/	/	/	
	150	/	X	/	/	/	/	/	X	X	X	
	300	/	X	/	/	/	/	/	X	X	X	
	600	X	X	X	/	X	/	/	/	/	X	
	1140	X	X	X	X	X	X	X	X	/	/	X
	1560	/	/	X	X	X	X	X	X	/	/	X
Photocatalysis with TiO₂-coated tube	0	/	/	/	/	/	/	/	/	/	/	
	120	/	X	/	/	/	/	/	X	X	X	
	420	/	X	/	/	/	/	/	X	X	X	
	840	/	X	X	/	/	/	/	/	X	X	
	1320	/	/	/	/	/	/	/	/	/	X	
	1980	/	/	/	/	/	/	/	/	/	/	
	2340	/	/	/	/	/	/	/	/	/	/	

T_R = retention time expressed in minutes

CHAPTER 4

Case study #3: homogeneous photocatalysis with hydrogen peroxide (H_2O_2), peroxymonosulphate (PMS, HSO_5^-) and peroxydisulphate (PS , $\text{S}_2\text{O}_8^{2-}$) for the degradation of levofloxacin

For this case of study, the aim was to give a comprehensive view of the different aspects linked to the degradation of levofloxacin with sulphate radicals based AOPs (SR-AOPs) and hydroxyl radicals AOPs (HR-AOPs). All experimental conditions and results are reported in this dissertation as an under review paper.

Comparison of sunlight-AOPs for levofloxacin removal: kinetics, transformation products and toxicity assay on *Escherichia coli* and *Micrococcus flavus* (submitted to Environmental Science and Pollution Research (ESPR) - under revision)

4.1 Introduction

Water pollution is an increasing environmental hot-spot due to the continuous introduction of recalcitrant organic compounds into the aquatic ecosystem (Geissen et al., 2015). Antibiotics are pharmaceuticals extensively used to treat and prevent bacterial infectious diseases. Despite being poorly regulated worldwide, antibiotics continue to be the most detected pharmaceuticals given their extensive use in human and veterinary medicine (Boy-Roura et al. 2018; Klein et al. 2018; Pascale et al. 2020). Effective removal of antibiotic trace levels from the environment is urgently required for a reason beyond the environmental impacts, such as toxicity to plants and other organisms (Backhaus et al., 2000; Mukhtar et al., 2020a). Trace levels of antibiotics in aquatic ecosystems may induce the development of antibiotic resistance genes and bacteria, which will decrease or completely inhibit the therapeutic potential of antibiotics against human and animal pathogens (Rizzo et al., 2013; Zainab et al., 2020). This is a major risk for human health that should be prevented through effective antibiotic removal from the environment. The most detected classes of antibiotics in wastewater and surface water are fluoroquinolones (FQs) (Gothwal and Shashidhar, 2015; Rizzo et al., 2013) because they are not removed in conventional wastewater treatment plants and can cause long-term bioaccumulation and toxicity

in the environment (Liu et al., 2020). Usually, these fluorinated antibiotics are found at low concentrations, ranging from ng L^{-1} to $\mu\text{g L}^{-1}$, but concentrations up to several mg L^{-1} were already detected in effluents from pharmaceutical industries (Larsson et al., 2007). Fluoroquinolones are highly recalcitrant organic pollutants hardly removed by conventional water treatment technologies. The biodegradation of FQs has rarely been reported. To our knowledge, only a few bacteria (Pan et al., 2018) and fungi (Manasfi et al., 2020) species have been identified as organisms capable of biotransforming these antibiotic traces. However, the consequences due to the presence of fluoroquinolones in the environment are not fully understood, but they are known to be toxic to plants and aquatic organisms (Backhaus et al., 2000; Mukhtar et al., 2020a). For this reason, the development of AOPs holds the promise of entirely mineralising pharmaceutical footprint in water environments if those are included as additional polishing to conventional wastewater treatment plants (Brienza and Katsoyiannis, 2017). The fundamental principle of AOPs resides in the generation *in situ* of robust oxidising radical species such as hydroxyl radicals (OH^\bullet), which interact with the molecules of the organic pollutants and lead to the progressive degradation of the contaminants (Lelario et al., 2016; Vagi and Petsas, 2017). Hydroxyl radicals (HR) can be produced by different systems such as UV/ H_2O_2 (Jung et al., 2012), UV/ O_3 (Šojić et al., 2012), UV/ TiO_2 (Azzaz et al., 2018; Zuorro et al., 2019), Fenton and photo-Fenton technologies (Kamagate et al., 2018; Zhu et al., 2019). In the last decade, oxidants like peroxydisulphate ($\text{PDS} = \text{S}_2\text{O}_8^{2-}$) or peroxymonosulphate ($\text{PMS} = \text{HSO}_5^-$) have been studied as an alternative to conventional OH^\bullet based AOPs (Ahmed et al., 2014). In fact, through their activation, sulphate radicals ($\text{SR}(\text{SO}_4^{\bullet-})$) can be produced for the removal of an extensive array of organic contaminants, including pharmaceuticals and pesticides (Kan et al., 2021). The activation of PMS and PDS can be achieved mainly by thermal, photolytic, sonolytic, radiolytic activation, and the reactions of the oxidants with iron oxide magnetic composites, including *in situ* formed iron hydroxides and quinones (Waclawek et al., 2017). Among the various SR-AOPs, sunlight technologies are desirable because of their low operational costs and high organic contaminants removal efficiency (Yang et al., 2019). After activation, PDS produces sulphate radicals, while PMS produces both sulphate and hydroxyl radicals, as reported in Eq. 4.1 - 4.2:



Compared to HO^\bullet , $\text{SO}_4^{\bullet-}$ radicals have a series of advantages: higher redox potential ($E^0 = 2.65 - 3.1$ V), higher selectivity and efficiency on the oxidation of compounds with unsaturated bonds or aromatic ring, higher pH range and higher half-life in some cases (Ahmed et al., 2012; Hayat et al., 2020). Therefore, sulphate radicals can remove emerging contaminants more efficiently (Wang and Wang, 2018; Yang et al., 2019).

This work provides a framework to compare the effectiveness of homogeneous AOPs processes based on the generation of OH^\bullet and $\text{SO}_4^{\bullet-}$ by solar-driven methods. Levofloxacin (LFX) is used as a model compound since it is the widest fluoroquinolone pharmaceutical and has been widely prescribed in the period of the Covid-19 pandemic due to its usefulness in the treatment of opportunistic bacterial infections that can co-occur during bacterial pathogenesis. In addition, the LFX transformation pathway has been investigated upon different oxidative treatments (Epold et al., 2015; Yahya et al., 2015) biodegradation (Shu et al., 2021), which might facilitate intermediates identification. The oxidants used are H_2O_2 , PMS and PDS, which produce HO^\bullet , HO^\bullet and $\text{SO}_4^{\bullet-}$, $\text{SO}_4^{\bullet-}$ radicals respectively. In the first step, the performance of different AOPs was investigated in other pH conditions according to essential kinetic criteria, mainly the comparison between apparent first-order kinetic rate constants obtained by different SR-AOPs and HR-AOPs. Then, in a second step, treatment of LFX was conducted in a complex water matrix as representative wastewater composition to assess competitive and targeted reduction of fluoroquinolone at a realistic concentration level. To demonstrate the hazard of the starting molecule and its degradation products, the evaluation of the inactivation of specific bacterial strains is beneficial (Cai et al., 2016). For this purpose, the effective inactivation of antibactericidal effects of LFX and by-products was evaluated using the culture of *Escherichia coli* and *Micrococcus flavus* microorganisms. The bactericidal effect evaluation is essential to define the effectiveness of technology to prevent the undesired development of bacteria resistant strains.

4.2 Material and methods

4.2.1 Reagents, catalyst and wastewater

For chemical analysis, acetonitrile (ACN) and formic acid were LC-MS grade from Honeywell (Wabash, Indiana, US), and water was ultrapure Milli-Q grade ($18.2 \text{ M}\Omega \text{ cm}^{-1}$ resistivity at 25°C). Analytical standard of levofloxacin (LFX) (purity 99.4%) was purchased from Lab Instruments S.r.l. (Castellana Grotte, Puglia, Italy). Potassium peroxymonosulphate, with the commercial name of Oxone® (PMS, $\text{KHSO}_5 \cdot 0.5\text{KHSO}_4 \cdot 0.5\text{K}_2\text{SO}_4$), sodium peroxydisulphate (PDS, reagent grade, $\geq 98\%$), hydrogen peroxide (H_2O_2 , 30%), potassium iodide (KI, $\geq 99.5\%$),

sodium acetate trihydrate ($\text{CH}_3\text{COONa}\cdot 3\text{H}_2\text{O}$, $\geq 99\%$), monobasic potassium phosphate (KH_2PO_4 , $\geq 99\%$), dibasic potassium phosphate (K_2HPO_4 , $\geq 98\%$), sodium chloride (NaCl , $\geq 99.5\%$), calcium sulphate dihydrate ($\text{CaSO}_4\cdot 2\text{H}_2\text{O}$, $\geq 99\%$), magnesium sulphate (MgSO_4 , $\geq 97\%$), magnesium sulphate heptahydrate ($\text{MgSO}_4\cdot 7\text{H}_2\text{O}$, $\geq 98\%$), potassium chloride (KCl , $\geq 99\%$), urea ($\geq 99.5\%$), peptone, yeast extract, agar, tryptone, enzymatic digest of soybean meal were purchased from Sigma Aldrich (St. Louis, USA), sodium hydrogen carbonate (NaHCO_3 , $\geq 99.5\%$) from VWR Chemicals (Radnor, Pennsylvania, US), glacial acetic acid (CH_3COOH , $\geq 99.9\%$) and methanol (CH_3OH , LC-MS grade) from Carlo Erba reagents (Milano, Italy), calcium chloride dihydrate ($\text{CaCl}_2\cdot 2\text{H}_2\text{O}$, $\geq 97\%$). All chemicals were used as received without further purification.

4.2.2 AOPs and experimental conditions

The photocatalytic experiments were conducted using an amber cylindrical reactor covered with a quartz cap. The photochemical reactor was placed in a solar simulator device (Heraeus-Atlas Suntest CPS+, Chicago, USA), equipped with a Xenon Arc lamp (1.8 KW) as irradiation source, with a light power of 400 W/m^2 and a spectral wavelength range of 290 - 800 nm. The temperature was kept constant ($26 \pm 0.1^\circ\text{C}$) through an air conditioning system, and the solutions were maintained under continuous stirring to ensure an optimum mixing flow. All photodegradation reactions were performed on a solution of LFX with an initial concentration of $10 \text{ mg}\cdot\text{L}^{-1}$, obtained from a stock solution of $2000 \text{ mg}\cdot\text{L}^{-1}$ in methanol and diluted in different aqueous media: distilled water $\text{pH} = 6.3$, acetate buffer solution 0.01 M $\text{pH} = 5$, phosphate buffer solution 0.05 M $\text{pH} = 7$, simulated wastewater (SWW) $\text{pH} = 7.8$. The initial concentration was fixed at $10 \text{ mg}\cdot\text{L}^{-1}$ because it is suitable for kinetic competition experiments and allows HPLC quantification without pre-concentration steps. The efficiency of H_2O_2 , PMS and PDS as oxidants at a concentration of $400 \mu\text{M}$ was assessed for each medium. Simulated wastewater (SWW) at pH around eight was employed in this work. The exact composition is as follows (Polo-López et al., 2012): NaHCO_3 ($96 \text{ mg}\cdot\text{L}^{-1}$), NaCl ($7 \text{ mg}\cdot\text{L}^{-1}$), $\text{CaSO}_4\cdot 2\text{H}_2\text{O}$ ($60 \text{ mg}\cdot\text{L}^{-1}$), urea ($6 \text{ mg}\cdot\text{L}^{-1}$), MgSO_4 ($60 \text{ mg}\cdot\text{L}^{-1}$), KCl ($4 \text{ mg}\cdot\text{L}^{-1}$), K_2HPO_4 ($0.28 \text{ mg}\cdot\text{L}^{-1}$), $\text{CaCl}_2\cdot 2\text{H}_2\text{O}$ ($4 \text{ mg}\cdot\text{L}^{-1}$), peptone ($32 \text{ mg}\cdot\text{L}^{-1}$), $\text{MgSO}_4\cdot 7\text{H}_2\text{O}$ ($2 \text{ mg}\cdot\text{L}^{-1}$).

4.2.3 Analytical methods

4.2.3.1 HPLC-UV and MS method

The time course concentration of LFX was monitored using a high-performance liquid chromatography (HPLC) system (Agilent Technologies 1200 series, USA) equipped with a Kinetex C18 100Å column (250 x 4.6 mm i.d. and 5 µm particle size) coupled to a diode array detector, set at $\lambda = 295$ nm. The mobile phase consists of a biphasic gradient, ultrapure water with 0.1% formic acid (solvent A) and acetonitrile (solvent B), structured as follows: 0 - 3 min, 0% B; 3 - 5 min, 15% B; 5 - 16 min, 15% B; 16 - 18 min, 100% B; 18 - 22 min, 100% B; 22 - 23 min, 0% B; 23 - 25 min, 0% B. The flow rate is $1.0 \text{ mL}\cdot\text{min}^{-1}$, and the injection volume is 20 µL. The study of metabolites for LFX degradation in SWW by simulated irradiation/PDS was carried out using an LC-ESI(+)-linear trap quadrupole (LTQ) MS (Thermo Fisher Scientific, Bremen, Germany). Chromatographic conditions were maintained identical to those described above for the HPLC-UV method. The MS optimised experimental conditions for the ESI ion source were: ESI needle voltage, +4.5 kV; cone voltage, +3.00 kV; the temperature of the heated capillary, 350°C; and sheath gas (N_2) flow rate of 60 arbitrary units (a.u.). The instrument was externally calibrated with appropriate standards, and mass spectrometric data were acquired in the positive ion mode while scanning m/z 50–2000.

4.2.3.2 Spectrophotometric method for PDS quantification

During degradation, residual PDS concentration in SWW samples was monitored using a UV/visible single-ray spectrophotometer Cary 50 at $\lambda = 352$ nm and $\lambda = 400$ nm. The analysed solutions consisted of 1 mL of the selected sample, 1 mL of NaHCO_3 $5.0 \text{ mg}\cdot\text{mL}^{-1}$, 1 mL of KI $0.1 \text{ g}\cdot\text{mL}^{-1}$. Samples were maintained under dark conditions for 15 minutes and then placed into the spectrophotometer for analysis (Liang et al., 2008).

4.2.4 Antibacterial activity evaluation

The antibacterial effect of treated solutions was assessed on *E. coli* (LMG2092) and *M. flavus* (DSM1790). These analyses aimed to quantify the effective inhibition of antibacterial character to the effluent to prevent the development of antibiotic-resistant strains. Therefore, studies were carried out by testing the samples obtained from photodegradation experiments of LFX in SWW with simulated irradiation/PDS. Tryptic Soy Broth (TSB) and Lysogeny Broth (LB) were used as agar medium. TSB was prepared to dissolve 15.0 g tryptone, 5.0 g enzymatic digest of soybean

meal, 5.0 g sodium chloride, 15.0 g agar in 1 L of distilled water; In comparison, LB medium was made up of 10.0 g peptone, 5.0 g yeast extract, 5.0 g sodium chloride and 12.0 g agar in 1 L of distilled water. Both the mediums were sterilised in a high-pressure steriliser at 121°C for 15 minutes and deposited into Petri dishes with a diameter of 60 mm (**MacWilliams and Liao, 2006**). The suspensions of *E. coli* and *M. flavus* bacteria were prepared to contain approximately 10^8 CFU mL⁻¹. Each Petri dish was spiked in four different points with 20 µL of four different samples, then finally incubated at a temperature of 37 °C for 18 hours.

4.3 Results and discussion

4.3.1 *Degradation efficiency of levofloxacin by simulated irradiation-drive processes*

Before undertaking the LFX photodegradation studies in distilled water, acetate buffer and phosphate buffer, a control experiment was carried out under dark conditions with an initial concentration of LFX at 10 mg·L⁻¹, with and without H₂O₂, PMS and PDS. In these conditions, there was no evidence for LFX degradation in the presence of H₂O₂. As far as PDS is concerned, a decrease in the percentage of degradation is observed with increasing pH, except distilled water, which has a zero-degradation rate. Finally, concerning PMS, there is an increase in the degradation percentage as the pH increases, except for distilled water again. This anomalous behaviour in distilled water could be attributed to the absence of ions in the solution. In particular, after 30 seconds adding of PDS, we obtained a decrease of 1%, 17% and 10% in LFX concentration, while after adding PMS, we obtained a reduction of 10%, 40% and 100% in distilled water, acetate buffer and phosphate buffer, respectively. In the case of PMS in phosphate buffer solution, we observe a complete transformation of LFX in just 30 seconds, as shown in the chromatogram of **Fig. 4.1**.

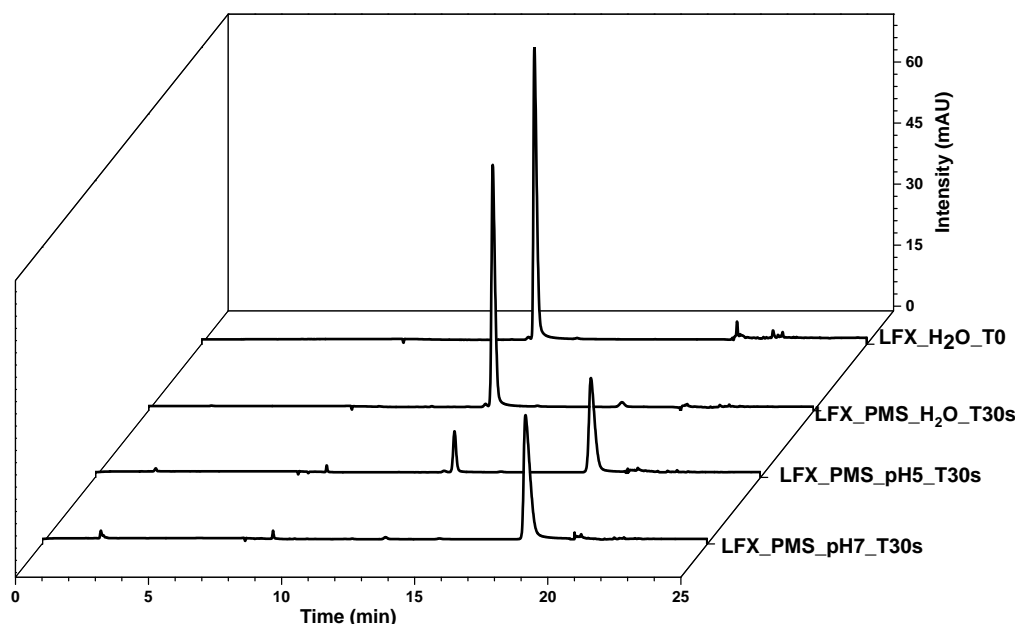


Fig. 4.1: Chromatograms of LFX $10 \text{ mg}\cdot\text{L}^{-1}$ in distilled water and after adding PMS [$400 \text{ }\mu\text{M}$] in distilled water, acetate buffer solution $\text{pH} = 5$ and phosphate buffer solution $\text{pH} = 7$.

All the LFX (retention time 13.3 min.) was transformed into another compound with a retention time of 18.4 min. This was identified as LFX N-oxide (Merel et al., 2017). Indeed, as reported for other fluoroquinolone antibiotics and nitrogenous heterocyclic compounds (Brienza et al., 2020, 2019; Nihemaiti et al., 2020), especially PMS can degrade organic contaminants without radicals involvement through an oxidation process, and it has been demonstrated that the piperazine ring is the leading reaction site for quinolone compounds. This mechanism is still little studied, but it is closely related to the range of pH used in the experimental setup and seems to be improved in alkaline conditions (Wang and Wang, 2018).

To compare the efficiency of sunlight driven advanced oxidation processes, a kinetic study of LFX photodegradation using different oxidant systems such as H_2O_2 , PMS and PDS and represented by the following reactions in Eq. 4.3 - 4.5 was carried out, and the results obtained were reported in Table 1:



Table 4.1: Percentage (%) of LFX degraded in acetate buffer solution, distilled water and phosphate buffer solution by different simulated irradiation/oxidant systems (t = 10 min).

	% PHOTODEGRADATION		
	Acetate buffer solution (pH = 5)	Distilled water (pH = 6.3)	Phosphate buffer solution (pH = 7)
Photolysis	3.0	2.5	13.9
H₂O₂	8.0	6.8	17.2
PMS	52.5	25.0	100.0
PDS	92.8	100.0	89.2

From the results obtained, minimal degradation is observed during photolysis processes and in the presence of H₂O₂; meanwhile, high percentage degradation in a range of 25 to 100 and 89.2 to 100% was observed by PMS and PDS, respectively. This result can be explained by the small yield of OH[•] induced by simulated irradiation. It is important to remark that photolysis of H₂O₂ from reaction (1) only takes place under UVC wavelengths. The spectrum of solar radiation has a small component of UV- light (< 4.0 %), from which UVC represents an almost null percentage (Serrà et al., 2021). Therefore, it cannot be expected a high efficiency in the photoactivation of H₂O₂ to produce a high concentration of OH[•] for LFX degradation.

In the case of PDS, there is an increase of degradation rate when switching from acetate buffer solution pH 5 to distilled water pH 6.3 and a decrease when switching to phosphate buffer pH 7. At the same time, for H₂O₂, there is a continuous increase when changing from acidic to neutral pH, in agreement with the results reported by Lau et al. (2007) and Liu et al. (2013). There are some main reasons for this observed behaviour: i) the increase of pH in the solution determines a different degree of molecule protonation, which will therefore have a distinct affinity for the radicals present; moreover, ii) the more or less acidic aqueous environment may determine an abundant production of radicals, which results in a different number of degraded molecules depending on their total concentration. Furthermore, all the variations occurring in a solution determine a different degree of light absorption and, therefore, an extra degradation efficiency (Lau et al., 2007; Liu et al., 2013).

The kinetics of degradation of the various oxidants at different pH under simulated irradiation conditions are shown in Fig. 4.2.

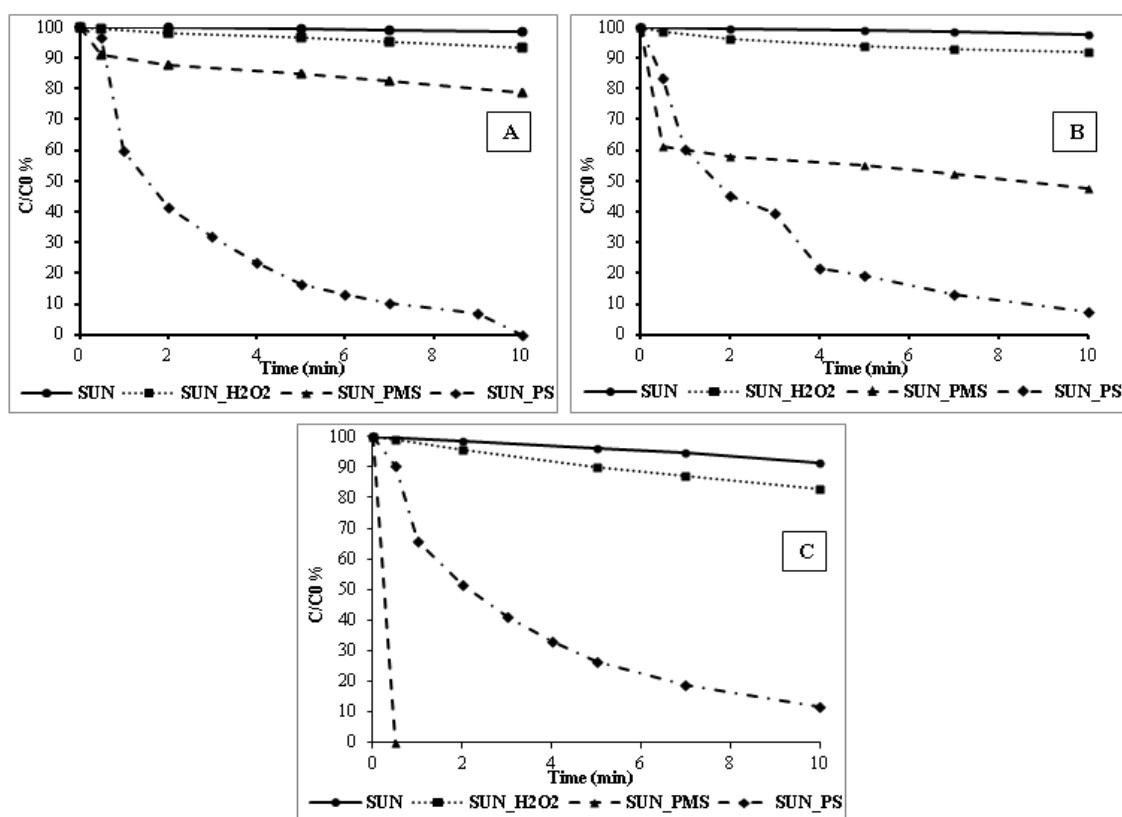


Fig. 4.2: Photodegradation curve of LFX in **A)** distilled water, **B)** acetate buffer solution and **C)** phosphate buffer solution, by different simulated irradiation/oxidant system ($t = 10$ min; $C_0 = 10$ mg·L⁻¹).

Under photolysis and simulated irradiation/H₂O₂ system, we have linear one-step degradation kinetics in all the solutions tested. In contrast, for simulated irradiation/PDS and affected irradiation/PMS systems, we have a first step where there is a rapid decrease in the concentration of the LFX due to a possible direct and immediate action of the oxidants adding and depending on the pH of the solutions tested, as said above, followed by a second step where we have a much slower degradation. However, the effect of pH value in the simulated irradiation/PDS process was smaller than that in the simulated irradiation/PMS process. In all cases, the first process led to complete degradation of LFX in 10 minutes and 20 minutes for distilled water and acetate/phosphate-buffered solutions, respectively.

Beyond direct comparison between the different reactions of AOPs, the simulated sunlight radiation activates the oxidants, resulting in hydroxyl and sulphate radicals forming depending on the chemical nature of the oxidants (Eq. 4.3 and Eq. 4.5). However, the results obtained indicate that SO₄^{•-} radicals are more reactive towards the molecule of LFX concerning OH[•] radicals (Brienza et al., 2014). These results also demonstrate that, in this specific case, the activation of PDS through the use of only simulated radiation is sufficient to degrade LFX at a concentration of 10 mg·L⁻¹. However, in literature, most researchers focus on the metal-induced

activation of PDS using metal ions such as Cu^{2+} , Fe^{2+} , Zn^{2+} or Mn^{2+} (Gao and Zou, 2020; Liu et al., 2021; Wang et al., 2018).

4.3.2 *Kinetic study of simulated irradiation/PDS system in simulated wastewater (SWW), and optimisation of the process*

Wastewater matrices present a complex composition that may affect the overall treatment performance of a treatment technology due to the existence of competitive species that may consume radicals produced (Garcia-Segura et al., 2020). Although methanol is an excellent scavenger for hydroxyl radicals (Bartlett and Cotman, 1949; Jiménez et al., 2003), in our case, the small amount of methanol was considered part of the complex and its influence in this scenario was not significant. Given the high performance of the simulated irradiation/PDS treatment, this process was selected to conduct further studies in a complex wastewater sample. Due to the ongoing Covid-19 pandemic, it was impossible to use an accurate wastewater sample for safety reasons; therefore, we used simulated wastewater, according to Polo-López et al. (2012). It can be observed that, despite the complex composition, the simulated irradiation/PDS treatment attains complete degradation of target LFX in 10 min with 400 μM PDS dose. The remaining PDS in the solution was quantified through spectrophotometric analyses (Liang et al., 2008). A remaining concentration of 275 μM PDS was quantified after treatment, suggesting that only 125 μM PDS was required to attain complete abatement of LFX. Dose optimisation is crucial to minimise capital expenditures and decrease risks associated with unwanted remaining concentrations of oxidants in treated water effluents. Additional experiences were conducted using lower initial doses of PDS of 100 μM and 200 μM (Fig. 4.3).

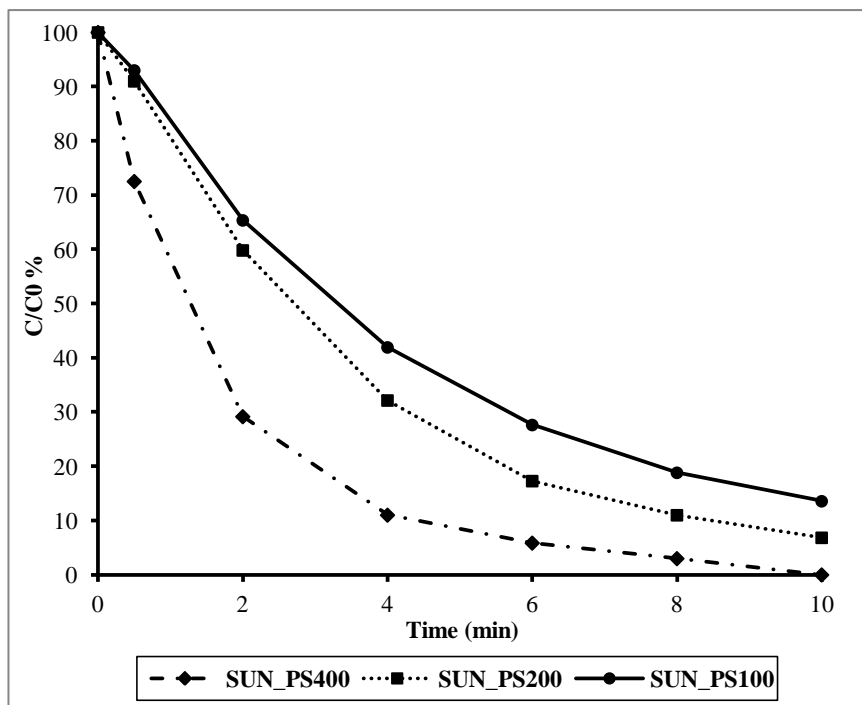


Fig. 4.3: Kinetics degradation by simulated irradiation/PDS system at different PDS concentrations [400 μM ; 200 μM ; 100 μM] in simulated wastewater (pH=7.8; $t = 10$ min; $C_0 = 10 \text{ mg}\cdot\text{L}^{-1}$).

In **Figure 4.3**, it can be seen that all three concentrations achieved almost complete degradation of LFX. Considering 10 min of residence time, LFX removal reached 86.4%, 93.1% and 100% for increasing doses of PDS of 100 μM , 200 μM and 400 μM , respectively. Thus, it can be observed that a lower amount of 200 μM can be used to attain one log removal of trace pollutant LFX in wastewater samples. All normalised concentration of LFX was fitted according to a simple first-order kinetic model (**Fig. 4.4**) described by **Eq. 4.6**. The kinetic rate constant (k) (min^{-1}) and the corresponding half-reaction time (**Eq. 4.7**) (**Table 4.2**) were determined to find the best fit between the experimental and the calculated concentration of LFX profiles obtained with the simulated irradiation/PDS system.

$$\ln ([A_0]) = -kt \quad \text{Eq. 4.6}$$

$$t_{1/2} = \frac{(\ln 2)}{k} \quad \text{Eq. 4.7}$$

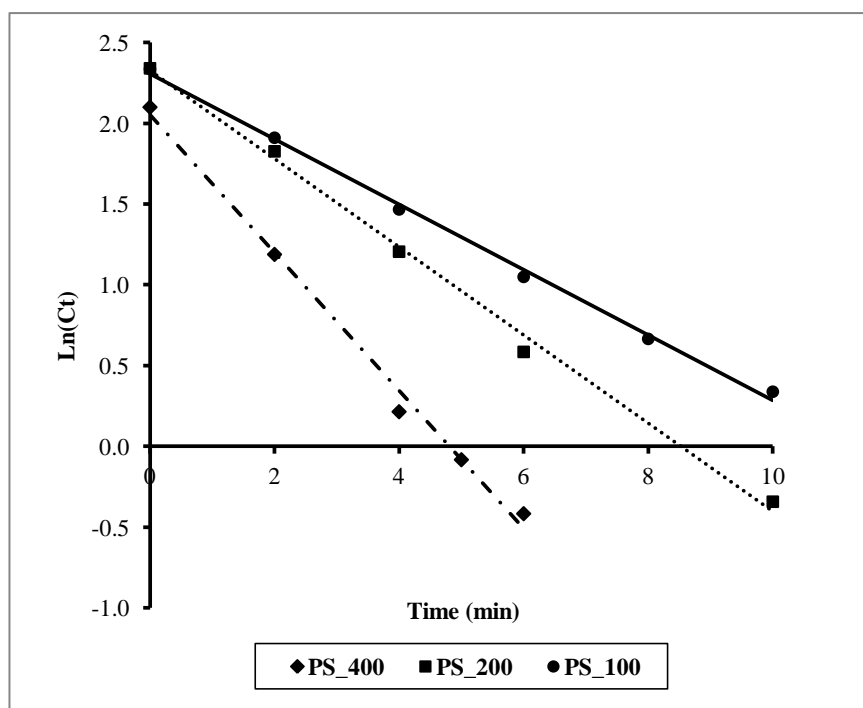


Fig. 4.4: Trends of the first-order linearised equation used to calculate kinetic parameters reported in **Table 4.2**.

Table 4.2: Kinetic parameters of LFX degradation in synthetic wastewater with three different concentrations of PDS.

System	$(C_{\text{exp}} - C_{\text{calc}})^2$	R^2	$t_{1/2}$ (min)	k (min^{-1})
Simulated irradiation/PDS_100	0.1584	0.9975	3.43	0.2019
Simulated irradiation/PDS_200	0.1125	0.9960	2.54	0.2726
Simulated irradiation/PDS_400	0.1025	0.9934	1.63	0.4261

Fig. 4.4 indicates that a decrease in the initial oxidant dose slowed the kinetics of LFX abatement. The kinetic analysis shows pseudo-first-order rate constants (k_l) of $4.261 \times 10^{-1} \text{ min}^{-1}$ ($R^2 = 0.993$) for 400 μM , 2.726×10^{-1} ($R^2 = 0.996$) for 200 μM , $2.019 \times 10^{-1} \text{ min}^{-1}$ ($R^2 = 0.997$) for 100 μM . The faster decrease observed in the wastewater concerning ultrapure water suggests that some components may facilitate the degradation of LFX. The decrease in k_l with decreasing dose of PDS can be explained by the lower yield when decreasing the concentration of precursor, which would decrease the availability of oxidant to react with the same concentration of target pollutant LFX.

4.3.3 Antibacterial activity (*E. coli* and *M. flavus*)

The LFX molecule contains several active functional groups that effectively induce toxicity to microorganisms in an aqueous ecosystem. Those vibrant centres are responsible for the antibacterial activity of LFX that is used to treat both Gram-negative and Gram-positive bacterial infections. Trace concentration levels of antibacterial pharmaceuticals in water samples below the lethal dose for bacteria (LD50) can cause the proliferation of multi-resistant strains. This analysis aims to evaluate the successful inhibition of the antibacterial activity of LFX and by-products to demonstrate that simulated irradiation/PDS can be an effective treatment technology to remove LFX and prevent the development of bacteria strains resistant to antibacterial drugs. Therefore, an antibacterial activity test was performed against Gram-negative *E. coli* (LMG2092) in the TSB medium and Gram-positive *M. flavus* (DSM1790) in the LB medium. The toxicity results were expressed by measuring the diameter of the culture inhibition halo. Blank experiments were conducted before the antibacterial activity assessment on the samples obtained during the simulated irradiation/PDS treatment to evaluate the potential toxicity of PDS, methanol and simulated wastewater. The results obtained showed that none of the tested concentrations of PDS (50 μ M \div 400 μ M), methanol and SWW had any inhibition activity on the tested bacteria. Based on these results, it was also possible to test the mix of LFX transformation products in SWW with PDS.

The samples tested were the solution containing LFX 10 mg·L⁻¹ in SWW (t₀) and the solutions obtained after 5, 10, 30, 60, and 120 minutes of irradiation in the presence of PDS. The results obtained from the first sample (t₀) analysis showed a growth inhibition halo with a diameter of 19 mm and 20 mm for *E. coli* and *M. flavus*, respectively, thus demonstrating the toxicity of LFX. In subsequent analysis after 5 minutes of treatment, we observed a notorious decrease in the inhibition halo on *E. coli* down to a diameter of 10 mm, almost 50% decrease in diameter. Meanwhile, no halo was observed for *M. flavus*, suggesting that after 5 min of treatment, there is no remaining antibacterial activity for Gram-positive microorganisms. Any halo was observed in the other samples tested on *E. coli* and *M. flavus*. The decrease in the antibacterial activity may be attributed to the breaking down of the molecular structure and the elimination of some functional groups (quinolonic ring and piperazine ring) responsible for the toxicity of quinolone antibiotics thanks to the binding with DNA gyrase enzyme. The DNA gyrase is an essential bacterial enzyme that allows the replication of DNA (Chu and Fernandest, 1989). Furthermore, it has been reported that some moieties, such as piperazine, carboxylic acid and keto groups in quinolones molecules, played essential roles in killing Gram-positive bacteria (Neth et al.,

2019). The toxicity studies demonstrate the effectiveness of simulated irradiation/PDS treatment to completely degrade the functional groups of LFX and its degradation by-products associated with the antibacterial character of the pharmaceutical (Li et al., 2015; Zhou et al., 2021). These promising results suggest that simulated irradiation/PDS treatment might be a feasible solution to prevent the undesired release of trace antibacterial fluoroquinolone pharmaceuticals to the environment.

4.3.4 Elucidation on degradation pathways of levofloxacin

The toxicity analyses allow inferring the degradation of different functional groups with antibacterial effects such as the piperazine ring. To elucidate the possible degradation pathway of LFX induced by simulated irradiation/PDS, aliquots were analysed by the HPLC–MS to identify intermediates and by-products yielded from the radical-mediated oxidation. Structure analysis of the main degradation products was based on literature and fragmentation data obtained by positive ion collision dissociation (data not shown). In Fig. 4.5, the structure and the m/z ratio of all photo-products detected as $[M+H]^+$ ions and the proposed degradation pathway are reported.

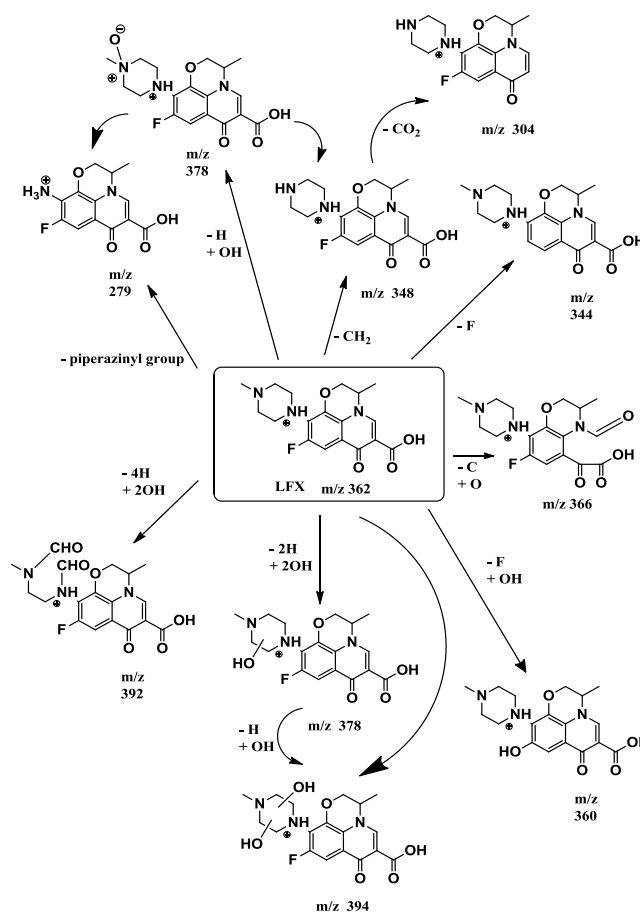


Figure 4.5: Possible degradation pathway of LFX in SWW by simulated irradiation/PDS system, after 5 minutes of irradiation.

The parent compound LFX exhibits as $[M+H]^+$ ion a nominal m/z ratio of 362 and, as highlighted in **Fig. 4.5**, undergoes further losses and substitutions forming, directly, eight main photoproducts. These primary products were themselves degraded, and we observed a quick increase during the first minutes and then a rapid decrease. After 10 minutes, the concentrations of LFX and all by-products identified were below the LOD, suggesting the complete disappearance of aromatic structures. The breakage of aromatic rings is commonly reported for other AOPs resulting in the yield of biodegradable carboxylic acids of low molecular weight (e.g., oxalic acid, oxamic acid, formic acid). The classification of identified by-products allows depicting different organic events of relevance that justify the loss of the antibiotic character of the effluent. As described above, certain functional groups are associated with toxic effects on Gram-positive and Gram-negative bacteria. These results agree with the previous discussion and suggest the competitive degradation of LFX and effective inactivation of the antibiotic character of the effluent. Identifying stable intermediates presents the significant events for LFX degradation mediated by sulphate radicals involving hydroxylation reactions. One of the degradation pathways is associated with the defluorination of LFX.

The intermediate at m/z 344 is due to the neutral loss of fluorine atom in the C-5 position, and, at the same time, the ion at m/z 360 can be obtained by substituting fluorine with OH (**Scrano et al., 2020**). Previous literature identified the piperazine ring as the most reactive site towards sulphate radicals attack (**De Witte et al., 2009; Jiang et al., 2016**).

A compound identified at nominal m/z of 348 exhibited a difference of 14 amu concerning the m/z ratio of the protonated LFX suggesting the direct formation of de-methylated derivative by loss of a methyl group bonded to N-3, according to previous studies (**Jiang et al., 2016; Li et al., 2020**). Further neutral loss of CO_2 generates the product at m/z 304, agreeing with **Li et al. (2020)**. The vulnerability of the piperazine group to sulphate radicals attack was confirmed by the other three compounds identified at m/z 378 and 394, and 392. The first two, probably, derived from single and double hydroxylation of piperazine ring, respectively; the third, a di-aldehyde derivative, due to the cleavage of piperazine ring following the formation of peroxy radicals on two N atoms (**Jiang et al., 2016**). Because hydroxyl radicals are not selective towards different functional groups, it is impossible to identify the exact position of hydroxylation in the two compounds at m/z 378 and 394. At the same time, based on the fragmentation pathway, retention time and comparison with the product formed by the addition of PMS, it is possible to attribute the structure of the other compounds identified at m/z 378 to N-oxide levofloxacin (**De Witte et al., 2008; Jiang et al., 2016**). The direct oxidation of the piperazine side-chain until forming an amino group in position 2 leads to the formation of de-

piperazinyl LFX at m/z 279. These by-products define sulphate radicals' selective attack that induces the piperazine ring opening. In addition, a product with m/z 366 was identified that was associated with the cleavage of the quinolone moieties instead of the piperazine ring.

4.4 Conclusions

Photon-driven advanced oxidation processes can effectively remove recalcitrant antibacterial pharmaceuticals such as levofloxacin. This work benchmarked the performance of three different precursors of radical oxidant species (H_2O_2 , PMS and PDS) in other pH conditions.

Experiments demonstrated that simulated irradiation/ H_2O_2 treatment showed less impact on LFX reduction than the combined AOPs of simulated irradiation/PMS and simulated irradiation/PDS due to the low content of UVC radiation in the solar spectra. In contrast, PMS and PDS were able to degrade levofloxacin completely.

The simulated irradiation/PDS AOP showed the best performance compared to the other oxidation processes evaluated in all mediums investigated, except for phosphate buffer, where PMS resulted in the best. For this medium, exciting results was the complete removal of LFX in 30 seconds and the formation through the non-radicals mechanism of LFX N-oxide in the presence of PMS. Further studies will focus on product yield quantification to better understand these results.

However, the simulated irradiation/PDS system showed the best performance, achieving a complete degradation of LFX after 10 minutes of irradiation in all mediums investigated. In simulated wastewater, PDS at different concentrations was tested, and in all cases, the degradation followed a first-order kinetic. Mass balance after treatment indicated that only 125 μ M PDS was required to attain complete abatement of levofloxacin. However, decreasing the PDS dose may reduce the kinetic rate of levofloxacin abatement. A concentration of 100 μ M of PDS resulted in optimal removal of LFX in simulated wastewater. The toxicity test allowed inferring that simulated irradiation/PDS can inhibit the antibacterial character of waste effluents, which is relevant to preventing multi-resistant strains' development. The culture of Gram-positive and Gram-negative bacteria was not affected after the effective degradation of levofloxacin by the sulphate radical based AOP. Finally, a degradative pathway was suggested from the by-products and intermediates identified by LC-MS. Results demonstrate that the degradation of specific functional groups (i.e., piperazine ring) is associated with the loss of antibacterial character of the molecule. Thus, the mechanism demonstrates the successful degradation of levofloxacin and suggests promising niche application opportunities to ensure pharmaceutical abatement in wastewater effluents. Aromatic by-products were wholly depleted

within 10 min of treatment, highlighting simulated irradiation/PDS as a promising technology to mitigate the undesired effects of trace pharmaceuticals pollution in real wastewater effluents.

CHAPTER 5

Scientific activity in University of Ioannina (Department of Chemistry)

5.1 MTT assay for the toxicity evaluation of photocatalytic treatment of levofloxacin with PDS

During my PhD course, despite the restrictions related to the COVID-19 pandemic, I have had the opportunity to carry out some analyses at University of Ioannina (Greece), with Mrs Lekka's research group. In particular, we tested the toxicity of the samples obtained from levofloxacin treatment ($C = 10 \text{ mg}\cdot\text{L}^{-1}$) with peroxydisulphate ($C = 400 \text{ }\mu\text{M}$) in pure water, through MTT bioassay. MTT assays assessed the toxicity of selected samples on human epithelial-like lung carcinoma cell line A549, to obtain another critical feedback about the potential eco-compatibility of sulphate radicals treatment for levofloxacin removal.

5.2 *Chemicals*

MTT [3-(4,5-dimethylthiazol-2-yl)-2,5-diphenyltetrazolium bromide], ethanol, dimethylsulfoxide (DMSO), ascorbic acid, cholesterol acetate, 25-hydroxycholesterol, methyl- β -cyclodextrin, apolipoprotein A-1, and trypan blue were a product of Sigma Chemical. Cholesterol of enhanced purity was obtained from Avanti Polar Lipids. The sterile 96-well clear polystyrene-tissue culture plates were obtained from Corning Incorporated. Propidium iodide was obtained from Molecular Probes.

5.3 *Experimental section*

Selected samples obtained during homogeneous photocatalysis of levofloxacin ($C = 10 \text{ mg}\cdot\text{L}^{-1}$) with peroxydisulphate ($C = 400 \text{ }\mu\text{M}$) in pure water were used for MTT assay on human epithelial-like lung carcinoma cell line A549. All the samples were lyophilised and then re-suspended in the same F-12K growth medium volume to obtain the same initial concentration. We prepared four dilutions for each sample:

- Standard solution of levofloxacin at several concentrations:
 1. Initial concentration: $10 \text{ mg}\cdot\text{L}^{-1}$

2. 1st dilution: 7.5 mg·L⁻¹
 3. 2nd dilution: 5 mg·L⁻¹
 4. 3rd dilution: 2.5 mg·L⁻¹
 5. 4th dilution: 1 mg·L⁻¹
- Standard solution of peroxydisulphate at several concentrations:
 1. Initial concentration: 400 μM
 2. 1st dilution: 200 μM
 3. 2nd dilution: 100 μM
 4. 3rd dilution: 50 μM
 5. 4th dilution: 40 μM
 - MIX 1: standard solution of levofloxacin (10 mg·L⁻¹) and peroxydisulphate (400 μM) before irradiation: four serial 1:2 dilutions;
 - MIX 2: sample obtained after 2 minutes of irradiation of MIX 1 → four serial 1:2 dilutions;
 - MIX 3: sample obtained after 7 minutes of irradiation of MIX 1 → four serial 1:2 dilutions.

The American Type Culture Collection obtained the human epithelial-like lung carcinoma cell line A549. Cells were grown in 100-mm polystyrene tissue culture dishes in 10 mL of F-12K growth medium containing 10% fetal calf serum, penicillin (100 U/mL), and streptomycin (100 mg/mL) incubated at 37°C under a humidified atmosphere of air containing 5% CO₂. Cells were routinely passaged by trypsinisation and subcultured at an initial plating density of 0.5 million cells per plate.

Reduction of water-soluble tetrazolium salt, 3-[4,5-dimethyl-thiazol-2-yl]-2,5-diphenyltetrazolium bromide (MTT), to the water-insoluble formazan was measured. Cells were plated in 96-well half-area tissue culture plates, and the medium was replaced by 100 μL of the samples reported above, in the positions reported in **Fig. 5.1**.

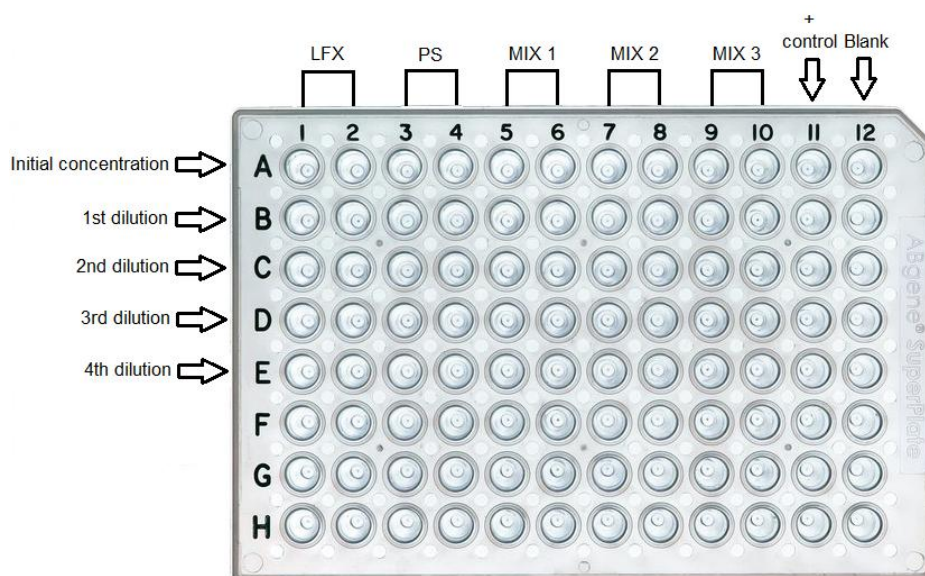


Fig. 5.1: Elisa's plate positions used for MTT assay of tested samples.

Then, fifty microliters of MTT ($4.0 \text{ mg}\cdot\text{mL}^{-1}$) was added, and the plate was incubated for 4h at 37°C . The purple formazan crystals thus formed were dissolved in $100 \mu\text{L}$ DMSO, and the optical densities on the plate were read at 540 nm using a plate reader, as summarised in **Fig. 5.2**. Trypan blue exclusion was performed by adding $25 \mu\text{L}$ of 0.1% trypan blue solution to $100 \mu\text{L}$ of cells suspended in phosphate-buffered saline (PBS). As described earlier, the cells that excluded the dye were counted on a hemocytometer.

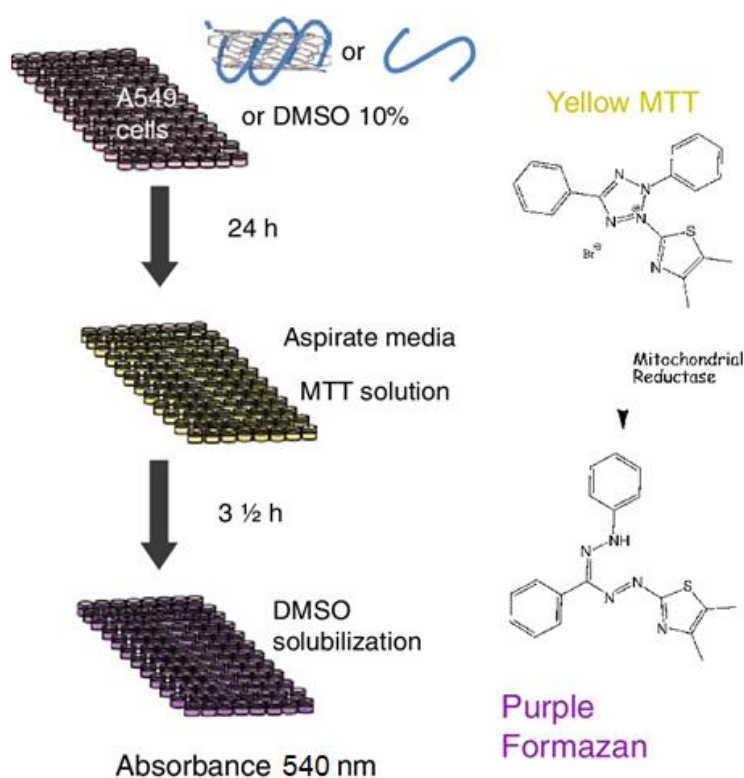


Fig. 5.2: Schematic procedure of MTT assay.

5.4 Results and discussion

To evaluate the potential effects of levofloxacin, peroxydisulphate and the samples obtained during the photocatalytic process on the viability of tumour cells, the cell viability assay (MTT) was performed on human epithelial-like lung carcinoma cell line A549. Through this assay, it was possible to compare the effects of the samples tested to see if the presence of levofloxacin by-products could be toxic on A549 cells, and it was possible to calculate the cell viability, expressed as:

$$\text{Cell viability (\%)} = \bar{A}_{\text{sample}} / \bar{A}_{\text{control}} \times 100 \quad \text{Eq. 5.1}$$

where \bar{A}_{sample} is the arithmetical average of the lecture at 540 nm using a plate reader, while \bar{A}_{control} is the average of control signal (only cells in F12K medium). Each sample was analysed in duplicate. The main results are reported in **Table 5.1**.

Table 5.1: Results of MTT assay on A549 cells.

Sample	Cells viability (%)
Levofloxacin (10 mg·L ⁻¹)	117.28
Peroxydisulphate (400 μM)	97.38
MIX 1 (LFX + PDS)	104.88
MIX 2 (after 2 minutes of irradiation)	119.36
MIX 3 (after 7 minutes of irradiation)	107.76

MIX 1: residual concentration of levofloxacin = 10 mg·L⁻¹

MIX 2: residual concentration of levofloxacin = 4.75 mg·L⁻¹

MIX 3: residual concentration of levofloxacin = 1 mg·L⁻¹

As can be shown from **Table 5.1** none of the tested samples affected significantly the viability of the cells.

5.5 Conclusions

Experimental results indicate that neither levofloxacin and samples contained the transformation products are cytotoxic. This aspect assumes particular importance because it seems to confirm the effectiveness of the treatment with sulphate radicals for levofloxacin degradation and also the potential application of the this degradation system on a larger scale.

CHAPTER 6

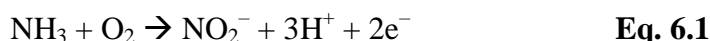
Training period at Hydros S.r.l.

During my PhD course I have had the opportunity to follow a six months internship period at Hydros S.r.l., a company that produces machines, packages and plants for:

- Water, wastewater and groundwater treatment;
- Waste treatment, composting and biogas production;
- Treatment of air and vapours from industrial processes;
- Special mechanical constructions.

In particular, I have attended to optimising of process parameters for the correct nitrification/denitrification treatment of wastewater.

Nitrification is a microbial process by which ammonia contained in the wastewater to treat is sequentially oxidised to nitrite and then to nitrate. The nitrification process is accomplished primarily by two groups of autotrophic nitrifying bacteria that can build organic molecules by using energy obtained from inorganic sources (in this case, ammonia or nitrite). In the first step of nitrification, ammonia-oxidising bacteria oxidise ammonia to nitrite, according to **Eq. 6.1**:



Nitrosomonas is the most frequently identified genus associated with this step, although other genera may be involved, including *Nitrosococcus* and *Nitrosospira*.

In the second step of the process, nitrite-oxidising bacteria oxidise nitrite to nitrate, according to **Eq. 6.2**:



Nitrobacter in the genus is most frequently associated with this second step.

Denitrification is when nitrates are reduced to gaseous nitrogen by facultative anaerobes. Facultative anaerobes, such as fungi, can flourish in anoxic conditions because they break down oxygen-containing compounds to obtain oxygen. Once introduced into the aquatic environment, nitrogen can exist in several forms – dissolved nitrogen gas (N_2), ammonia (NH_4^+ and NH_3), nitrite (NO_2^-), nitrate (NO_3^-), and organic nitrogen as proteinaceous matter or in dissolved or particulate phases. The organisms carrying out this process are called *denitrifiers*. In general,

General conclusion and perspectives

The presence of emerging contaminants in water is a worldwide problem. The main input source of micropollutants into the environment is wastewater effluents. It is confirmed by numerous scientific publications that their presence constitutes a risk for human and environmental health. In this scenario, the advanced oxidation processes (AOPs) offer a real opportunity for the removal of these pollutants from wastewater. The main objective of this PhD thesis was precisely to apply heterogeneous and homogeneous photolysis and photocatalysis systems in the liquid phase, for the removal of levofloxacin (LFX), a widely used antibiotic belonging to the quinolone family. Photolysis, photocatalysis by using titanium dioxide (TiO_2), hydrogen peroxide (H_2O_2), peroxymonosulphate (PMS) and peroxydisulphate (PDS) showed a good way to remove this antibiotic from water. Photocatalysis with TiO_2 powder is able to remove LFX and its by-products in four hours and seems to follow a second-order kinetic, but the necessity of an additional post-treatment for catalyst recovery limits its use. For this reason, a different system that used TiO_2 immobilised on the surface of a borosilicate tube was used as second aim of investigation. However, the results obtained from this treatment were not what was hoped for: this system follows a too slow kinetic, leading to a complete removal of LFX in almost 26 hours. *Vibrio fischeri* bioluminescence inhibition assay (VFBIA) and phytotoxicity tests revealed a toxicity increase during the process, maybe due to the coexistence and/or to a synergistic effect of TPs, or due to a possible detachment of TiO_2 from the borosilicate tube coating. Further investigations will be focused on this field. Another potential treatment used in this thesis for levofloxacin removal is represented from sulphate radicals. These reactive species, produced by the irradiation of oxidant agents like PMS and PDS, revealed a strong effect for the degradation of LFX and its transformation products. In particular, PDS was tested under simulated sunlight to remove LFX in distilled water and simulated wastewater (SWW), giving satisfactory results in both cases, with a complete degradation of the tested compound in only 10 minutes. In addition, toxicity tests conducted on *Micrococcus flavus* and *Escherichia coli*, and MTT assay on human epithelial-like lung carcinoma cell line A549 did not show any toxic effect. However, a cost-benefit analysis must be carried out for a potential application of sulphate radicals in real systems for decontamination of wastewater.

The experimental results obtained in this thesis tend to demonstrate that solar advanced oxidation processes has the potential to open new feasible remediation strategies for WWTPs effluent tertiary treatment before wastewater reuse in irrigation for instance. However, most investigations are done at lab-scale. For a practical view and commercial uses, much more work

is necessary to switch from batch work to a large scale to find out the efficiency and ecotoxicity of the processes.

REFERENCES

- Abbas, M., Adil, M., Ehtisham-ul-Haque, S., Munir, B., Yameen, M., Ghaffar, A., Shar, G.A., Asif Tahir, M., Iqbal, M., 2018. *Vibrio fischeri* bioluminescence inhibition assay for ecotoxicity assessment: A review. *Sci. Total Environ.* 626, 1295–1309. <https://doi.org/10.1016/J.SCITOTENV.2018.01.066>
- Adachi, F., Yamamoto, A., Takakura, K.I., Kawahara, R., 2013. Occurrence of fluoroquinolones and fluoroquinolone-resistance genes in the aquatic environment. *Sci. Total Environ.* 444, 508–514. <https://doi.org/10.1016/J.SCITOTENV.2012.11.077>
- Adriaenssens, N., Bruyndonckx, R., Versporten, A., Hens, N., Monnet, D.L., Molenberghs, G., Goossens, H., Weist, K., Coenen, S., 2021. Consumption of quinolones in the community, European Union/European Economic Area, 1997–2017. *J. Antimicrob. Chemother.* 76, ii37–ii44. <https://doi.org/10.1093/JAC/DKAB176>
- Aguiar, L.L., Andrade-Vieira, L.F., de Oliveira David, J.A., 2016. Evaluation of the toxic potential of coffee wastewater on seeds, roots and meristematic cells of *Lactuca sativa* L. *Ecotoxicol. Environ. Saf.* 133, 366–372. <https://doi.org/10.1016/J.ECOENV.2016.07.019>
- Ahmed, M.M., Barbati, S., Doumenq, P., Chiron, S., 2012. Sulfate radical anion oxidation of diclofenac and sulfamethoxazole for water decontamination. *Chem. Eng. J.* 197, 440–447. <https://doi.org/10.1016/j.cej.2012.05.040>
- Ahmed, M.M., Brienza, M., Goetz, V., Chiron, S., 2014. Solar photo-Fenton using peroxymonosulfate for organic micropollutants removal from domestic wastewater: Comparison with heterogeneous TiO₂ photocatalysis. *Chemosphere* 117, 256–261. <https://doi.org/10.1016/j.chemosphere.2014.07.046>
- Al Mayyahi, A., Ali Abed Al-Asadi, H., 2018. Advanced Oxidation Processes (AOPs) for Wastewater Treatment and Reuse: A Brief Review. *Asian J. Appl. Sci. Technol.* 2, 18–30.
- Alalwan, H.A., Kadhom, M.A., Alminshid, A.H., 2020. Removal of heavy metals from wastewater using agricultural byproducts. *J. Water Supply Res. Technol.* 69, 99–112. <https://doi.org/10.2166/aqua.2020.133>
- Alcaraz, M.R., Culzoni, M.J., Goicoechea, H.C., 2016. Enhanced fluorescence sensitivity by coupling yttrium-analyte complexes and three-way fast high-performance liquid

- chromatography data modeling. *Anal. Chim. Acta* 902, 50–58.
<https://doi.org/10.1016/J.ACA.2015.10.038>
- Ambulkar, A., Nathanson, J.A., 2021. Wastewater treatment [WWW Document]. *Encycl. Br.*
URL <https://www.britannica.com/technology/wastewater-treatment>.
- Andreozzi, R., Caprio, V., Insola, A., Marotta, R., 1999. Advanced oxidation processes (AOP) for water purification and recovery. *Catal. Today* 53, 51–59. [https://doi.org/10.1016/S0920-5861\(99\)00102-9](https://doi.org/10.1016/S0920-5861(99)00102-9)
- Anipsitakis, G.P., Dionysiou, D.D., 2003. Degradation of Organic Contaminants in Water with Sulfate Radicals Generated by the Conjunction of Peroxymonosulfate with Cobalt. *Environ. Sci. Technol.* 37, 4790–4797. <https://doi.org/10.1021/ES0263792>
- Arvanitoyannis, I.S., Kassaveti, A., 2008. Olive Oil Waste Management: Treatment Methods and Potential Uses of Treated Waste, in: *Waste Management for the Food Industries*. Academic Press, pp. 453–568. <https://doi.org/10.1016/B978-012373654-3.50011-0>
- Azzaz, A.A., Assadi, A.A., Jellali, S., Bouzaza, A., Wolbert, D., Rtimi, S., Bousselmi, L., 2018. Discoloration of simulated textile effluent in continuous photoreactor using immobilized titanium dioxide: Effect of zinc and sodium chloride. *J. Photochem. Photobiol. A Chem.* 358, 111–120. <https://doi.org/10.1016/J.JPHOTOCHEM.2018.01.032>
- Babuponnusami, A., Muthukumar, K., 2014. A review on Fenton and improvements to the Fenton process for wastewater treatment. *J. Environ. Chem. Eng.* 2, 557–572. <https://doi.org/10.1016/J.JECE.2013.10.011>
- Backhaus, T., Scholze, M., Grimme, L.H., 2000. The single substance and mixture toxicity of quinolones to the bioluminescent bacterium *Vibrio fischeri*. *Aquat. Toxicol.* 49, 49–61. [https://doi.org/10.1016/S0166-445X\(99\)00069-7](https://doi.org/10.1016/S0166-445X(99)00069-7)
- Bagur-González, M.G., Estepa-Molina, C., Martín-Peinado, F., Morales-Ruano, S., 2011. Toxicity assessment using *Lactuca sativa* L. bioassay of the metal(loid)s As, Cu, Mn, Pb and Zn in soluble-in-water saturated soil extracts from an abandoned mining site. *J. Soils Sediments* 11, 281–289. <https://doi.org/10.1007/S11368-010-0285-4>
- Balasuriya, A., 2018. Coastal area management: Biodiversity and ecological sustainability in sri lankan perspective, in: *Biodiversity and Climate Change Adaptation in Tropical Islands*.

- Elsevier, pp. 701–724. <https://doi.org/10.1016/B978-0-12-813064-3.00025-9>
- Bartlett, P.D., Cotman, J.D., 1949. The Kinetics of the Decomposition of Potassium Persulfate in Aqueous Solutions of Methanol. *J. Am. Chem. Soc.* 71, 1419–1422. <https://doi.org/10.1021/JA01172A078>
- Baxendale, J.H., Wilson, J.A., 1957. The photolysis of hydrogen peroxide at high light intensities. *Trans. Faraday Soc.* 53, 344–356.
- Bedford, N.M., Pelaez, M., Han, C., Dionysiou, D.D., Steckl, A.J., 2012. Photocatalytic cellulosic electrospun fibers for the degradation of potent cyanobacteria toxin microcystin-LR. *J. Mater. Chem.* 22, 12666–12674. <https://doi.org/10.1039/C2JM31597A>
- Behnajady, M.A., Modirshahla, N., Daneshvar, N., Rabbani, M., 2007. Photocatalytic degradation of an azo dye in a tubular continuous-flow photoreactor with immobilized TiO₂ on glass plates. *Chem. Eng. J.* 127, 167–176. <https://doi.org/10.1016/J.CEJ.2006.09.013>
- Beltrán, F.J., González, M., González, J.F., 1997. Industrial wastewater advanced oxidation. Part 1. UV radiation in the presence and absence of hydrogen peroxide. *Water Res.* 31, 2405–2414. [https://doi.org/10.1016/S0043-1354\(97\)00077-8](https://doi.org/10.1016/S0043-1354(97)00077-8)
- Bendz, D., Paxéus, N.A., Ginn, T.R., Loge, F.J., 2005. Occurrence and fate of pharmaceutically active compounds in the environment, a case study: Höje River in Sweden. *J. Hazard. Mater.* 122, 195–204. <https://doi.org/10.1016/J.JHAZMAT.2005.03.012>
- Berridge, M. V., Herst, P.M., Tan, A.S., 2005. Tetrazolium dyes as tools in cell biology: New insights into their cellular reduction. *Biotechnol. Annu. Rev.* 11, 127–152. [https://doi.org/10.1016/S1387-2656\(05\)11004-7](https://doi.org/10.1016/S1387-2656(05)11004-7)
- Berridge, M. V., Tan, A.S., 1993. Characterization of the Cellular Reduction of 3-(4,5-dimethylthiazol-2-yl)-2,5-diphenyltetrazolium bromide (MTT): Subcellular Localization, Substrate Dependence, and Involvement of Mitochondrial Electron Transport in MTT Reduction. *Arch. Biochem. Biophys.* 303, 474–482. <https://doi.org/10.1006/ABBI.1993.1311>
- Blatchley, E.R., Gong, W.L., Alleman, J.E., Rose, J.B., Huffman, D.E., Otaki, M., Lisle, J.T., 2007. Effects of Wastewater Disinfection on Waterborne Bacteria and Viruses. *Water Environ. Res.* 79, 81–92. <https://doi.org/10.2175/106143006X102024>

- Blinova, I., 2004. Use of freshwater algae and duckweeds for phytotoxicity testing. *Environ. Toxicol.* 19, 425–428. <https://doi.org/10.1002/TOX.20042>
- Blok, C., Baumgarten, A., Baas, R., Wever, G., Lohr, D., 2019. Analytical Methods Used With Soilless Substrates, in: *Soilless Culture: Theory and Practice*. Elsevier, pp. 509–564. <https://doi.org/10.1016/B978-0-444-63696-6.00011-6>
- Bottoni, P., Caroli, S., Caracciolo, A.B., 2010. Pharmaceuticals as priority water contaminants. *Toxicol. Environ. Chem.* 92, 549–565. <https://doi.org/10.1080/02772241003614320>
- Bottoni, P., Fidente, R., 2005. A pilot study for the assessment of pharmaceuticals as water contaminants. *Ann. Ist. Super. Sanita* 41, 333–342.
- Boy-Roura, M., Mas-Pla, J., Petrovic, M., Gros, M., Soler, D., Brusi, D., Menció, A., 2018. Towards the understanding of antibiotic occurrence and transport in groundwater: Findings from the Baix Fluvià alluvial aquifer (NE Catalonia, Spain). *Sci. Total Environ.* 612, 1387–1406. <https://doi.org/10.1016/j.scitotenv.2017.09.012>
- Brienza, M., Katsoyiannis, I.A., 2017. Sulfate Radical Technologies as Tertiary Treatment for the Removal of Emerging Contaminants from Wastewater. *Sustain.* 2017, Vol. 9, Page 1604 9, 1604. <https://doi.org/10.3390/SU9091604>
- Brienza, M., Mahdi Ahmed, M., Escande, A., Plantard, G., Scrano, L., Chiron, S., A. Bufo, S., Goetz, V., 2014. Relevance of a photo-Fenton like technology based on peroxymonosulphate for 17 β -estradiol removal from wastewater. *Chem. Eng. J.* 257, 191–199. <https://doi.org/10.1016/J.CEJ.2014.07.061>
- Brienza, M., Manasfi, R., Chiron, S., 2019. Relevance of N-nitrosation reactions for secondary amines in nitrate-rich wastewater under UV-C treatment. *Water Res.* 162, 22–29. <https://doi.org/10.1016/J.WATRES.2019.06.055>
- Brienza, M., Manasfi, R., Sauvêtre, A., Chiron, S., 2020. Nitric oxide reactivity accounts for N-nitroso-ciprofloxacin formation under nitrate-reducing conditions. *Water Res.* 185, 116293. <https://doi.org/10.1016/J.WATRES.2020.116293>
- Brillas, E., Sirés, I., Oturan, M.A., 2009. Electro-Fenton Process and Related Electrochemical Technologies Based on Fenton's Reaction Chemistry. *Chem. Rev.* 109, 6570–6631. <https://doi.org/10.1021/CR900136G>

- Busca, G., Berardinelli, S., Resini, C., Arrighi, L., 2008. Technologies for the removal of phenol from fluid streams: a short review of recent developments. *J. Hazard. Mater.* 160, 265–288. <https://doi.org/10.1016/J.JHAZMAT.2008.03.045>
- Bustillo-Lecompte, C., 2020. Advanced Oxidation Processes: Applications, Trends, and Prospects. InTechOpen. <https://doi.org/10.5772/intechopen.85681>
- Byrne, J.A., Eggins, B.R., Brown, N.M.D., McKinney, B., Rouse, M., 1998. Immobilisation of TiO₂ powder for the treatment of polluted water. *Appl. Catal. B Environ.* 17, 25–36. [https://doi.org/10.1016/S0926-3373\(97\)00101-X](https://doi.org/10.1016/S0926-3373(97)00101-X)
- Cai, H., Hauser, M., Naider, F., Becker, J.M., 2016. Halo Assay for Toxic Peptides and Other Compounds in Microorganisms. *Bio-protocol* 6, e2025. <https://doi.org/10.21769/BIOPROTOCOL.2025>
- Calderón-Parra, J., Muiño-Míguez, A., Bendala-Estrada, A.D., Ramos-Martínez, A., Muñoz-Rubio, E., Carracedo, E.F., Montes, J.T., Rubio-Rivas, M., Arnalich-Fernandez, F., Pérez, J.L.B., Bruñén, J.M.G., Beamonte, E. del C., Fontan, P.M.P., Carmona, M. del M., Martínez, R.F.-M., García, A.G., Mosteiro, C.S., Almeida, C.T. de, Moraleja, J.G., Deodati, F., Escalante, M.D.M., Tomás, M.L.A., Huelgas, R.G., Rojo, J.M.C., Núñez-Cortés, J.M., 2021. Inappropriate antibiotic use in the COVID-19 era: Factors associated with inappropriate prescribing and secondary complications. Analysis of the registry SEMI-COVID. *PLoS One* 16. <https://doi.org/10.1371/JOURNAL.PONE.0251340>
- Calza, P., Massolino, C., Pelizzetti, E., 2008. Photo-induced transformation of hexaconazole and dimethomorph over TiO₂ suspension. *J. Photochem. Photobiol. A Chem.* 200, 356–363. <https://doi.org/10.1016/J.JPHOTOCHEM.2008.08.018>
- Ceglie, F.G., Elshafie, H., Verrastro, V., Tittarelli, F., 2011. Evaluation of olive pomace and green waste composts as peat substitutes for organic tomato seedling production. *Compost Sci. Util.* 19, 293–300. <https://doi.org/10.1080/1065657X.2011.10737011>
- Chen, X., Liu, L., Yu, P.Y., Mao, S.S., 2011. Increasing solar absorption for photocatalysis with black hydrogenated titanium dioxide nanocrystals. *Science* 331, 746–750. <https://doi.org/10.1126/SCIENCE.1200448>
- Chen, Y., Stathatos, E., Dionysiou, D.D., 2008. Microstructure characterization and photocatalytic activity of mesoporous TiO₂ films with ultrafine anatase nanocrystallites.

- Surf. Coatings Technol. 202, 1944–1950.
<https://doi.org/10.1016/J.SURFCOAT.2007.08.041>
- Chhaya, Raychoudhury, T., Prajapati, S.K., 2020. Bioremediation of Pharmaceuticals in Water and Wastewater. *Microb. Bioremediation Biodegrad.* 425–446. https://doi.org/10.1007/978-981-15-1812-6_16
- Chu, D.T.W., Fernandest, P.B., 1989. Structure-Activity Relationships of the Fluoroquinolones. *Antimicrob. Agents Chemother.* 33, 131–135. <https://doi.org/10.1128/AAC.33.2.131>
- Climate Policy Watcher, 2021. Ion Exchange - Wastewater Treatment [WWW Document]. URL <https://www.climate-policy-watcher.org/wastewater-treatment/ion-exchange.html>.
- Comninellis, C., Kapalka, A., Malato, S., Parsons, S.A., Poulios, I., Mantzavinos, D., 2008. Advanced oxidation processes for water treatment: advances and trends for R&D. *J. Chem. Technol. Biotechnol.* 83, 769–776. <https://doi.org/10.1002/JCTB.1873>
- Cunha, D.L., Kuznetsov, A., Achete, C.A., Machado, A.E. da H., Marques, M., 2018. Immobilized TiO₂ on glass spheres applied to heterogeneous photocatalysis: Photoactivity, leaching and regeneration process. *PeerJ* 2018, e4464. <https://doi.org/10.7717/PEERJ.4464>
- D'Arienzo, S., Carmignani, C., 2021. L'utilizzo di antibiotici in ospedale durante la pandemia, uno sguardo alla letteratura [WWW Document]. Agenzia Reg. di Sanità - Toscana. URL <https://www.ars.toscana.it/2-articoli/4619-utilizzo-di-antibiotici-in-ospedale-durante-pandemia-covid-uno-sguardo-della-letteratura.html>.
- Dash, M., Panda, S.K., 2001. Salt Stress Induced Changes in Growth and Enzyme Activities in Germinating Phaseolus Mungo Seeds. *Biol. Plant.* 44, 587–589. <https://doi.org/10.1023/A:1013750905746>
- Davies, J., Davies, D., 2010. Origins and Evolution of Antibiotic Resistance. *Microbiol. Mol. Biol. Rev.* 74, 1092–2172. <https://doi.org/10.1128/MMBR.00016-10>
- De Witte, B., Dewulf, J., Demeestere, K., Van De Vyvere, V., De Wispelaere, P., Van Langenhove, H., 2008. Ozonation of ciprofloxacin in water: HRMS identification of reaction products and pathways. *Environ. Sci. Technol.* 42, 4889–4895. <https://doi.org/10.1021/es8000689>
- De Witte, B., Langenhove, H. Van, Hemelsoet, K., Demeestere, K., Wispelaere, P. De, Van

- Speybroeck, V., Dewulf, J., 2009. Levofloxacin ozonation in water: Rate determining process parameters and reaction pathway elucidation. *Chemosphere* 76, 683–689. <https://doi.org/10.1016/j.chemosphere.2009.03.048>
- Deblonde, T., Cossu-Leguille, C., Hartemann, P., 2011. Emerging pollutants in wastewater: A review of the literature. *Int. J. Hyg. Environ. Health* 214, 442–448. <https://doi.org/10.1016/j.ijheh.2011.08.002>
- Doña, I., Barrionuevo, E., Montañez, M.I., Fernández, T.D., Torres, M.J., 2018. Quinolone Allergy, in: *Drug Allergy Testing*. Elsevier, pp. 137–144. <https://doi.org/10.1016/B978-0-323-48551-7.00013-4>
- Dunn, A.K., Rader, B.A., Stabb, E. V., Mandel, M.J., 2015. Regulation of bioluminescence in *Photobacterium leiognathi* strain KNH6. *J. Bacteriol.* 197, 3676–3685. <https://doi.org/10.1128/JB.00524-15>
- Ebert, I., Bachmann, J., Kühnen, U., Küster, A., Kussatz, C., Maletzki, D., Schlüter, C., 2011. Toxicity of the fluoroquinolone antibiotics enrofloxacin and ciprofloxacin to photoautotrophic aquatic organisms. *Environ. Toxicol. Chem.* 30, 2786–2792. <https://doi.org/10.1002/ETC.678>
- El Najjar, N.H., Deborde, M., Journal, R., Vel Leitner, N.K., 2013. Aqueous chlorination of levofloxacin: Kinetic and mechanistic study, transformation product identification and toxicity. *Water Res.* 47, 121–129. <https://doi.org/10.1016/J.WATRES.2012.09.035>
- El Yadini, A., Saufi, H., Dunlop, P.S.M., Byrne, J.A., El Azzouzi, M., El Hajjaji, S., 2014. Supported TiO₂ on Borosilicate Glass Plates for Efficient Photocatalytic Degradation of Fenamiphos. *J. Catal.* 1–8. <https://doi.org/10.1155/2014/413693>
- Elshafie, H.S., Sakr, S.H., Sadeek, S.A., Camele, I., 2019. Biological Investigations and Spectroscopic Studies of New Moxifloxacin/Glycine-Metal Complexes. *Chem. Biodivers.* 16, e1800633. <https://doi.org/10.1002/CBDV.201800633>
- Emmanuel, E., Perrodin, Y., Keck, G., Blanchard, J.M., Vermande, P., 2005. Ecotoxicological risk assessment of hospital wastewater: a proposed framework for raw effluents discharging into urban sewer network. *J. Hazard. Mater.* 117, 1–11. <https://doi.org/10.1016/J.JHAZMAT.2004.08.032>

- Environmental Protection Agency, 2007. Wastewater Technology Fact Sheet - Denitrification Filters.
- Epold, I., Trapido, M., Dulova, N., 2015. Degradation of levofloxacin in aqueous solutions by Fenton, ferrous ion-activated persulfate and combined Fenton/persulfate systems. *Chem. Eng. J.* 279, 452–462. <https://doi.org/10.1016/j.cej.2015.05.054>
- European Medicines Agency, 2018. Disabling and potentially permanent side effects lead to suspension or restrictions of quinolone and fluoroquinolone antibiotics.
- Expósito, A.J., Patterson, D.A., Mansor, W.S.W., Monteagudo, J.M., Emanuelsson, E., Sanmartín, I., Durán, A., 2017. Antipyrine removal by TiO₂ photocatalysis based on spinning disc reactor technology. *J. Environ. Manage.* 187, 504–512. <https://doi.org/10.1016/J.JENVMAN.2016.11.012>
- Faust, B.C., Hoigné, J., 1990. Photolysis of Fe (III)-hydroxy complexes as sources of OH radicals in clouds, fog and rain. *Atmos. Environ. Part A. Gen. Top.* 24, 79–89. [https://doi.org/10.1016/0960-1686\(90\)90443-Q](https://doi.org/10.1016/0960-1686(90)90443-Q)
- Fent, K., 2015. Progestins as endocrine disrupters in aquatic ecosystems: Concentrations, effects and risk assessment. *Environ. Int.* 84, 115–130. <https://doi.org/10.1016/J.ENVINT.2015.06.012>
- Fick, J., Söderström, H., Lindberg, R.H., Phan, C., Tysklind, M., Larsson, D.G.J., 2009. Contamination of surface, ground, and drinking water from pharmaceutical production. *Environ. Toxicol. Chem.* 28, 2522–2527. <https://doi.org/10.1897/09-073.1>
- Fink, L., Dror, I., Berkowitz, B., 2012. Enrofloxacin oxidative degradation facilitated by metal oxide nanoparticles. *Chemosphere* 86, 144–149. <https://doi.org/10.1016/J.CHEMOSPHERE.2011.10.002>
- Frade, V.M.F., Dias, M., Teixeira, A.C.S.C., Palma, M.S.A., 2014. Environmental contamination by fluoroquinolones. *Brazilian J. Pharm. Sci.* 50, 41–54. <https://doi.org/10.1590/S1984-82502011000100004>
- Gao, Y., Zou, D., 2020. Efficient degradation of levofloxacin by a microwave–3D ZnCo₂O₄/activated persulfate process: Effects, degradation intermediates, and acute toxicity. *Chem. Eng. J.* 393, 124795. <https://doi.org/10.1016/j.cej.2020.124795>

- Garcia-Segura, S., Nienhauser, A.B., Fajardo, A.S., Bansal, R., Conrad, C.L., Fortner, J.D., Marcos-Hernández, M., Rogers, T., Villagran, D., Wong, M.S., Westerhoff, P., 2020. Disparities between experimental and environmental conditions: Research steps toward making electrochemical water treatment a reality. *Curr. Opin. Electrochem.* 22, 9–16. <https://doi.org/10.1016/J.COEELEC.2020.03.001>
- Geissen, V., Mol, H., Klumpp, E., Umlauf, G., Nadal, M., Van der Ploeg, M., Van de Zee, S.E.A.T.M., Ritsema, C.J., 2015. Emerging pollutants in the environment: A challenge for water resource management. *Int. Soil Water Conserv. Res.* 3, 57–65. <https://doi.org/10.1016/J.ISWCR.2015.03.002>
- Gerba, C.P., Pepper, I.L., 2019. Municipal Wastewater Treatment. *Environ. Pollut. Sci.* 393–418. <https://doi.org/10.1016/B978-0-12-814719-1.00022-7>
- Ghasemi, M., Turnbull, T., Sebastian, S., Kempson, I., 2021. The MTT Assay: Utility, Limitations, Pitfalls, and Interpretation in Bulk and Single-Cell Analysis. *Int. J. Mol. Sci.* 22, 12827. <https://doi.org/10.3390/IJMS222312827>
- Ghatak, H.R., 2014. Advanced Oxidation Processes for the Treatment of Biorecalcitrant Organics in Wastewater. *Crit. Rev. Environ. Sci. Technol.* 44, 1167–1219. <https://doi.org/10.1080/10643389.2013.763581>
- Ghime, D., Ghosh, P., 2020. Advanced Oxidation Processes: A Powerful Treatment Option for the Removal of Recalcitrant Organic Compounds, in: *Advanced Oxidation Processes - Applications, Trends, and Prospects.* IntechOpen. <https://doi.org/10.5772/INTECHOPEN.90192>
- Glaze, W.H., Kang, J.-W., Chapin, D.H., 1987. The Chemistry of Water Treatment Processes Involving Ozone, Hydrogen Peroxide and Ultraviolet Radiation. *Ozone Sci. Eng.* 9, 335–352. <https://doi.org/10.1080/01919518708552148>
- Golet, E.M., Alder, A.C., Giger, W., 2002a. Environmental Exposure and Risk Assessment of Fluoroquinolone Antibacterial Agents in Wastewater and River Water of the Glatt Valley Watershed, Switzerland. *Environ. Sci. Technol.* 36, 3645–3651. <https://doi.org/10.1021/ES0256212>
- Golet, E.M., Strehler, A., Alder, A.C., Giger, W., 2002b. Determination of Fluoroquinolone Antibacterial Agents in Sewage Sludge and Sludge-Treated Soil Using Accelerated Solvent

- Extraction Followed by Solid-Phase Extraction. *Anal. Chem.* 74, 5455–5462. <https://doi.org/10.1021/AC025762M>
- González-Pleiter, M., Gonzalo, S., Rodea-Palomares, I., Leganés, F., Rosal, R., Boltes, K., Marco, E., Fernández-Piñas, F., 2013. Toxicity of five antibiotics and their mixtures towards photosynthetic aquatic organisms: Implications for environmental risk assessment. *Water Res.* 47, 2050–2064. <https://doi.org/10.1016/J.WATRES.2013.01.020>
- Gothwal, R., Shashidhar, T., 2015. Antibiotic Pollution in the Environment: A Review. *Clean - Soil, Air, Water* 43, 479–489. <https://doi.org/10.1002/clen.201300989>
- Gothwal, R., Thatikonda, S., 2017. Role of environmental pollution in prevalence of antibiotic resistant bacteria in aquatic environment of river: case of Musi river, South India. *Water Environ. J.* 31, 456–462. <https://doi.org/10.1111/WEJ.12263>
- Gros, M., Petrović, M., Ginebreda, A., Barceló, D., 2010. Removal of pharmaceuticals during wastewater treatment and environmental risk assessment using hazard indexes. *Environ. Int.* 36, 15–26. <https://doi.org/10.1016/J.ENVINT.2009.09.002>
- Gros, M., Rodríguez-Mozaz, S., Barceló, D., 2013. Rapid analysis of multiclass antibiotic residues and some of their metabolites in hospital, urban wastewater and river water by ultra-high-performance liquid chromatography coupled to quadrupole-linear ion trap tandem mass spectrometry. *J. Chromatogr. A* 1292, 173–188. <https://doi.org/10.1016/J.CHROMA.2012.12.072>
- Guo, Q., Zhou, C., Ma, Z., Yang, X., 2019. Fundamentals of TiO₂ Photocatalysis: Concepts, Mechanisms, and Challenges. *Adv. Mater.* 31, 1901997. <https://doi.org/10.1002/ADMA.201901997>
- Haber, F., Weiss, J., 1934. The catalytic decomposition of hydrogen peroxide by iron salts. *Proc. R. Soc. London. Ser. A - Math. Phys. Sci.* 147, 332–351. <https://doi.org/10.1098/RSPA.1934.0221>
- Han, H., Bai, R., 2010. Highly effective buoyant photocatalyst prepared with a novel layered-TiO₂ configuration on polypropylene fabric and the degradation performance for methyl orange dye under UV–Vis and Vis lights. *Sep. Purif. Technol.* 73, 142–150. <https://doi.org/10.1016/J.SEPPUR.2010.03.017>

- Han, H., Bai, R., 2009. Buoyant photocatalyst with greatly enhanced visible-light activity prepared through a low temperature hydrothermal method. *Ind. Eng. Chem. Res.* 48, 2891–2898. <https://doi.org/10.1021/IE801362A>
- Hashimoto, K., Irie, H., Fujishima, A., 2005. TiO₂ photocatalysis: A historical overview and future prospects. *Jpn. J. Appl. Phys.* 44, 8269–8285. <https://doi.org/10.1143/JJAP.44.8269/XML>
- Hayat, W., Zhang, Y., Hussain, I., Huang, S., Du, X., 2020. Comparison of radical and non-radical activated persulfate systems for the degradation of imidacloprid in water. *Ecotoxicol. Environ. Saf.* 188, 109891. <https://doi.org/10.1016/j.ecoenv.2019.109891>
- He, X., Wang, Z., Nie, X., Yang, Yufen, Pan, D., Leung, A.O.W., Cheng, Z., Yang, Yongtao, Li, K., Chen, K., 2012. Residues of fluoroquinolones in marine aquaculture environment of the Pearl River Delta, South China. *Environ. Geochem. Health* 34, 323–335. <https://doi.org/10.1007/S10653-011-9420-4>
- Hernando, M.D., Gómez, M.J., Agüera, A., Fernández-Alba, A.R., 2007. LC-MS analysis of basic pharmaceuticals (beta-blockers and anti-ulcer agents) in wastewater and surface water. *TrAC Trends Anal. Chem.* 26, 581–594. <https://doi.org/10.1016/J.TRAC.2007.03.005>
- Hoigne, J., Bader, H., 1979. Ozonation Of Water: Selectivity And Rate Of Oxidation Of Solutes. *Ozone Sci. Eng.* 1, 73–85. <https://doi.org/10.1080/01919517908550834>
- Hoigné, J., Bader, H., Haag, W.R., Staehelin, J., 1985. Rate constants of reactions of ozone with organic and inorganic compounds in water—III. Inorganic compounds and radicals. *Water Res.* 19, 993–1004. [https://doi.org/10.1016/0043-1354\(85\)90368-9](https://doi.org/10.1016/0043-1354(85)90368-9)
- Hongxia, Y., Jing, C., Yuxia, C., Huihua, S., Zhonghai, D., Hongjun, J., 2004. Application of toxicity identification evaluation procedures on wastewaters and sludge from a municipal sewage treatment works with industrial inputs. *Ecotoxicol. Environ. Saf.* 57, 426–430. <https://doi.org/10.1016/J.ECOENV.2003.08.024>
- Hou, J., Wang, L., Wang, C., Zhang, S., Liu, H., Li, S., Wang, X., 2019. Toxicity and mechanism of action of titanium dioxide nanoparticles in living organisms. *J. Environ. Sci.*, 40–53. <https://doi.org/10.1016/j.jes.2018.06.010>

- House, D.A., 1962. Kinetics and mechanism of oxidations by peroxydisulfate. *Chem. Rev.* 62, 185–203. <https://doi.org/10.1021/CR60217A001>
- Hreiz, R., Latifi, M.A., Roche, N., 2015. Optimal design and operation of activated sludge processes: State-of-the-art. *Chem. Eng. J.* 281, 900–920. <https://doi.org/10.1016/J.CEJ.2015.06.125>
- Huggett, D.B., Brooks, B.W., Peterson, B., Foran, C.M., Schlenk, D., 2001. Toxicity of Select Beta Adrenergic Receptor-Blocking Pharmaceuticals (B-Blockers) on Aquatic Organisms. *Arch. Environ. Contam. Toxicol.* 43, 229–235. <https://doi.org/10.1007/S00244-002-1182-7>
- Hughes, S.R., Kay, P., Brown, L.E., 2013. Global Synthesis and Critical Evaluation of Pharmaceutical Data Sets Collected from River Systems. *Environ. Sci. Technol.* 47, 661–677. <https://doi.org/10.1021/ES3030148>
- Ibhadon, A.O., Fitzpatrick, P., 2013. Heterogeneous Photocatalysis: Recent Advances and Applications. *Catalysts* 3, 189–218. <https://doi.org/10.3390/CATAL3010189>
- Jain, A., Vaya, D., 2017. Photocatalytic activity of TiO₂ nanomaterial. *J. Chil. Chem. Soc.* 62, 3683–3690. <https://doi.org/10.4067/S0717-97072017000403683>
- Janecko, N., Pokludova, L., Blahova, J., Svobodova, Z., Literak, I., 2016. Implications of fluoroquinolone contamination for the aquatic environment - A review. *Environ. Toxicol. Chem.* 35, 2647–2656. <https://doi.org/10.1002/ETC.3552>
- Jia, A., Wan, Y., Xiao, Y., Hu, J., 2012. Occurrence and fate of quinolone and fluoroquinolone antibiotics in a municipal sewage treatment plant. *Water Res.* 46, 387–394. <https://doi.org/10.1016/J.WATRES.2011.10.055>
- Jiang, C., Ji, Y., Shi, Y., Chen, J., Cai, T., 2016. Sulfate radical-based oxidation of fluoroquinolone antibiotics: Kinetics, mechanisms and effects of natural water matrices. *Water Res.* 106, 507–517. <https://doi.org/10.1016/j.watres.2016.10.025>
- Jiménez, E., Gilles, M.K., Ravishankara, A.R., 2003. Kinetics of the reactions of the hydroxyl radical with CH₃OH and C₂H₅OH between 235 and 360 K. *J. Photochem. Photobiol. A Chem.* 157, 237–245. [https://doi.org/10.1016/S1010-6030\(03\)00073-X](https://doi.org/10.1016/S1010-6030(03)00073-X)
- Johansson, C.H., Janmar, L., Backhaus, T., 2014. Toxicity of ciprofloxacin and sulfamethoxazole to marine periphytic algae and bacteria. *Aquat. Toxicol.* 156, 248–258.

- <https://doi.org/10.1016/J.AQUATOX.2014.08.015>
- Johnson, R.L., Tratnyek, P.G., Johnson, R.O.B., 2008. Persulfate persistence under thermal activation conditions. *Environ. Sci. Technol.* 42, 9350–9356. <https://doi.org/10.1021/ES8019462>
- Jung, Y.J., Kim, W.G., Yoon, Y., Kang, J.-W., Hong, Y.M., Kim, H.W., 2012. Removal of amoxicillin by UV and UV/H₂O₂ processes. *Sci. Total Environ.* 420, 160–167. <https://doi.org/10.1016/j.scitotenv.2011.12.011>
- Juretic, D., Kusic, H., Dionysiou, D.D., Bozic, A.L., 2013. Environmental aspects of photooxidative treatment of phenolic compounds. *J. Hazard. Mater.* 262, 377–386. <https://doi.org/10.1016/J.JHAZMAT.2013.08.060>
- Kaeding, A.J., Ast, J.C., Pearce, M.M., Urbanczyk, H., Kimura, S., Endo, H., Nakamura, M., Dunlap, P. V., 2007. Phylogenetic diversity and cosymbiosis in the bioluminescent symbioses of “*Photobacterium mandapamensis*.” *Appl. Environ. Microbiol.* 73, 3173–3182. <https://doi.org/10.1128/AEM.02212-06>
- Kamagate, M., Assadi, A.A., Kone, T., Giraudet, S., Coulibaly, L., Hanna, K., 2018. Use of laterite as a sustainable catalyst for removal of fluoroquinolone antibiotics from contaminated water. *Chemosphere* 195, 847–853. <https://doi.org/10.1016/J.CHEMOSPHERE.2017.12.165>
- Kan, H., Wang, T., Yu, J., Qu, G., Zhang, P., Jia, H., Sun, H., 2021. Remediation of organophosphorus pesticide polluted soil using persulfate oxidation activated by microwave. *J. Hazard. Mater.* 401, 123361. <https://doi.org/10.1016/J.JHAZMAT.2020.123361>
- Kang, Y.W., Hwang, K.Y., 2000. Effects of reaction conditions on the oxidation efficiency in the Fenton process. *Water Res.* 34, 2786–2790. [https://doi.org/10.1016/S0043-1354\(99\)00388-7](https://doi.org/10.1016/S0043-1354(99)00388-7)
- Khalaf, S., Shoqeir, J.H., Lelario, F., Scrano, L., Karaman, R., Bufo, S.A., 2017. Removal of Diclofenace Sodium from Aqueous Environments Using Heterogeneous Photocatalysis Treatment. *Imp. J. Interdiscip. Res.* 3, 766–776.
- Khalaf, S., Shoqeir, J.H., Scrano, L., Karaman, R., Bufo, S.A., 2019. Photodegradation using

- TiO₂-activated borosilicate tubes. *Environ. Sci. Pollut. Res.* 26, 19025–19034. <https://doi.org/10.1007/S11356-018-2858-5>
- Khataee, A.R., Fathinia, M., Joo, S.W., 2013. Simultaneous monitoring of photocatalysis of three pharmaceuticals by immobilized TiO₂ nanoparticles: Chemometric assessment, intermediates identification and ecotoxicological evaluation. *Spectrochim. Acta Part A Mol. Biomol. Spectrosc.* 112, 33–45. <https://doi.org/10.1016/J.SAA.2013.04.028>
- Klein, E.Y., Van Boeckel, T.P., Martinez, E.M., Pant, S., Gandra, S., Levin, S.A., Goossens, H., Laxminarayan, R., 2018. Global increase and geographic convergence in antibiotic consumption between 2000 and 2015. *Proc. Natl. Acad. Sci.* 115, E3463–E3470. <https://doi.org/10.1073/pnas.1717295115>
- Krýsa, J., Waldner, G., Měšt'ánková, H., Jirkovský, J., Grabner, G., 2006. Photocatalytic degradation of model organic pollutants on an immobilized particulate TiO₂ layer: Roles of adsorption processes and mechanistic complexity. *Appl. Catal. B Environ.* 64, 290–301. <https://doi.org/10.1016/J.APCATB.2005.11.007>
- Kumar, R.R., Lee, J.T., Cho, J.Y., 2012. Fate, occurrence, and toxicity of veterinary antibiotics in environment. *J. Korean Soc. Appl. Biol. Chem.* 55, 701–709. <https://doi.org/10.1007/S13765-012-2220-4>
- Kümmerer, K., Al-Ahmad, A., Mersch-Sundermann, V., 2000. Biodegradability of some antibiotics, elimination of the genotoxicity and affection of wastewater bacteria in a simple test. *Chemosphere* 40, 701–710. [https://doi.org/10.1016/S0045-6535\(99\)00439-7](https://doi.org/10.1016/S0045-6535(99)00439-7)
- Kwon, B.G., Lee, D.S., Kang, N., Yoon, J., 1999. Characteristics of p-chlorophenol oxidation by Fenton's reagent. *Water Res.* 33, 2110–2118. [https://doi.org/10.1016/S0043-1354\(98\)00428-X](https://doi.org/10.1016/S0043-1354(98)00428-X)
- Langford, B.J., So, M., Raybardhan, S., Leung, V., Soucy, J.P.R., Westwood, D., Daneman, N., MacFadden, D.R., 2021. Antibiotic prescribing in patients with COVID-19: rapid review and meta-analysis. *Clin. Microbiol. Infect.* 27, 520–531. <https://doi.org/10.1016/J.CMI.2020.12.018>
- Langford, B.J., So, M., Raybardhan, S., Leung, V., Westwood, D., MacFadden, D.R., Soucy, J.P.R., Daneman, N., 2020. Bacterial co-infection and secondary infection in patients with COVID-19: a living rapid review and meta-analysis. *Clin. Microbiol. Infect.* 26, 1622–

1629. <https://doi.org/10.1016/J.CMI.2020.07.016>
- Larsson, D.G.J., 2014. Antibiotics in the environment. *Ups. J. Med. Sci.* 119, 108–112. <https://doi.org/10.3109/03009734.2014.896438>
- Larsson, D.G.J., de Pedro, C., Paxeus, N., 2007. Effluent from drug manufactures contains extremely high levels of pharmaceuticals. *J. Hazard. Mater.* 148, 751–755. <https://doi.org/10.1016/J.JHAZMAT.2007.07.008>
- Lau, T.K., Chu, W., Graham, N.J.D., 2007. The aqueous degradation of butylated hydroxyanisole by UV/S 2082-: Study of reaction mechanisms via dimerization and mineralization. *Environ. Sci. Technol.* 41, 613–619. <https://doi.org/10.1021/es061395a>
- Legrini, O., Oliveros, E., Braun, A.M., 1993. Photochemical Processes for Water Treatment. *Chem. Rev.* 93, 671–698. <https://doi.org/10.1021/CR00018A003>
- Lelario, F., Brienza, M., Bufo, S.A., Scrano, L., 2016. Effectiveness of different advanced oxidation processes (AOPs) on the abatement of the model compound mepanipyrin in water. *J. Photochem. Photobiol. A Chem.* 321, 187–201. <https://doi.org/10.1016/j.jphotochem.2016.01.024>
- Li, L., Niu, C.G., Guo, H., Wang, J., Ruan, M., Zhang, L., Liang, C., Liu, H.Y., Yang, Y.Y., 2020. Efficient degradation of Levofloxacin with magnetically separable ZnFe₂O₄/NCDs/Ag₂CO₃ Z-scheme heterojunction photocatalyst: Vis-NIR light response ability and mechanism insight. *Chem. Eng. J.* 383, 123192. <https://doi.org/10.1016/j.cej.2019.123192>
- Li, M., Wei, D., Du, Y., 2014. Acute toxicity evaluation for quinolone antibiotics and their chlorination disinfection processes. *J. Environ. Sci.* 26, 1837–1842. <https://doi.org/10.1016/J.JES.2014.06.023>
- Li, Y., Tang, H., Hu, Y., Wang, X., Ai, X., Tang, L., Matthew, C., Cavanagh, J., Qiu, J., 2016. Enrofloxacin at environmentally relevant concentrations enhances uptake and toxicity of cadmium in the earthworm *Eisenia fetida* in farm soils. *J. Hazard. Mater.* 308, 312–320. <https://doi.org/10.1016/J.JHAZMAT.2016.01.057>
- Li, Y., Wei, D., Du, Y., 2015. Oxidative transformation of levofloxacin by d-MnO₂: Products, pathways and toxicity assessment. *Chemosphere* 119, 282–288.

- <https://doi.org/10.1016/j.chemosphere.2014.06.064>
- Liang, C., Bruell, C.J., 2008. Thermally Activated Persulfate Oxidation of Trichloroethylene: Experimental Investigation of Reaction Orders. *Ind. Eng. Chem. Res.* 47, 2912–2918. <https://doi.org/10.1021/IE070820L>
- Liang, C., Huang, C.F., Mohanty, N., Kurakalva, R.M., 2008. A rapid spectrophotometric determination of persulfate anion in ISCO. *Chemosphere* 73, 1540–1543. <https://doi.org/10.1016/j.chemosphere.2008.08.043>
- Liang, C., Su, H.-W., 2009. Identification of Sulfate and Hydroxyl Radicals in Thermally Activated Persulfate. *Ind. Eng. Chem. Res.* 48, 5558–5562. <https://doi.org/10.1021/IE9002848>
- Lima Gomes, P.C.F., Tomita, I.N., Santos-Neto, Á.J., Zaiat, M., 2015. Rapid determination of 12 antibiotics and caffeine in sewage and bioreactor effluent by online column-switching liquid chromatography/tandem mass spectrometry. *Anal. Bioanal. Chem.* 407, 8787–8801. <https://doi.org/10.1007/S00216-015-9038-Y>
- Lin, S.H., Lin, C.M., Leu, H.G., 1999. Operating characteristics and kinetic studies of surfactant wastewater treatment by Fenton oxidation. *Water Res.* 33, 1735–1741. [https://doi.org/10.1016/S0043-1354\(98\)00403-5](https://doi.org/10.1016/S0043-1354(98)00403-5)
- Liu, B., Li, Y., Wu, Y., Xing, S., 2021. Enhanced degradation of ofloxacin by persulfate activation with Mn doped CuO: Synergetic effect between adsorption and non-radical activation. *Chem. Eng. J.* 417, 127972. <https://doi.org/10.1016/j.cej.2020.127972>
- Liu, L., Liu, Z., Bai, H., Sun, D.D., 2012. Concurrent filtration and solar photocatalytic disinfection/degradation using high-performance Ag/TiO₂ nanofiber membrane. *Water Res.* 46, 1101–1112. <https://doi.org/10.1016/J.WATRES.2011.12.009>
- Liu, X., Fang, L., Zhou, Y., Zhang, T., Shao, Y., 2013. Comparison of UV/PDS and UV/H₂O₂ processes for the degradation of atenolol in water. *J. Environ. Sci.* 25, 1519–1528. [https://doi.org/10.1016/S1001-0742\(12\)60289-7](https://doi.org/10.1016/S1001-0742(12)60289-7)
- Liu, X., Liu, Y., Lu, S., Wang, Z., Wang, Y., Zhang, G., Guo, X., Guo, W., Zhang, T., Xi, B., 2020. Degradation difference of ofloxacin and levofloxacin by UV/H₂O₂ and UV/PS (persulfate): Efficiency, factors and mechanism. *Chem. Eng. J.* 385, 123987.

- <https://doi.org/10.1016/j.cej.2019.123987>
- Liu, X., Lu, S., Guo, W., Xi, B., Wang, W., 2018. Antibiotics in the aquatic environments: A review of lakes, China. *Sci. Total Environ.* 627, 1195–1208. <https://doi.org/10.1016/J.SCITOTENV.2018.01.271>
- Liu, X.Y., Wang, B.J., Jiang, C.Y., Liu, S.J., 2007. *Micrococcus flavus* sp. nov., isolated from activated sludge in a bioreactor. *Int. J. Syst. Evol. Microbiol.* 57, 66–69. <https://doi.org/10.1099/IJS.0.64489-0>
- Liu, Y., Li, J., Qiu, X., Burda, C., 2006. Novel TiO₂ nanocatalysts for wastewater purification: tapping energy from the sun. *Water Sci. Technol.* 54, 47–54. <https://doi.org/10.2166/WST.2006.733>
- López-Serna, R., Jurado, A., Vázquez-Suñé, E., Carrera, J., Petrović, M., Barceló, D., 2013. Occurrence of 95 pharmaceuticals and transformation products in urban groundwaters underlying the metropolis of Barcelona, Spain. *Environ. Pollut.* 174, 305–315. <https://doi.org/10.1016/J.ENVPOL.2012.11.022>
- MacWilliams, M.P., Liao, M.K., 2006. Luria broth (LB) and Luria agar (LA) media and their uses protocol. ASM MicrobeLibrary. Am. Soc. Microbiol.
- Mahlie, W.S., 1934. Sulphur in Sewage. *Sewage Work. J.* 6, 547–579. <https://www.jstor.org/stable/25028417>
- Mahmood, A.R., Al-Haideri, H.H., Hassan, F.M., 2019. Detection of Antibiotics in Drinking Water Treatment Plants in Baghdad City, Iraq. *Adv. Public Heal.* 2019, 1–10. <https://doi.org/10.1155/2019/7851354>
- Maia, A.S., Paíga, P., Delerue-Matos, C., Castro, P.M.L., Tiritan, M.E., 2020. Quantification of fluoroquinolones in wastewaters by liquid chromatography-tandem mass spectrometry. *Environ. Pollut.* 259, 113927. <https://doi.org/10.1016/J.ENVPOL.2020.113927>
- Manasfi, R., Chiron, S., Montemurro, N., Perez, S., Brienza, M., 2020. Biodegradation of fluoroquinolone antibiotics and the climbazole fungicide by *Trichoderma* species. *Environ. Sci. Pollut. Res.* 27, 23331–23341. <https://doi.org/10.1007/s11356-020-08442-8>
- Mansilla, H.D., Yeber, M.C., Freer, J., Rodríguez, J., Baeza, J., 1997. Homogeneous and heterogeneous advanced oxidation of a bleaching effluent from the pulp and paper industry.

- Water Sci. Technol. 35, 273–278. [https://doi.org/10.1016/S0273-1223\(97\)00035-8](https://doi.org/10.1016/S0273-1223(97)00035-8)
- Martin Marietta Magnesia Specialities, 2015. The Role of Alkalinity in Aerobic Wastewater Treatment Plants: Magnesium Hydroxide vs. Caustic Soda.
- Maselli, B. de S., Luna, L.A.V., Palmeira, J. de O., Tavares, K.P., Barbosa, S., Beijo, L.A., Umbuzeiro, G.A., Kummrow, F., 2015. Ecotoxicity of raw and treated effluents generated by a veterinary pharmaceutical company: a comparison of the sensitivities of different standardized tests. *Ecotoxicology* 24, 795–804. <https://doi.org/10.1007/S10646-015-1425-9>
- Matthews, R.W., 1987. Photooxidation of organic impurities in water using thin films of titanium dioxide. *J. Phys. Chem.* 91, 3328–3333. <https://doi.org/10.1021/J100296A044>
- Meighen, E.A., 1993. Bacterial bioluminescence: organization, regulation, and application of the lux genes. *FASEB J.* 7, 1016–1022. <https://doi.org/10.1096/FASEBJ.7.11.8370470>
- Meighen, E.A., 1991. Molecular biology of bacterial bioluminescence. *Microbiol. Rev.* 55, 123–142. <https://doi.org/10.1128/MR.55.1.123-142.1991>
- Merel, S., Lege, S., Yanez Heras, J.E., Zwiener, C., 2017. Assessment of N-Oxide Formation during Wastewater Ozonation. *Environ. Sci. Technol.* 51, 410–417. <https://doi.org/10.1021/acs.est.6b02373>
- Michael, I., Rizzo, L., McArdell, C.S., Manaia, C.M., Merlin, C., Schwartz, T., Dagot, C., Fatta-Kassinos, D., 2013. Urban wastewater treatment plants as hotspots for the release of antibiotics in the environment: A review. *Water Res.* 47, 957–995. <https://doi.org/10.1016/J.WATRES.2012.11.027>
- Milovac, N., Juretic, D., Kusic, H., Dermadi, J., Bozic, A.L., 2014. Photooxidative degradation of aromatic carboxylic acids in water: Influence of hydroxyl substituents. *Ind. Eng. Chem. Res.* 53, 10590–10598. <https://doi.org/10.1021/IE501338Q>
- Mitscher, L.A., 2005. Bacterial Topoisomerase Inhibitors: Quinolone and Pyridone Antibacterial Agents. *Chem. Rev.* 105, 559–592. <https://doi.org/10.1021/CR030101Q>
- Mokhbi, Y., Korichi, M., Akchiche, Z., 2019. Combined photocatalytic and Fenton oxidation for oily wastewater treatment. *Appl. Water Sci.* 9. <https://doi.org/10.1007/S13201-019-0916-X>
- Mokrini, A., Ousse, D., Esplugas, S., 1997. Oxidation of aromatic compounds with UV

- radiation/ozone/hydrogen peroxide. *Water Sci. Technol.* 35, 95–102.
[https://doi.org/10.1016/S0273-1223\(97\)00014-0](https://doi.org/10.1016/S0273-1223(97)00014-0)
- Moretto, F., Sixt, T., Devilliers, H., Abdallahoui, M., Eberl, I., Rogier, T., Buisson, M., Chavanet, P., Duong, M., Esteve, C., Mahy, S., Salmon-Rousseau, A., Catherine, F., Blot, M., Piroth, L., 2021. Is there a need to widely prescribe antibiotics in patients hospitalized with COVID-19? *Int. J. Infect. Dis.* 105, 256–260.
<https://doi.org/10.1016/J.IJID.2021.01.051>
- Mukhtar, A., Manzoor, M., Gul, I., Zafar, R., Jamil, H.I., Niazi, A.K., Ali, M.A., Park, T.J., Arshad, M., 2020a. Phytotoxicity of different antibiotics to rice and stress alleviation upon application of organic amendments. *Chemosphere* 258, 127353.
<https://doi.org/10.1016/J.CHEMOSPHERE.2020.127353>
- Mukhtar, A., Manzoor, M., Gul, I., Zafar, R., Jamil, I., Khan Niazi, A., Ali, M.A., Park, T.J., Arshad, M., 2020b. Phytotoxicity of different antibiotics to rice and stress alleviation upon application of organic amendments. *Chemosphere* 258, 127353.
<https://doi.org/10.1016/j.chemosphere.2020.127353>
- Munter, R., 2001. Advanced oxidation processes - Current status and prospects, in: *Proceedings of the Estonian Academy of Sciences, Chemistry*. pp. 59–80.
- Nakata, K., Fujishima, A., 2012. TiO₂ photocatalysis: Design and applications. *J. Photochem. Photobiol. C Photochem. Rev.* 13, 169–189.
<https://doi.org/10.1016/J.JPHOTOCHEMREV.2012.06.001>
- Neth, N.L.K., Carlin, C.M., Keen, O.S., 2019. Emerging investigator series: Transformation of common antibiotics during water disinfection with chlorine and formation of antibacterially active products. *Environ. Sci. Water Res. Technol.* 5, 1222–1233.
<https://doi.org/10.1039/c9ew00182d>
- Ni, M., Leung, M.K.H., Leung, D.Y.C., Sumathy, K., 2007. A review and recent developments in photocatalytic water-splitting using TiO₂ for hydrogen production. *Renew. Sustain. Energy Rev.* 11, 401–425. <https://doi.org/10.1016/J.RSER.2005.01.009>
- Nihemaiti, M., Permala, R.R., Croué, J.P., 2020. Reactivity of unactivated peroxy monosulfate with nitrogenous compounds. *Water Res.* 169, 115221.
<https://doi.org/10.1016/j.watres.2019.115221>

- Nikolaou, A., Meric, S., Fatta, D., 2007. Occurrence patterns of pharmaceuticals in water and wastewater environments. *Anal. Bioanal. Chem.* 2007 3874 387, 1225–1234. <https://doi.org/10.1007/S00216-006-1035-8>
- Nzila, A., Razzak, S.A., Zhu, J., 2016. Bioaugmentation: An Emerging Strategy of Industrial Wastewater Treatment for Reuse and Discharge. *Int. J. Environ. Res. Public Health* 13, 846. <https://doi.org/10.3390/IJERPH13090846>
- Odonkor, S.T., Ampofo, J.K., 2013. Escherichia coli as an indicator of bacteriological quality of water: an overview. *Microbiol. Res. (Pavia)*. 4, 2. <https://doi.org/10.4081/MR.2013.E2>
- Oliphant, C.M., Green, G., 2002. Quinolones: A Comprehensive Review. *Am. Fam. Physician* 65, 455–465.
- Ory, J., Bricheux, G., Togola, A., Bonnet, J.L., Donnadiou-Bernard, F., Nakusi, L., Forestier, C., Traore, O., 2016. Ciprofloxacin residue and antibiotic-resistant biofilm bacteria in hospital effluent. *Environ. Pollut.* 214, 635–645. <https://doi.org/10.1016/J.ENVPOL.2016.04.033>
- Orzoł, A., Piotrowicz-Cieślak, A.I., 2017. Levofloxacin is phytotoxic and modifies the protein profile of lupin seedlings. *Environ. Sci. Pollut. Res.* 24, 22226–22240. <https://doi.org/10.1007/S11356-017-9845-0>
- Oturan, M.A., Aaron, J.-J., 2014. Advanced Oxidation Processes in Water/Wastewater Treatment: Principles and Applications. A Review. *Crit. Rev. Environ. Sci. Technol.* 44, 2577–2641. <https://doi.org/10.1080/10643389.2013.829765>
- Pan, L. jia, Li, J., Li, C. xing, Tang, X. da, Yu, G. wei, Wang, Y., 2018. Study of ciprofloxacin biodegradation by a *Thermus* sp. isolated from pharmaceutical sludge. *J. Hazard. Mater.* 343, 59–67. <https://doi.org/10.1016/J.JHAZMAT.2017.09.009>
- Pan, M., Chu, L.M., 2016. Phytotoxicity of veterinary antibiotics to seed germination and root elongation of crops. *Ecotoxicol. Environ. Saf.* 126, 228–237. <https://doi.org/10.1016/J.ECOENV.2015.12.027>
- Pascale, R., Bianco, G., Coviello, D., Cristina Lafiosca, M., Masi, S., Mancini, I.M., Bufo, S.A., Scrano, L., Caniani, D., 2020. Validation of a liquid chromatography coupled with tandem mass spectrometry method for the determination of drugs in wastewater using a three-phase solvent system. *J. Sep. Sci.* 43, 886–895. <https://doi.org/10.1002/jssc.201900509>

- Pavel, V.L., Sobariu, D.L., Diaconu, M., Statescu, F., Gavrilesco, M., 2013. Effects of heavy metals on *Lepidium sativum* germination and growth. *Environ. Eng. Manag. J.* 12, 727–733. <https://doi.org/10.30638/eemj.2013.089>
- Pekakis, P.A., Xekoukoulotakis, N.P., Mantzavinos, D., 2006. Treatment of textile dyehouse wastewater by TiO₂ photocatalysis. *Water Res.* 40, 1276–1286. <https://doi.org/10.1016/J.WATRES.2006.01.019>
- Pena, A., Chmielova, D., Lino, C.M., Solich, P., 2007. Determination of fluoroquinolone antibiotics in surface waters from Mondego River by high performance liquid chromatography using a monolithic column. *J. Sep. Sci.* 30, 2924–2928. <https://doi.org/10.1002/JSSC.200700363>
- Petrie, B., Barden, R., Kasprzyk-Hordern, B., 2015. A review on emerging contaminants in wastewaters and the environment: Current knowledge, understudied areas and recommendations for future monitoring. *Water Res.* 72, 3–27. <https://doi.org/10.1016/J.WATRES.2014.08.053>
- Peyton, G.R., Glaze, W.H., 1988. Destruction of Pollutants in Water with Ozone in Combination with Ultraviolet Radiation. 3. Photolysis of Aqueous Ozone. *Environ. Sci. Technol.* 22, 761–767. <https://doi.org/10.1021/es00172a003>
- Pignatello, J.J., 1992. Dark and Photoassisted Iron (Fe³⁺)-Catalyzed Degradation of Chlorophenoxy Herbicides by Hydrogen Peroxide. *Environ. Sci. Technol.* 26, 944–951. <https://doi.org/10.1021/ES00029A012>
- Polo-López, M.I., García-Fernández, I., Velegraki, T., Katsoni, A., Oller, I., Mantzavinos, D., Fernández-Ibáñez, P., 2012. Mild solar photo-Fenton: An effective tool for the removal of Fusarium from simulated municipal effluents. *Appl. Catal. B Environ.* 111–112, 545–554. <https://doi.org/10.1016/J.APCATB.2011.11.006>
- Poyatos, J.M., Muñio, M.M., Almecija, M.C., Torres, J.C., Hontoria, E., Osorio, F., 2009. Advanced Oxidation Processes for Wastewater Treatment: State of the Art. *Water. Air. Soil Pollut.* 205, 187–204. <https://doi.org/10.1007/S11270-009-0065-1>
- Prat, M.D., Ramil, D., Compañó, R., Hernández-Arteseros, J.A., Granados, M., 2006. Determination of flumequine and oxolinic acid in sediments and soils by microwave-assisted extraction and liquid chromatography-fluorescence. *Anal. Chim. Acta* 567, 229–

235. <https://doi.org/10.1016/J.ACA.2006.03.051>
- Ramos Payán, M., Bello López, M.Á., Fernández-Torres, R., González, J.A.O., Callejón Mochón, M., 2011. Hollow fiber-based liquid phase microextraction (HF-LPME) as a new approach for the HPLC determination of fluoroquinolones in biological and environmental matrices. *J. Pharm. Biomed. Anal.* 55, 332–341. <https://doi.org/10.1016/J.JPBA.2011.01.037>
- Rashed, M.N., 2013. Adsorption Technique for the Removal of Organic Pollutants from Water and Wastewater. *Org. Pollut. - Monit. Risk Treat.* 7, 167–194. <https://doi.org/10.5772/54048>
- Rastogi, A., Al-Abed, S.R., Dionysiou, D.D., 2009. Sulfate radical-based ferrous–peroxymonosulfate oxidative system for PCBs degradation in aqueous and sediment systems. *Appl. Catal. B Environ.* 85, 171–179. <https://doi.org/10.1016/J.APCATB.2008.07.010>
- Reddy, K.R., Reddy, C.V., Nadagouda, M.N., Shetti, N.P., Jaesool, S., Aminabhavi, T.M., 2019. Polymeric graphitic carbon nitride (g-C₃N₄)-based semiconducting nanostructured materials: Synthesis methods, properties and photocatalytic applications. *J. Environ. Manage.* 238, 25–40. <https://doi.org/10.1016/J.JENVMAN.2019.02.075>
- Repubblica Italiana, 2006. Decreto Legislativo 3 aprile 2006, n. 152, Gazzetta Ufficiale.
- Riaz, L., Mahmood, T., Khalid, A., Rashid, A., Siddique, M.B.A., Kamal, A., Coyne, M.S., 2018. Fluoroquinolones (FQs) in the environment: A review on their abundance, sorption and toxicity in soil. *Chemosphere* 191, 704–720. <https://doi.org/10.1016/J.CHEMOSPHERE.2017.10.092>
- Richards, S.M., Wilson, C.J., Johnson, D.J., Castle, D.M., Lam, M., Mabury, S.A., Sibley, P.K., Solomon, K.R., 2009. Effects of pharmaceutical mixtures in aquatic microcosms. *Environ. Toxicol. Chem.* 23, 1035–1042. <https://doi.org/10.1897/02-616>
- Rigol, A., Latorre, A., Lacorte, S., Barceló, D., 2004. Bioluminescence inhibition assays for toxicity screening of wood extractives and biocides in paper mill process waters. *Environ. Toxicol. Chem.* 23, 339–347. <https://doi.org/10.1897/02-632>
- Rizzo, L., Manaia, C., Merlin, C., Schwartz, T., Dagot, C., Ploy, M.C., Michael, I., Fatta-

- Kassinis, D., 2013. Urban wastewater treatment plants as hotspots for antibiotic resistant bacteria and genes spread into the environment: A review. *Sci. Total Environ.* 447, 345–360. <https://doi.org/10.1016/j.scitotenv.2013.01.032>
- Robinson, A.A., Belden, J.B., Lydy, M.J., 2005. Toxicity of fluoroquinolone antibiotics to aquatic organisms. *Environ. Toxicol. Chem.* 24, 423–430. <https://doi.org/10.1897/04-210R.1>
- Rodrigues-Silva, C., Porto, R.S., Santos, S.G. dos, Schneider, J., Rath, S., 2019. Fluoroquinolones in Hospital Wastewater: Analytical Method, Occurrence, Treatment with Ozone and Residual Antimicrobial Activity Evaluation. *J. Braz. Chem. Soc.* 30, 1447–1458. <https://doi.org/10.21577/0103-5053.20190040>
- Rodriguez-Mozaz, S., Chamorro, S., Marti, E., Huerta, B., Gros, M., Sánchez-Melsió, A., Borrego, C.M., Barceló, D., Balcázar, J.L., 2015. Occurrence of antibiotics and antibiotic resistance genes in hospital and urban wastewaters and their impact on the receiving river. *Water Res.* 69, 234–242. <https://doi.org/10.1016/J.WATRES.2014.11.021>
- Romanos, G.E., Athanasekou, C.P., Katsaros, F.K., Kanellopoulos, N.K., Dionysiou, D.D., Likodimos, V., Falaras, P., 2012. Double-side active TiO₂-modified nanofiltration membranes in continuous flow photocatalytic reactors for effective water purification. *J. Hazard. Mater.* 211–212, 304–316. <https://doi.org/10.1016/J.JHAZMAT.2011.09.081>
- Rosal, R., Rodea-Palomares, I., Boltes, K., Fernández-Piñas, F., Leganés, F., Gonzalo, S., Petre, A., 2009. Ecotoxicity assessment of lipid regulators in water and biologically treated wastewater using three aquatic organisms. *Environ. Sci. Pollut. Res.* 17, 135–144. <https://doi.org/10.1007/S11356-009-0137-1>
- Rosal, R., Rodríguez, A., Perdígón-Melón, J.A., Petre, A., García-Calvo, E., Gómez, M.J., Agüera, A., Fernández-Alba, A.R., 2010. Occurrence of emerging pollutants in urban wastewater and their removal through biological treatment followed by ozonation. *Water Res.* 44, 578–588. <https://doi.org/10.1016/J.WATRES.2009.07.004>
- Ruppert, G., Bauer, R., Heisler, G., 1993. The photo-Fenton reaction — an effective photochemical wastewater treatment process. *J. Photochem. Photobiol. A Chem.* 73, 75–78. [https://doi.org/10.1016/1010-6030\(93\)80035-8](https://doi.org/10.1016/1010-6030(93)80035-8)
- Saien, J., Soleymani, A.R., Sun, J.H., 2011. Parametric optimization of individual and hybridized

- AOPs of Fe²⁺/H₂O₂ and UV/S₂O₈²⁻ for rapid dye destruction in aqueous media. *Desalination* 279, 298–305. <https://doi.org/10.1016/J.DESAL.2011.06.024>
- Salgado, R., Oehmen, A., Carvalho, G., Noronha, J.P., Reis, M.A.M., 2012. Biodegradation of clofibrac acid and identification of its metabolites. *J. Hazard. Mater.* 241–242, 182–189. <https://doi.org/10.1016/J.JHAZMAT.2012.09.029>
- Santana, C.M., Ferrera, Z.S., Padrón, M.E.T., Rodríguez, J.J.S., 2009. Methodologies for the Extraction of Phenolic Compounds from Environmental Samples: New Approaches. *Molecules* 14, 298–320. <https://doi.org/10.3390/MOLECULES14010298>
- Scheres, J., Kuszewski, K., 2019. The Ten Threats to Global Health in 2018 and 2019. A welcome and informative communication of WHO to everybody, *Zdrowie Publiczne i Zarządzanie* 17, 2–8. <https://doi.org/10.4467/20842627OZ.19.001.11297>
- Schneider, J., Matsuoka, M., Takeuchi, M., Zhang, J., Horiuchi, Y., Anpo, M., Bahnemann, D.W., 2014. Understanding TiO₂ Photocatalysis: Mechanisms and Materials. *Chem. Rev.* 114, 9919–9986. <https://doi.org/10.1021/CR5001892>
- Schwarzenbach, R.P., Egli, T., Hofstetter, T.B., Von Gunten, U., Wehrli, B., 2010. Global Water Pollution and Human Health. *Annu. Rev. Environ. Resour.* 35, 109–136. <https://doi.org/10.1146/annurev-environ-100809-125342>
- Scrano, L., Bufo, S.A., Perucci, P., Meallier, P., Mansour, M., 1999. Photolysis and hydrolysis of rimsulfuron. *Pestic. Sci.* 55, 955–961. [https://doi.org/10.1002/\(SICI\)1096-9063\(199909\)55:9<955::AID-PS29>3.0.CO;2-9](https://doi.org/10.1002/(SICI)1096-9063(199909)55:9<955::AID-PS29>3.0.CO;2-9)
- Scrano, L., Foti, L., Lelario, F., 2020. Fluoroquinolones in Water: Removal Attempts by Innovative Aops, in: *NATO Science for Peace and Security Series A: Chemistry and Biology*. Springer Science and Business Media B.V., pp. 259–263. https://doi.org/10.1007/978-94-024-2041-8_27
- Serpone, N., Borgarello, E., Harris, R., Cahill, P., Borgarello, M., Pelizzetti, E., 1986. Photocatalysis over TiO₂ supported on a glass substrate. *Sol. Energy Mater.* 14, 121–127. [https://doi.org/10.1016/0165-1633\(86\)90070-5](https://doi.org/10.1016/0165-1633(86)90070-5)
- Serrà, A., Philippe, L., Perreault, F., Garcia-Segura, S., 2021. Photocatalytic treatment of natural waters. Reality or hype? The case of cyanotoxins remediation. *Water Res.* 188, 116543.

- <https://doi.org/10.1016/J.WATRES.2020.116543>
- Sharma, V. K., 2009. Aggregation and toxicity of titanium dioxide nanoparticles in aquatic environment - A review. *J. Environ. Sci. Health, Part A*, 44, 1485–1495. <https://doi.org/10.1080/10934520903263231>
- Shu, W., Zhang, Y., Wen, D., Wu, Q., Liu, H., Cui, M.-H., Fu, B., Zhang, J., Yao, Y., 2021. Anaerobic biodegradation of levofloxacin by enriched microbial consortia: Effect of electron acceptors and carbon source. *J. Hazard. Mater.* 414, 125520. <https://doi.org/10.1016/j.jhazmat.2021.125520>
- Singh, S., Mahalingam, H., Singh, P.K., 2013. Polymer-supported titanium dioxide photocatalysts for environmental remediation: A review. *Appl. Catal. A Gen.* 462–463, 178–195. <https://doi.org/10.1016/J.APCATA.2013.04.039>
- Skoumal, M., Cabot, P.L., Centellas, F., Arias, C., Rodríguez, R.M., Garrido, J.A., Brillas, E., 2006. Mineralization of paracetamol by ozonation catalyzed with Fe²⁺, Cu²⁺ and UVA light. *Appl. Catal. B Environ.* 66, 228–240. <https://doi.org/10.1016/J.APCATB.2006.03.016>
- Snedecor, G.W., Cochran, W.G., 1989. *Statistical Methods*, 8th ed. Iowa State University Press: Ames, USA.
- Šojić, D., Despotović, V., Orčić, D., Szabó, E., Arany, E., Armaković, S., Illés, E., Gajda-Schranz, K., Dombi, A., Alapi, T., Sajben-Nagy, E., Palágyi, A., Vágvölgyi, C., Manczinger, L., Bjelica, L., Abramović, B., 2012. Degradation of thiamethoxam and metoprolol by UV, O₃ and UV/O₃ hybrid processes: Kinetics, degradation intermediates and toxicity. *J. Hydrol.* 472–473, 314–327. <https://doi.org/10.1016/J.JHYDROL.2012.09.038>
- Speight, J.G., 2017. Chemical Transformations in the Environment, in: *Environmental Organic Chemistry for Engineers*. Butterworth-Heinemann, pp. 305–353. <https://doi.org/10.1016/B978-0-12-804492-6.00007-1>
- Spellman, F.R., 2013. *Handbook of Water and Wastewater Treatment Plant Operations*. CRC Press. <https://doi.org/10.1201/B15579>
- Srinivasan, A., Chowdhury, P., Viraraghavan, T., 2009. Air stripping in industrial wastewater treatment, in: *Water and Wastewater Treatment Technologies*. Encyclopedia of Life

- Support Systems (EOLSS).
- Sriwong, C., Wongnawa, S., Patarapaiboolchai, O., 2008. Photocatalytic activity of rubber sheet impregnated with TiO₂ particles and its recyclability. *Catal. Commun.* 9, 213–218. <https://doi.org/10.1016/J.CATCOM.2007.05.037>
- Stanley, J.K., Ramirez, A.J., Mottaleb, M., Chambliss, C.K., Brooks, B.W., 2006. Enantiospecific toxicity of the β -blocker propranolol to *Daphnia magna* and *Pimephales promelas*. *Environ. Toxicol. Chem.* 25, 1780–1786. <https://doi.org/10.1897/05-298R1.1>
- Stott, R., 2003. Fate and behaviour of parasites in wastewater treatment systems, in: *Handbook of Water and Wastewater Microbiology*. Academic Press, pp. 491–521. <https://doi.org/10.1016/B978-012470100-7/50032-7>
- Sturini, M., Speltini, A., Maraschi, F., Profumo, A., Pretali, L., Fasani, E., Albini, A., 2012. Sunlight-induced degradation of soil-adsorbed veterinary antimicrobials Marbofloxacin and Enrofloxacin. *Chemosphere* 86, 130–137. <https://doi.org/10.1016/J.CHEMOSPHERE.2011.09.053>
- Sun, Y., Pignatello, J.J., 1993. Photochemical Reactions Involved in the Total Mineralization of 2,4-D by iron (3+)/hydrogen peroxide/UV. *Environ. Sci. Technol.* 27, 304–310. <https://doi.org/10.1021/ES00039A010>
- Svenson, A., Norin, H., Hynning, P.-A., 1996. Toxicity-Directed Fractionation of Effluents Using the Bioluminescence of *Vibrio fischeri* and Gas Chromatography/Mass Spectroscopy Identification of the Toxic Components. *Environ. Toxicol. Water Qual. An Int. J.* 11, 277–284. [https://doi.org/10.1002/\(SICI\)1098-2256\(1996\)11:3<277::AID-TOX15>3.0.CO;2-8](https://doi.org/10.1002/(SICI)1098-2256(1996)11:3<277::AID-TOX15>3.0.CO;2-8)
- Szpyrkowicz, L., Juzzolino, C., Kaul, S.N., 2001. A Comparative study on oxidation of disperse dyes by electrochemical process, ozone, hypochlorite and fenton reagent. *Water Res.* 35, 2129–2136. [https://doi.org/10.1016/S0043-1354\(00\)00487-5](https://doi.org/10.1016/S0043-1354(00)00487-5)
- The Pharmaceutical Journal, 2018. Global antibiotic consumption increased by 65% between 2000 and 2015, study finds [WWW Document]. *Pharm. J.* <https://doi.org/DOI:10.1211/PJ.2018.20204603>
- Turiel, E., Martín-Esteban, A., Tadeo, J.L., 2007. Molecular imprinting-based separation methods for selective analysis of fluoroquinolones in soils. *J. Chromatogr. A* 1172, 97–104.

- <https://doi.org/10.1016/J.CHROMA.2007.10.003>
- Tyumina, E.A., Bazhutin, G.A., Cartagena Gómez, A. d. P., Ivshina, I.B., 2020. Nonsteroidal Anti-inflammatory Drugs as Emerging Contaminants. *Microbiology* 89, 148–163. <https://doi.org/10.1134/S0026261720020125>
- Umadevi, M., Sangari, M., Parimaladevi, R., Sivanantham, A., Mayandi, J., 2013. Enhanced photocatalytic, antimicrobial activity and photovoltaic characteristics of fluorine doped TiO₂ synthesized under ultrasound irradiation. *J. Fluor. Chem.* 156, 209–213. <https://doi.org/10.1016/J.JFLUCHEM.2013.10.011>
- University of Minnesota, 2013. The Effects of Chloride from Waste Water on the Environment.
- Ushani, U., Lu, X., Wang, J., Zhang, Z., Dai, J., Tan, Y., Wang, S., Li, W., Niu, C., Cai, T., Wang, N., Zhen, G., 2020. Sulfate radicals-based advanced oxidation technology in various environmental remediation: A state-of-the-art review. *Chem. Eng. J.* 402, 126232. <https://doi.org/10.1016/J.CEJ.2020.126232>
- Uslu, M.Ö., Yediler, A., Balcıoğlu, I.A., Schulte-Hostede, S., 2008. Analysis and Sorption Behavior of Fluoroquinolones in Solid Matrices. *Water. Air. Soil Pollut.* 190, 55–63. <https://doi.org/10.1007/S11270-007-9580-0>
- Vagi, M., Petsas, A., 2017. Advanced oxidation processes for the removal of pesticides from wastewater: recent review and trends. 15th Int. Conf. Environ. Sci. Technol. CEST 2017 31.
- Valerio, M.E., García, J.F., Peinado, F.M., 2007. Determination of phytotoxicity of soluble elements in soils, based on a bioassay with lettuce (*Lactuca sativa* L.). *Sci. Total Environ.* 378, 63–66. <https://doi.org/10.1016/J.SCITOTENV.2007.01.007>
- Vallejo-Rodríguez, R., Sánchez-Torres, P.B., López-López, A., León-Becerril, E., Murillo-Tovar, M., 2017. Detection of Steroids in Tap and Drinking Water Using an Optimized Analytical Method by Gas Chromatography–Mass Spectrometry. *Expo. Heal.* 2017 103 10, 189–199. <https://doi.org/10.1007/S12403-017-0254-X>
- Van der Graaf, J.H.J.M., De Koning, J., Ravazzini, A., Miska, V., 2005. Treatment matrix for reuse of upgraded wastewater. *Water Sci. Technol. Water Supply* 5, 87–94. <https://doi.org/10.2166/ws.2005.0011>
- Van Doorslaer, X., Dewulf, J., Van Langenhove, H., Demeestere, K., 2014. Fluoroquinolone

- antibiotics: An emerging class of environmental micropollutants. *Sci. Total Environ.* 500–501, 250–269. <https://doi.org/10.1016/J.SCITOTENV.2014.08.075>
- Vogelsang, C., Grung, M., Jantsch, T.G., Tollefsen, K.E., Liltved, H., 2006. Occurrence and removal of selected organic micropollutants at mechanical, chemical and advanced wastewater treatment plants in Norway. *Water Res.* 40, 3559–3570. <https://doi.org/10.1016/J.WATRES.2006.07.022>
- Von Sperling, M., 2007. Wastewater Characteristics, Treatment and Disposal, in: *Biological Wastewater Treatment Series*. pp. 1–292.
- Wacławek, S., Lutze, H. V., Grübel, K., Padil, V.V.T., Černík, M., Dionysiou, D.D., 2017. Chemistry of persulfates in water and wastewater treatment: A review. *Chem. Eng. J.* 330, 44–62. <https://doi.org/10.1016/j.cej.2017.07.132>
- Walling, C., 1975. Fenton's Reagent Revisited. *Acc. Chem. Res.* 8, 125–131. <https://doi.org/10.1021/AR50088A003>
- Wang, C., Yediler, A., Lienert, D., Wang, Z., Kettrup, A., 2002. Toxicity evaluation of reactive dyestuffs, auxiliaries and selected effluents in textile finishing industry to luminescent bacteria *Vibrio fischeri*. *Chemosphere* 46, 339–344. [https://doi.org/10.1016/S0045-6535\(01\)00086-8](https://doi.org/10.1016/S0045-6535(01)00086-8)
- Wang, H., Che, B., Duan, A., Mao, J., Dahlgren, R.A., Zhang, M., Zhang, H., Zeng, A., Wang, X., 2014. Toxicity evaluation of β -diketone antibiotics on the development of embryo-larval zebrafish (*Danio rerio*). *Environ. Toxicol.* 29, 1134–1146. <https://doi.org/10.1002/TOX.21843>
- Wang, J., Wang, S., 2018. Activation of persulfate (PS) and peroxymonosulfate (PMS) and application for the degradation of emerging contaminants. *Chem. Eng. J.* 334, 1502–1517. <https://doi.org/10.1016/j.cej.2017.11.059>
- Wang, Q., Wang, B., Ma, Y., Xing, S., 2018. Enhanced superoxide radical production for ofloxacin removal via persulfate activation with Cu-Fe oxide. *Chem. Eng. J.* 354, 473–480. <https://doi.org/10.1016/j.cej.2018.08.055>
- Watkinson, A.J., Murby, E.J., Costanzo, S.D., 2007. Removal of antibiotics in conventional and advanced wastewater treatment: Implications for environmental discharge and wastewater

- recycling. *Water Res.* 41, 4164–4176. <https://doi.org/10.1016/J.WATRES.2007.04.005>
- Watkinson, A.J., Murby, E.J., Kolpin, D.W., Costanzo, S.D., 2009. The occurrence of antibiotics in an urban watershed: From wastewater to drinking water. *Sci. Total Environ.* 407, 2711–2723. <https://doi.org/10.1016/J.SCITOTENV.2008.11.059>
- Wei, Z., Villamena, F.A., Weavers, L.K., 2017. Kinetics and mechanism of ultrasonic activation of persulfate: an in situ EPR spin trapping study. *Environ. Sci. Technol.* 51, 3410–3417. <https://doi.org/10.1021/acs.est.6b05392>
- Whirledge, S., Cidlowski, J.A., 2019. Steroid Hormone Action. *Yen Jaffe's Reprod. Endocrinol. Physiol. Pathophysiol. Clin. Manag.* Eighth Ed. 115-131.e4. <https://doi.org/10.1016/B978-0-323-47912-7.00005-6>
- Williams, C.F., Geroni, G.M., Lloyd, D., Choi, H., Clark, N., Pirog, A., Lees, J., Porch, A., 2019. Bioluminescence of *Vibrio fischeri*: bacteria respond quickly and sensitively to pulsed microwave electric (but not magnetic) fields. *J. Biomed. Optics* 24, 051412. <https://doi.org/10.1117/1JBO.24.5.051412>
- World Health Organization, 2019. WHO releases the 2019 AWaRe Classification Antibiotics [WWW Document]. URL <https://www.who.int/news/item/01-10-2019-who-releases-the-2019-aware-classification-antibiotics>.
- World Health Organization, 2012. Pharmaceuticals in drinking-water [WWW Document]. URL https://apps.who.int/iris/bitstream/handle/10665/44630/9789241502085_eng.pdf;jsessionid=0187491E89E31BF8B98FE10990D8A5EA?sequence=1
- Yahya, M.S., Karbane, M. El, Oturan, N., Kacemi, K. El, Oturan, M.A., 2015. Mineralization of the antibiotic levofloxacin in aqueous medium by electro-Fenton process: kinetics and intermediate products analysis. *Environ. Technol.* 37, 1276–1287. <https://doi.org/10.1080/09593330.2015.1111427>
- Yamashita, N., Yasojima, M., Nakada, N., Miyajima, K., Komori, K., Suzuki, Y., Tanaka, H., 2006. Effects of antibacterial agents, levofloxacin and clarithromycin, on aquatic organisms. *Water Sci. Technol.* 53, 65–72. <https://doi.org/10.2166/WST.2006.338>
- Yang, C., Song, G., Lim, W., 2020. A review of the toxicity in fish exposed to antibiotics. *Comp. Biochem. Physiol. Part C Toxicol. Pharmacol.* 237, 108840.

- <https://doi.org/10.1016/J.CBPC.2020.108840>
- Yang, Q., Ma, Y., Chen, F., Yao, F., Sun, J., Wang, S., Yi, K., Hou, L., Li, X., Wang, D., 2019. Recent advances in photo-activated sulfate radical-advanced oxidation process (SR-AOP) for refractory organic pollutants removal in water. *Chem. Eng. J.* 378, 122149. <https://doi.org/10.1016/J.CEJ.2019.122149>
- Yarahmadi, H., Duy, S.V., Hachad, M., Dorner, S., Sauvé, S., Prévost, M., 2018. Seasonal variations of steroid hormones released by wastewater treatment plants to river water and sediments: Distribution between particulate and dissolved phases. *Sci. Total Environ.* 635, 144–155. <https://doi.org/10.1016/J.SCITOTENV.2018.03.370>
- Ye, Z., Weinberg, H.S., Meyer, M.T., 2007. Trace Analysis of Trimethoprim and Sulfonamide, Macrolide, Quinolone, and Tetracycline Antibiotics in Chlorinated Drinking Water Using Liquid Chromatography Electrospray Tandem Mass Spectrometry. *Anal. Chem.* 79, 1135–1144. <https://doi.org/10.1021/AC060972A>
- Yin, R., Sun, J., Xiang, Y., Shang, C., 2018. Recycling and reuse of rusted iron particles containing core-shell Fe-FeOOH for ibuprofen removal: Adsorption and persulfate-based advanced oxidation. *J. Clean. Prod.* 178, 441–448. <https://doi.org/10.1016/J.JCLEPRO.2018.01.005>
- Yiruhan, Wang, Q.J., Mo, C.H., Li, Y.W., Gao, P., Tai, Y.P., Zhang, Y., Ruan, Z.L., Xu, J.W., 2010. Determination of four fluoroquinolone antibiotics in tap water in Guangzhou and Macao. *Environ. Pollut.* 158, 2350–2358. <https://doi.org/10.1016/J.ENVPOL.2010.03.019>
- Yu, B., Leung, K.M., Guo, Q., Lau, W.M., Yang, J., 2011. Synthesis of Ag–TiO₂ composite nano thin film for antimicrobial application. *Nanotechnology* 22, 115603. <https://doi.org/10.1088/0957-4484/22/11/115603>
- Zainab, S.M., Junaid, M., Xu, N., Malik, R.N., 2020. Antibiotics and antibiotic resistant genes (ARGs) in groundwater: A global review on dissemination, sources, interactions, environmental and human health risks. *Water Res.* 187, 116455. <https://doi.org/10.1016/J.WATRES.2020.116455>
- Zhang, H., Huang, C.-H., 2005. Oxidative Transformation of Fluoroquinolone Antibacterial Agents and Structurally Related Amines by Manganese Oxide. *Environ. Sci. Technol.* 39, 4474–4483. <https://doi.org/10.1021/ES048166D>

- Zhang, R., Yu, K., Li, A., Wang, Y., Huang, X., 2019. Antibiotics in corals of the South China Sea: Occurrence, distribution, bioaccumulation, and considerable role of coral mucus. *Environ. Pollut.* 250, 503–510. <https://doi.org/10.1016/J.ENVPOL.2019.04.036>
- Zhao, H., Quan, W., Bekele, T.G., Chen, M., Zhang, X., Qu, B., 2018. Effect of copper on the accumulation and elimination kinetics of fluoroquinolones in the zebrafish (*Danio rerio*). *Ecotoxicol. Environ. Saf.* 156, 135–140. <https://doi.org/10.1016/J.ECOENV.2018.03.025>
- Zhou, Y., Gao, Y., Jiang, J., Shen, Y.M., Pang, S.Y., Song, Y., Guo, Q., 2021. A comparison study of levofloxacin degradation by peroxymonosulfate and permanganate: Kinetics, products and effect of quinone group. *J. Hazard. Mater.* 403, 123834. <https://doi.org/10.1016/j.jhazmat.2020.123834>
- Zhu, Y., Zhu, R., Xi, Y., Zhu, J., Zhu, G., He, H., 2019. Strategies for enhancing the heterogeneous Fenton catalytic reactivity: A review. *Appl. Catal. B Environ.* 255, 117739. <https://doi.org/10.1016/J.APCATB.2019.05.041>
- Zouaghi, R., David, B., Suptil, J., Djebbar, K., Boutiti, A., Guittonneau, S., 2011. Sonochemical and sonocatalytic degradation of monolinuron in water. *Ultrason. Sonochem.* 18, 1107–1112. <https://doi.org/10.1016/J.ULTSONCH.2011.03.008>
- Zuorro, A., Lavecchia, R., Monaco, M.M., Iervolino, G., Vaiano, V., 2019. Photocatalytic Degradation of Azo Dye Reactive Violet 5 on Fe-Doped Titania Catalysts under Visible Light Irradiation. *Catalysts* 9, 645. <https://doi.org/10.3390/CATAL9080645>